THE UNIVERSITY *of* EDINBURGH

PATHOPHYSIOLOGY OF LACUNAR STROKE: ISCHAEMIC STROKE OR BLOOD BRAIN BARRIER DYSFUNCTION?

EMMA LOUISE BAILEY BSc Hons

Doctor of Philosophy

University of Edinburgh

2011

CONTENTS

APPENDICIES

ACKNOWLEDGEMENTS

It's scientific fact that you cannot do a PhD without supervisors. Therefore I must extend my thanks to the following. Firstly Joanna Wardlaw whose unwavering patience, never ending ideas, work rate and infinite back catalogue of scientific knowledge cannot be matched, secondly, Colin Smith for his straight talking, the occasional reality check and friendly ear and finally Cathie Sudlow for her editorial skills on various manuscripts and her constant praise and encouragement.

Ultimately this project was collaboration; therefore I also express my gratitude to my additional advisors in Glasgow. Firstly, to Anna Dominiczak for allowing the collaboration to happen, providing laboratory facilities and editing manuscripts. Secondly to Martin McBride thank you for your precious time, your enthusiasm and restoring some self belief, thirdly, to Delyth Graham for providing tissue and data for the project and finally to Wendy Crawford and John McClure – molecular technician and statistician extraordinaire! You are both indispensable. Thank you to all of the BHF for making me laugh out loud everyday, providing baked goods was the least I could do in return.

In Edinburgh I would like to thank Ian Croy, Tommy Dingwall and Frances Carnie for their technical histopathology guidance and David Wiles from Media Cybernetics who gave up days at a time to train me on Image analysis software.

To all the PhD students, post docs and technicians at 1 George Square – thanks for being my 'surrogate lab'. It's hard flying solo and I am eternally grateful for all the time people spent listening (or pretending to listen) to my whinging. I hope I managed to give something back to the group. I must especially thank Jim McCulloch for his advice on the first systematic review and providing me with a base – I had no right to be there, but you understood that I needed it.

To all the PhD students, post docs and admin staff at DCN. Thank you for putting up with me and being my conference chums. In particular Kirsten Shuler who relentlessly chased all my expenses and kept me right in all matters admin. You have the patience of a saint.

I would like to thank the Medical Research Council, the Newby Fund and the British Neuropathological Society for supporting me financially.

Providing emotional support throughout a PhD is a full time job and I thank Laura, Phil, Hugo, Michelle, the F63 crowd and my brother David amongst others, for distracting me

from science in ways only they know how. I also thank my parents and my boyfriend's parents who, whilst not entirely understanding my PhD, always expressed their pride in me.

Finally I thank my partner in crime - Duncan, my coffee snob, best friend and statistics guru. Your previous PhD endeavours taught me well. You never know we might be able to afford that 'hypothetical' wedding one day!

DECLARATION

I declare that this thesis comprises my own original work and has not been submitted previously for any degree. The work comprising this thesis was carried out by me, except where acknowledged in the text, therefore ‘we’ within the text is indicative of me. All sources of data and information have been specifically referenced.

Emma Louise Bailey 2011

PUBLICATIONS

Published Papers

Bailey EL, McCulloch J, Sudlow C, Wardlaw JM (2009) Potential animal models of lacunar stroke. A systematic review. *Stroke* 40:e451-e458

Bailey EL, Wardlaw J, Graham D, Dominiczak A, Sudlow C, Smith C (2010) Cerebral small vessel endothelial structural changes predate hypertension in Stroke Prone Spontaneously Hypertensive Rats: a blinded, controlled immunohistochemical study of 5-21 week old rats. *Journal of Neuropathology and Applied Neurobiology. In Press.*

Bailey EL, Smith C, Sudlow C, Wardlaw J (2011). Is the spontaneously hypertensive stroke prone rat a pertinent model of subcortical ischaemic stroke? A systematic review. *International Journal of Stroke. In Press.*

Manuscripts accepted for publication

Bailey EL, Smith C, Sudlow C, Wardlaw J (2012). Pathology of lacunar ischaemic stroke in humans – A systematic review. *Brain Pathology.*

Manuscripts in preparation

E.L.Bailey, M.W.McBride, W.Crawford, J.D.McClure, D.Graham, A.F. Dominiczak, C.L.M. Sudlow, C.Smith and J.M.Wardlaw. "Discrete protein expression defects in several key pathways explain the susceptibility to cerebral small vessel disease in a model of human cerebral small vessel disease."

E.L.Bailey, M.W.McBride, W.Crawford, J.D.McClure, D.Graham, A.F. Dominiczak, C.L.M. Sudlow, C.Smith and J.M.Wardlaw. "Influence of sodium chloride on gene expression in the brain of spontaneously hypertensive stroke-prone and Wistar Kyoto rats

LIST OF FIGURES

CHAPTER 1

CHAPTER 2

CHAPTER 3

CHAPTER 4

CHAPTER 5

CHAPTER 6

CHAPTER 7

CHAPTER 8

CHAPTER 9

LIST OF TABLES

CHAPTER 1

No tables

CHAPTER 2

CHAPTER 3

CHAPTER 4

No tables

CHAPTER 5

CHAPTER 6

CHAPTER 7

CHAPTER 8

ABSTRACT

Lacunar strokes account for approximately a quarter of all ischaemic strokes and traditionally are thought to result from occlusion of a small deep perforating arteriole in the brain. Lacunar infarcts can be up to 2cm in diameter and are found in deep brain structures such as the thalamus and internal capsule. Despite their prevalence and specific accompanying clinical syndromes, the cause of lacunar stroke and its associated vascular pathology remain unclear.

Many hypotheses as to the cause exist, which fall broadly into two categories; firstly, a direct occlusion via emboli or thrombus usually from a cardiac or large artery source, microatheroma (intrinsic lenticulostriate occlusion) or macroatheroma (parent artery occlusion) all operating primarily via ischaemia. Secondly, there could be an indirect occlusion resulting from vasospasm, endothelial dysfunction or other forms of endovascular damage (e.g. inflammation). Therefore the question of whether the resulting lesions are truly "ischaemic" or actually arise secondary to an alternative process is still under debate.

To clarify the chain of pathological events ultimately resulting in lacunar stroke, in this thesis I firstly undertook a systematic assessment of human lacunar stroke pathology literature to determine the information currently available and the quality of these studies (including terminology). The majority of these studies were performed in patients who had died long after their stroke making it difficult to determine the early changes, and there were few patients with a clinically verified lacunar syndrome.

Therefore I adopted alternative approaches. In this thesis, I systematically looked for all potential experimental models of lacunar stroke and identified what appears at present to be the most pertinent - the spontaneous pathology of the stroke-prone spontaneously hypertensive rat (SHRSP). However, the cerebral pathology described in this model to date is biased towards end stage pathology, with little information concerning the microvasculature (as opposed to the brain parenchyma) and confounding by use of salt to exacerbate pathology.

Therefore, the aim of the experimental work in this thesis was to assess pathological changes within the cerebral vasculature and brain parenchyma of the SHRSP across a variety of ages (particularly young pre-hypertensive animals) and to look at the effects of salt loading on both the SHRSP and its parent strain (the Wistar Kyoto rat - WKY).

Three related studies (qualitative and quantitative histology, immunohistochemistry and a microarray study of gene expression confirmed by quantitative PCR), revealed that the presence of inflammation (via significant changes in gene expression in the acute phase response pathway and increased immunostaining of activated microglia and astrocytes) plus alterations in vascular tone regulation, (via genetic alteration of the nitric oxide signaling pathway probably secondary to abnormal oxidative state), impaired structural integrity of the blood brain barrier (histological evidence of endothelial dysfunction and significantly decreased Claudin-5 staining) and reduced plasma oncotic potential (reduced albumin gene expression) are all present in the native SHRSP at 5 weeks of age, i.e. well before the onset of hypertension and without exposure to high levels of salt. We also confirmed previous findings of vessel remodelling at older ages likely as a secondary response to hypertension (thickened arteriolar smooth muscle, increased smooth muscle actin immunostaining). Furthermore, we found not only that salt exacerbated the changes see in the SHRSP at 21 weeks, but also that the control animals (WKY) exposed to a high salt intake developed features of cerebral microvascular pathology independently of hypertension (e.g. white matter vacuolation and significant changes in myelin basic protein expression).

In conclusion, via the assessment of the most pertinent experimental model of lacunar stroke currently available, this thesis has provided two very important pieces of evidence: firstly that cerebral small vessel disease is primarily caused by a non-ischaemic mechanism and that any thrombotic vessel lesions occur as secondary end stage pathology; secondly that these features are not simply the consequence of exposure to raised blood pressure but occur secondary to abnormal endothelial integrity, inflammation, abnormal oxidative pathways influencing regulation of vascular tone and low plasma oncotic pressure. Patients with an innate susceptibility to increased blood brain barrier permeability and/or chronic inflammation could therefore have a higher risk of developing small vessel disease pathology and ultimately lacunar stroke and other features of small vessel disease. Research, addressing whether lacunar stroke patients should be treated differently to those with atherothromboembolic stroke is urgently needed.

LIST OF ABBREVIATIONS

(Abbreviations within figures are spelt out in the accompanying figure legend, all gene names are fully spelt out in chapter 8 before being subsequently abbreviated)

ABC = Avidin Biotin Complex

ACA = Anterior Cerebral Artery

ACTB = Beta Actin

AD = Alzheimers Disease

ADC = Apparent Diffusion Coefficient

ALB = Albumin

ANOVA = Analysis of Variance

BA = Basilar Artery

BBB = Blood Brain Barrier

CADASIL = Cerebral Autosomal Dominant Arteriopathy with Subcortical Infarcts and Leukoencephalopathy

CAMARADES = Collaborative Approach to Meta Analysis and Review of Animal Data from Experimental Stroke.

CBF = Cerebral Blood Flow

cDNA = Complementary DNA

CI = Confidence Intervals

COL I = Collagen type 1

COL IV = Collagen type 4

COL4A1 = Collagen Type IV alpha 1 subunit.

cRNA = complementary RNA

CSF = Cerebrospinal Fluid

CT (value) = Cycle Threshold

CT = Computerised Tomography

Cv = Coefficient of Variance

DAB = 3.3'-diaminobenzidine

E1 = Expression 1

E1BC = Expression 1 Bead Chip

EPVS = Enlarged Perivascular Spaces

ET-1 = Endothelin-1

FDR = False Discovery Rate

FLAIR = Fluid Attenuation Inversion Recovery

FU = Fluorescence Units

GFAP = Glial Fibrillary Acidic Protein

GLM = General Linear Model

H&E = Hematoxylin and Eosin

HCB = Humidity Control Buffer

HRP = Horse Radish Peroxidase

HyB = Hybridisation Buffer

Iba-1 = Ionised calcuim Binding Adaptor molecule 1

ICA = Internal Carotid Artery

ICAM1 = Inter-cellular Adhesion Molecule 1

ICP = Intracranial Pressure

IgG = Immunogloblin G

IL-6 = Interleukin 6

IPA = Ingenuity Pathway Analysis

IQR = Interquartile Range

JPD = Japanese Diet

LACI = Lacunar Infarct

LCM = Laser Capture Microdissection

LSA = Lenticulostriate Artery

MAP = Mean Arterial Pressure

MBP = Myelin Basic Protein

MCA = Middle Cerebral Artery

MCAO = Middle Cerebral Artery Occlusion

MeSH = Medical Subject Headings

MMP9 = Matrix Metallopeptidase 9

MOOSE = Meta-analysis Of Observational Studies in Epidemiology

MRI = Magnetic Resonance Imaging

mRNA = messenger RNA

NaCl = Sodium Chloride

NS – No Significance

OCT = Optimal Cutting Temperature compound

OSCP = Oxford Stroke Classification Project

PACI = Partial Anterior Circulation Infarct

PBS = Physiological Buffered Saline

PCA = Posterior Cerebral Artery

PCA = Principle Components Analysis

POCI = Posterior Circulation Infarct

qRT-PCR = Quantitative Real Time Polymerase Chain Reaction

RIN = RNA Integrity Number

RNA = Ribonucleic Acid

RP = Rank Product

rRNA = Ribosomal RNA

RQ = Relative Quantity

SEM = Standard Error of the Mean

SHR = Spontaneously Hypertensive Rat

SHRSP = Spontaneously Hypertensive Stroke Prone Rat

SMA = Smooth Muscle Actin

SNP = Single Nucleotide Polymorphism

STARD = Standards for the Reporting of Diagnostic Accuracy studies

STROBE = Strengthening the Reporting of Observational studies in Epidemiology

SVD = (cerebral) Small Vessel Disease

TACI = Total Anterior Circulation Infarct

TF = Tissue Factor

tPA = Tissue Plasminogen Activator

TRIS-EDTA = Trisaminomethane-Ethylenediaminetetraacetic Acid

UTP = Uridine Trisphosphate

UTR = Untranslated Region

Wk = Weeks

WKY = Wistar Kyoto Rat

WML = White Matter Lesions

SECTION 1) GENERAL INTRODUCTION AND SYSTEMATIC REVIEWS

CHAPTER 1 :GENERAL INTRODUCTION

1.1 Stroke – why is it important?

Stroke is defined as "a clinical syndrome characterized by an acute loss of focal cerebral function with symptoms lasting over 24 hours"(Warlow et al. 2008e). Depending on the region of the brain affected, a stroke may cause paralysis, speech impairment, loss of memory and reasoning ability, coma, or even death (www.who.int).

Stroke is extremely common – according to the UK Stroke Association every 5 minutes someone in the UK has a stroke (www.stroke.org.uk), which equates to approximately 150,000 strokes a year. The overall incidence of stroke has declined slightly in developed countries with estimates of incidence of 3-38% over the past 40 years(Feigin et al. 2003), however the majority of the decline tends to be in younger patients (aged 35-64)(Thorvaldsen et al. 1997) and does not include all subtypes – the incidence of subarachnoid haemorrhagic has not altered in the past 30 years(Rothwell et al. 2004). The crude annual incidence rate of all strokes (including first-ever-in-a-lifetime and recurrent strokes of all subtypes) in a Scottish population from the most recent estimation is approximately 2.8 per 1000 per year(Syme et al. 2005).

1.1.1 Disability and recurrence

Worldwide, stroke is the third leading cause of death and the leading cause of severe disability (www.who.int). Over 250,000 people in the UK live with disabilities caused by stroke (www.stroke.org.uk). A statistical model in 2003 predicted that for every patient who experiences a stroke, the cost to the NHS in the UK is £15,000 over 5 years and when informal care costs are included, the amount increases to £29,000(Youman et al. 2003).

1.1.2 What constitutes a stroke?

There are two principle types of stroke – ischaemic and haemorrhagic.

Ischaemic stroke accounts for over 80% of all strokes, whilst haemorrhagic stroke, although accounting for less than 20% of all strokes causes up to 30% of deaths due to its more severe nature(Lawlor et al. 2002;Rothwell et al. 2004). Haemorrhagic stroke results from the

rupture of a blood vessel, whereas ischaemic stroke is attributed to a blockage in the blood supply to the brain, usually via an artery becoming occluded, although veins can also be blocked. Numerous causes of these blockages are thought to exist, e.g. thrombosis, embolism and intrinsic disease of the small vessel of the brain(Warlow et al. 2008e).

1.2 Anatomy of stroke

1.2.1 The cerebral blood supply

The brain receives blood from two main sources: the internal carotid arteries and the vertebral arteries(Warlow et al. 2008d). The internal carotid arteries (ICA) branch inside the skull to form the anterior and middle cerebral arteries (ACA and MCA respectively), which supply the forebrain, whilst the right and left vertebral arteries join at the pons to form the basilar artery (BA)(Purves et al. 2007). The BA divides into the posterior cerebral arteries (PCA), which supply the occipital lobes and the thalamus. Communicating arteries join the internal carotids, the PCA's and the ACA to form the circle of Willis - an arterial ring at the base of the brain (figure 1.1).

The arteries of the anterior circulation (the ACA and MCA and PCA) are the origin for numerous branches that supply the cortical tissue and others, which penetrate the basal surface of the brain, supplying subcortical brain structures like the thalamus, internal capsule and basal ganglia(Purves et al. 2007).

The lenticulostriate arteries (LSA's), which can branch from the ICA, PCA, BA and MCA in particular, are prominent penetrating arterioles(Warlow et al. 2008d). The perforating arteries and arterioles within deep brain structures control the exposure of the brain to changes in vascular reactivity and blood flow. They are essentially, 'end arteries' and do not have a collateral blood supply like their cortical equivalents. Cortical pial vessels anastomose with each other enabling any interruptions in blood flow to be managed more effectively(Warlow et al. 2008d).

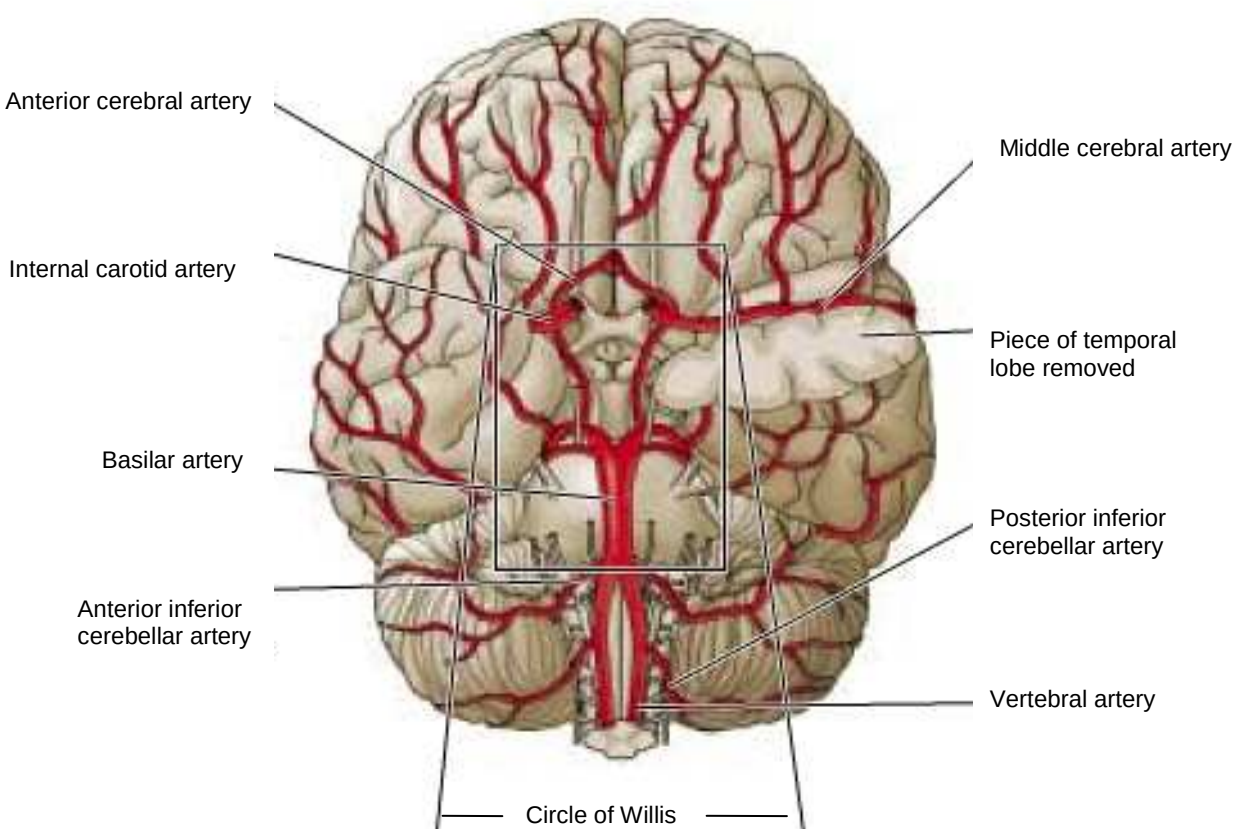

Figure 1.1 The blood supply to the brain as seen from the inferior side.

Figure adapted from 'Neuroscience' chapter 1. Purves et al. 4th Edition 2007.

1.2.2 Autoregulation

Cerebral blood flow (CBF) needs to be tightly controlled in order to meet the metabolic needs of the brain. Maintenance of CBF depends on maintaining a balance between intracranial pressure (ICP) and mean arterial pressure (MAP), known as autoregulation(Warlow et al. 2008a). The cerebral blood vessels (in particular arterioles) are able to regulate the flow of blood through them by altering their diameters and subsequently maintain intracranial pressure within an optimal range to counteract both an increase in ICP, which can lead to edema and brain enlargement(Eames et al. 2002) (Dawson et al. 2003), as well as a decrease in pressure, which can result in ischaemic damage(Walters FJM 1998). Autoregulation is still a relatively poorly understood mechanism; however metabolic,

myogenic and neurogenic factors are all said to be involved. Neural (neurogenic) activity is by far the largest determinant of CBF in the brain. In addition to this however, the diameters of the proximal vessels are thought to be mostly under myogenic control(Ursino and Gianessi 2010) responding to intraluminal pressure fluctuations. If the intraluminal pressure increases, smooth muscle fibres within the vessel walls stretch to a point where reflex contraction of reflex fibres results in the constriction of the vessel diameter(Eames et al. 2002;Dawson et al. 2003). Myogenic mechanisms also include endothelial dependent dilatation and constriction controlled by the L-arginine – nitric oxide – cGMP pathway(Schlaich et al. 2004). Vasomotion of the small arteries and arterioles is influenced more by metabolic stimulation. Fluctuations in extracellular pH, levels of carbon dioxide, adenosine and glycolytic intermediates can trigger very rapid changes in flow (~1 second after neuronal excitation) in the microvasculature(Wagerle et al. 1983;Eames et al. 2002).

1.3 The effect of ischaemia on different vascular territories determines the clinical classification of stroke subtypes.

If a major cerebral artery such as the MCA or ACA is occluded, the area of resulting ischaemic damage is widespread and these infarcts are often referred to as 'hemispheric', 'territorial'(Lee et al. 2004) or in some classifications, such as the Oxford Community Stroke Project (OSCP)(Bamford et al. 1991), which classifies clinical stroke subtypes based on their vascular territory and site of occlusion, as total anterior circulation infarcts (TACI) (see figure 1.2). Patients suffering this type of proximal MCA occlusion (~20% of the ischaemic stroke population); incur the most severe levels of disability, as ischaemia has occurred in both the deep and superficial territories of the artery. Multiple motor, cognitive and behavioural deficits result(Bamford et al. 1991). The underlying cause is mostly atherothrombolic, embolic or closely associated with carotid stenosis(Warlow et al. 2008d). Therapeutic interventions are generally geared towards this subtype e.g. the use of antiplatelet agents and thrombolysis(Feigin et al. 2003).

Occlusion of a second order branch of the MCA or other parent cerebral artery can also result in a large area of ischaemic brain damage and severe disability, although collateral flow from anastomoses within the cortical vasculature can go some way to abating the local loss of blood flow (see figure 1.2)(Bamford et al. 1991;Ng et al. 2007). This type of stroke is classified as a partial anterior circulation infarct (PACI) by the OSCP(Bamford et al. 1991). Patients with PACI present with characteristic cortical deficits, such as, aphasia, neglect or

hemianopia. PACI occur in approximately 40% of all strokes and affect only the superficial territory of the parent artery or the basal ganglia, but not both. Atrial fibrillation and atherothromboembolism are considered more as risk factors for cortical stroke (both TACI and PACI) over the other subtypes(Dulli et al. 1998;Jackson and Sudlow 2005a). Cortical PACI have an approximate survival rate at 4 weeks of 77%(Milan et al. 1991).

Striatocapsular infarcts (another type of PACI) result from either a transient occlusion of the MCA or a longer occlusion of the same artery, but in a patient with a good cortical collateral blood supply. The resulting infarction can encompass several structures of the basal ganglia (see figure 1.2)(Nishida et al. 2000). The OSCP classes this type of infarct as either a TACI or a PACI depending on the associated clinical symptoms(Bamford et al. 1991).

Lacunar infarcts (known as LACI by the OSCP) by contrast, are restricted areas of parenchymal damage due to the occlusion of a single perforating vessel (see figure 1.2). It is this subtype of stroke, which forms the focus of this thesis. Lacunar lesions rarely reach over 2cm in diameter in any direction(Lammie 2002a). 25% of ischaemic strokes are thought to be lacunar and infarcts are thought to be caused by intrinsic disease of a single basal perforating artery, rather than atherosclerosis of a parent artery(Bamford et al. 1987;Bamford et al. 1991). It is thought that a restriction in blood flow to second / third order branches of perforating arterioles can cause small lacunar lesions usually under 1cm in diameter and clinically silent (see figure 1.2) or leukoaraiosis, both of which can ultimately contribute to cognitive decline(Feekes et al. 2005). The causative factors of lacunar stroke are discussed later in this introduction.

The final stroke subtype defined in the OSCP concerns posterior circulation infarcts (POCI). These infarcts are clearly associated with the vertebrobasilar arterial territory (cerebellum, brainstem and occipital lobes) (see figure.1.1). POCI account for approximately 15% of ischaemic strokes and result from embolism (either cardiac or artery-artery in situ thrombosis) or hemodynamic disruption(Bamford et al. 1991;Piechowski-Józwiak and Bogousslavsky 2008). They present with a wide variety of symptoms and episodes are often staggered and more protracted than anterior circulation strokes. Mortality rates vary from 20-60%, but patients presenting with bilateral vertebral artery occlusion fare worse, with a mortality rate of ~90%(Piechowski-Józwiak and Bogousslavsky 2008).

1.4 Lacunar Stroke

1.4.1 Clinical Syndromes

Lacunar stroke is thought to cause one of 4 so called classic lacunar syndromes;

1.4.1.1 Pure Motor Stroke

The most common amongst symptomatic lacunar stroke patients accounting for up to 2/3rds of admissions(Warlow et al. 2008d). It is marked by hemiparesis or hemiplegia that typically affects the face, arm, or leg of one side.

1.4.1.2 Pure Sensory Stroke

The opposite of pure motor stroke. Patients with pure sensory stroke present with transient or persistent numbness and mild sensory loss on one side of the body. Only 6% patients usually present with pure sensory stroke and often have thalamic lesions(Warlow et al. 2008d).

1.4.1.3 Sensorimotor Stroke

A combined sensory and motor deficit. Estimates of prevalence for sensorimotor stroke range from 20-38% of symptomatic patients. On magnetic resonance imaging (MRI), lesions that cause a sensorimotor syndrome are larger than lesions that cause other lacunar syndromes and are often located in the internal capsule(Papamitsakis 2007;Warlow et al. 2008d).

1.4.1.4 Ataxic Hemiparesis & Dysarthria Clumsy Hand Syndrome

Approximately 20% of symptomatic lacunar stroke patients present with weakness of the lower limb (especially the ankle and toes), or dysmetria of the arm and leg on the same side(Bejot et al. 2008;Warlow et al. 2008d).

Aside from these recognised syndromes however, there are up 10% of lacunar stroke patients who present with atypical symptoms. Dysarthria, facial paresis and hemiballismus(Arboix et al. 2006) are just three of several atypical presentations caused by a verified lacunar infarct(Ghandehari and Izadi 2009).

1.4.2 Prognosis

The acute prognosis (e.g. 30 days post stroke) of lacunar stroke is the best of all the stroke subtypes, with some studies reporting a mortality rate of as little as 1%(Bamford et al. 1987). The long term prognosis for lacunar stroke however, is not so favourable and is similar to that of larger anterior circulation strokes(Jackson and Sudlow 2005b). There is also the risk of recurrent stroke. For all stroke subtypes, there is approximately a 10% chance of a recurrent stroke and the recurrent stroke tends to be the same type as the initial stroke, so patients who have had a lacunar stroke are more likely to have a recurrent lacunar stroke than a large artery stroke and vice versa(Jackson and Sudlow 2005b).

1.4.3 Risk Factors

Smoking, obesity, high salt intake and hypercholesterolemia are all risk factors for stroke in general. High blood pressure is also a significant risk factor for stroke in general and for the prevalence of WMLs on MRI(de Leeuw et al. 2002). Large artery stroke has a more defined set of risk factors including atrial fibrillation, atherothromboembolism and carotid stenosis – all shown to be more commonly associated with large artery stroke(Jackson and Sudlow 2005a). There is no evidence however, that these risk factors are more associated with lacunar stroke than cortical stroke(Jackson et al. 2010) and specific risk factors for lacunar stroke are less well defined, but are likely to be different(Jackson et al. 2010) due to the differing clinical symptoms and specific vascular territories involved. There is evidence that lacunar arteriopathy may differ from atherosclerotic arterial disease(Wardlaw et al. 2009), ischaemic heart disease and carotid stenosis – both atherosclerotic disorders have a lower prevalence in lacunar stroke when compared to non-lacunar stroke(Jackson et al. 2010).

1.4.4 Brain and vascular territory

Recognition of a small vessel (or lacunar) subtype of stroke was first documented in 1901 by Marie and Ferrand(Marie P 1901;Ferrand J 1902). Via pathological examination of human autopsy specimens, they described the appearance of a typical lacunar cavity as a “healed infarct resulting from rupture or obliteration of a perforating artery and/or its branches due to local atherosclerosis.” Topographical distribution of lacunar lesions encompassed the lenticular nucleus, thalamus, internal capsule, caudate nucleus, pons, centrum semiovale and finally the corpus callosum(Ferrand J 1902). These brain areas are supplied by the LSA’s

(i.e. perforating arteries), which branch off at approximately a 90° angle from the MCA, ACA, ICA or PCA. See figure 1.3 for a diagrammatical representation of a lacunar stroke relative to the vascular territory within the brain. The majority of lacunar strokes occur within the anterior cerebral circulation(Warlow et al. 2008f) and are associated with the perforating arteries and/or arterioles of the MCA and ACA arteries. The precise nature of the vascular territory in which lacunar lesions are found, limits their size and explains why lacunar strokes are rarely fatal and more often than not silent on imaging(Chen et al. 2009). However, even though lacunar strokes are small, if situated in a region of high connectivity within the brain, they can cause severe disability.

The exact vascular territory of lacunar infarcts is still under debate with 2/3rds said to be anatomically related to the $1^{st}/2^{nd}$ order branches of penetrating arterioles in the basal ganglia(Challa et al. 1990). A more general picture however, places over 90% of lacunar infarcts as resulting from occlusion or stenosis of the $2^{nd}/3^{rd}$ order branches from the major penetrators(Moody et al. 2004). Others, describe infarcts of a pertinent size and territory as a consequence of occluding 3^{rd} order arterioles(Feekes et al. 2005). In general the volume of an individual lacunar infarct is dependent on the site of occlusion - the more proximal to the parent artery the larger the infarct(Warlow et al. 2008d). These differences however, may reflect sampling bias in small studies, as pathology studies in lacunar stroke generally are on few patients. This will be discussed further in chapter 2 of this thesis.

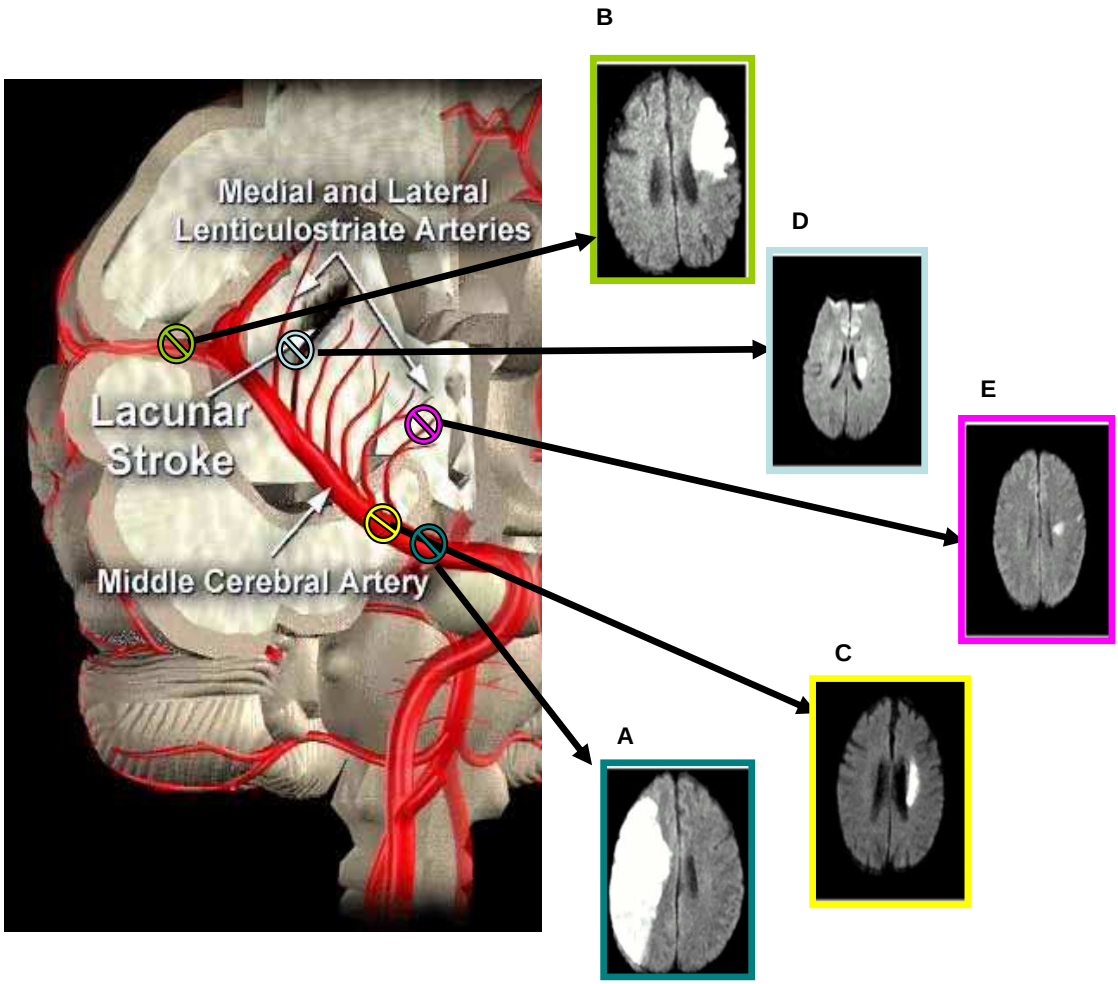

Figure 1.2. The effect of occluding different arterial territories within the anterior circulation of the brain.

A = occlusion of the main branch of the MCA. This results in a 'hemispheric' infarct and results in widespread ischaemic damage. B = occlusion of a secondary branch (M2) of the MCA. This results in a more contained area of ischaemic damage but still affects roughly 1/3 of the hemisphere. C = occlusion of the MCA not affecting cortical tissue due to good collateral flow and/or a transient episode. These are known as striatocapsular infarcts. D = occlusion of one LSA or similar sized vessel. These are lacunar infarcts. E = occlusion of the second / third order branches of LSA's. This type of occlusion can result in small often asymptomatic lesions on imaging. All images captured by diffusion weighted MRI. Figure compromised of figures adapted from Lee et al 2004. JNNP: 75: 727-732 and www.thestrokefoundation.com.

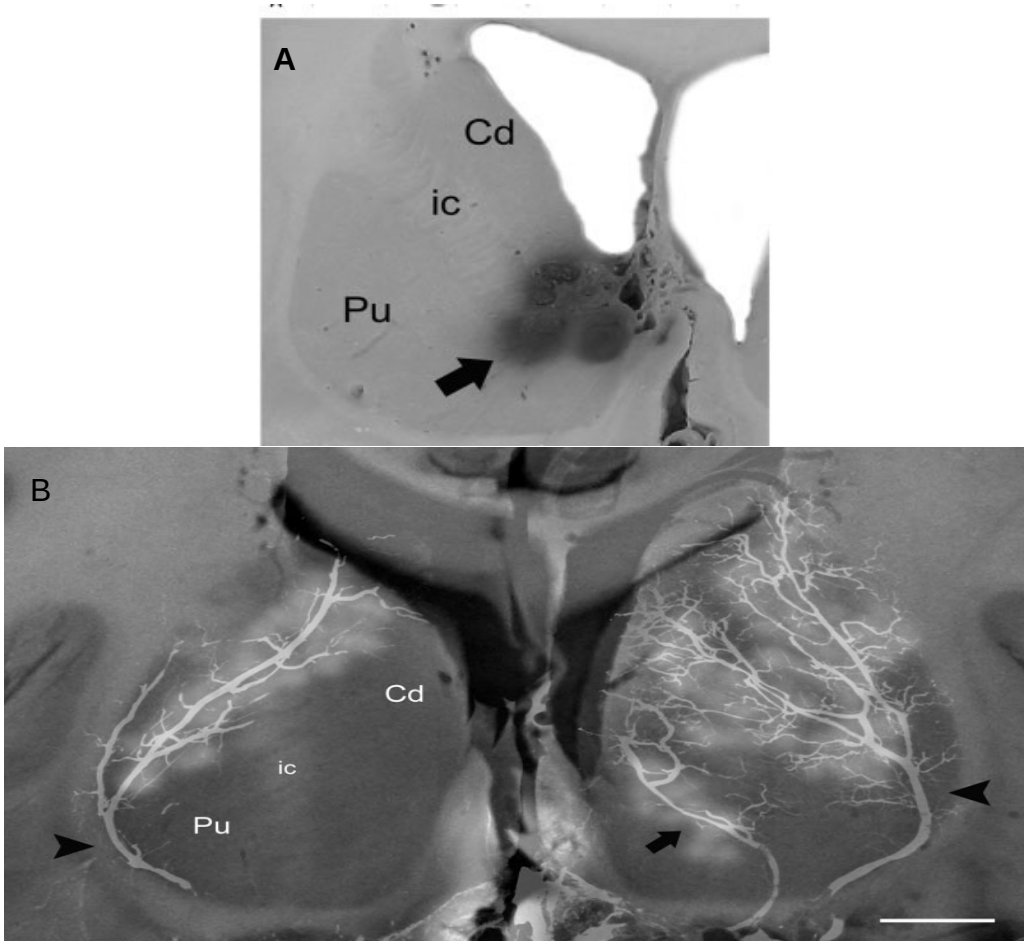

Figure 1.3. Images of lacunar lesions and the associated vascular territories.

A) Lacunar lesions within the territory of the basal ganglia (arrow). B) Radiographs / fluorescent dye overlap of injected medial and lateral LSA's (arrowheads) and recurrent artery of Heubner (arrow) in the human basal ganglia, Cd = caudate nucleus; ic = internal capsule; Pu = putamen. Line bar _ 1cm. Figures adapted from Feekes et al 2005. Annals of Neurology 58: 18-30.

1.5 The appearance of acute lacunar lesions on imaging (see figure 1.4).

Detection of lacunar lesions on imaging is based on the development of intracellular or extracellular edema within the damaged region, which appears hyperintense on some MRI sequences or low attenuation on CT(Warlow et al. 2008c). Diffusion MRI (DWI) is particularly sensitive to acute ischaemic change and so is good for detecting small lesions like lacunar ischaemic stroke that may be hard to see on CT. MRI generally shows more small lesions than CT. Overall approximately only 50% of lacunar infarcts at most are picked up on CT(Wardlaw et al. 2001). CT scans therefore underestimate the burden of

small deep infarcts compared to MRI(Longstreth, Jr. et al. 1998). CT is good however, for displaying old lesions(Warlow et al. 2008c).

Lacunar lesions can be missed on imaging due to having wide interslice gaps on both, CT and MRI, partial volume averaging on CT and limitations in contrast and spatial resolution. Furthermore, up to a fifth of lacunar infarcts are misdiagnosed clinically, as cortical infarcts(Potter et al. 2010a). Variation in imaging sequences used by different groups and variation within the terminology used to describe lacunar lesions and overlapping small vessel disease entities, have also contributed to this potential underestimation of lacunar lesion prevalence.

In addition, clinically imaging the small perforating arteries responsible for lacunar lesions can be extremely difficult, as scanners do not possess the resolution to display them reliably(Wardlaw 2005). They can be seen on high resolution intra arterial angiography and some are visible on high field MRI (7T), but the resolution is limited. Hyperintensities on T2 weighted images are often required to distinguish small deep infarcts from dilated perivascular spaces or other manifestations of SVD(Bokura et al. 1998). Trying to image the small vessels is therefore difficult, but trying to pinpoint exactly which vessel has caused the symptomatic lesion is even more so. One study found only 9/80 symptomatic lacunar stroke patients had evidence of an abnormal or occluded perforating artery in a pertinent brain region(Wardlaw et al. 2001).

1.5.1 Cavitation of lacunar lesions

Aside from imaging parameters, another reason for underestimating the burden of lacunar lesions is the incidence of cavitation. Lacunar lesions are often defined as ‘cerebrospinal fluid filled cavities’ on imaging, however evidence is emerging that the majority of lacunar lesions do not actually cavitate to form a true ‘lacune’ and some only partially go through this process (see figure 1.4). Potter et al(Potter et al. 2010b) discovered that only approximately 20% of symptomatic lacunar lesions definitely go on to cavitate on MRI, whereas the majority persisted as lesions that looked similar to WMLs (median 227 days after stroke onset). Age, stroke severity, hypertension and other imaging features (WMLs, EPVS etc) were not associated with cavitation(Potter et al. 2010b).

Due to this observation many lacunar lesions in patients presenting with a lacunar syndrome may be missed due to delays in obtaining suitable imaging therefore studies which count only cavitated lacunes, may be seriously underestimating the incidence of lacunar lesions.

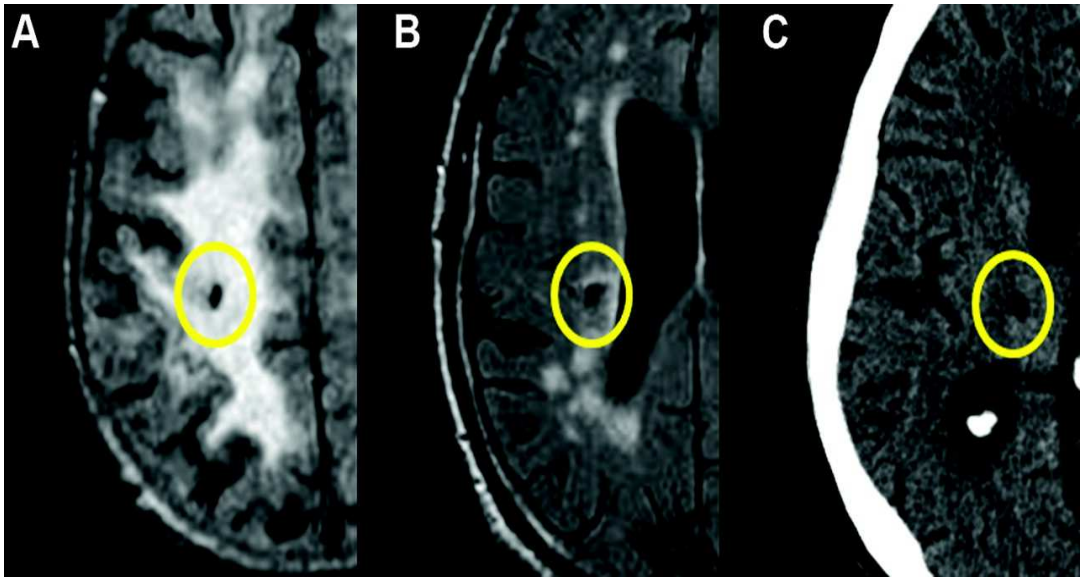

Figure 1.4. The appearance of cavitated and non cavitated lacunar lesions on imaging.

A) A definite cavitated lacunar lesion on fluid attenuation inversion recovery (FLAIR) MRI, in the centrum semiovale. B) A partially cavitated lacunar lesion in the centrum semiovale again on FLAIR MRI. C) A lacunar lesion in the thalamus on CT. Image taken from Potter et al. Stroke 2010:41:267-272.

1.6 The wider implications and features of disease in the small deep perforating arterioles

It is now more widely recognised that lacunar lesions may in fact be a single manifestation of a whole spectrum of pathology, clinical and imaging markers of a diffuse abnormality in the small deep vessels. These markers include WML, enlarged perivascular spaces (EPVS) and brain microbleeds.

For example, this cerebral small vessel disease (SVD) is thought to be a major cause of vascular dementia as well as lacunar stroke, with an incidence over 6 times that of any symptomatic stroke(Leary and Saver JL 2003). SVD generally refers to the pathological and radiological changes, along with clinical syndromes, associated with disease of the small perforating arteries supplying the subcortical areas of the brain. SVD is found mainly in the white matter and deep grey structures of the brain(Mohr 1982). It manifests as WMLs seen on MRI or computerised tomography (CT) plus lacunar stroke, enlarged perivascular spaces (EPVS) and microbleeds(Morris et al. 2009). Age alone is said to be a risk factor for SVD

with evidence of WML on MRI scans found in over 40% of people aged over 80(Bryan et al. 1997). There are currently several types of vascular pathology described in SVD, including intracranial atherosclerosis, in some cases small vessel atherosclerosis, and lipohyalinosis (concentric rings of thickening in the vessel wall caused by the build up of fatty hyaline material and often also referred to as hyaline arteriolosclerosis)(Lammie 2002a). Small vessel atherosclerosis appears to be related to hypertension with, in simple terms, the hypertension extending the distribution of atherosclerotic changes to small vessels. Most autopsy derived specimens will show old, or healed lipohyalinosis, however, occasionally a case will be examined which shows the acute phase of this process, with fibrinoid necrosis of the vessel wall(Lammie 2002a). The term fibrinoid necrosis is used to describe eosinophilic fibrin-like deposits, usually of degenerated collagen in arterial walls(Lammie 2002a).

1.7 General Pathophysiology

1.7.1 Parenchymal lesions

Imaging and pathological descriptions of lacunar lesions share similar features. According to the available literature, lacunar lesions pathologically, are usually 2 to 20 mm in diameter and are presumed to result from the occlusion of single, small, perforating arteries supplying the deep subcortical areas of the brain(Hughes et al. 1954;Fisher 1965). See figure 1.5 for the macroscopic pathological appearance of lacunar lesions. A pathological classification system for lacunes was proposed by Poirier & Derouesne(Poirier et al. 1985), which divided lacunar lesions into three types – type I, II and III. Lammie et al added a subclassification (type 1b lacunes)(Lammie et al. 1998) and more recently there have been calls to add a further type IV lacune. Further descriptions of the pathology of lacunar lesions are provided in chapter 2 of this thesis. Briefly however;

Type I(a) is an old small cavity containing brain fragments and small patent arterioles and/or capillaries(Poirier et al. 1985).

Type I(b) – ‘incomplete’ or ‘partially’ cavitated lacunar lesions(Lammie et al. 1998).

Type II - old small haemorrhages(Poirier et al. 1985).

Type III – dilated perivascular spaces (Virchow Robin spaces)(Derouesne and Poirier 1999)

Type IV – expanding lacunes. A more extreme dilatation of the perivascular space sometimes accompanied by an inflammatory reaction of the blood vessel, which results in fibrinoid

necrosis of the vessel wall. This type is rare and thought to be due to an impairment in the lymphatic drainage system within the brain(Homeyer et al. 1996).

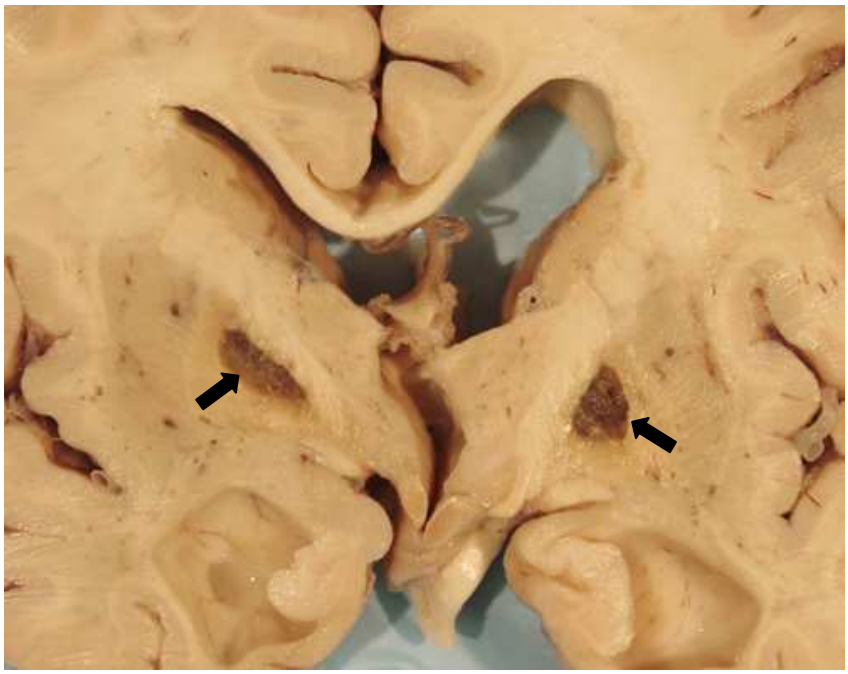

Figure 1.5.The macroscopic pathological appearance of type I lacunar infarcts (arrows) taken from a coronal brain slice.

This particular specimen has bilateral thalamic lacunes. Image courtesy of www.neuropathologyweb.org.

1.7.2 Vascular pathology

SVD has, for many years, been thought to be closely related to atherosclerosis, a disorder of large vessels which underlies cortical infarcts, and which has well defined risk factors including hypertension(Lammie 2002b). The assumption has been that atherosclerosis and SVD share common risk factors and are similar pathological processes. This association has its origins in the detailed studies of Fisher in the 1960s(Fisher 1965;Fisher 1968), in which lipohyalinosis, or "segmental arterial disorganisation" as he described it, was considered to be responsible for 46 of 68 lacunes examined(Fisher 1968) (see figure 1.6). In those vessels where no occlusive lesion was seen, embolus was assumed.

The relationship between lipohyalinosis and hypertension is uncertain and in this era of aggressive pharmacological intervention in the management of hypertension, lipohyalinotic lesions are still seen at autopsy, albeit less commonly(Lammie 2002b). The relationship between healed lipohyalinosis and intracerebral haemorrhage also remains uncertain and while aneurysmal dilatations are well described in healed lipohyalinosis, there is no evidence of subsequent increased incidence of rupture and haemorrhage.

Since Miller Fisher's research into lacunar stroke pathology in the 1960's, the treatment of hypertension has improved and Lammie(Lammie 2000) amongst others(Ogata 1999), proposes that lacunar strokes are nowadays more likely to result from decreases in local cerebral blood flow (see above section on autoregulation), plus small vessel stenosis, rather than occlusive lipohyalinosis caused by hypertension, because poorly controlled hypertension occurs less frequently, although hypertension is extremely common amongst stroke patients.

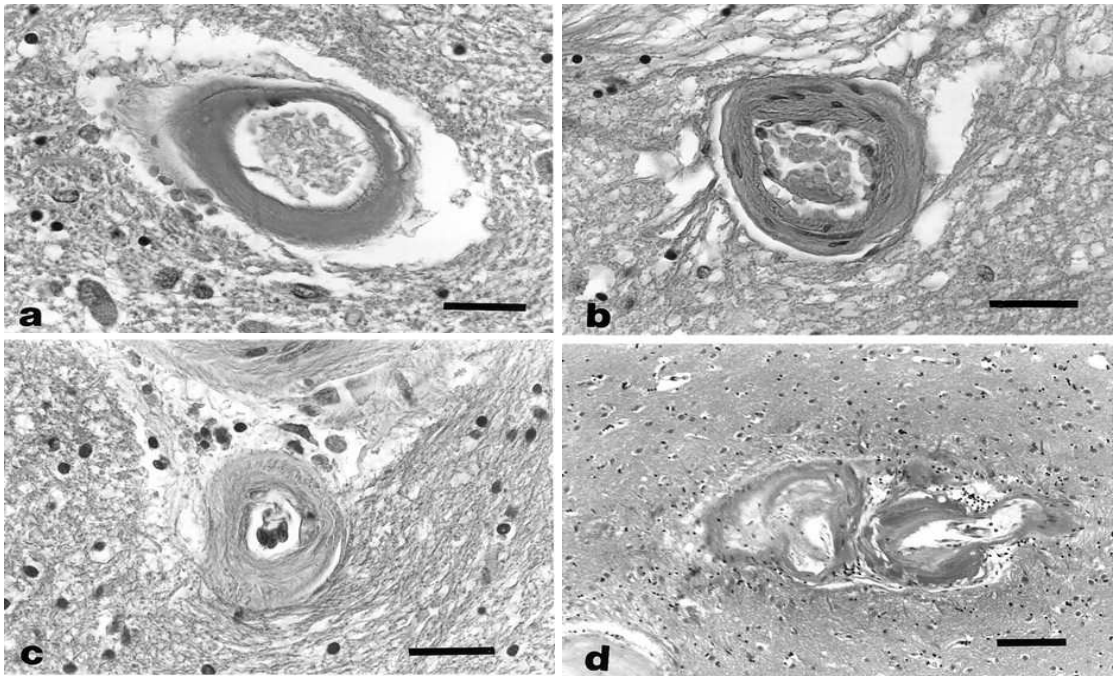

Figure 1.6. The progression of small vessel disease.

A) shows mild hyaline thickening of a small thalamic artery. B) is a similar sized vessel from the putamen with moderate concentric hyaline thickening. C) is a severely affected vessel again from the putamen this time with noticeable encroachment upon the lumen. D) represents the final stages of complex small vessel disease displaying an arterial lesion from the putamen. Scale bar = 40μm. Figure adapted from Lammie et al 1997. Stroke 28:2222-2229.

The above sections, briefly assessing the parenchymal and vascular lesions encountered in lacunar stroke, provide a background to this area of stroke research that is conventional, but still open to interpretation and therefore is not necessarily complete or correct. A more thorough review of human lacunar stroke pathology, the potential causative mechanisms and the evidence for them, will be given in chapter 2 of this thesis.

1.8 What causes lacunar stroke? Evidence for a distinct arteriopathy.

Although abnormalities in the small deep perforating, or lenticulostriate, arteries are often cited as the cause of lacunar stroke, how often other abnormalities affecting the small vessels might also lead to lacunar stroke, is unknown(Davis and Donnan 2004). Many hypotheses exist, including embolic or thrombotic occlusion usually from a cardiac or large artery source, microatheroma - consisting of intrinsic lenticulostriate occlusion, as well as parent artery occlusion also known as macroatheroma(Wardlaw 2005). Additionally vasospasm, endothelial dysfunction(Knottnerus ILH et al. 2009;Stevenson et al. 2010) or other forms of endovascular damage (e.g. inflammation) have also been implicated(Arboix and Marti-Vilalta 2004). See figure 1.7 for a diagrammatical representation of the range of possible causative mechanisms. Furthermore, it is not known if the resulting lesions are truly "ischaemic" or actually arise secondary to an alternative process, such as perivascular edema following blood-brain barrier (BBB) derangement and therefore endovascular leakage(Lammie et al. 1997;Lammie et al. 1998;Wardlaw et al. 2003).

Evidence in support of an embolic source is often conflicting(Futrell 2004;Norrving 2004;Jackson and Sudlow 2005a). While most will agree that emboli can cause lacunar lesions, the discovery of a clear embolic source in a lacunar stroke patient is rare. In a study of 10 patients, Chowdury et al could only attribute a potential embolic cause to a single patient suggesting that emboli are not a common cause of lacunar lesions(Chowdhury et al. 2004). Atrial fibrillation and carotid stenosis are also considered uncommon etiologies in lacunar stroke patients(Jackson et al. 2010). Macroatheroma in the large parent arteries is also unlikely to account for the majority of lacunar lesions, as Fisher found little evidence to suggest that the obstruction of the mouths of the parent artery by atherosclerosis was to blame(Fisher 1965) and there has been no evidence since to contradict this finding. Thrombosis of the penetrating vessels is often cited as a cause of lacunar lesions, however the thrombus directly responsible for the vessel occlusion has rarely been found(Fisher 1968). This may be because the vessels recanalized before death and so verifying this

mechanism at autopsy will always be difficult. Others have suggested that thrombus is a late stage event and that the primary cause of pathology is related to the integrity of the blood brain barrier (BBB)(Wardlaw 2005).

Evidence of endothelial dysfunction in human lacunar stroke has been present for many years, but has been overlooked until recently(Samuelsson et al. 1994;Wardlaw et al. 2008). Increased levels of markers representing endothelial dysfunction (e.g. Inter-cellular adhesion molecule 1 (ICAM1), Tissue Factor (TF) and homocysteine) have been found in lacunar stroke and leukoaraiosis patients independent of hypertension, diabetes and age(Hassan et al. 2004;Zylberstein et al. 2008). Most studies of endothelial function however, used normal age matched controls with no neurological disease present, or age and risk factor matched controls, but failed to compare them to other stroke subtypes. When compared with cortical stroke patients for example, there is little good evidence that endothelial dysfunction in lacunar stroke is more than just exposure to risk factors, but there are few relevant studies(Stevenson et al. 2010). More recently, a paper assessing generalized cerebral blood brain barrier (BBB) leak between mild cortical and lacunar stroke patients with MRI and intravenous gadolinium has been published(Wardlaw et al. 2008). Post stroke measurement demonstrated higher background BBB leakage in the cerebrospinal fluid and white matter in lacunar patients than cortical stroke controls(Wardlaw et al. 2008). Others have found increased BBB leak in patients with lacunar stroke and leukoaraiosis (but not versus cortical stroke controls) and in vascular dementia(Farrall and Wardlaw 2009;Topakian et al. 2010).

1.9 The problems of studying lacunar stroke pathology.

Pathological studies of human tissues have informed our understanding of SVD, even though they are limited by being a static, often late analysis of a dynamic process. Unfortunately, recognised risk factors and pathological descriptions from scarce and often old material do little to describe the underlying mechanisms of the vessel damage. In addition to the limiting factors described above, the added obstacles of trying to assess lacunar stroke pathology include the difficulty of dissecting subcortical small vessels, the unavailability of human tissue from autopsy - autopsy rates have declined over the past 40 years(Burton and Underwood 2007)- and post mortem material is often obtained late after the initial event.

Lacunar stroke is rarely a fatal condition meaning that any brain tissue recovered will display old vessel abnormalities, which will have partially or extensively healed and the likelihood of scanning a patient immediately pre and post infarct formation is as mentioned previously,

minute. Imaging techniques are becoming more sophisticated, but the available levels of resolution on MRI scans are still not enough to capture perforating vessels at the level of detail required. Consequently, animal models could be very valuable in this area.

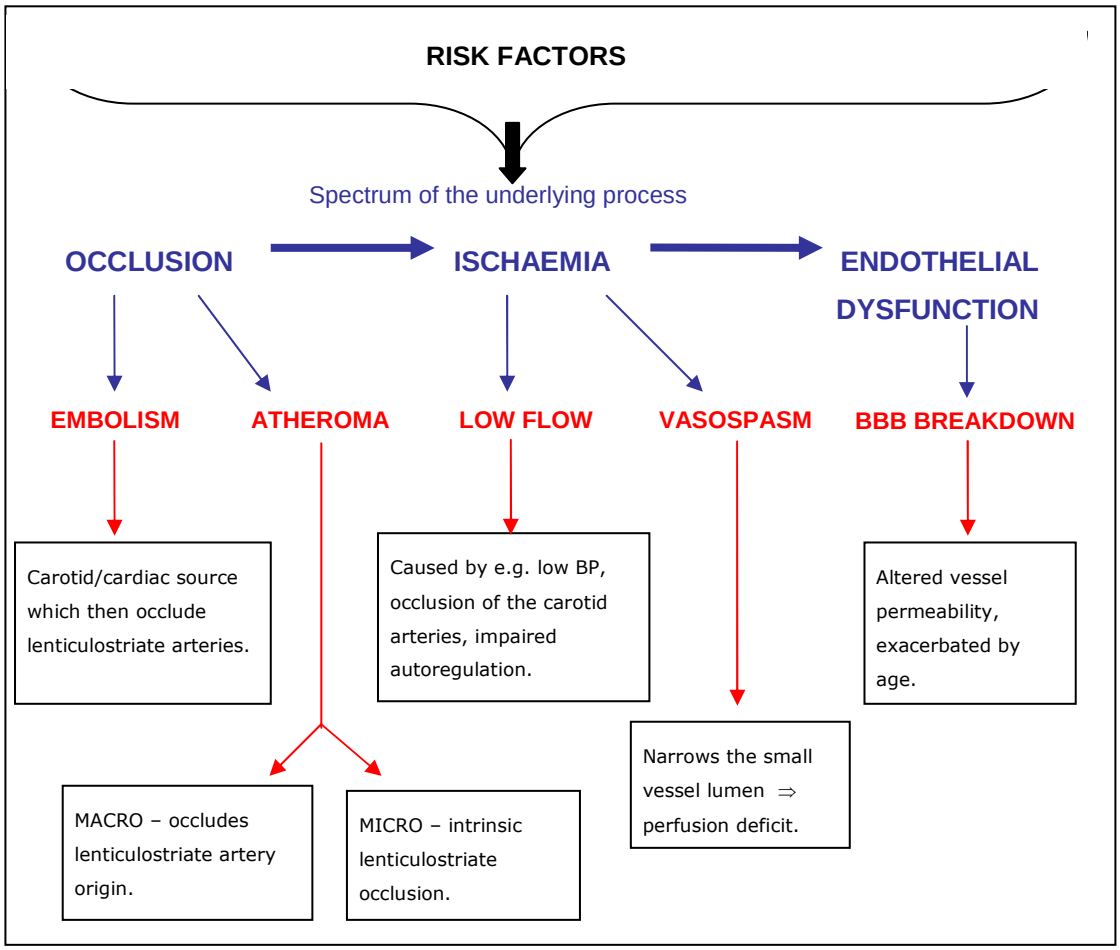

Figure 1.7. The possible causes of lacunar stroke lesions displayed with regards to the spectrum of the underlying process.

BP = blood pressure. BBB = blood brain barrier.

1.9.1 Why would an animal model be useful?

Animal models are useful in research of cerebral ischaemia, as they can replicate human ischaemic damage in some ways, in particular the middle cerebral artery occlusion model(Belayev et al. 1999). In lacunar stroke the difference in opinion on and lack of defined terminology regarding the pathophysiological events, makes it impossible (as with

most animal models) to faithfully recreate the entire human disease state. Ideally an animal model of lacunar stroke should display both the vascular and parenchymal pathology associated with the disease and the disease should be introduced by a pathologically relevant mechanism e.g. occluding a large artery with an intraluminal thread is not appropriate for producing lacunar lesions. At present there are still several proposed causative mechanisms that could be modelled including reduced cerebral blood flow, vasospasm and endothelial (BBB) dysfunction. A model that can mimic at least some features of one or more of the proposed mechanisms of human lacunar stroke, or can imitate some of the pathological features would undoubtedly be valuable to improve understanding of the disease and to test potential treatments. Lacunar stroke is now a recognised distinct stroke subtype, however acute treatment and secondary prevention are not tailored towards it and this can only be done once the underlying mechanisms are understood.

1.10 Systematic Reviews – the value of and design

In order to find and clarify the potential causative mechanisms of lacunar stroke, it was necessary to review both the available human and animal data in an unbiased and systematic way. Systematic reviews consequently, play an important role in this thesis.

A systematic review is a literature review focused on a single question that tries to identify, appraise, select and synthesize all relevant high quality research evidence. Systematic reviews are often needed whenever there are several primary studies with disparate findings related to the same substantive question, thereby causing uncertainty.

A systematic review uses an objective and transparent approach for research synthesis, with the aim of minimizing bias. It often uses statistical techniques (meta-analysis) to combine the data from valid studies. This approach can also be applied to a whole range of different studies and guidance is available from the Equator Network (see below). Systematic reviews are generally based on a peer-reviewed protocol, so that they can be easily replicated**.** Systematic reviews offer a way to interpret the findings of studies in an unbiased manner and present a balanced and impartial summary of the findings, taking into account any flaws in the evidence.

Conducting systematic reviews has been aided in recent years by the publication of recommended reporting guidelines for observational studies, clinical trials and experimental studies. The Equator Network website (www.equator-network.org) lists most of these tools, enabling the author to generate a study quality checklist, relevant to the type of studies their

review will be mostly comprised of. There are now specific databases for systematic reviews in particular subject areas (e.g. the Cochrane collaboration covers treatments and diagnostic tests).

1.11 Aims of the thesis

In light of questions and gaps in our knowledge demonstrated by the above introduction the aims of this thesis were as follows;

i) Systematically review the cerebral pathology of human lacunar stroke in order to make unbiased comparisons between animal and man and identify the exact gaps in our knowledge of lacunar stroke pathology.

ii) Conduct a systematic review of potential animal models of lacunar stroke currently in the published literature.

iii) Consequently, systematically assess the cerebral pathology of the most suitable animal model.

iv) Conduct histopathological assessment of vascular pathology in the most suitable animal model in brain regions, encompassing the territory of lacunar stroke.

v) Conduct RNA microarray analysis of pertinent markers of vascular pathology in this model.

In this thesis we have assigned each of the systematic reviews to an individual chapter. In addition we have conducted our own original laboratory work therefore this thesis will be split into three sections –

Section 1) General introduction and systematic reviews – incorporating this chapter, an introduction to systematic reviews and chapters 2-4, each of which is a systematic review.

Section 2) Original laboratory work - incorporating general materials and methods and three results chapters (chapters 5-8).

Section 3) A general discussion of the entire thesis plus appendices and references.

CHAPTER 2 : HUMAN LACUNAR STROKE PATHOLOGY – A SYSTEMATIC REVIEW

2.1 Background

As stated in the general introduction to this thesis, about 20% of all strokes (about 25% of all ischaemic stroke) are lacunar in type(Sudlow and Warlow 1997). These small lesions (<2cm in diameter, <1.5cm in some definitions) affect the white matter and deep grey matter of the cerebral hemispheres and brainstem and are associated with several discrete neurological syndromes(Fisher 1982b;Arboix et al. 2006;Ghandehari and Izadi 2009). They are associated with an abnormal deep perforating arteriole but the small size of the brain and vascular lesions make pathological examination of lacunar lesions technically difficult. In addition lacunar stroke is rarely fatal and the autopsy rate is declining.

A previous review of lacunar stroke pathology found only 10 studies (11 including their own), most from before 1980(Arboix et al. 1996). Various descriptive reviews of lacunar stroke pathology have been published since then(Lammie 2000;Arboix and Marti-Vilalta 2004;Pantoni et al. 2006), but descriptive reviews rarely provide an in depth appreciation of the quality, breadth and reliability of the published knowledge. Other reviews focused more generally on ageing rather than lacunar stroke(Grinberg and Thal 2010) or compared multiple features of small vessel disease seen on imaging with pathology(Gouw et al. 2010). Hence we performed a systematic examination of all human lacunar stroke pathology to help summarise all of the available published studies of the pathology of lacunar stroke.

2.2 Materials and methods

2.2.1 Search strategy

We searched for all available studies describing lacunar stroke pathology using, at the very least, a macroscopic assessment of brain slices. We developed a comprehensive electronic search strategy using terms such as lacun$, lipohyalinosis, patholo$, stroke and autopsy in Embase and Medline from inception to February 2011 (see appendix A for full search strategy), hand searched reference lists in review papers and text books and two relevant journals (Stroke and Acta Neuropathologica). We excluded editorials, conference abstracts and review papers that did not contain any new primary data.

2.2.2 Inclusion/Exclusion criteria

We included studies published in full, in any language, that described the pathology of human lacunar lesions, whether symptomatic (the patient had a documented lacunar syndrome) or asymptomatic (including truly asymptomatic or initial stroke of uncertain subtype, or with atypical symptoms). We included lacunar lesions of any age (from acute to old) and appearance (cavitated or not), studies of brain banked tissue if they specifically described lacunar lesions, and all lesions explicitly described as lacunar in nature by the study authors, as well as lesions we considered to be lacunar from the descriptions given, even if the term 'lacunar' was not specifically used by the authors. We defined lacunar lesions based on Poirier et al and Lammie et al(Lammie et al. 1998;Derouesne and Poirier 1999) where a type 1a lacune is a cavitated lesion with a ring of gliosis and a type 1b lacune is a partially cavitated lesion, but also included non-cavitated lacunar ischaemic stroke lesions to avoid undue focus on cavitated lesions. Types II (old haemorrhage), III and IV lacunes (dilated and very dilated perivascular spaces respectively) were not relevant.

We excluded studies of: leukoaraiosis, Binswanger's disease or vascular dementia (but checked for descriptions of lacunar lesions within these studies and included pathological details if given); patients with primary intracerebral haemorrhage (as our focus was on ischaemic lesions); experimental models (because the absence of agreement on what causes human lacunar stroke limits the relevance of animal studies); cerebral autosomal dominant arteriopathy with subcortical infarcts and leukoencephalopathy (CADASIL) and other monogenic disorders; and striatocapsular infarcts (which are larger than lacunar infarcts and due to middle cerebral artery (MCA) atherothromboembolic occlusion(Fisher 1979;Donnan et al. 1991)).

2.2.3 Data extraction

One reviewer (E.L.B) extracted information on: study population, number of patients, symptoms, vascular risk factors, previous stroke, age of patients at time of stroke and death or time lapse from stroke to death, cause of death, use of imaging, pathological methods, brain regions and vessels examined and brain/vascular lesion findings (see appendix B for full data extraction form) including lesion location and size and specific evidence of ischaemia, inflammation or blood brain barrier disruption. We noted any other terms used by authors to describe what we considered to be lacunar lesions. A second reviewer (J.M.W)

checked the extracted information. Differences were resolved by consensus with a third reviewer (C.L.M.S).

2.2.4 Study quality

We assessed study quality using a checklist based on the STROBE statement(von Elm et al. 2007) and the MOOSE criteria(Stroup et al. 2000) which factors such as; study population (e.g. an aging cohort, stroke population, brain bank study etc), number of patients, reporting of risk factors (e.g. hypertension, smoking, diabetes etc), the number and expertise of observers (e.g. neuropathologist, neurologist, radiologist etc), whether the observers were blinded to clinical data and whether lesion size (in any dimension) and / or lesion location was reported. Factors such as whether the pathology interpretation was appropriately blinded to clinical data are important as they highlight the potential problem that knowledge of risk factors may influence the examination of the specimen and bias the results.

Table 2.1 The 9 point study quality checklist applied to all included studies

Study population reported– stroke, aging cohort, etc	
How patients were sampled – inclusion criteria	
Number of patients	
Risk factors reported (including age)	
Number of & expertise of observers	
Observers blinded to clinical data?	
Use of validated histopathological methods	
Size of Infarcts recorded	
Location of infarcts recorded	
Total /9	

We devised the checklist using influences from the STROBE statement (von Elm et al. 2007) and the MOOSE criteria (Stroup et al. 2000).

2.2.5 Data analysis

We entered data into a spreadsheet and performed summary statistical analysis. We planned to perform a formal meta-analysis of the association of lesion location and size with symptoms, and of the frequency of features indicating ischaemia, inflammation or blood brain barrier leakage.

2.3 Results

2.3.1 Search results

Our initial search produced 1796 studies (figure 2.1): excluding animal studies, non cerebral lacunes, duplicates and review papers left 1240 studies. Of these, 672 were full journal articles. We excluded 362/673 studies which only reported on vascular dementia and/or Alzheimer's pathology, 165 studies of imaging or retinopathy only and 106 studies of leukoaraiosis, none of which included data on lacunar lesions, of CADASIL, two studies that looked relevant but provided no data on lacunar pathology(van Swieten et al. 1991;Yamada et al. 1995) and the early reports of Dechambre(Dechambre 1838) and Durant-Fardel(Durand-Fardel 1843) whose patient populations are not specific and do not provide enough detailed pathological information. This left 39 relevant studies (see table 2.2).

2.3.2 Study characteristics

38/39 studies included a total of 2340 subjects (1 study did not report the number of subjects), with a median of 14 subjects per study (interquartile range [IQR] 2-45, range 1 to >1000)(Dozono et al. 1991a). The number of lesions studied was reported in 22 studies (total lesions 4110) but not in the other 17 studies. Nine studies reported the median number of lesions studied per patient (2, range 1-5).

Fifteen studies (38%) described symptomatic brain lesions and six studies (15%) reported asymptomatic lacunar lesions on pre-mortem imaging followed by autopsy in aging studies. The remaining 18/39 studies (46%) described lacunar lesions in patients with a history of stroke (subtype unspecified and not clearly linked to a lesion on pathology, 10 studies) or who had stroke risk factors but had died of non-neurological causes (8 studies). The time interval between symptoms and death ranged from one month to approximately ten years. 29/39 studies (74%) reported on hypertension (which affected >50% of subjects in those studies), 14/39 studies reported on diabetes (less frequent than hypertension) and a few studies reported other risk factors e.g. atrial fibrillation or serum cholesterol (table 2.2).

The 15 studies of symptomatic lesions included 554 patients but the actual number of individual lesions assessed was unclear (some gave the total and some the mean per patient) and six studies did not state the number at all. From those studies that gave the total or mean number of lesions per patient, we calculated that at least 1200 lesions were assessed in patients with a lacunar syndrome, although it was unclear how many of these were truly

symptomatic. In patients with multiple lacunar lesions, it was noted that at least half the patients had lesions which did not fit their symptoms(Pullicino et al. 1980).

24 studies of subjects with asymptomatic (including not definitely symptomatic) lacunar lesions included six aging cohorts with asymptomatic lacunar lesions on pre-mortem imaging (71 subjects) and 18 studies of autopsy brains from patients without neurological symptoms in life or who had a previous history of stroke but of undefined subtype. 9/24 studies reported the number of lesions (total approximately 2700), 2567 of which came from one study with 1086 subjects(Dozono et al. 1991a). Nine studies did not report the total number of lesions. Sixteen studies used brain imaging (nine CT, four MRI and two used CT and MRI), nine before death, one after death and four both before and after death, to match lesions in life to those at autopsy – none of these lesions were symptomatic (table 2.2).

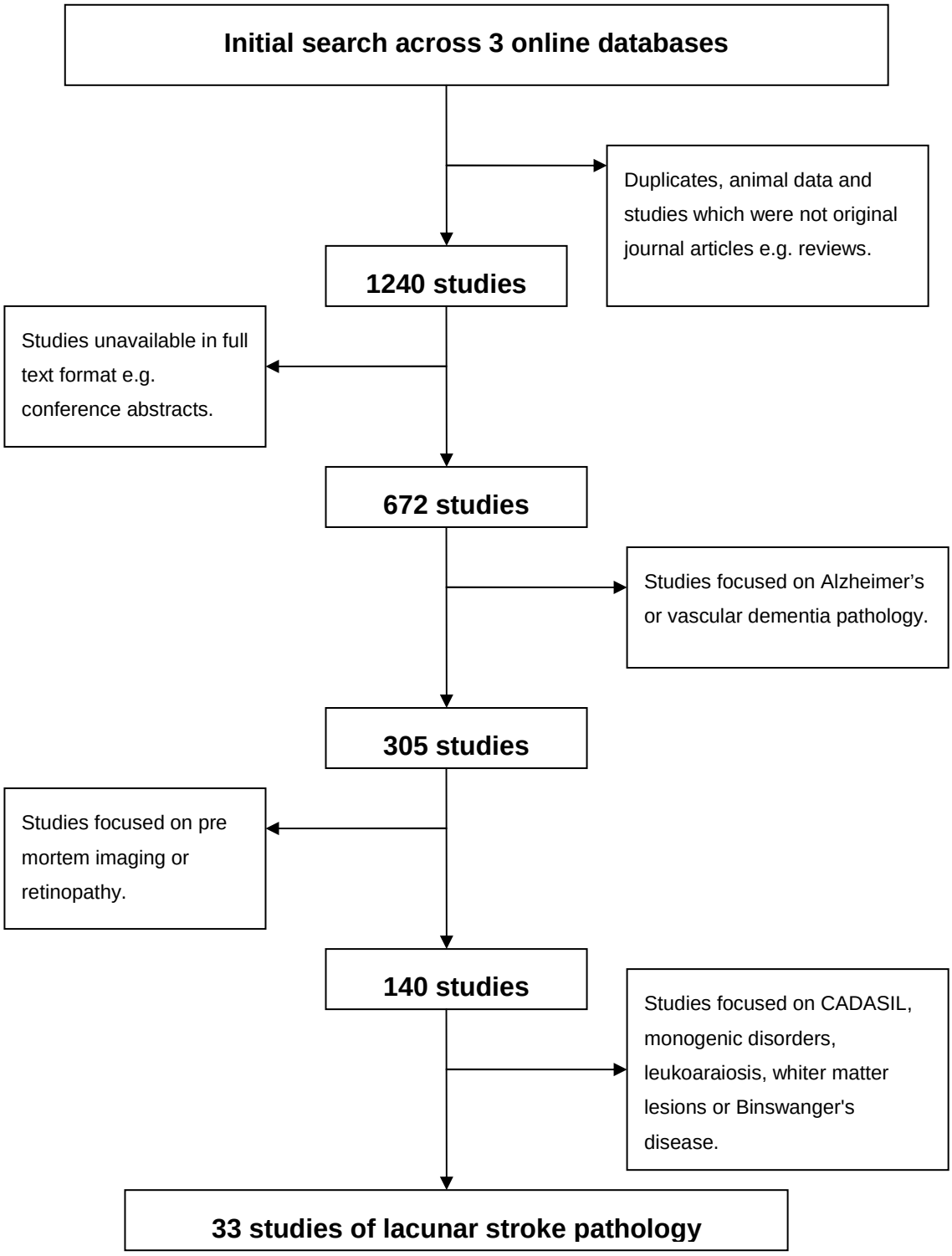

Figure 2.1 The results of the search strategy along with exclusion criteria applied to the studies in order to retrieve pertinent literature.

Table 2.2 A full list of studies which met our inclusion criteria, arranged in chronological order.

Author	Date	Number of patients	Study type	Reported risk factors	Imaging	Fixation & embedding	Focus on vessels / tissue	Stains / antibodies used	Number of observers	Study Quality Score /9
Marie(Marie P 1901)	1901	50	Non neurologic brain bank specimens	None except age	N/A	Unknown	Tissue & Vessels	Unknown	1 - Neurologist	5
Ferrand(Ferrand J 1902)	1902	98	Lacunar symptoms & corresponding pathology	HT	N/A	Formalin, Celloidin embedding	Tissue & Vessels	H&E, Weigert	2 – 1 Neurologist	6
Hughes(Hughes et al. 1954)	1954	15	Lacunar symptoms & corresponding pathology	HT,Urea, dementia	N/A	Unknown	Tissue & vessels	Unknown	Unknown	6
Alex(Alex et al. 1962)	1962	107	Non neurologic brain bank specimens	HT, DM	N/A	Fixation unknown, paraffin embedding.	Tissue	H&E. EVG, PAS, Colloidal Iron	3 - pathologists	6.5
Fisher(Fisher 1965)	1965	114	Lacunar symptoms & corresponding pathology	HT, DM, AF & "other special conditions"	N/A	Unknown	Tissue & vessels	Unknown	1- Neurologist?	6.5
Cole(Cole and Yates 1967)	1967	15	Non neurologic brain bank specimens	HT	N/A	Micropaque/Gelatin Mix injected through IC. Fixative unknown	Tissue & Vessels	Unknown	2 pathologists?	7.5
Fisher(Fisher 1968)	1968	4	Lacunar symptoms & corresponding pathology	HT & "history of small strokes"	N/A	Fixation unknown, paraffin & celloidin embedding.	Tissue & Vessels	Phloxine, saffron, H&E, EVG & "myelin stains"	1 - Neurologist	5.5
Fisher(Fisher 1978)	1978	2	Lacunar symptoms & corresponding pathology	HT, Dementia	CT (premortem)	Formalin Paraffin	Tissue & Vessels	PTAH	1 - Neurologist	4.5
Pullicino(Pullicino et al. 1980)	1980	42	Lacunar symptoms & corresponding pathology	HT, Dementia	CT (premortem)	Unknown	Tissue & Vessels	Unknown	Unknown	6
Mihara/Ogata(Ogata 1999)	1980	22	Autopsy specimens with documented stroke incident	Unknown	N/A	Gelatin & Barium infused into arteries paraffin embedded	Tissue & vessels	Unknown	1 - specialism unknown	5.5

Nelson(Nelson et al. 1980)	1980	37	Lacunar symptoms & corresponding pathology	HT, DM, Cholesterol	CT (premortem)	Unknown	Tissue	Unknown	Unknown	9
Masuda(Masuda et al. 1983)	1983	202	Autopsy specimens with documented stroke incident	HT, cholesterol	N/A	Unknown	Tissue & vessels	H&E, EVG.	Unknown	7
Awad(Awad et al. 1986)	1986	1	Autopsy specimen with documented stroke incident	Unknown	MRI (fresh and fixed states) - T2	Formaldehyde paraffin	Tissue & Vessels	H&E, LFB, GFAP	1 - specialism unknown	7
Benhaiem-Sigaux(Benhaiem-Sigaux et al. 1987)	1987	1	Lacunar symptoms & corresponding pathology	HT	N/A	Formalin Celloidin/Paraffin	Tissue & Vessels	H&E, Loyez, Masson Trichrome, Bodian silver & LFB	Unknown	6
Braffman(Braffman et al. 1987)	1987	6	Cohort with asymptomatic lacunes on imaging	HT, neurologic symptoms, CVD, DM, smoking	CT & MRI (3 had in vivo imaging) postmortem	Formalin, embedding material unknown	Tissue	H&E, LFB, Bodian	4 Neuropathologists 2 Neuroradiologists	7
Mancardi(Mancardi GL et al. 1988)	1988	46	Lacunar symptoms & corresponding pathology	HT,DM,CVD, Smoking	N/A	Paraffin unknown fixative	Tissue & Vessels	H&E, PAS, EVG, PTAH, Weigert. GFAP.	Unknown	5.5
Marshall(Marshall et al. 1988)	1988	6	1 patient - asymptomatic on imaging. Rest non neurologic brain bank.	Unknown	MR premortem 1 patient. MR post for the rest	Formalin - unknown embedding	Tissue	H&E, Congo Red, LFB, Alcian Blue. GFAP, Albumin, IgG.	Unknown	6
Tuszynski(Tuszynski et al. 1989)	1989	167	Lacunar symptoms & corresponding pathology	HT,DM,CVD, Smoking	N/A	Formalin Paraffin	Tissue & Vessels	H&E	Unknown	7
Challa(Challa et al. 1990)	1990	15 + 'others'	Non neurologic brain bank specimens	HT	N/A	Formaldehyde, celloidin & paraffin	Tissue & Vessels	AP, CV, H&E	Unknown	6

Loeb(Loeb et al. 1990)	1990	34	Lacunar symptoms & corresponding pathology	HT, DM, Smoking, Dyslipidemia	CT (premortem)	Unknown	Tissue & Vessels	H&E, PAS, EVG, PTAH. GFAP	Unknown	7.5
Dozano(Dozono et al. 1991a)	1991	1086	Non neurologic brain bank specimens	HT	N/A	Formalin, embedding material unknown	Tissue	Unknown	Unknown	6.5
Laloux(Laloux and Brucher 1991)	1991	1	Lacunar symptoms & corresponding pathology	HT, Inflammatory syndrome	CT (premortem)	Unknown	Tissue & Vessels	Kluver-Barrera, Masson Trichrome	Unknown	6
Chimowitz(Chimowitz et al. 1992)	1992	2	Non neurologic brain bank specimens	HT, DM, Smoking	N/A	Formalin Paraffin	Tissue & Vessels	Kluver Barrera, Congo Red, Desmin. GFAP	1- Neuropatholo gist?	8
Reed(Reed et al. 1994)	1994	45	Autopsy specimens with documented stroke incident	HT, cholesterol, alcohol others available?	N/A	Unknown	Tissue & vessels	H&E	At least 3 pathologists	6.5
Arboix(Arboix et al. 1996)	1996	25	Lacunar symptoms & corresponding pathology	HT	N/A	Unknown	Tissue	Unknown	Unknown	6
Ma(Ma and Olsson 1997)	1997	3 / 167	Cohort with asymptomatic lacunes on imaging	HT, Dementia	CT (premortem)	Formalin Paraffin	Brain & Vessels	H&E, LFB, Acid fuchsin, Masson Trichrome, Congo red Toludene blue. Albumin, IgG, Fibrinogen, Fibronectin.	Unknown	8
Lammie(Lammie et al. 1998)	1998	19	Autopsy specimens with documented stroke incident	HT & DM	CT (premortem) - 5 cases only	Formalin Paraffin	Tissue & Vessels	H&E, LFB, CV, EVG, MSB, GFAP & Fibrinogen	1 – Neuropatholo gist	5.5
Vinters(Vinters et al. 2000)	2000	12	Cohort with asymptomatic lacunes on imaging	Cognitive Impairment / Dementia	N/A	Unknown	Tissue & Vessels	H&E, Congo Red, Bielschowsky. Abeta, tau, ubiquitin, GFAP.	At least 2 (1 at a neuropatholog y centre)	5

Rossi(Rossi et al. 2004)	2004	35	Cohort with asymptomatic lacunes on imaging	AD, Dementia	CT & SPECT (premortem)	Unknown	Tissue & vessels	H&E, LFB, PAS, Bielschowsky	2 – specialism unknown	6
Schneider(Schneider et al. 2005)	2005	64	Autopsy specimens with documented stroke incident	AD & ApoE genotype	N/A	Paraformaldehyde, paraffin	Tissue	Unknown	1-Neuropathologist	5
Kawamoto(Kawamoto et al. 2006)	2006	8	Non neurologic brain bank specimens	Unknown	N/A	Formalin Paraffin	Tissue?	H&E, Kluver Barrera, Bielschowsky. 14-3-3, GFAP, anti-vimentin, transferrin, CD11b	Unknown	6
Pico(Pico et al. 2007)	2007	108	Autopsy specimens with documented stroke incident	No DM	N/A	Formalin Paraffin	Tissue & Vessels	H&E, Bodian, LFB, Masson Trichome, Congo Red	2 - specialism unknown	6
Ogata(Ogata et al. 2008)	2008	2	Autopsy specimens with documented stroke incident	HT, DM, AF, dyslipidemia	N/A	Formalin, embedding material unknown	Vessels	H&E, Masson trichrome, PTAH	Unknown	6.5

Number of patients refers to the number of patients with lacunar lesions (therefore not necessarily the total number in the study). HT = hypertension. DM = diabetes mellitus. AF = atrial fibrillation. CVD = cerebrovascular disease. AD = Alzheimer's disease. IC = internal carotids. H&E = hematoxylin and eosin. EVG = elastic van gieson. PAS = periodic acid-Schiff. PTAH = phosphotungstic acid hematoxylin. LFB = luxol fast blue. GFAP = glial fibrillary acidic protein. AP = alkaline phosphatase. IgG = immunoglobulin G. CV = cresyl violet. MSB =martius scarlet blue.

2.3.3 Pathological assessments

Ten studies provided only a macroscopic assessment of brain slices. Amongst the 29/39 studies reporting microscopic data, 25 different histological stains were used, the most common being hematoxylin & eosin (22 studies) then luxol fast blue (seven studies). Sixteen different antibodies for immunohistochemistry were used of which Glial Fibrillary Acidic Protein (GFAP) was the most common (nine studies). Sixteen studies (41%) reported findings of typical type I cavitated lacunar lesions without reference to the lesion age, 9 studies (23%) reported cavitated lacunar lesions with some reference to lesion age (i.e. subacute or old) and the remaining 14 studies (36%) reported on lesions in varying stages of development describing softenings, partially cavitated lesions, gliosis and associated perivascular space dilatations.

2.3.4 Terminology and definitions

Descriptions of lacunar lesions varied widely, making it difficult to distinguish whether authors were referring to lacunar lesions, related pathology and/or imaging features (table 2.3). Terms used for clinical or imaging features included lacunar infarct(ion), lacune, small deep infarcts and lacunar cavities. Pathological descriptions favoured the term ‘lacune’, followed by various descriptions of cavities (small, lacunar, trabeculated etc) (table 2.3). ‘Softening’ was most often used to describe more acute lesions(Hughes et al. 1954;Fisher 1965). Although 23/39 (59%) of studies defined what they meant by a lacunar lesion, descriptions ranged from only the lesion size and location to more detailed pathological descriptions of lacunar lesion types; six studies used terms such as ‘small deep infarcts’ or ‘small subcortical infarcts’; and ten studies did not define what they meant by lacunar lesions at all. Terms used to describe vessel lesions included lipohyalinosis, hyalinization, hyaline arteriosclerosis and segmental arteriolar disorganization, all of which described apparently similar lesions.

2.3.5 Study quality score

The average study quality score was 6/9 (range 4-9). The most common items omitted were blinding between clinical and pathological data, the number and expertise of observers and lesion size. Where reported, neuropathologists were the most common observers (7/15 studies), but others were reported as simply ‘pathologists’ and 24 studies (62%) did not

report the specialty of the person performing the pathology. Only five studies blinded the observer to potentially confounding clinical data (13%).

2.3.6 Pathological findings

29 studies (74%) examined both parenchymal and associated vascular pathology, nine studies (23%) reported only parenchymal pathology and one study only reported vascular pathology(Ogata et al. 2008).

2.3.6.1 Parenchymal Lesions

Location: Most studies sampled many areas of the brain, if not the entire brain, with little evidence of sampling bias, but data were not provided on the exact number of lesions found in each brain structure. Studies of symptomatic lesions more often reported precise locations (e.g. caudate or lentiform nucleus) than those of asymptomatic lesions (e.g. "basal ganglia"). Most lesions were in the thalamus (18/39), putamen (12/39), caudate and internal capsule (11/39). Studies of symptomatic subjects reported almost double the number of lesions in the internal capsule (seven versus four studies) and almost 3 times as many studies reported lesions in the caudate nucleus (eight versus three studies), compared to studies in asymptomatic subjects (see table 2.4).

Size: Twenty-five studies (64%) reported lacunar lesion size, by: diameter (<5 to 30mm, 17 studies); volume (0.1 to 525m^3, 8 studies); area (0.1- to 28mm^2, 6 studies) and some used more than one unit of measurement. Many studies used 1cm as the maximum diameter for a lacunar lesion. There was no difference in size between symptomatic and asymptomatic lesions with a range of 1-30mm diameter encompassing both types of lesion. Determining the mean size of symptomatic versus asymptomatic lesions was impossible due to the different types of measurements reported.

Table 2.3.The varying terminology used to describe lacunar lesions in both clinical and pathology settings.

Clinical/General descriptions	N	Imaging	N	Pathology	N
Lacunar infarct(ion)(s)	7	Lacune (ae)(s)	6	Lacune(as)(s)	14
Lacune (ae)(s)	7	Lacunar infarct(ion)(s)	4	Cavities (small/cystic/cribriform/slit like/trabeculated/lacunar)	12
Small deep (cerebral) infarct(s)	6	Small lesions	3	Lacunar infarct(ion)(s)	10
Lacunar cavities	2	Small deep lesions	3	small (subcortical) infarcts	8
Lacunar stroke	2	Small infarcts	2	Microinfarcts	6
Little/mild/small strokes	2	Lacunar lesion	2	Subcortical/brain stem/WM/thalamic infarctions	6
Patches / patchy lesions	2	Etat crible	1	Cystic infarcts/lesions/encephalomalacia	6
Subcortical lesions	2	Slit like/ ovoid infarct(s)	1	Small deep infarcts	5
Caps	1	Slit like irregular cavity	1	Etat crible	4
Cystic infarct	1	Patchy lesions	1	Softenings (small&/ischaemic)	4
Etat lacunaire	1	Microinfarcts	1	Ischaemic necrotic foci	2
Expanding lacunes	1	Small deep infarct	1	WM infarcts	2
Lacunar disease	1	Lacunar sized infarct/lesion	1	Lacunar stroke	2
Lacunar lesions	1	Lacunar cavities	1	Lacunar scars	1
Lacunar sized infarct/lesion	1	Lacunar state	1	Parenchymal rarefaction	1
Piriform lacunes	1	Multiple ischaemic infarctions	1	Etat lacunaire	1
Punctate lesions	1			Etat vermoulu	1
Rims	1			Status cribrosus	1
Slient infarct/lesion/stroke	1			Space-occupying/expanding infarcts	1
Small cerebrovascular lesions	1			Infarcted lesion	1
Small deep lesions	1			Silent infarct	1
Small ischaemic brain lesions	1			Proliferative/inflammatory/atheromatus lesions	1
Status lacunaris	1				
Total	**23**	**Total**	**16**	**Total**	**22**

KEY	
	Stand alone terms
	Term used in both clinical and imaging settings
	Term used in both imaging and pathology settings
	Term used in both clinical and pathology settings
	Term used in all three settings

WM = white matter. N= number of studies using the term.

Macroscopic appearance – Lesions were of varying sizes, generally bilateral, in the territory of the lenticulostriate arterioles (>75%) and a mixture of old and more acute(Marie P 1901;Ferrand J 1902). Those in the deep grey matter were often more irregular shaped and collapsed than those in the white matter(Fisher 1965). Occasional haemorrhage and Charcot-Bouchard / saccular aneurysms (or microaneursyms) were also found close to lacunar lesions(Cole and Yates 1967;Fisher 1978;Benhaiem-Sigaux et al. 1986;Tuszynski et al. 1989;Revesz et al. 1989).

Table 2.4 A comparison of the territory of symptomatic versus asymptomatic lacunes in the brain.

Symptomatic	Number of studies	Asymptomatic	Number of studies
Thalamus	8	Basal Ganglia	9
Caudate	8	Thalamus	8
Putamen	7	Putamen	5
Internal Capsule	6	Pons	4
Pons	4	Frontal/deep WM	4
Globus pallidus	4	Cerebellum	3
Frontal/deep WM	4	Caudate	3
Cerebellum	3	Internal Capsule	3
Corpus Callosum	2	Brain Stem	2
Basis Pontis	2	Centrum Semiovale	2
Basal Ganglia	2	Globus pallidus	1
Mid Brain	1	Mid Brain	1
Medulla Oblongata	1	Medulla Oblongata	1
Unknown	1	Dentate Nuclei	1
		Lenticular nucleus	1
		Optic tract	1
		Unknown	6

Microscopic appearance - Old lesions were described as small pale cavities with irregular borders, often trabeculated with connective tissue and accompanied by a ring of gliosis(Benhaiem-Sigaux et al. 1987;Bokura et al. 1998;Kawamoto et al. 2006). Macrophages and fibrous astrocytes were observed at the lesion border(Mancardi GL et al. 1988;Chimowitz et al. 1992;Mayer et al. 1993). Acute lesions more often had plump macrophages, liquefaction necrosis and little gliosis(Fisher 1968) and were often described as "softenings"(Cole and Yates 1967). Hemosiderin laden macrophages were occasionally encountered. The surrounding parenchyma showed varying degrees of edema and spongiosis as well as reactive astrocytes(Mancardi GL et al. 1988;Lammie et al. 1998), but little direct specific evidence of infarction. Small capillaries/arterioles often lay within or crossed the lesion(Fisher 1968;Benhaiem-Sigaux et al. 1987). Some lacunar lesions had perivascular rarefaction and selective neuronal loss without full cavitation(Ma and Olsson 1997;Lammie et al. 1998) and were labelled as 'oedema associated lesions' reflecting the impression that edema was a key factor in their formation(Ma and Olsson 1997;Lammie et al. 1998). Dilated perivascular spaces with a round regular border surrounded by rarefied and gliotic nervous tissue were often found close to lacunar lesions(Benhaiem-Sigaux et al. 1987;Mancardi GL et al. 1988;Loeb et al. 1990;Bokura et al. 1998) e.g. in the putamen at the point of entry of the lenticulostriate arteries(Loeb et al. 1990) and were rarely associated with lacunar clinical syndromes. This appearance was common in normal aging brains(Braffman et al. 1987) or in those with vascular dementia(Revesz et al. 1989;Vinters et al. 2000). Neuronal loss around the lesions was rare(Hughes et al. 1954), but increased levels of inflammatory markers were common(Tomimoto et al. 2002).

2.3.7 Vascular lesions

Fourteen studies (44%) attempted to trace the arteriole thought to be responsible for the symptomatic lesion. Nine studies that measured the affected arteriole reported diameters ranging from 14-400µm. No arteriole >400µm diameter was cited as having directly caused a lacunar lesion. Changes in arteries, arterioles and capillaries were reported; veins and/or venules were rarely mentioned(Alex et al. 1962). In general, the size of a lacunar lesion was proportional to the size of the affected vessel(Fisher 1968).

2.3.7.1 Large vessels – circle of Willis and major branches

We found similar descriptions of large vessel pathology in both symptomatic and asymptomatic patients, including atherosclerosis and dolichoectasia. Ferrand(Ferrand J 1902) described the basilar artery (BA) of patients with lacunes at autopsy as being 'atheromatous', with alterations of the internal membrane, proliferation of elastic tissue and infiltration of macrophages. Atherosclerosis of the circle of Willis, ICA, BA, posterior cerebral (PCA), MCA and anterior cerebral (ACA) arteries in symptomatic lacunar stroke patients was reported in several studies as either 'moderate' or 'severe' in at least 50% of patients ('moderate' and 'severe' were not defined), more commonly in patients with hypertension in life than in normotensive patients(Fisher 1965;Tuszynski et al. 1989). Mancardi(Mancardi GL et al. 1988) described atherosclerotic changes consisting of collagen or fibrin deposits, cholesterol crystals, duplication and splitting of the elastic lamina and thickening of the adventitia in patients with lacunar syndromes and other neurological symptoms (but did not provide information on hypertension). Patients with incomplete lacunar lesions (not clearly associated with symptoms) showed mild (60% of patients) to moderate (30% of patients) atheroma in the ipsilateral ICAs(Lammie et al. 1998) but these patients had various previous stroke episodes not just lacunar. Asymptomatic patients showed similar changes, with more atherosclerosis typically associated with more lacunes(Bokura et al. 1998), particularly in patients with vascular dementia(Revesz et al. 1989;Vinters et al. 2000). Widening of the internal and external diameters of the vertebral, ICA and MCAs (dolichoectasia) was also described, for example the median diameter of the BA was almost doubled in patients with asymptomatic lacunar lesions and those with a 'history of stroke'(Pico et al. 2007).

2.3.7.2 Small penetrating arteries, arterioles and capillaries

We found no quantitative differences in the small vessel lesions in symptomatic versus asymptomatic patients. Ferrand described small penetrating arterioles in symptomatic lacunar stroke patients as having thick walls and dilated perivascular spaces in areas with lacunes as well as in areas in the ipsilateral hemisphere devoid of lacunes(Ferrand J 1902). Hughes(Hughes et al. 1954) described perforating arterioles as being sclerotic and without occlusion but it was unclear whether these arterioles were directly related to lacunar lesions.

The first detailed description of small arteriolar changes directly related to lacunar lesions came from Fisher who found abnormal penetrating arterioles or their branches in six patients, some of which were occluded, and which he stated was not due to atheroma(Fisher 1965). In a separate study, he identified 'segmental arteriolar disorganisation' in 45/50 lacunar lesions in four patients(Fisher 1968). The

'segmental arteriolar disorganization' was distributed along the length of arterioles, 40-200µm in diameter and included a disintegrating arteriolar wall consisting of a loose mesh of collagenous strands, infiltration of fatty macrophages and/or foam cells and deposition of fibrinoid material(Fisher 1982b). 'Lipohyalinosis' was not mentioned until 1978 when he described thalamic infarcts in two hypertensive patients(Fisher 1978) in whom the external diameters of the small arterioles were enlarged to twice the diameter of any adjacent normal artery, the wall architecture was lost and the lumenae were occluded by a fine trabecular meshwork of hyaline material(Fisher 1978).

Intimal thickening and hyalinization, fibrosis of the wall and occasional microaneurysms were seen in the putamen(Masuda et al. 1983;Benhaiem-Sigaux et al. 1987), thalamoperforating and lenticulostriate arterioles(Mancardi GL et al. 1988) and other small intraparenchymal vessels(Benhaiem-Sigaux et al. 1986;Tuszynski et al. 1989). Intraluminal thrombi were rare and the arterioles were assumed to have recanalised(Mancardi GL et al. 1988). Ferrand described leukocytes infiltrating the walls of small arterioles and macrophages and active microglia in perivascular parenchymal lesions(Ferrand J 1902). One exception to the above is a single case report describing a patient with multiple cholesterol emboli in the perforating arteries with no evidence of vascular hyalinosis(Laloux and Brucher 1991).

There were additional comments pertaining to arterioles in asymptomatic patients. Most lacunes occurred on the 1st or 2nd order branches of the penetrating arterioles of hypertensive patients(Challa et al. 1990). Arteriosclerosis with medial hyalinization(Challa et al. 1990;Reed et al. 1994;Schneider et al. 2005), dense adventitial fibrosis and foamy macrophages in the vessel wall were common in patients with lacunar lesions dying of non-stroke neurologic or non-neurologic causes(Vinters et al. 2000). The degree of small arteriolar pathology increased with the number of lacunes visible pathologically in an ageing hypertensive population(Dozono et al. 1991a) or with the number of lacunar lesions and leukoaraiosis visible on imaging(Gupta et al. 1988;Rossi et al. 2004). One study suggested that fibrinoid necrosis was commoner in patients with diastolic hypertension than in those with systolic and borderline hypertension(Masuda et al. 1983).

Intimal hyalinization and thickening were more frequent in patients with lacunar ischaemic stroke than in those with haemorrhage(Reed et al. 1994). In non-cavitated (type Ib) lacunar lesions, hyaline arteriolar wall thickening was present but fibrinoid necrosis, luminal thrombi and foam cells were not(Lammie et al. 1998;Vinters et al. 2000). There was no cerebral amyloid angiopathy on staining with Congo Red(Marshall et al. 1988;Pico et al. 2007).

2.4 Discussion

Lacunar stroke is part of the spectrum of cerebral small vessel disease and represents an expanding global public health problem(Hachinski 2002). With out better understanding of the cause, it will be difficult to deliver better treatments. Amongst 39 studies including approximately 4000 lacunar lesions in 2300 subjects, we found consistent descriptions of a segmental non-atheromatous thickening of small artery/arteriole walls, along with breakdown of muscular and elastic fibres. Information on venular pathology was rare. There were signs of inflammation in the arteriolar wall and perivascular tissue, of perivascular edema-related damage, but little evidence of infarction or arteriolar occlusion except as an occasional late stage phenomenon secondary to extreme vessel wall damage(Ogata 1999). The inflammation had been noted as long ago as 1900(Ferrand J 1902). The absence of much direct evidence of true infarction could be because most studies were performed late in the disease course by which time the initiating features could have been obliterated. However, there were many studies that reported on the various evolutionary stages of lacunar lesions, including areas of initial softening and edema and/or partially cavitated lesions. Symptomatic lesions may occur in the internal capsule or caudate nucleus more often than asymptomatic ones, but otherwise there was little difference in the size or location of parenchymal or vascular lesions between symptomatic and asymptomatic patients/lesions. The notion that symptomatic lesions were larger than asymptomatic ones may have originated from studies of striatocapsular infarcts(Fisher 1979) – striatocapsular lesions occur due to transient MCA main stem occlusion or longer duration MCA occlusion in patients with good collateral pathways to protect the peripheral MCA territory, are due to large artery atherothromboembolic disease(Nishida et al. 2000). Other points of note were that the microvascular changes were spread throughout the deep grey and white matter (i.e. not just around one symptomatic lesion), moderate large artery atheroma and dolichoectasia were common and, where stated, many of the patients were hypertensive. However, the absence of comparisons between patients with other stroke subtypes, e.g. cortical ischemic stroke, makes it difficult to say whether the large artery atheroma is relevant, or whether it simply indicates exposure to vascular risk factors such as hypertension which was present in more than 50% of patients where stated. Further than that, considerable variation in pathological approaches, terminology, reporting of risk factors and clinical syndromes precluded further comparisons.

2.4.1 Strengths & weaknesses of the review and primary studies:

This is the first review of this topic to take a systematic approach. Hence, we hope that it provides additional insights into this topic. There was no evidence to suggest that the lack of difference between symptomatic and asymptomatic patients was due to sampling bias. However it was difficult to be certain we had found all the relevant papers. Publication bias is almost certain to affect this topic, but in the absence of much quantitative data, we did not test formally for it. We excluded studies of leukoaraiosis, Binswanger's encephalopathy, Alzheimer's disease and vascular dementia (unless they specifically described lacunar lesions) and genetic disorders (e.g. CADASIL). However, the reliance on the author's description and interpretation of lacunar lesions, even with our inclusive approach, may have inadvertently excluded papers or introduced bias.

We noted the very early and frequently quoted studies by Durand-Fardel(Durand-Fardel 1843) and Dechambre(Dechambre 1838) but did not formally include them because we found that, when translated, they contained only a small number of patients and these were of very mixed often non stroke-related backgrounds. For example, epileptic patients featured in both studies, some patients had previous episodes of encephalitis and others had severe cognitive impairments loosely described as 'idiotisme'. Therefore it is difficult to attribute any of the pathological descriptions to solely to a diagnosis of stroke.

There were other limitations of the included studies. Studies using brain bank material often stated there had been a stroke in life but not the stroke subtype. Studies of symptomatic patients need to pinpoint the relevant lacunar lesion. However efforts to do this, and/or to match a lacunar lesion to the responsible vessel lesion/s were often futile, due to normal imaging appearances(Gouw et al. 2010), difficulties singling out one lesion often among many, difficulties tracing vascular trees and the delay between clinical diagnosis and autopsy(Nelson et al. 1980). Changes resulting from fixation (e.g. shrinkage and changes in tissue proton relaxation characteristics) must also be considered when trying to correlate post mortem pathology or imaging with in vivo MRI findings(Gouw et al. 2010). Lacunar lesions rarely occurred in isolation (white matter lesions, dilated perivasular spaces etc were frequently encountered within the same subject) and as much patient information as possible is needed here in order to distinguish clinically relevant lesions from asymptomatic findings. Reporting of risk factors varied precluding attempts to differentiate causative from co-associated findings such as large artery atheroma and lacunar stroke. The exact brain regions examined were often poorly described. Most, after cutting 2cm coronal sections, only took regions which were macroscopically interesting, potentially missing many smaller lacunar lesions and other primary pathology. Studies differed in their diameter definition of lacunar lesions, some classifying lesions <1cm diameter as lacunar and other studies including lesions of up to 2cm diameter. However 36% of studies did not mention lesion size.

2.4.2 Interpretation

The notion that most lacunar stroke is due to "occlusion of small perforating arterioles" is not supported by this in depth, structured, examination of the literature. Perhaps, by association with large artery ischaemic stroke which is due largely to atherothromboembolic occlusion of large intracranial arteries, investigators assumed that lacunar stroke was also largely ischaemic and also due to arterial occlusion. Investigators may have assumed that, when not occluded, that arterioles must have recanalised as do thromboembolic occlusions of large arteries, rather than that the arterioles might never have been occluded in the first place.

There are many parallels between these findings in lacunar stroke and findings in other forms of small vessel disease, particularly in leukoaraiosis and features that are generally associated with ageing(Fazekas et al. 1993;Baloh and Vinters 1995;Vinters et al. 2000;Udaka et al. 2002;Wang et al. 2009;Grinberg and Thal 2010). In leukoariaosis and indeed normal aging, atherosclerosis of large intracranial arteries has been reported accompanied by vessel wall and / or perivascular macrophage infiltration and activated microglia(Vinters et al. 2000;Grinberg and Thal 2010). Enlarged perivascular spaces are a feature of cerebral small vessel disease(Zhu et al. 2010;Doubal et al. 2010) are also associated with active inflammation(Wuerfel et al. 2008) and impaired drainage of cerebral interstitial spaces. All, of the above are also associated with hypertension. Hence the association between increased brain features of small vessel disease and large artery atheroma could be because both are the result of hypertensive damage rather than because large artery atheroma causes cerebral small vessel disease. The blood brain barrier becomes increasingly permeable with advancing age, even more so in dementias (especially vascular dementia) and leukoaraiosis(Farrall and Wardlaw 2009). Patients with lacunar stroke have more permeable blood brain barrier than do those with cortical stroke: larger numbers of enlarged perivascular spaces are associated with further increases in blood brain barrier permeability(Wardlaw et al. 2009). Hence, inflammatory damage to the small vessel endothelium, perhaps triggered by or as part of hypertension, could aggravate the arteriolar wall segmental disintegration and perivascular tissue damage that manifests as lacunar stroke clinically or as leukoaraiosis on imaging.

2.5 Conclusion

Terminology and definitions used for lacunar disease in pathology have been highlighted as a continuing problem in this field since the 1960's(Fisher 1982a;Pantoni et al. 2006) but also affect descriptions of lacunar lesions clinically and on imaging(Wardlaw 2008;Potter et al. 2010a). When compared to the numerous imaging studies of lacunar stroke patients, the lack of pathology reports is explained by lacunar stroke rarely resulting in death soon after onset(Mihara 1980;Jackson and Sudlow 2005b), meaning that any acute abnormalities will have evolved. The difficulty of preserving and dissecting subcortical small vessels means that better use should be made of high field strength scanners, that are now much more widely available (e.g. 7T for experimental or human imaging), to match pre-mortem clinical and imaging features to post mortem imaging to help localise the relevant lacunar lesion and quantify associated features of small vessel disease(Wardlaw et al. 2011). Studies of lacunar lesions in general lack histology targeting specific pathological processes, e.g. using newer methods such as immunohistochemistry or mRNA expression analysis. Given the continually dwindling autopsy rate and difficulties in retaining material for research, perhaps some material from previous studies could even be re-examined with these methods? Brain tissue banks are becoming essential to overcome these problems, but are of limited use without detailed clinical and other in vivo information. More detailed information on the patient in life especially stroke symptoms, subtype and vascular risk factors, should be recorded in primary research on lacunar disease or kept with brain tissue in brain banks(Gouw et al. 2010). We should aim, through these approaches, to make the best use of existing and future human pathological material to study small vessel disease and its pathogenesis.

CHAPTER 3 : A SYSTEMATIC REVIEW OF POTENTIAL ANIMAL MODELS OF LACUNAR STROKE.

3.1 Background

Our systematic review of human lacunar stroke pathology (see previous chapter) and available epidemiological evidence suggests that the prognosis of lacunar stroke differs from large artery stroke with carotid stenosis and atrial fibrillation less common and the risk of early recurrence lower in lacunar stroke patients(Jackson and Sudlow 2005a;Jackson and Sudlow 2005b). This evidence thereby indicates that the underlying causes of lacunar stroke probably differ from other ischaemic stroke subtypes.

The small subcortical 'Lacunes' which characterize the condition are generally considered to be "ischaemic", however some data from patients suggests that they could arise secondary to an alternative initial process such as perivascular edema following BBB derangement(Lammie et al. 1998).

Animal models are useful in cerebral ischaemia research to replicate ischaemic damage encountered in humans. In contrast to large artery occlusive ischaemic stroke, the lack of clarity regarding the pathophysiological events in lacunar stroke makes it particularly difficult to model. However a model that can mimic at least some features of human lacunar stroke would undoubtedly be valuable to improve understanding of the disease in humans and to test treatments. We therefore undertook a systematic review to assess the suitability of all available animal models pertinent to lacunar stroke. Subsequently, we assessed their likely pathological mechanisms in order to determine their relevance to the human condition.

3.2 Materials and Methods

3.2.1 Study Identification

We used Cochrane Collaboration methodology for systematic reviews modified for observational studies (www.equator-network.org)(von Elm et al. 2007). We also applied the CAMARADES (Collaborative Approach to Meta Analysis and Review of Animal Data from Experimental Stroke) checklist for systematic reviews of animal models in stroke(Macleod et al. 2004). We sought to include a broad range of studies that claimed to (or could be taken to) mimic the vascular pathology and/or the brain damage associated with lacunar stroke (i.e. that produced small lesions secondary to a

disorder of a perforating artery of a size and distribution consistent with human lacunar lesions). We also sought models of conditions associated with similar pathology (e.g. generalised white matter disease or vascular dementia) as unlike our systematic review of human pathology we wanted to capture any potential animal model of related pathology that could be pertinent to lacunar stroke not just those which explicitly claimed to be so.

3.2.2 Search Strategy

We identified studies with a search strategy developed with advice from the Cochrane Collaboration Stroke Group, across three English language databases (Medline, Embase and Biosis Previews) adjusted to accommodate different medical subject heading (MeSH) terms or subcategories available on each database (see appendix C). We searched from 1st January 1950 to 30th June 2007, and included English and non-English language publications. We also hand searched two journals which had published a large proportion of relevant material (*Stroke* and *Journal of Cerebral Blood Flow and Metabolism*) and cross-checked reference lists of primary papers, review articles and books on subcortical stroke.

3.2.3 Inclusion and Exclusion Criteria

We sought animal models which could produce small subcortical lesions, in white or deep grey matter, by ischaemic or other mechanisms. We excluded studies published only in abstract (due to insufficient information). We were careful to include each study only once (although in the case of multiple publications, all available relevant data from each study were included). We specifically excluded (Figure 3.1): non-stroke literature; human studies; primary cerebral haemorrhage, global ischaemia and distal middle cerebral artery occlusions (MCAO, as only cortical infarcts are produced); models which only produced lesions over $100mm^3$ in volume, (too large); and the collagen type IV alpha 1 subunit (COL4A1) genetic mouse(Gould et al. 2006) (develops primary intracerebral haemorrhage at birth). We included the CADASIL transgenic mouse(Ruchoux et al. 2003) as it displays small vessel pathology pertinent to human CADASIL.

3.2.4 Data Extraction

From each study we extracted data pertaining to; purpose of the model and the aspect of pathology being modelled, characteristics of animals used (species, strain, weight, sex, age, any comorbidity), number of animals, method of stroke induction, use of randomization (if appropriate), outcomes assessed (histology, imaging, neurobehavioural tests, etc), blinding of outcome assessment to key variables, lesion size and brain territory affected. For the full data extraction form see appendix (D).

3.2.5 Study Quality Assessment

We assessed study quality using the CAMARADES database(Macleod et al. 2004). We focused on seven of the 10 CAMARADES items relevant to observational studies (see table 3.1). We categorised studies by induction method and analysed the type and distribution of tissue and vessel lesions produced in each model and their relevance to human lacunar stroke.

Table 3.1 The 7 point study quality checklist applied to all included studies

Blood characteristics – was blood pressure taken and /or blood gases monitored?	
Published in a peer review journal?	
Was body temperature controlled?	
Anaesthesia - does the anaesthetic used have intrinsic neuroprotective properties?	
Sample size calculation performed?	
Statement of compliance with regulatory requirements – e.g. UK Home Office regulations.	
Conflict of interest statement?	
Total /7	

Checklist based on the CAMARADES checklist devised by MacLeod et al(Macleod et al. 2004).

3.3 Results

Our systematic search produced 17821 articles in the first instance (figure 3.1). We reviewed (and where necessary translated) the abstracts of 5670 publications with relevant titles. After meeting abstracts and review articles were excluded, 340 primary papers were examined in full. Following discussion amongst co-authors, 46 papers were deemed appropriate describing 41 studies (table 3.1).

3.3.1 Methodological characteristics of included studies

Eight publications openly stated (either within the aim, conclusion or title) that their model represented lacunar stroke. Three models were cited as representing lacunar stroke in subsequent literature by others but were not claimed as a model of lacunar stroke by the original authors. Seventeen appeared to us to be pertinent (although were not directly attributed by the authors to) lacunar stroke because they produced small deep lesions in relevant areas of brain. The remaining 12 models attempted to recreate an aspect of small vessel stroke pathology (e.g. vasoconstriction via endothelin-1 injection) which might be relevant and so where included.

Most models used rodents, but dogs, primates and rabbits were also used (table 3.1). The mean number of animals per study was 42 (range 6-242), with considerable variation in number between induction techniques. The sex and age of animals were particularly difficult to extract: 42% of studies used male animals only, 5% female only, 30% both and 23% did not specify the sex. At least 18% used adults (age not given), 10% used adolescents, 25% used a range of ages; 47% did not specify the age and only one study specifically used older animals. Few animals had co-morbidities like hypertension.

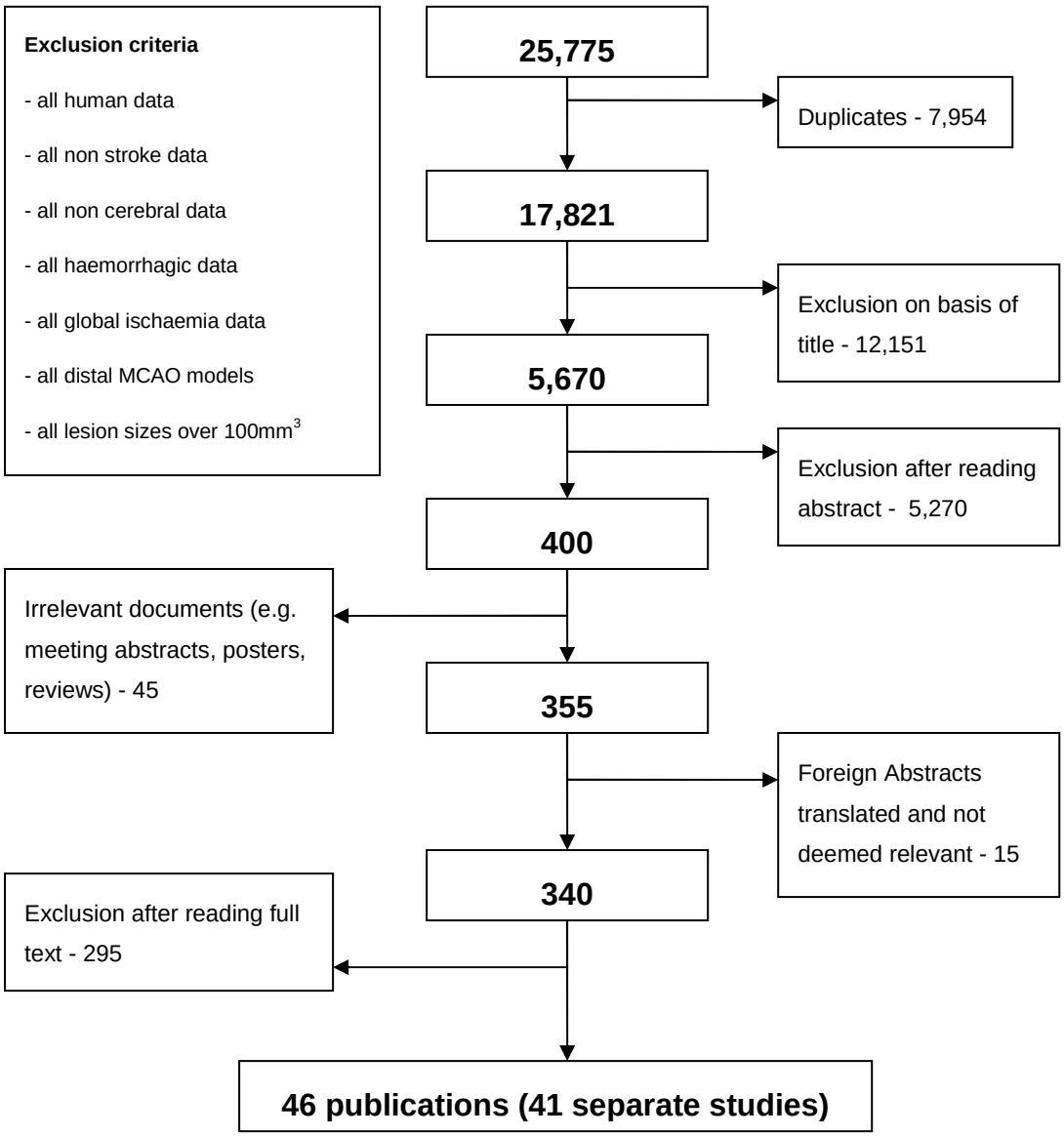

Figure 3.1. Summary of the search strategy and exclusion criteria for experimental studies of lacunar stroke.

Infarct size was poorly described and standardised. 39% did not give infarct measurements at all. Of those that did, there were ten different measurement methods (figure 3.2). Standardised comparisons of infarct size between or within models were therefore limited to descriptive analyses. From descriptions and figures provided, infarcts from many studies were diversely spread around the brain in cortical grey and white matter. Many subcortical lesions better resembled a human striatocapsular than a lacunar infarct. Figure 3.3 demonstrates the size of a lacunar lesion relative to each species' brain assuming a similar lesion:brain size ratio to humans. These small deep lesions are not only extremely difficult to create but also difficult to measure accurately with current techniques. The figure also demonstrates the added complication of the substantial differences in white:grey matter ratios between primates and rodents.

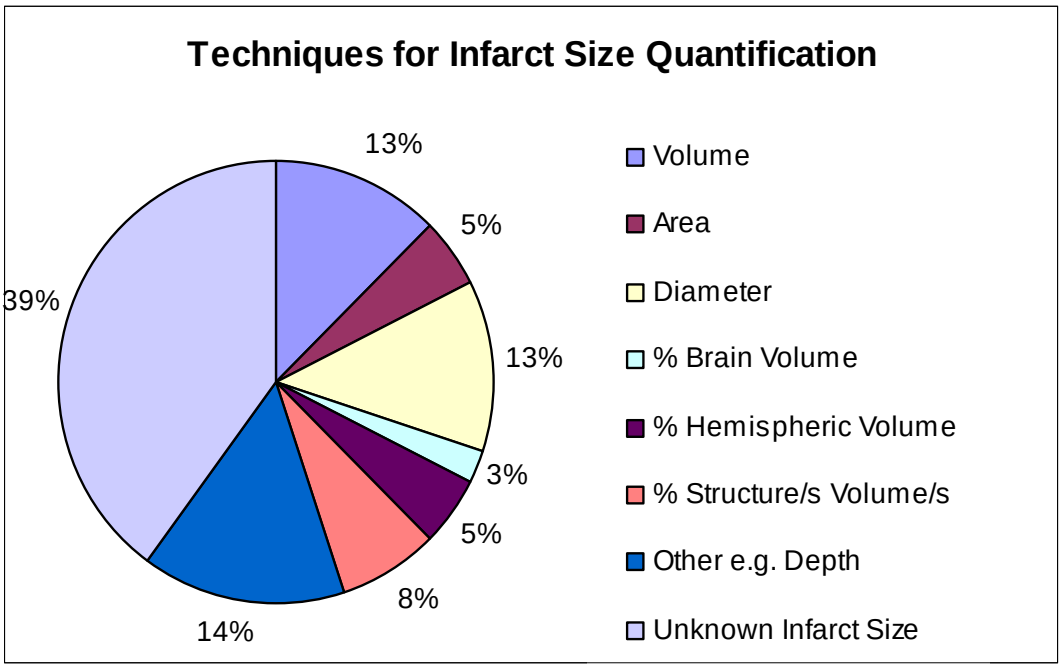

Figure 3.2 Methods of infarct quantification used within the 41 studies selected for inclusion.

Physiological variables during surgery were poorly reported: 28/41 studies stated that body temperature was controlled, but blood pressure and respiration were only stated to be controlled in eight (20%) and five (12%) respectively. Most models sacrificed animals within a week of surgery: 9/41 (22%) within 24 hours, 23/41 (56%) between one and seven days. Long term survival experiments were conducted mainly in transgenic animals or spontaneously hypertensive stroke-prone rats (SHRSP). There were few neurological assessments: 10/41 (24%) publications used a validated neurological test; 12/41 others (29%) used a self-devised scale usually described as 'mild', 'moderate' and 'severe'. The median score on the CAMARADES study quality checklist(Macleod et al. 2004) was 3/7 (range of 2-6/7), reflecting rather poor reporting of key methodological criteria.

3.3.2 Lesion induction methods

There were six categories of primary stroke induction technique: embolism, MCAO, individual perforating vessel occlusion, parenchymal endothelin-1 (ET-1) injection, spontaneous lesions and miscellaneous (table 3.1).

3.3.2.1 *Embolism:*

(8 studies(Molinari 1970a;Molinari 1970b;Futrell et al. 1991;Macdonald et al. 1995;Roos et al. 1996;Roos and Sperber 1998;Chen et al. 2001;Atochin et al. 2004;Lozano et al. 2007),433 animals, mostly rodents): Injection of different amounts and sizes of emboli (microspheres, black beads, silicone rubber cylinders, preformed clots) into the internal carotid artery produced unpredictable infarcts(Molinari 1970a;Molinari 1970b;Roos et al. 1996;Roos and Sperber 1998;Chen et al. 2001;Atochin et al. 2004). Whilst small emboli in sparse numbers could produce subcortical infarcts, most emboli produced cortical infarcts(Macdonald et al. 1995). Some models irradiated the internal/common carotid arteries in the presence of a photosensitive dye to produced an embolic source said to mimic thrombus generation on an atherosclerotic carotid artery plaque(Lozano et al. 2007). This produced multiple infarcts, mostly cortical with a few in the basal ganglia and the caudate nucleus, but the subcortical lesions were poorly documented making their relevance to lacunar infarction uncertain.

3.3.2.2 *MCA occlusion:*

(7 studies(Crowell et al. 1970;DeGirolami et al. 1984;Memezawa et al. 1992;Belayev et al. 1999;He et al. 1999;He et al. 2000;Lindner et al. 2003;Gharbawie et al. 2006) ,385 animals; primates, pigs and rodents): Two approaches were described: a) the intraluminal MCA thread occlusion; and b) selective anterior choroidal or hypothalamic artery occlusion. The intraluminal thread occlusion model is a widely used large artery ischaemic stroke model, which first damages subcortical and later cortical structures(Crowell et al. 1970). 30 minutes of MCA occlusion produced purely subcortical lesions <1cm diameter in primates(DeGirolami et al. 1984). Occlusion for up to 4 hours created infarcts in subcortical structures in primates(DeGirolami et al. 1984) that mimicked human striatocapsular infarcts(Warlow et al. 2008f) in terms of size and structures affected. Striatocapsular infarcts affect the majority of the basal ganglia or adjacent white matter and are accounted for by either transient MCA mainstream occlusion with early reperfusion, or if the occlusion persists, then with very good collateral flow from the anterior or posterior arteries to the cortical MCA territory. Selective occlusion of the anterior choroidal and hypothalamic artery origins by precise placing of the intraluminal thread in the artery mouth(He et al. 1999;He et al. 2000) produced subcortical infarcts. The anterior choroidal lesions were generally of striatocapsular dimensions; the hypothalamic lesions seemed particularly pertinent to lacunar stroke but were poorly described.

3.3.2.3 *Perforating artery occlusion:*

(8 studies(Yonas et al. 1981;Vajda et al. 1985;del Zoppo et al. 1986;Kuwabara et al. 1988;Brenowitz and Yonas 1990;Pevsner et al. 2001;Wang and Walz 2003;Hua and Walz 2006), 119 animals; rat, monkey, dog): Small cortical infarcts, produced in rats by occluding a cortical pial artery on the brain surface using forceps or photochemical irradiation(Pevsner et al. 2001;Wang and Walz 2003) were described as mimicking lacunar infarction because the showed “cavitation caused specifically by ischaemia of smaller vessels” (however the lesions were cortical)(Hua and Walz 2006). In primates, a balloon cuff placed around the proximal MCA and inflated for 3 hours produced thrombus formation within the lenticulostriate arteries(del Zoppo et al. 1986)and resulted in tissue softening, necrosis and cyst formation with an average volume of 3.9cm^3. Others coagulated or crushed many arterioles (thalamoperforators, lenticulostriates, etc). These lenticulostriate occlusion models produced lesions equivalent in size to a striatocapsular infarct in a variety of brain regions, rather than lacunar lesions in more characteristically defined areas.

3.3.2.4 *ET-1 injection:*

(4 studies(Fuxe et al. 1992;Hughes et al. 2003;Whitehead et al. 2005;Frost et al. 2006), 114 animals; rats): ET-1, a powerful vasoconstrictor, when injected into the subcortical tissues in a dose-dependent manner produces ischaemic lesions(Sharkey et al. 1993). The powerful vasoconstrictive action may affect several microvessels. ET-1 injected into deep grey matter caused a small lesion with neuronal and astrocyte loss and delayed macrophage/microglia response;(Fuxe et al. 1992) into white matter caused axonal and oligodendrocyte disruption followed by myelin damage and increased astrocyte reactivity(Whitehead et al. 2005). The histological changes in the vasoconstricted vessels were not reported.

3.3.2.5 Spontaneous lesions:

(9 studies(Knox et al. 1980;Ogata et al. 1981;Ogata et al. 1982;Fredriksson et al. 1985;Tagami et al. 1987;Fredriksson et al. 1988;Su et al. 1998;Lin et al. 2001;Sironi et al. 2004;Garosi et al. 2006;Rossmeisl, Jr. et al. 2007), 466 animals; rats, dogs): The SHRSP(Okamoto et al. 1974) develops hypertension followed by stroke-like neurological symptoms with increasing age. Studies in rats from 4-52 weeks of age showed that a combination of malignant hypertension, a genetic predisposition to stroke and high salt diet were all risk factors for spontaneous stroke(Knox et al. 1980;Ogata et al. 1981;Ogata et al. 1982;Fredriksson et al. 1985;Fredriksson et al. 1988;Lin et al. 2001;Sironi et al. 2004). Pathology, all in the perforating arteriolar territories, included microinfarcts, small haemorrhages and multiple white matter cysts. The primary event was endothelial disruption, with BBB breakdown (shown using multiple techniques) being the likely cause of the “ischaemic” lesions(Sironi et al. 2004) with arteriolar wall thickening, luminal narrowing or dilatation and thrombotic occlusion being late secondary features, long after extensive subcortical damage was already apparent. Elderly dogs also suffer spontaneous strokes with neurological deficits (hemiparesis, facial hypalgesia and hemianopia), but are less researched(Su et al. 1998;Garosi et al. 2006;Rossmeisl, Jr. et al. 2007).

3.3.2.6 Miscellaneous:

(5 studies(Yoshimoto et al. 1978;Matsumoto et al. 1990;Toshima et al. 2000;Ruchoux et al. 2003;Shibata et al. 2004), 194 animals; various species): Simultaneous occlusion of four main cerebral arteries for 60-120mins in dogs produced thalamic infarction alone, and was considered to be a low perfusion model(Yoshimoto et al. 1978). Sodium Laurate injected into a cortical cerebral artery in rats

induced endothelial necrosis, intravascular thrombus formation and occlusive stroke but caused damage that was predominantly cortical and too extensive for lacunar stroke(Toshima et al. 2000). Unilateral carotid occlusion from 5 to 30 minutes in the gerbil produced a large artery territorial infarct(Matsumoto et al. 1990). A transgenic notch3 mouse modelling CADASIL pathology produced smooth muscle proliferation in the small arteriolar walls similar to human CADASIL (mostly in the tail not the brain) and few stroke lesions(Ruchoux et al. 2003). Bilateral carotid artery stenosis, created by placing microcoils around the carotid arteries in mice, produced hypoperfusion accompanied 14 days later by white matter lesions(Shibata et al. 2004) judged to be a cumulative consequence of hypoperfusion. However these white matter lesions share common features with those seen in subcortical vascular dementia and were considered primarily to reflect BBB disruption(Shibata et al. 2004).

Table 3.2. Summary of included studies by induction method.

	Author/Reference	Year	Induction method	Species	n	Age & Co-morbidity?	Infarct Size	Study Quality Score
Embolism	Molinari(Molinari 1970a)	1970	Silicone Rubber Emboli	Dog	25	unknown	unknown	3
	Futrell(Futrell 1991)	1991	Photo-coagulation of ICA	Rat	33	unknown	200-1200uM diam	3
	Miyake(Miyake et al. 1993)	1993	Microsphere emboli	Rat	242	unknown	77% of ipsil hemis	6
	MacDonald(Macdonald et al. 1995)	1995	Microsphere emboli	Monkey	9	unknown	unknown	5
	Roos(Roos et al. 1996)	1996	Black bead emboli	Rabbit	18	unknown	0.5-3mm diam	4
	Chen(Chen et al. 2001)	2001	Preformed fibrin clot into right ICA	Rat	27	unknown	unknown	4
	Atochin(Atochin et al. 2004)	2004	Fibrin Microemboli	Mice	44	Adult	<40mm^3 UK	4
	Lozano(Lozano et al. 2007)	2007	Photo-coagulation of ICA	Mice	35	Range	7-15% brain volume	4
MCA occlusion	Crowell(Crowell et al. 1970)	1970	Scoville clip on MCA origin	Monkey	65	unknown	3mm diameter average	3
	DeGirolami(DeGirolami et al. 1984)	1984	Transorbital snare ligation of MCA	Monkey	87	unknown	< 2cm diameter	2
	Memezawa(Memezawa et al. 1992)	1992	Intraluminal thread MCA occlusion	Rat	42	unknown	40% of Caudoputamen	4
	Belayev(Belayev et al. 1999)	1999	Intraluminal thread MCA occlusion	Mice	49	unknown	4.5 - 9mm^2	5
	He(He et al. 1999)	1999	Intraluminal occlusion of AChA & HTA	Rat	80	Adolescent	6-48mm^3	6
	Lindner(Lindner et al. 2003)	2003	Intraluminal thread MCA occlusion	Rat	50	Adult	4-27% of hemisphere	4
	Gharbawie(Gharbawie et al. 2006)	2006	Intraluminal thread MCA occlusion	Rat	12	Adolescent	% of 3 structures damaged	4
Perforating artery occlusion	Yonas(Yonas et al. 1981)	1981	Retro-orbital occlusion of lateral lenticulostriates	Monkey	9	unknown	Unknown	3
	Vajda(Vajda et al. 1985)	1985	Posterior thalamic arteries occluded	Monkey	10	unknown	unknown	2
	Del Zoppo(del Zoppo et al. 1986)	1986	Balloon cuff around MCA	Monkey	22	Adolescent	3.9cm^3	4
	Kuwabara(Kuwabara et al. 1988)	1988	Occlusion of Posterior Cerebral perforators	Dog	24	unknown	Unknown	3
	Brenowitz(Brenowitz and Yonas 1990)	1990	Occlusion of Anterior cerebral artery branches	Dog	42	unknown	0.73cm^3	3
	Pevsner(Pevsner et al. 2001)	2001	Cortical Photo-coagulation	Rat	12	Adult	1.7-4.2mm depth	3
	Wang(Wang and Walz 2003)	2003	Cortical pial vessel crush	Rat	UK	Adult	1629 +/- 261um diameter	3
	Hua(Hua and Walz 2006)	2006	Cortical pial vessel crush	Rat	UK	Adult	1.09mm^3	3

	Author	Year	Induction method	Species	n	Age & Co-morbidity?	Infarct Size	Study Quality
Endothelin-1 injection	Fuxe(Fuxe et al. 1992)	1992	ET-1 injection (Intra-striatal)	Rat	11	unknown	1-6mm^3	3
	Hughes(Hughes et al. 2003)	2003	ET-1 injection (striatum and subcortical WM)	Rat	38	Adult	17.5ul / 20um^2	5
	Frost(Frost et al. 2006)	2005	ET-1injection (striatum)	Rat	40	unknown	unknown	4
	Whitehead(Whitehead et al. 2005)	2006	ET-1 injection (Internal Capsule)	Rat	25	unknown	~500uM diameter	5
Spontaneous stroke	Knox(Knox et al. 1980)	1980	Naturally occurring strokes in SHRSP	Rat	43	Range + Hypertension	Unknown	4
	Ogata(Ogata et al. 1981)	1981	Naturally occurring strokes in SHRSP	Rat	88	Range + Hypertension	150um - 1.5mm diameter	3
	Fredriksson(Fredriksson et al. 1985)	1985	Naturally occurring strokes in SHRSP	Rat	55	Range + Hypertension	Unknown	3
	Tagami(Tagami et al. 1987)	1987	Naturally occurring strokes in SHRSP	Rat	84	Range + Hypertension	Unknown	2
	Su(Su et al. 1998)	1998	Naturally occurring strokes	Dogs	18	Range	Unknown	3
	Lin(Lin et al. 2001)	2001	Naturally occurring strokes in SHRSP	Rat	38	Range + Hypertension	Unknown	2
	Sironi(Sironi et al. 2004)	2004	Naturally occurring strokes in SHRSP	Rat	96	unknown + Hypertension	Unknown	2
	Garosi(Garosi et al. 2006)	2006	Naturally Occurring strokes	Dog	38	Range	Unknown	2
	Rossmeisl(Rossmeisl, Jr. et al. 2007)	2007	Naturally Occurring strokes	Dog	6	Range	9-21mm diameter	3
Miscellaneous	Yoshimoto(Yoshimoto et al. 1978)	1978	Simultaneous occlusion of ICA, ACA, MCA and PCA	Dogs	43	Adult	Amount of thalamus damaged	3
	Matsumoto(Matsumoto et al. 1990)	1990	Unilateral carotid occlusion	Gerbil	20	unknown	</> 0.2mm	3
	Toshima(Toshima et al. 2000)	2000	2 injections of sodium laurate into ICA	Rat	56	Adult	8% of slice area?	3
	Ruchoux(Ruchoux et al. 2003)	2003	Genetic model of CADASIL	Mice	15	Range	0.2-0.6um?	3
	Shibata(Shibata et al. 2004)	2004	Bilateral Carotid Artery Occlusion	Mice	60	Adolescent	Unknown	3

N = number of animals; SHRSP = Spontaneously Hypertensive Stroke-Prone Rat = MCA, Middle Cerebral Artery; ICA = Internal Carotid Artery; ACA = Anterior Cerebral Artery; PCA = Posterior Cerebral Artery; HTA = Hypothalamic Artery; AChA = Anterior Choroidal Artery; WM = White matter; ET-1 = Endothelin-1; CADASIL = Cerebral Autosomal Dominant Arteriopathy with Subcortical Infarcts and Leukoencephalopathy.

3.4 Discussion

Our systematic search discovered animal models (using over 10 different induction techniques) which were able to reproduce brain lesions, microvessel pathology, or both, which could be representative of lacunar stroke. However, most models produced infarcts which were too large or affected the wrong brain territory to be fully pertinent. Some models could be useful for evaluating novel treatments for lacunar-sized ischaemic subcortical lesions, but few attempted to explain the small vessel changes associated with most lacunar stroke in humans. Only one established model, the SHRSP, produced lesions that mimicked the small vessel and brain parenchymal pathology. In this particular model, the primary event is BBB disruption, with vessel occlusion and brain ischaemia occurring well after tissue damage caused by edema fluid is visible. The widespread and primarily cortical infarct distribution encountered in models using emboli indicated that emboli or microthrombi were an unlikely cause of most human lacunar stroke. This finding is consistent with human epidemiological data(Jackson and Sudlow 2005a).

This review has limitations. The methodology for systematic reviews of observational studies in animals is still evolving. Trying to capture the exact literature is difficult as currently, key word usage is too generalised and potentially subjective. We used multiple overlapping study ascertainment methods but may still have missed some key models. Any full assessment of the relevance of experimental models of subcortical stroke is hampered by the incomplete knowledge and confusing terminology of lacunar stroke pathology in humans. The location and small lesion size makes modelling of lacunar stroke difficult in small mammals. Reproducing a $1cm^3$ human infarct relative in size to a mouse or rat's brain requires skill and advanced measuring techniques (figure 3.3)(Yang et al. 1998;Zhang and Sejnowski 2000;Bush and Allman 2003). A further limitation is the substantially lower white:grey matter ratio in rodents (approximately 14:86%) compared with primates (40:60%)(Bush and Allman 2003).

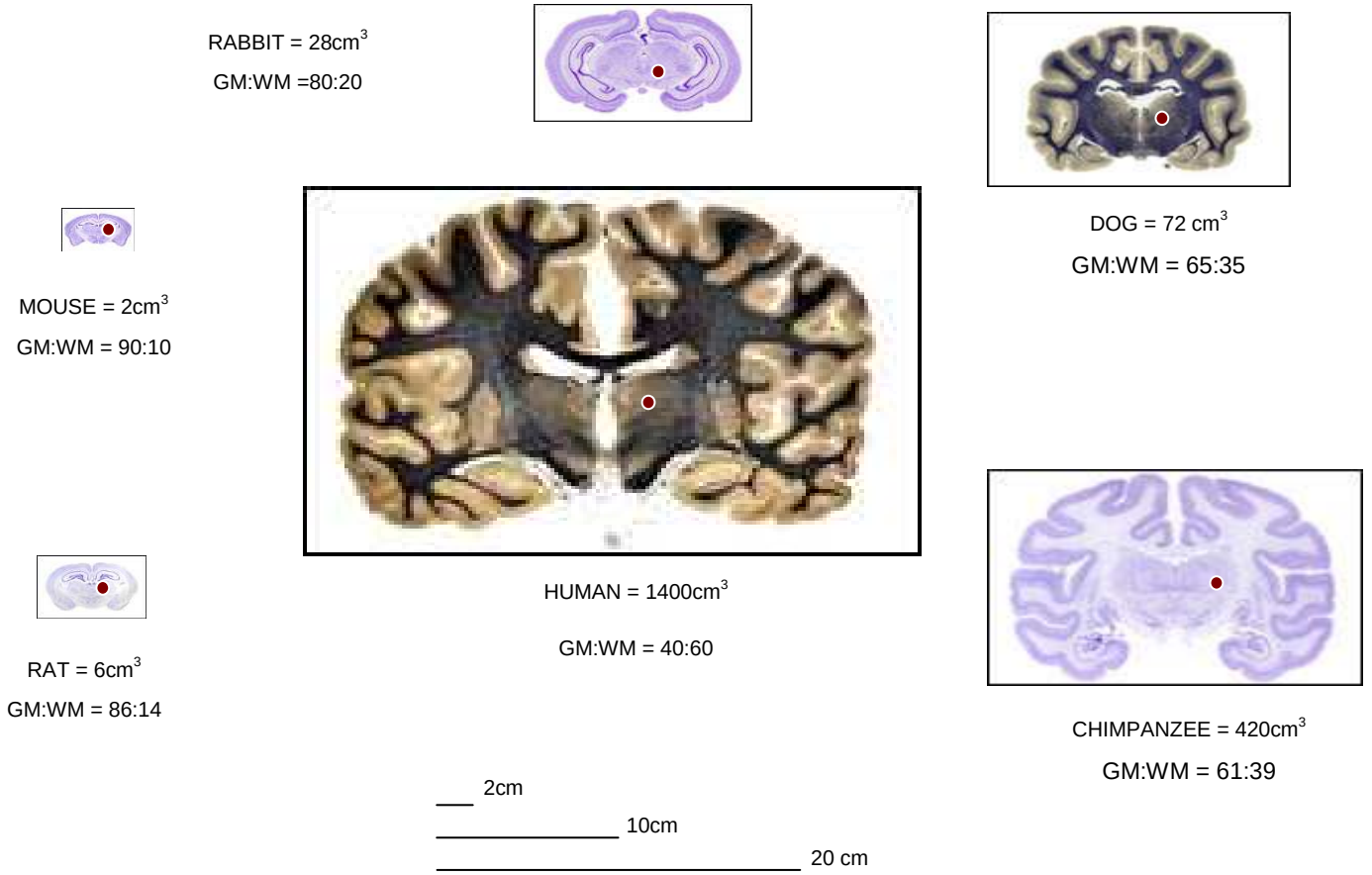

Figure 3.3 Approximate brain volume (cm^3) and grey: white matter ratio in healthy (young) animals shown relative to the human brain

Red dots indicate a human sized lacunar lesion superimposed onto animal species' brains. The red dots also illustrate the difficulty in targeting a small lacunar-like lesion to white matter, particularly in smaller rodents, due to the paucity of white matter.

Study reporting was suboptimal, with the average score for key methodological factors (based on the CAMARADES score) of only 3/7. Few studies used older animals or animals with pre-existing vascular problems, even though most lacunar stroke patients are considered old and present with vascular risk factors (Dozono et al. 1991b). Few neurological / behavioural assessments occurred in animal models, whilst clinical examination for 'lacunar syndromes'(Warlow et al. 2008e) is the first assessment of a potential lacunar stroke patient. Therefore behavioural tests which are sensitive enough to detect the effects of lacunar-like syndromes in animals are important in order to establish the symptomatic relevance of any inflicted lesions. Additionally, some models cause damage that restricts neurological assessment (e.g. blindness)(Shibata et al. 2004). The short time from induction to sacrifice did not allow the affected areas to mature, further limiting determination of lesion size and relevance.

All of the models had limitations, when trying to extrapolate results to human lacunar disease. The embolic technique produced small infarcts, but most were cortical not subcortical. Poor documentation of subcortical lesions in several models precluded reliable assessment of whether the lesions were large subcortical (i.e. striatocapsular equivalent) or true lacunar. Human lacunar stroke may be caused by MCA atheroma occluding the lenticulostriate artery origin. The most promising model equivalent was selective occlusion of the anterior choroidal or hypothalamic arteries which produced some small infarcts (He et al. 1999). The hypothalamic infarcts in particular appeared comparable with lacunar infarcts (author's comment), but were overlooked in favour of the anterior choroidal artery lesions(He et al. 2000). Other models that occluded lenticulostriate trunks or multiple ostia produced striatocapsular-like not lacunar lesions(Brenowitz and Yonas 1990). ET-1 injection produced small subcortical lesions but caused several microvessels to be constricted simultaneously so was inconsistent with the "single vessel" theory of lacunar stroke. The CADASIL transgenic mouse mimics some aspects of human CADASIL(Ruchoux et al. 2003), but the vessel changes are mainly encountered in the tail with minimal effects on the cerebral vessels and few if any cerebral lesions. A lacunar stroke model in the miniature pig was published after the June 2007 cut off(Tanaka et al. 2008).

3.5 Conclusion

The only model that mimics both microvessel and parenchymal changes is the spontaneous stroke in SHRSP(Blezer et al. 1998;Sironi et al. 2004). However the initiating step is BBB disruption leading to parenchymal and arteriolar damage, so the mechanism is not primarily ischaemic, in that although arteriolar wall thickening could lead to luminal narrowing and thrombosis, these only occur late, secondary to earlier events, after much brain damage due to perivascular edema fluid has already occurred. Several other features commonly associated with human lacunar stroke have also been observed in SHRSP (e.g. dilated perivascular spaces). This species is highly inbred and may therefore be of limited relevance, but the microvascular and brain morphological features are so similar to those described in humans that it is hard to ignore. However, if the SHRSP truly does mimic human lacunar disease, then a major move away from traditional occlusive/ischaemic mechanisms towards endothelial/BBB disruption mechanisms will be required in order to advance understanding of the development of lacunar stroke and associated features of small vessel disease in humans(Yamori et al. 1976a). Further studies to characterise the small vessel morphological changes in SHRSP in more detail would be worthwhile.

CHAPTER 4 : THE SPONTANEOUSLY HYPERTENSIVE STROKE PRONE RAT AS A MODEL OF SUBCORTICAL ISCHAEMIC STROKE. A SYSTEMATIC REVIEW.

4.1 Background

The Spontaneously Hypertensive Rat family was developed by selective cross breeding of out bred Wistar Kyoto Rats (WKY) and consists of two main members: the Spontaneously Hypertensive Rat (SHR) (1963) which has elevated blood pressure (~180mmHg systolic) but rarely shows signs of stroke (sometimes known as the stroke-resistant SHR – SHRSR)(Okamoto and Aoki 1963) and the Spontaneously Hypertensive Stroke Prone Rat (SHRSP) (1974)(Okamoto et al. 1974) selectively bred from a substrain of the SHR that showed signs of stroke and had malignant hypertension (~220mmHg systolic); The precise mechanisms underlying the stroke-proneness and stroke-resistance are unclear. The SHR family has been used to model a wide range of conditions from attention deficit hyperactivity disorder to osteoporosis. In stroke research, the SHRSP has mainly been used in middle cerebral artery (MCA) occlusion models to produce large MCA territory infarcts. In contrast, the spontaneous strokes suffered by SHRSP have received less attention but are generally assumed to be consequent upon elevated blood pressure and manifest as cortical and subcortical infarcts and haemorrhages(Takiguchi 1983).

In systematic reviews of potential animal models of lacunar stroke, we(Bailey et al. 2009) and others(Hainsworth and Markus 2008) noted that SHRSP seemed to demonstrate similar pathological features to the small vessel disease underlying human lacunar stroke pathology(Fisher 1968). Given human small cerebral vessels are difficult to study and tissue for histopathology is difficult to obtain, the cause of human lacunar stroke remains unclear(Wardlaw 2005). Numerous studies describe the cerebral pathology encountered in SHRSP, but no systematic summary of this literature is available. Clarification of the pathology underlying the spontaneous vascular and tissue lesions in SHRSP would aid understanding of human lacunar stroke and related small vessel disease.

Therefore, we gathered all published studies documenting spontaneous cerebral pathological changes in both vessels and tissue of SHRSP for a detailed assessment of the type and sequence of vascular and tissue damage(Masineni et al. 2005).

4.2 Materials and Methods

4.2.1 Search strategy

We searched using the terms 'SHRSP' and/or 'Spontaneously-Hypertensive Stroke Prone Rat' and all possible variants of these text strings in three online databases, Medline, Embase and Biosis Previews. We limited the search to full text primary research articles, describing cerebral vascular or tissue pathology, published between 1974 (the SHRSP was developed in 1974) and May 2010. We removed duplicate publications, conference abstracts, reviews, publications on artificially induced ischemia, non-cerebral changes, drug interventions and genetics. Where multiple publications arose from the same animal cohort, we attributed all results to one study to avoid artificially inflating total sample size.

4.2.2 Data extraction

We extracted data on: the pathology studied (e.g. vessels, tissue or both); methodologies; the number of SHRSP and control animals, their age; the area of the vasculature and/or brain studied; blood pressure and its relationship to pathological changes; and whether the rats were raised on a "Japanese diet" (high sodium (4%):low potassium (0.75%)), had sodium chloride (1%) supplemented into their drinking water ("salt loaded")(DiNicolantonio and Silvapulle 1988) or were fed standard rat chow.

We subcategorized studies into those which focused on blood vessels alone, brain tissue alone, both vessels and tissue, and those which examined other hematological and biochemical changes (using serum, urine or CSF biomarkers, e.g. nitric oxide concentration or platelet aggregation). We defined small cerebral vessels as arterioles that penetrated into the brain tissue and were less than 150μm diameter and larger arteries as arteries over 150μm in diameter including the basal intracranial large arteries, carotid/vertebral arteries and other systemic large arteries.

4.2.3 Study quality

We assessed study methodology with the CAMARADES criteria(Sena et al. 2007), the STARD (Standards for the Reporting of Diagnostic Accuracy studies) statement(Bossuyt et al. 2003) and MOOSE (The Meta-analysis Of Observational Studies in Epidemiology) criteria(Stroup et al. 2000) (www.equatornetwork.org). We did not seek data on body temperature, anaesthesia or compliance with animal welfare regulations as surgical procedures were rare.

4.3 Results

4.3.1 The available literature.

The initial search produced 4000 potentially relevant articles (Figure 4.1). Excluding conference abstracts, reviews, duplicates and artificially-induced ischemia left 496 papers. Of these, 132 papers described cerebral pathology, of which 30 were multiple publications arising from the same animals, leaving 102 independent studies.

Of the 102 studies, 10 primarily described brain tissue histopathology, 27 described vessel pathology, 14 addressed both tissue and vessel changes and 51 described serum, urine or CSF biomarkers. All studies used WKY, SHR (SHRSR) or occasionally Sprague Dawley rats as controls, although Sprague Dawley's were always used in conjunction with WKY (summary data of all the studies included are listed in appendix E of this thesis).

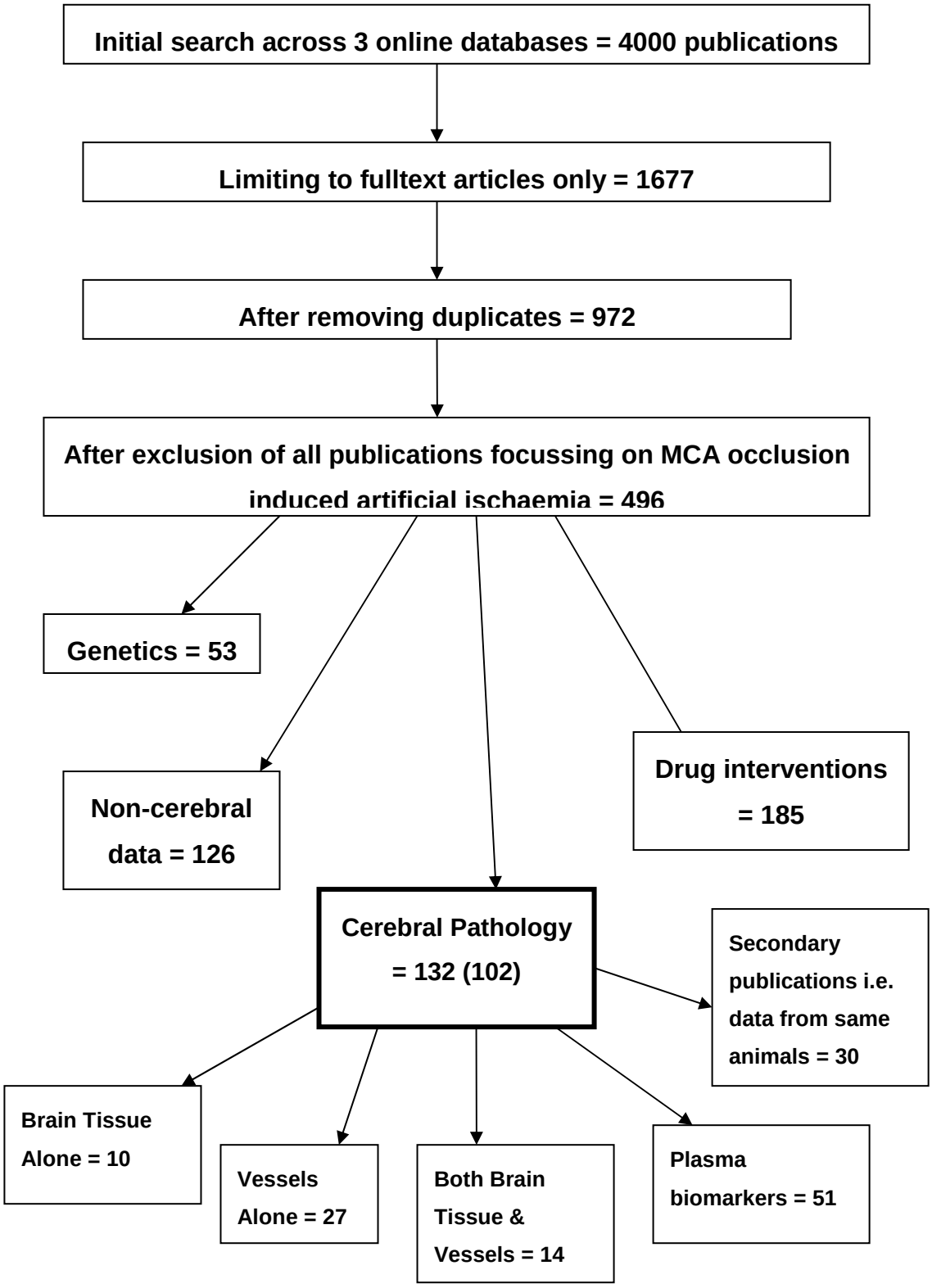

Figure.4.1 Search strategy for the retrieval of pathological papers to be included in the review.

4.3.2 Study methodology

No study mentioned whether authors were blinded to SHRSP or control rat status. Blood pressure readings were rarely documented. The total number of experimental animals per study ranged from 5(Ogata et al. 1981) (an in depth characterization of tissue and vessel pathology) to 1278(Yamori et al. 1976a), median 43 (inter quartile range 24 to 77). Nineteen studies (18%) did not state the number of rats used. Age at sacrifice (given in 97 studies) ranged from animals that were developing hypertension (i.e. >9 weeks old), had established hypertension (>12 weeks old) or had reached the high risk age for stroke (>16 weeks). Only 9 studies documented changes in pre-hypertensive animals (i.e. <9 weeks old) (figure 4.2). Five studies did not state age of sacrifice. In 24 studies (23%), rats were fed a Japanese diet (JPD) or had salt added to their drinking water (figure 4.3). Use of salt was rare prior to the 1980's but increased from 1990 onwards. We indicate whether animals were salt-loaded in relevant sections of the results. All studies that assessed inflammatory biomarkers (e.g. thiostatin) used animals raised on high salt (via diet or water supplements, n=5) or did not state the diet used (n=2).

Examination of tissue/vessel changes was mostly by histology (e.g. haematoxylin and eosin), immunohistochemistry or electron microscopy. Other methods included in vivo MRI, proteomics or combinations of these. Cerebral blood flow was measured with laser Doppler or hydrogen clearance methods.

Vascular pathology was described in 41 studies (27 vessels only; 14 both tissue and vessel changes): 23 described large artery changes (MCA, posterior cerebral artery (PCA), basilar artery (BA) and the internal carotid artery (ICA)); eight described arterioles of 150µm diameter or less. The remaining 10 studies analysed vessels of an unspecific size and / or brain region. We found no studies of venular pathology or pre-hypertensive changes in arterioles (only large arteries) as all studies describing small vessel pathology sacrificed animals after 13 weeks of age. Tissue damage was described in 23 studies, but most (n=19) described data from the cortex (predominantly frontal cortex) with only occasional references to deep grey matter and little information (n=2) on white matter. Data on numbers of animals in each study, plus other study characteristics are available in appendix D of this thesis.

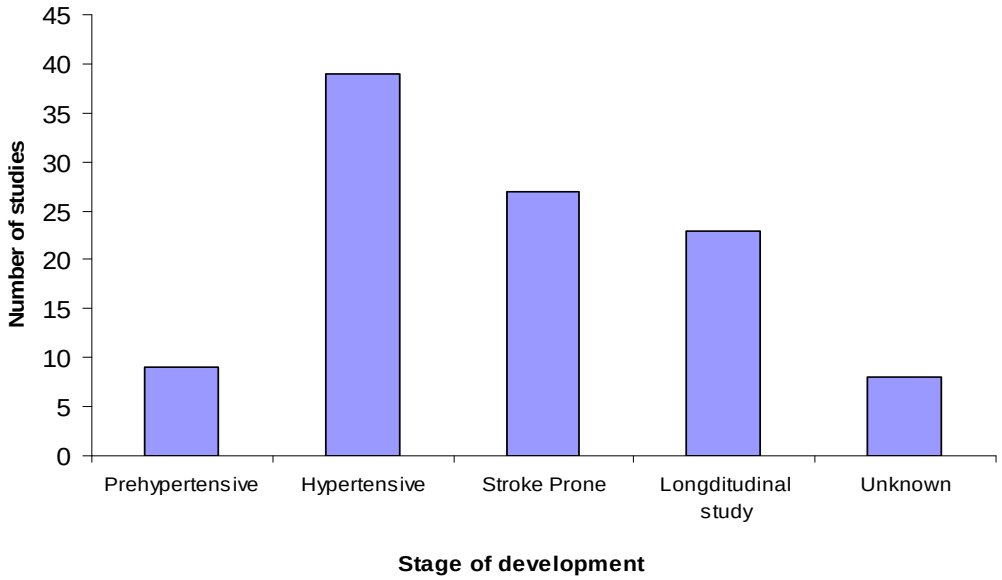

Figure.4.2. Ages of animals used in pathological studies.

Prehypertensive = majority of animals sacrificed at 9 weeks of age or less. Hypertensive = majority of animals sacrificed between 10-16 weeks of age. Stroke Prone = animals sacrificed at any time over 16 weeks of age. Longitudinal study = animals sacrificed at various ages over 9 weeks of age. Unknown = data unobtainable.

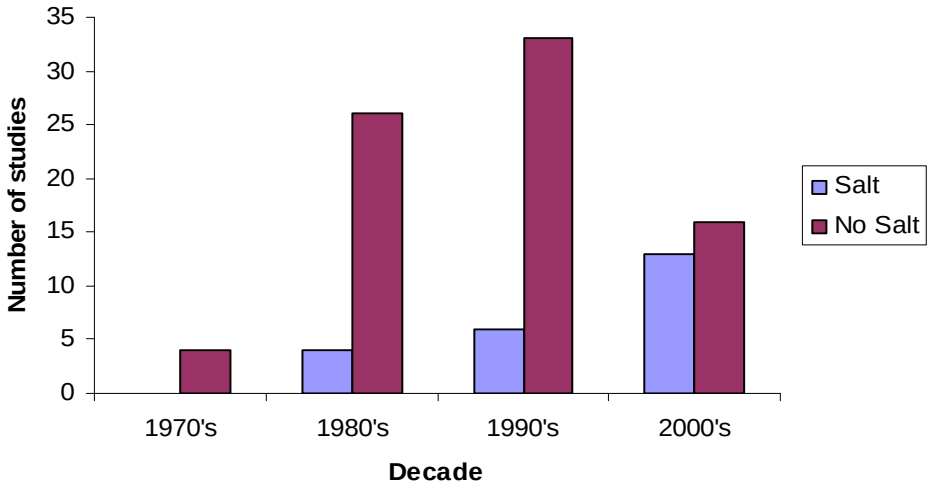

Figure 4.3. Number of studies using salt- in pathological studies by decade.

Studies that stated whether salt was administered salt- n= 24. Studies that did not add salt to the rat's diet n = 78. Some groups administered salt from as young as 4 weeks old others did not introduce salt until 9 weeks old and beyond. Salt included the JPD on its own, JPD plus 1% NaCl in drinking water or just varying levels of NaCl within drinking water (~1-4% solution).

4.3.3 Structural Pathological Findings - Brain parenchyma (Figure. 4.4):

Most (12/14) studies examined animals during or after the onset of hypertension. Tissue damage in SHRSP seemed mostly to occur in the frontal cortex and basal ganglia(Yamori et al. 1976a;Rodda et al. 1983;Tabuchi et al. 2002), usually within the territory of the MCA/ACA, MCA/PCA borderzones(Coyle and Feng 1993) and the lenticulostriate arteries(Yamori et al. 1976a). Cerebral pathology included cortical infarcts, enlarged perivascular spaces(Tagami et al. 1987;Fredriksson et al. 1988), white matter damage, microinfarcts and microaneurysms(Yamori et al. 1976a;Takiguchi 1983;Minami et al. 1985;Chue et al. 1993) although the overall incidence of each type of these lesions is unclear. Studies that examined lesion distribution found most lesions occurred in the basal ganglia(Yamori et al. 1976a). The earliest brain tissue abnormalities in SHRSP were documented with MRI(Sironi et al. 2004)'(Guerrini et al. 2002). Here, animals raised on a Japanese diet from 6 weeks of age, by 10-12 weeks had blood brain barrier (BBB) failure on intravenous gadolinium-enhanced MRI(Sironi et al. 2004) and tissue lesions consisting of small foci of perivascular extracellular edema as shown by abnormal apparent diffusion coefficient (ADC) of water(Guerrini et al. 2002). Lesions started in the caudate and putamen(Rieke et al. 1981) and spread through the subcortical region. At sacrifice, lesions were associated with fibrinoid necrosis in the media, although the type/size of vessel displaying this pathology was unclear(Sironi et al. 2004).

White matter lesions (WML) were more often seen in SHRSP than in SHR and increased with advancing age(Lin et al. 2001). At 20 weeks, WML were more frequent ($p<0.05$) in four separate brain regions (corpus callosum, anterior commisure, internal capsule and caudate) in SHRSP compared to WKY and SHR. SHR had lesions in the caudate only(Lin et al. 2001). In SHRSP aged >24 weeks, white matter was rarefied and cystic, particularly in deeper layers where myelinated fibres are abundant(Ogata et al. 1982). At 24 weeks, in areas with BBB leakage demonstrated with Evans Blue(Fredriksson et al. 1985), the deep arterioles showed fibrinoid necrosis and subcortical gray/white matter showed haemorrhages, vacuoles and 'necrotic cysts'. By one year of age 75% of SHRSP with WML on MRI had bilateral lesions(Henning et al. 2010).

In SHRSP aged >24 weeks, perivascular spaces were dilated around perforating arterioles(Tagami et al. 1987) and within BBB leakage sites(Fredriksson et al. 1988). In SHRSP, the number of affected segments of vessels increased towards the arterial borderzones. In SHRSP aged >40 weeks, microinfarcts less than 150µm in diameter were frequently encountered in the neocortex around arterioles showing fibrinoid necrosis, infarcts of varying ages were present in the cortex and subcortex(Ogata et al. 1982).

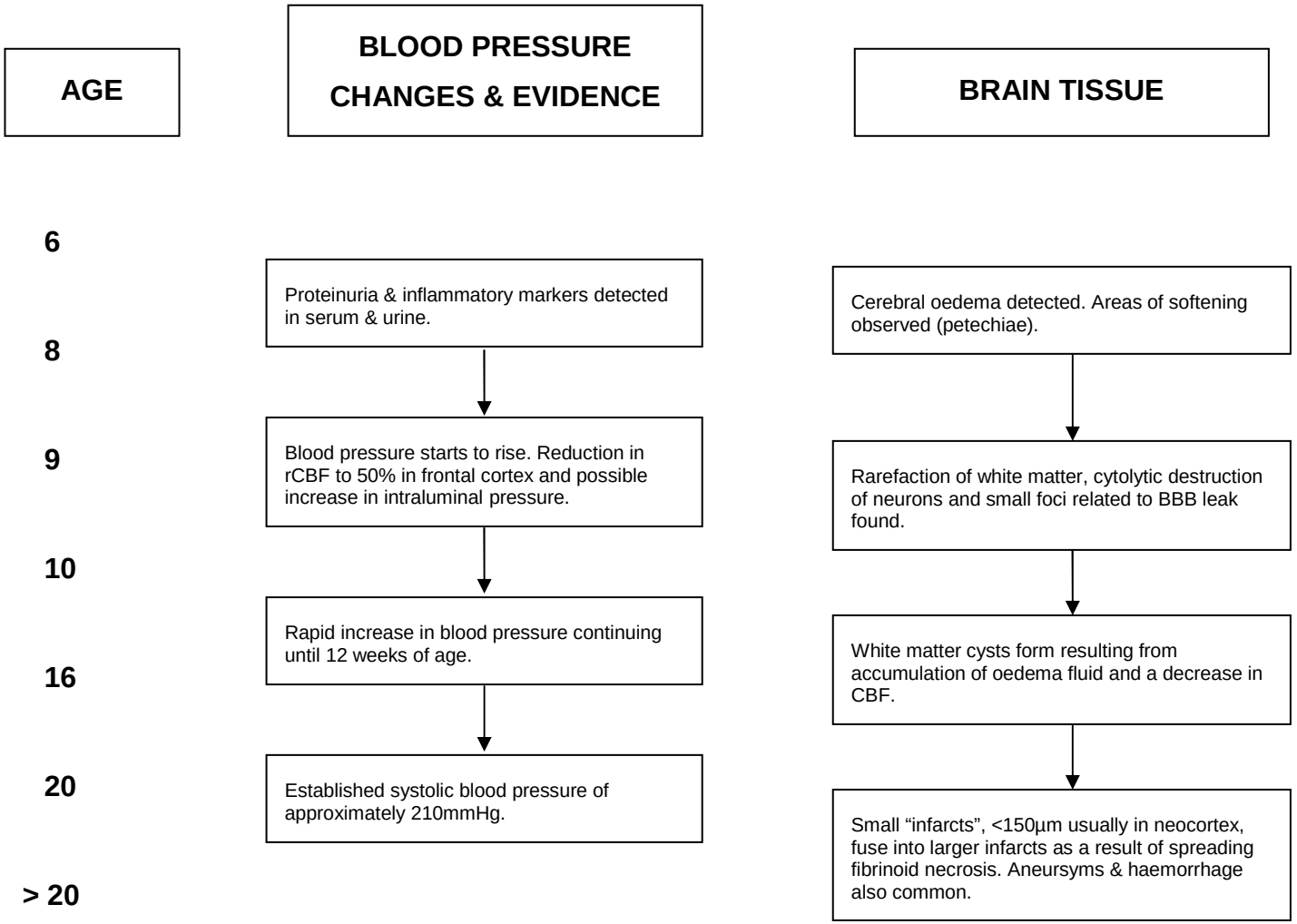

Figure 4.4. Summary of the timescale of cerebral pathological changes and their relation to age in SHRSP.

rCBF = regional cerebral blood flow. BBB = Blood brain barrier

4.3.4 Structural findings: Vessels (Figure 4.5.)

4.3.4.1 Large vessels (>150μm)

A) Prior to, or unattributed to hypertension.

Publications between 1974 and 1990 reported few structural changes in the large arteries. Ogata found no evidence of atherosclerosis or thrombosis in the major arteries(Ogata et al. 1982), however, a later study reported the external diameter of the carotid artery was less in SHRSP aged 4-8 weeks compared to WKY(Zanchi et al. 1997). Another study found vascular smooth muscle cell disorganisation (deviation from the normal 90° orientation) in all three layers of the media in the basilar artery of eight week old SHRSP compared to age-matched WKY(Arribas et al. 1996). This was not corrected by antihypertensive agents.

B) Following development of/directly attributable to hypertension

Numerous studies (17/40) described large vessel changes attributed to hypertension. Hypertrophic remodelling was common in the large arteries of SHRSP over 12 weeks of age versus WKY(Kanbe et al. 1983;Tamaki et al. 1984b;Shimizu et al. 1988;Contard et al. 1993) and media: lumen ratios were increased in SHRSP versus SHR from 8 weeks of age. In the basilar artery, PCA and MCA, this was attributed to increased smooth muscle cell layers in the media(Mangiarua and Lee 1992). Increasing media thickness also caused a progressive increase in the external diameter of the MCA. Others reported a thicker media and/or smaller internal diameter in the basilar artery, MCA and PCA versus age-matched WKY(Nordborg et al. 1985). A scanning and transmission electron microscopy study revealed as many as 10% of all smooth muscle cells in the MCA of SHRSP were necrotic by 24 weeks with no necrotic vessels in age-matched WKY(Fujiwara et al. 1990). Increased amounts of fibronectin in large vessel arterial walls in 13 week old SHRSP versus WKY was attributed to activation of smooth muscle cells in the media(Boumaza et al. 2001).

4.3.4.2 Small vessels (<150µm)

A) Prior to, or unattributed to hypertension.

Only one study examined the small vessels prior to development of hypertension(Tagami et al. 1987). In this study, SHRSP were sacrificed from 4 weeks of age, then every 4 subsequent weeks. The authors reported no small vessel changes visible with lead citrate and uranyl acetate staining before 12 weeks of age; a full description of changes was not given until 16 weeks.

B) Following development of / directly attributable to hypertension

After the onset of hypertension, most pathological changes described were in the arterioles and smaller arteries ~30µm in diameter(Mies et al. 1999), particularly the lateral group of lenticulostriate arteries in the basal ganglia(Yamori et al. 1976a), at bifurcations and anastomoses between subcortical and cortical vessels.

In 10 week old SHRSP, the mean internal diameter of ACA, MCA branches and the ACA-MCA anastomotic collateral arterioles were significantly smaller than in WKY rats(Coyle 1987). While this may be an early response to rising blood pressure, it may also suggest the arterioles in SHRSP are constitutionally smaller than WKY (in addition to the large arteries(Zanchi et al. 1997)) as hypertension is not fully established at 10 weeks. At 16 weeks, focal deposition of collagen and cytoplasmic necrosis were noted in the outer layers of the media of penetrating vessels in SHRSP(Tagami et al. 1987). This spread along the media with advancing age resulting in widespread medial necrosis and atrophy with eventual replacement of the medial muscle with collagen and cell debris(Yamori et al. 1975;Tagami et al. 1987).

In 24 week old SHRSP, the internal (84µm) and external diameters (104µm) of the 3rd order branches of the PCA were smaller than WKY (127µm and 140µm respectively) at all levels of intravascular pressure(Hajdu and Baumbach 1994). There was no accompanying hypertrophy, suggesting the arterioles were constitutionally small, although this may have been secondary to hypertension which is well established at 24 weeks. At 28 weeks, small/medium arterioles close to cerebral lesions showed hyaline degeneration, fibrinoid necrosis and thrombosis(Tagami et al. 1981). The presence of thrombi within the deep arterioles of nine month old SHRSP was considered a secondary event following luminal narrowing and accumulation of fibrin-rich material found at BBB leakage sites(Fredriksson

et al. 1985;Tagami et al. 1987). Interestingly, in SHRSP without evidence of BBB leakage, no necrotic lesions were seen in the gray matter and white matter appeared normal(Fredriksson et al. 1985). At 28 weeks, Tagami et al(Tagami et al. 1987) noted monocyte adhesion to endothelial cells with migration through the arteriolar wall into the media; the monocytes carried plasma components and then degranulated in the media, leading to further monocyte and fibrin adhesion, with eventual luminal narrowing, occlusion and enlarged perivascular spaces. No studies described venular changes.

4.3.5 Functional Changes – Vessels

4.3.5.1 Large vessels (>150μm)

A) Prior to, or independent of hypertension

One study found loss of cerebral blood flow autoregulation in SHRSP at six weeks(Tamaki et al. 1984a), suggesting an impaired vasoactive response may precede the onset of hypertension, although the precise location and timing of this loss wasn't clear. We found no reports of vasoactive changes in large vessels prior to hypertension. At 12 and 52 weeks, endothelial-dependent relaxation was markedly reduced in the basilar arteries in response to acetyl choline or substance P in SHRSP versus SHR and SHRSP/SHR hybrids(Volpe et al. 1996;Sekiguchi et al. 2001). This reduction was described as not entirely due to blood pressure as comparisons were made between animals with similar blood pressures(Takeshita et al. 1982).

B) Following development of, or directly attributable to hypertension

Functional changes were attributed directly to hypertension(Smeda and King 1999;Taka et al. 2002;Izzard et al. 2003;Izzard et al. 2006). In early hypertension (eight weeks), regional cerebral blood flow (CBF) in SHRSP was reduced to 50% of normal (versus WKY) in the frontal cortex, and fell further as blood pressure increased(Yamori and Horie 1977). At nine weeks, SHRSP also showed decreased baroreceptor sensitivity and increased sympathetic nerve outflow versus age-matched WKY, possibly indicating greater sensitivity to blood pressure changes or failure of the feedback loop(Luft et al. 1986;Yang et al. 1995). However, another study found 10 week old SHRSP showed normal autoregulation versus WKY despite falling CBF(Smeda et al. 1999;Smeda and King 2000;Jesmin et al. 2004). Autoregulatory ability in SHRSP was eventually lost by 13 weeks in the MCA and PCA in

areas of prominent tissue damage(Smeda et al. 1999). At one year, large artery resistance in SHRSP was at least double that of WKY indicating increased arterial stiffness or impaired vascular reactivity(Werber and Heistad 1984).

4.3.5.2 Small vessels (<150µm)

We found no data prior to the development of hypertension. We found the available data on small vessel reactivity difficult to interpret as reports were conflicting and much could be secondary to hypertension(Sunano et al. 1999). For example, at 5-10 weeks, the distensibility of small PCA branches was reported to increase in SHRSP, but larger PCA branches had decreased distensibility versus WKY(Zanchi et al. 1997). 32 week old SHRSP also had increased passive distensibility in cerebral arterioles in vitro(Zanchi et al. 1997). At one year, the resistance and pressure in pial arterioles was greater in SHRSP(Werber and Heistad 1984), they also showed a “sausage string” appearance(Werber and Heistad 1984). No studies described venules.

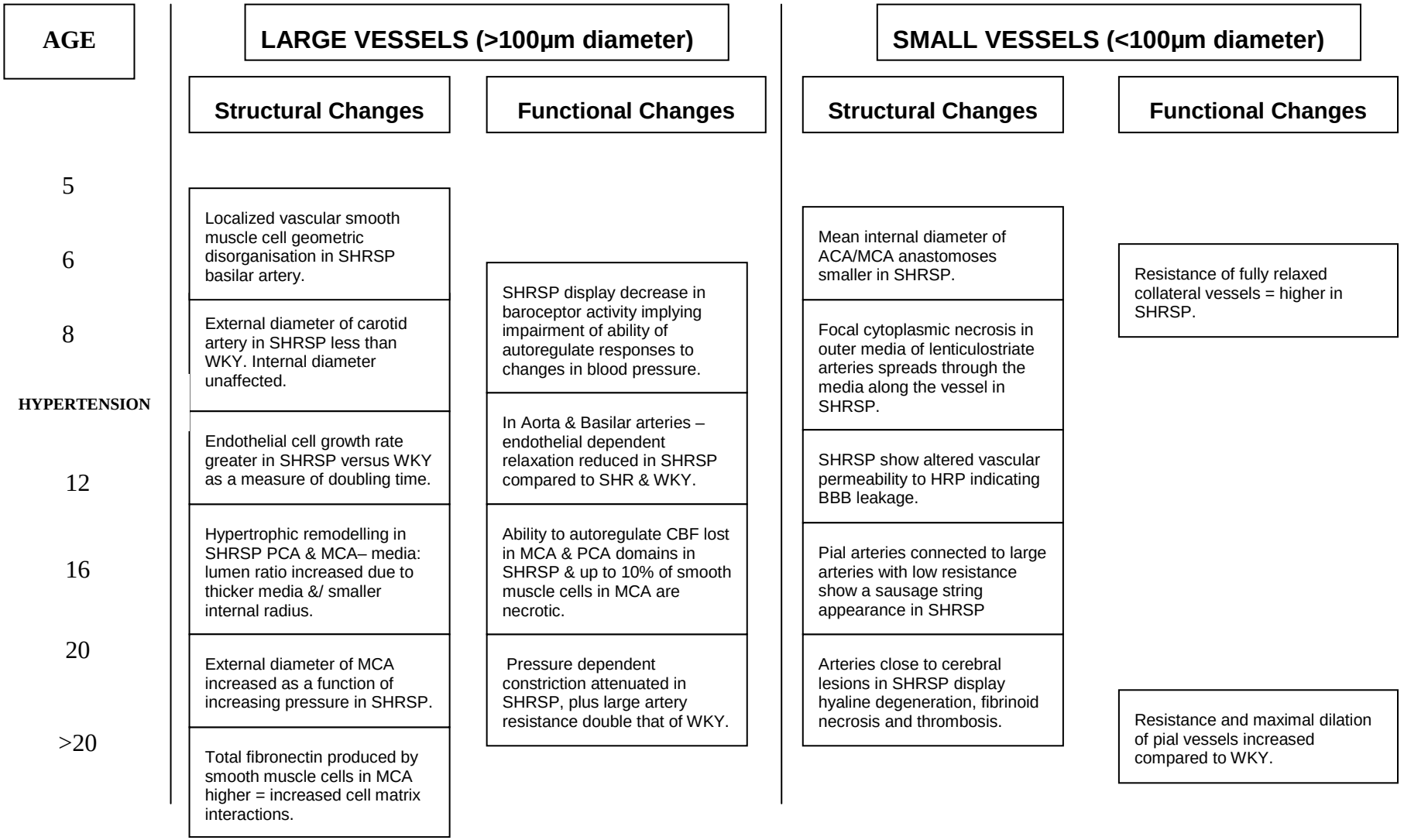

Figure 4.5. Summary of the timescale of structural and functional changes affecting both large & small vessels with increasing age.

Levels of blood pressure begin to rise at approximately 8 weeks with hypertension fully established at 12 weeks. WKY = Wistar Kyoto. SHRSP = Spontaneously Hypertensive Stroke Prone Rat. BBB = Blood Brain Barrier. PCA = Posterior Cerebral Artery. MCA = Middle Cerebral Artery. ACA = Anterior Cerebral Artery. HRP = Horse Radish Peroxidase.

4.3.6 Endothelial and systemic abnormalities

4.3.6.1 Prior to, or unattributed to hypertension

Cerebral endothelial function was impaired in SHRSP, manifesting as BBB impairment documented histopathologically(Yamori et al. 1976a;Hazama et al. 1979;Sadoshima and Heistad 1982;Fredriksson et al. 1985;Tagami et al. 1987;Lee et al. 2007) or on imaging(Guerrini et al. 2002;Sironi et al. 2004). However, all studies of inflammatory markers in SHRSP used animals with a high salt intake. At 10 weeks of age, proteinuria(Sironi et al. 2003), raised inflammatory blood markers (see table 1) and BBB impairment were detected in SHRSP on MRI(Sironi et al. 2004). Thiostatin, an acute-phase reactant, increased sharply in the urine and serum of SHRSP on a Japanese diet plus 1% salt-loading from six weeks of age, peaking at least four weeks before stroke (~15 weeks)(Ballerio et al. 2007). Additionally, two groups found early cerebral vasogenic edema secondary to BBB leak using both proteomics and MRI(Blezer et al. 1998;Sironi et al. 2001;Guerrini et al. 2002). Salt-loading from six weeks resulted in an 'atypical inflammatory condition' in SHRSP versus both SHR and WKY, manifesting as an acute-phase protein accumulation in the serum and urine (table 1)(Shimamura et al. 1999;Sironi et al. 2001). Excretion of inflammatory serum proteins in the urine preceded cerebral edema by three to 15 days(Blezer et al. 1998).

4.3.6.2 Following development of/directly attributable to hypertension.

Several studies showed that endothelial function deteriorated with increasing hypertension(Knox et al. 1980;Kitazono et al. 1995;Lee et al. 2007). Ogata et al found edema fluid around abnormal perforating arterioles(Ogata et al. 1980), whilst Tagami(Tagami et al. 1987) described monocyte adhesion and infiltration of plasma components through endothelial cells in 16 week old SHRSP on an undisclosed diet. In 12 week old SHRSP injected in vivo with Horse Radish Peroxidase (HRP) via a tail vein, a greater proportion of HRP reaction product appeared around arterioles of the hippocampus and hypothalamus (particularly in proximal segments), versus age-matched WKY, indicating leakage(Ueno et al. 2004a;Ueno et al. 2004b). Spontaneous BBB leakage detected using intravenous Evans Blue was found in 33% of SHRSP aged 5-9 months versus WKY(Fredriksson et al. 1987). Injections of albumin and trypan blue have also demonstrated spontaneous leakage in hypertensive 32 week old SHRSP versus both WKY and SHR(Yamori et al. 1975). In addition, arteriolar endothelial cells in SHRSP had

disturbed electrophysiological function of the tight junctions, which could lead to subtle changes in BBB polarity(Lippoldt et al. 2000). SHRSP capillaries showed increased endothelial cell contraction which resulted in leakage between endothelial cells(Tagami et al. 1981). Cultured cerebral endothelial cells from large vessels of 8-9 week old SHRSP grew faster(Ito et al. 1995b) but produced less than half the amount of tissue plasminogen activator (tPA) as age-matched WKY rats(Matsuo et al. 1992).

Oxidative stress is increased by hypertension and increased reactive oxygen species were found in the rostral ventrolateral medulla of 14 week old SHRSP rats (diet unknown)(Kishi et al. 2004). Nitric oxide expression was increased in areas of BBB leak and was implicated in the development of tissue lesions in SHRSP at 16 weeks(Gotoh et al. 1996).

4.4 Discussion

4.4.1 Primary Findings

We identified 102 studies of cerebral pathology in the SHRSP. This review, a comprehensive and systematic analysis of the SHRSP, highlights gaps in knowledge which could be fundamental to understanding the causes of subcortical stroke in patients, a point that was recognised almost immediately after the strain was developed(Yamori et al. 1976a;Ogata et al. 1982). Although SHRSP suffer both cortical infarcts and cerebral haemorrhages, the predominant lesions are small subcortical lesions. Of note, five separate research groups(Yamori et al. 1975;Fredriksson et al. 1987;Blezer et al. 1998;Mies et al. 1999;Sironi et al. 2004) have found evidence of, or actively demonstrated, BBB leakage in SHRSP starting prior to overt vessel or tissue damage, with and without added dietary salt. We found no evidence of atheroma in the SHRSP.

Early publications describe extensive histopathological investigations of tissue and vascular changes after stroke, whilst more recent studies focus on plasma biomarkers, changes in CBF and genetics. We found only one potential sequential histopathological investigation of arteriolar and tissue changes throughout the SHRSPs life(Tagami et al. 1987) This study sacrificed SHRSP every 4 weeks, reported on electron microscopic changes in perforatoring arterioles and documented serial vessel wall damage. They found monocyte adhesion and invasion of the arteriolar wall, fibrin deposition, disruption of the vessel wall with enlargement of the perivascular space and secondary luminal thrombosis in latter

stages(Tagami et al. 1987). The relationship of these small vessel changes to stroke lesions has not been specifically studied, despite much agreement that the small vessels suffer the major impact of the vascular changes(Mies et al. 1999).

4.4.2 Discussion of the pathological data

In SHRSP, small vessel lipohyalinosis and fibrinoid necrosis are associated with microinfarcts, white matter lesions and hemorrhage(Yamori et al. 1976a). However, the root cause of the small vessel pathology is unclear. The general absence of infarcts in the territory of arterioles occluded by thrombus, the late appearance of thrombus and sparse evidence of large artery atheroma, mitigate against a mainly thrombotic cause(Chander et al. 2003). However, the difficulty of identifying which small arteriole was associated with a particular vascular territory could be partly to blame. We found vascular damage and functional changes were more often encountered in the smaller arterioles (<150µm). However, the lack of information regarding arteriolar integrity before hypertension makes it difficult to ascertain whether hypertension was the main or initial cause of at least some of the arteriolar features. In contrast, most of the large vessel changes (especially functional) occurred after 12 weeks of age suggesting they are a response to hypertension, although evidence was conflicting, especially regarding dilatory and resistance mechanisms. There was no information on venules, yet venules are increasingly recognised to be important markers of small vessel pathology in human lacunar stroke(Lindley et al. 2009;Doubal et al. 2009) and of inflammation in the brain(Hamilton et al. 2001;Black and Garbutt 2002;Wuerfel et al. 2008).

Multiple experimental approaches pointed to a primary causative role for BBB leakage and inflammation with evidence of increased BBB permeability in SHRSP preceding the development of full hypertension (12 weeks)(Yamori et al. 1975;Fredriksson et al. 1985;Ito et al. 1995a;Blezer et al. 1998;Mies et al. 1999;Sironi et al. 2001;Michihara et al. 2001;Guerrini et al. 2002;Sironi et al. 2004). Several studies demonstrated spontaneous BBB leakage(Yamori et al. 1975;Hazama et al. 1979;Sadoshima and Heistad 1983;Fredriksson et al. 1987) although frequency varied, possibly due to differences in salt intake, genetic factors(Hazama et al. 1979;Ito et al. 2001), or whether BBB leakage was actually sought. The inflammatory acute-phase reaction seen in SHRSP on a high salt intake was not observed in SHR under identical environment conditions(Sironi et al. 2001). This reaction

may exacerbate vascular dysfunction by increasing BBB permeability through alterations at the endothelial tight junctions.

The above findings suggest the initiating cerebral pathological event in SHRSP could be BBB disruption rather than vasospasm, thrombosis or ischemia. Indeed no vessel alterations were seen in regions with preserved BBB function(Fredriksson et al. 1988). This suggests that endothelial damage could lead to the lipohyalinosis/fibrinoid necrosis observed in older animals alongside white matter rarefaction and cysts(Ogata et al. 1981). However, further studies are needed to determine whether this change can be attributed to high salt intake(Henning et al. 2010).

There are alternative causative hypotheses. Some vasoactive responses and structural changes such as vessel wall thickening(Mizuno et al. 1999) may all be the result of adaptive responses to limit the effects of rising blood pressure. Other changes, such as the loss of autoregulation at 10 weeks, may expose the brain to elevated systemic blood pressure and increase the damage(Werber and Heistad 1984;Smeda et al. 1999;Smeda and King 2000). Falling CBF could also lead to ischaemia, which in turn causes BBB disruption and edema(Henning et al. 2010). However the falling CBF could represent a loss of brain tissue to supply following brain damage from an alternative cause.

4.4.3 Methodological considerations

Our review has some weaknesses. We have not described renal vessels, mesenteric arteries and other systemic vessels. SHRSP, like humans, do not just suffer from a cerebral disease(Thompson and Hakim 2009). Even though our literature search was robust we cannot exclude having overlooked some literature.

There are methodological issues within the SHRSP literature. In particular, no studies mentioned blinding of analysis to rat strain, meaning the pathological results reported are potentially susceptible to opinion bias. Not all authors stated the age of animals at sacrifice. Most animals (where age was given) were at least 12 weeks old, by which time hypertension is fully established. Many vessels included in histopathological investigations were cortical rather than subcortical, probably because it is technologically less demanding to analyse cortical vessels. Therefore, further study of the exact sequence of pathological differences in the small subcortical arterioles is required. Some studies did not give the number of animals studied and none provided an estimate of sample size. This may be because many were undertaken as exploratory pilot studies. If this is true it would mean larger definitive studies

are required. Recent studies use a high salt intake(Enea et al. 2000) to hasten pathological changes, potentially masking the natural development of disease. The Japanese diet contains on average, 4% sodium chloride rather than the usual 0.4% in standard rat chow(Matsuo and Nagaoka 1981) and accelerates the development of hypertension in SHRSP(Stier et al. 1988;Schmidlin et al. 2005); most SHRSP on a high salt intake die before 28 weeks. Salt-loading via drinking water usually includes 1% NaCl. Compared to WKY, SHRSP are said to prefer salty water(Stier et al. 1988;Hilgers et al. 1993;Bourjeili et al. 1995). Dietary salt modulates the blood pressure of SHR and SHRSP but is said to have little effect on WKY(DiNicolantonio and Silvapulle 1988). A higher salt intake in SHRSP may increase BBB permeability, increase production of reactive oxygen species and lead to early death(Kim-Mitsuyama et al. 2005;Ishizuka et al. 2007). However, as no studies provided direct comparisons between animals randomly allocated to high salt intake or not, it is difficult to say what components of brain or vessel pathology are influenced by salt rather than other factors. Furthermore high salt is no more a risk factor for lacunar stroke than any other stroke subtype(Jackson et al. 2010) and therefore we would discourage the use of salt when assessing pathology in relation to human small vessel disease. These studies were performed on several different colonies of SHRSP, all with differing genetic phenotypes, breeding programs, levels of systolic hypertension etc. However, it is encouraging to see concordant results from several different groups. Testing hypotheses on rats from several colonies would help overcome problems of colony-specific rats. Finally, the use of both in vitro and in vivo methods to study small vessels may have contributed to contrasting results as the environment around the vessel influences its function, so studies of isolated cell or other in vitro preparations should be interpreted cautiously(Hajdu and Baumbach 1994).

4.5 Conclusions

This review has added weight to the case made in two recent reviews of potential animal models of subcortical stroke(Hainsworth and Markus 2008;Bailey et al. 2009) that the spontaneous cerebral pathology of the SHRSP (and without dietary or surgical interventions) mimics human subcortical stroke. However, there is missing data which needs to be addressed in order to fully utilise this model of the human disease. Future studies should include profiling inflammatory markers in SHRSP that have not been exposed to excess salt, more quantitative assessments of biomarkers at pre-hypertensive ages (<9 weeks), detailed analysis of the differences in all levels of vessels between SHRSP and controls and how

changes in the arterioles and venules relate to the sequence of spontaneous tissue pathological changes.

The above conclusions provided the rationale for the original laboratory work presented in the second half of this thesis.

SECTION 2) EXPERIMENTAL WORK

CHAPTER 5 :GENERAL MATERIALS AND METHODS

The conclusions from the three systematic reviews conducted at the beginning of the thesis highlighted the Spontaneously Hypertensive Stroke-Prone Rat (SHRSP) to be the best potential animal model of lacunar stroke. Consequently all of the original laboratory work contained within this thesis has been conducted on this rat strain.

5.1 The SHRSP rat (Rattus Norvegicus) – genetic background, breeding history, Glasgow colony.

The Spontaneously Hypertensive Rat family was developed by selective cross breeding of Wistar Kyoto Rats (WKY) and consists of three members; the Spontaneously Hypertensive Rat (SHR) developed in 1963,(Okamoto and Aoki 1963) the Spontaneously Hypertensive Stroke Prone Rat (SHRSP) in 1974(Okamoto et al. 1974).

We obtained SHRSP and Wistar Kyoto rats (WKY) from the Glasgow colony(Graham et al. 2007). The Glasgow colony (SHRSP/Gcrc) has been running since 1991 and is the result of strain specific brother-sister mating of 13 SHRSP (6 males and 7 females) from Dr D.F. Bohr (Department of Physiology, University of Michigan, Ann Arbor). The colony is maintained by selecting rats with particular levels of systolic blood pressure for mating. Males with blood pressure of 170-190mmHg are bred with females with blood pressure readings of 130-150mmHg at approximately 10 weeks of age. This process produces offspring with an approximate mean systolic blood pressure of 187mmHg compared to WKY rats at 134mmHg at 9 weeks of age (figure 5.1). Normal blood pressure for a WKY rat is considered to be approximately 130/90mmHg(Higashino et al. 1995).

5.1.1 Animal maintenance

We administered a normal diet (standard rat chow) to one group of animals that we sacrificed at 5 & 16 weeks of age. We assessed 21 week old rats reared on both a normal diet and animals which were salt-loaded from 18 weeks of age by adding 1% NaCl to their drinking water. All animals were male and maintained on a 12 hour light/dark cycle with

food and water freely available in compliance with UK home office regulations. All brain extractions and exsanguinations were performed by Dr. Delyth Graham (University of Glasgow) and were conducted under a project and personal license issued by the UK home office under the animals (scientific procedures) act 1986.

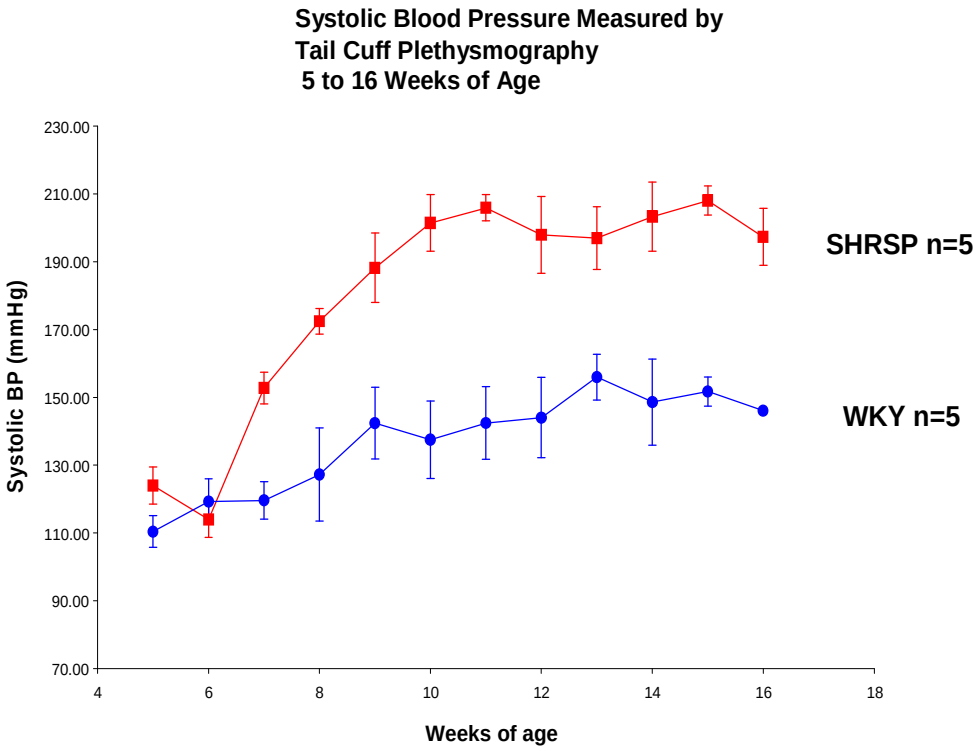

Figure 5.1. Systolic blood pressure readings measured by tail cuff plethysmography taken from male SHRSP and WKY rats aged 5 to 16 weeks in the Glasgow colony.

Error bars represent standard error of the mean. Data points represent the mean of 6-8 measurements from each animal in one sitting.

5.2 Tissue collection, fixation and storage.

We sacrificed animals by overdose of isofluorane at 5, 16 and 21 weeks of age, to enable assessment of the SHRSP at a normotensive, hypertensive and malignant hypertensive stage and age matched controls. After extraction we divided all brains in half along the saggital

plane with a scalpel. We fixed one hemisphere in formalin for subsequent paraffin embedding and histology, the other we froze in liquid nitrogen for cryostat sectioning and ribonucleic acid (RNA) extraction. We stored the formalin fixed brains at room temperature for paraffin processing and the frozen hemispheres in a -80°C freezer until required for cutting on a cryostat.

5.3 Histology – formalin fixed tissue.

5.3.1 Development of a standard sampling protocol for quantitative assessment of histology - part 1.

No standardised sampling method for extracting a specified area brain tissue from animals of varying ages (and therefore varying brain sizes) currently exists in the literature therefore we tried to rectify this by devising a protocol. Each sample of tissue we received from the Glasgow colony was assigned an ID number (e.g. C6157) which gave no indication of the age, strain and /or diet of each animal to ensure that our analysis was as blinded as possible. Full blinding is difficult to achieve as 5 week old brains are smaller to the naked eye than 16 and 21 week brains. We cut each hemisphere into 2mm thick coronal slices using a matrix (Zivic™) to produce consistent and replicable results. This resulted in approximately 6 sections per brain (7 in 21 week old animals). We processed and embedded the slices in paraffin blocks, which we then cut into thinner sections (7µm for H&E staining and 4µm for immunohistochemistry) on a microtome. From the coronal slices we selected one from approximately +1.8mm Bregma to capture a frontal section and one from approximately -1.72mm Bregma to capture areas of the basal ganglia and internal capsule (mid coronal section)(Paxinos and Watson 2007)(figure.5.2). These areas are said to display the majority of brain abnormalities in SHRSP(Fredriksson et al. 1985). To account for differences in brain size across the different ages and ensure standard sampling from consistent brain regions regardless of age, we used a stereotactic atlas to identify prominent structures within our two desired sections (e.g. the anterior commissure and lateral ventricle for the frontal section and the internal capsule and anterior hippocampus for the mid coronal section)(Paxinos and Watson 2007). We based our final decision on a series of haematoxylin and eosin stained sections pinpointing these relevant structures.

5.3.2 Hematoxylin and Eosin staining.

We used Hematoxylin and Eosin (H&E) staining as a standard method which has been used in previous studies and against which we could interpret any changes seen using other pathology techniques. H&E staining delineates anatomical regions and cell morphology as well as defining ischaemic neuronal damage(Bancroft and Gamble 2002). Haematoxylin stains nuclei blue/black and Eosin stains cytoplasm red. White matter stains a deeper pink than grey matter and stains the following structures accordingly;

Muscle fibres – deep pinky red

Collagen – pale pinky red

Red blood cells – orange/red

Fibrin – deep pink

5.3.2.1 Protocol:

For the full H&E staining protocol see appendix E. Briefly, we dewaxed slides in xylene and hydrated them via absolute alcohol and 99% Industrial Methylated Spirit to 70% alcohol, before incubating the slides in picric acid for 30 minutes. We rinsed the slides in water and placed them in Harris haematoxylin solution for 10 minutes. After a second wash with water and differentiation in acid alcohol we placed the slides in lithium carbonate solution until blue (usually 3-5 dips). Emersion in Putts Eosin solution for 10-12 minutes, followed by dehydration in alcohols completed the process. We left the slides in xylene to clear then mounted them with cover slips.

5.4 Qualitative assessment of morphological changes

Three observers (EB, Dr Colin Smith & Prof. Joanna Wardlaw) assessed slides for any gross pathology under a light microscope (Olympus BX51). Precise features were discussed to clarify features relevant to prior studies and to map to other data. We recorded incidences of vessel thickening and the size of the vessel affected, white matter rarefaction, inflammation and any other evidence of microinfarction, haemorrhage or white matter lesions. We also looked at the ependyma of the ventricle for ependymal thickening or periventricular rarefaction as evidence of structural damage which could suggest leakage of CSF.

5.4.1 Development of a standard sampling protocol for quantitative assessment of histology - part 2.

We developed a standard sampling protocol to assess the same 3 regions of interest across all animals; cortical grey matter, white matter and deep grey matter (see figure 5.3 for anatomical representation of these regions). We defined a cross sectional area using prominent features which were clearly visible across all age groups and strains of rat. For frontal sections, the most lateral edge of the lateral ventricle provided one boundary whilst the entorhinal cortex provided the other. In mid coronal sections the most lateral part of the emerging hippocampus provided one boundary whilst the rhinal fissure provided the other (see figure 5.3). Using these boundaries we could then define each region using the free hand tool on ImagePro™.

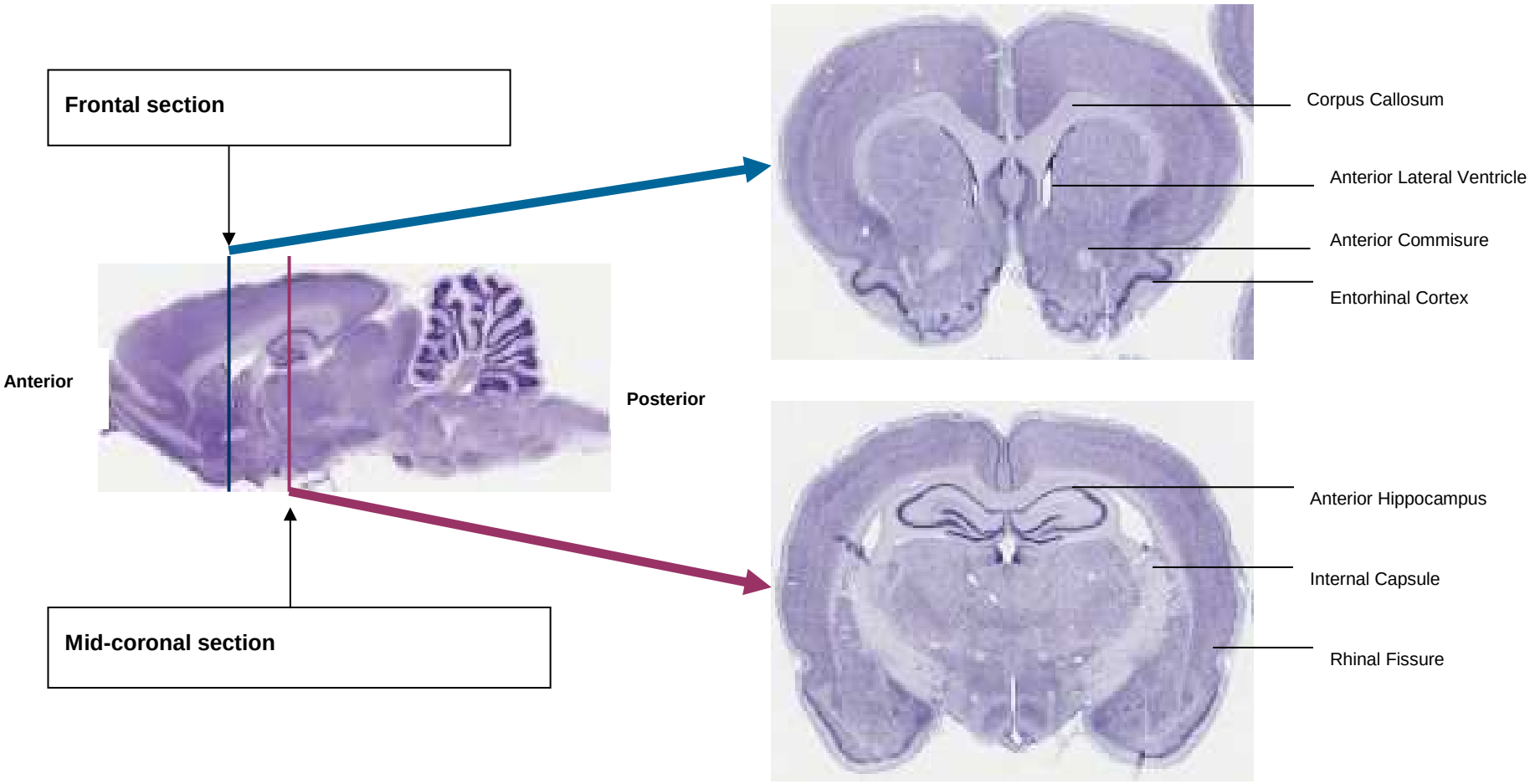

Figure 5.2. Sections of the rat brain taken for histology experiments (both staining and immunohistochemistry).

Images based on sections in the Rat Brain Atlas (Paxinos & Watson 6th Edition). In the frontal section the anterior lateral ventricle is visible along with the anterior commisure and entorhinal cortex. Within the mid coronal section the anterior hippocampus is visible and we aimed to obtain the largest area of the internal capsule possible to maximise the amount of white matter sampled.

5.4.2 Quantitative assessments

5.4.2.1 Vessel density and Cell Counts –

Using image analysis consisting of a CoolSNAP^{TM} camera (Roper Scientific Photometrics) attached to a light microscope (Olympus BX40 with x10 eye pieces) complete with platform (Prior Scientific), we counted various features on our anonymously coded slides using a random sampling protocol of three regions on Image-Pro^{TM} plus 6.3 software. These included; vessel density (capillaries and large vessels separately), neurons and oligodendrocytes. All structures which could be confidently identified by the observer (see chapter 6 for further details).

Using the software, we designed a stereology experiment. Each slide was tiled (using snapshots tiled side by side) to create a full on screen image at x4 magnification. We set preferences within the stereology menu as follows;

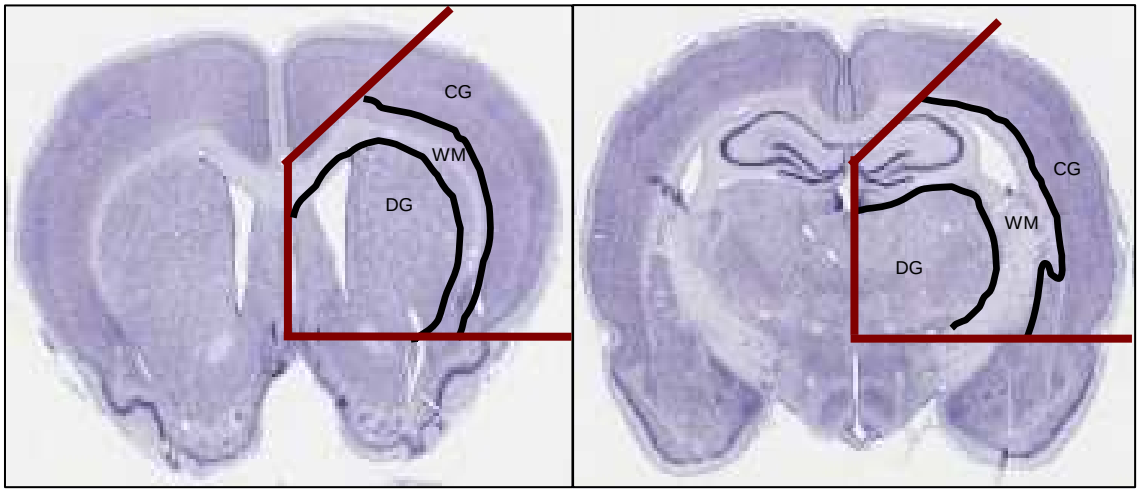

Figure 5.3. The cross sectional areas used in A) the frontal section and B) the mid coronal section to sample cortical grey, white matter and deep grey regions from all SHRSP and WKY animals regardless of age.

The red boundary lines were defined using A) the most lateral edge of the lateral ventricle and the entorhinal cortex and B) the rhinal fissure and the most lateral point of the hippocampus. CG = Cortical Grey. WM = White matter. DG = Deep grey.

Regions – Cortical Grey, White Matter and Deep Grey

Count frame – 300µm^2

Random points per region – 3

Thickness – 7µm

Experimental objective – x20

Counts – capillaries, large vessels, neurons, oligodendrocytes.

We then drew the first region of interest (i.e. cortical grey) using the free hand tool on ImagePro™. Once this region was defined we generated three random sampling points within the area using the software (figure.5.4). Within each point (300µm^2) we then performed the above counts. Once the experiment was running, each count frame (random point per region) was brought up independently and we performed the counts for all objects one after the other. The software colour coded the separate structures accordingly (figure 5.5). Once we had counted all the large vessels, capillaries, neurons and oligodendrocytes for that count frame, the software transferred to the next count frame and the process continued until all three random points had been counted for that region. We then drew the next region of interest (i.e. white matter) and repeated the process until the last sampling point within the deep grey matter had been counted. We loaded the next slide, drew the cortical grey region and so on.

Both frontal and mid coronal sections were analysed using the described protocol. We exported data to an excel spreadsheet for analysis.

5.4.2.2 Measurement of sclerotic index:

Using the same defined regions (cortical grey, white matter and deep grey) we also measured evidence of atherosclerosis in both cortical and perforating arterioles using Lammie's sclerotic index(Lammie et al. 1997) where the following formula is applied;

Ratio = 1-(internal diameter/external diameter).

From this formula normal vessels are considered to lie within the range of ratios of 0.2-0.3, 0.3-0.5 constitutes moderate sclerosis, and severe sclerosis is anything over a value of 0.5.We sampled 5 vessels from the cortical and deep grey matter and three from the white matter for each animal (the likelihood of finding vessels preserved well enough to measure in the white matter was lower due to the area of white matter being smaller).

Using the measurement tool on Image Pro^{TM} we measured the diameter of both the lumen (internal) and the entire vessel. We took measurements at the same point along the vessel so that the lines superimposed one another. This minimised human error (figure.5.6).

We exported the data to an excel spreadsheet for calculation of the ratio and further statistical analyses.

5.4.3 Data analysis

We performed statistical analysis using R software. We adjusted counts for age by calculating ratios - 5:16 weeks & 16:21 weeks for all cross section areas and applying the ratio to the counts.

For example;

21wk cortical grey area/16wk cortical grey area = 1.34

16wk count stays the same

21 week count divided by 1.34 = new adjusted count.

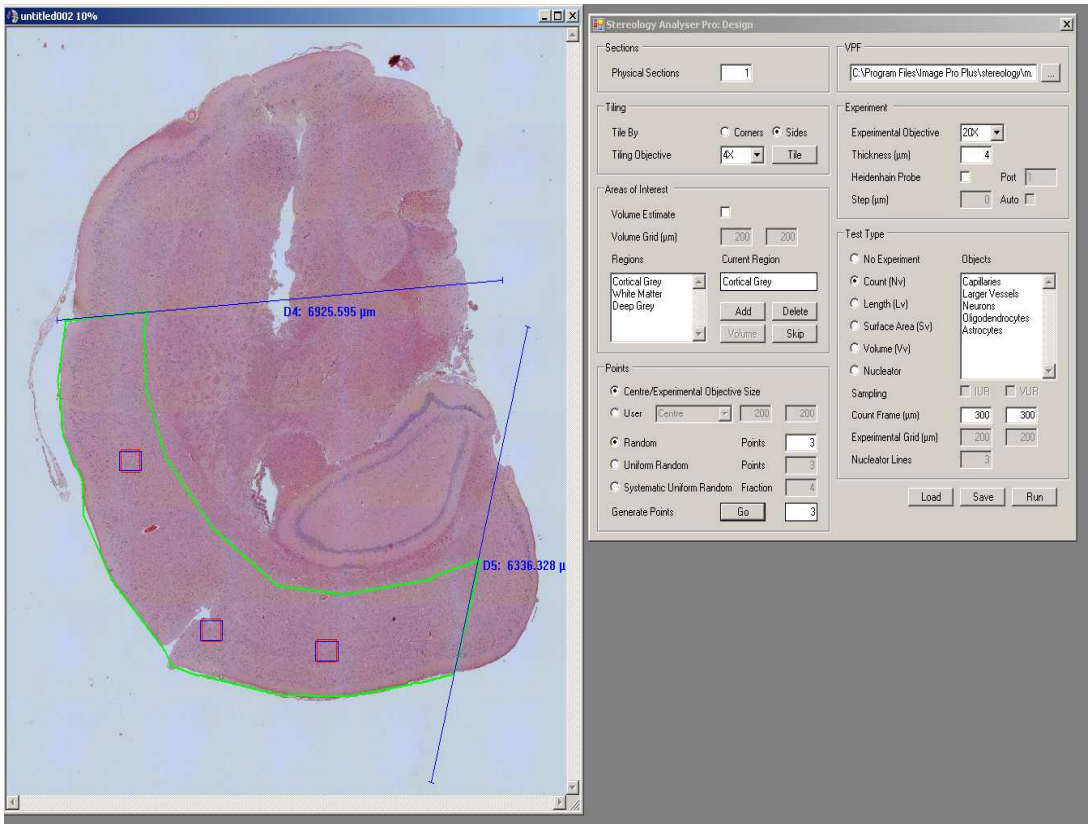

Figure 5.4. A screenshot from ImagePro™ showing the generation of random sampling points within the cortical grey matter of a mid coronal section for quantitative assessment of H&E sections.

With these adjusted values we performed a general linear model (GLM). For each region we firstly took the median count from the three randomly generated sampling points in each animal. Then we took the median value from all 5 animals to use in the final analysis and based the GLM on a quasi poisson distribution because the data were over-dispersed.

For all of the statistical analysis, we analysed frontal and mid-coronal sections separately as there were significant differences in the distribution of grey and white matter within the sections. We also analysed each region (cortical grey, white matter and deep grey) separately as there are substantial anatomical differences as well as differences in the area between regions. P values of <0.05 were considered statistically significant.

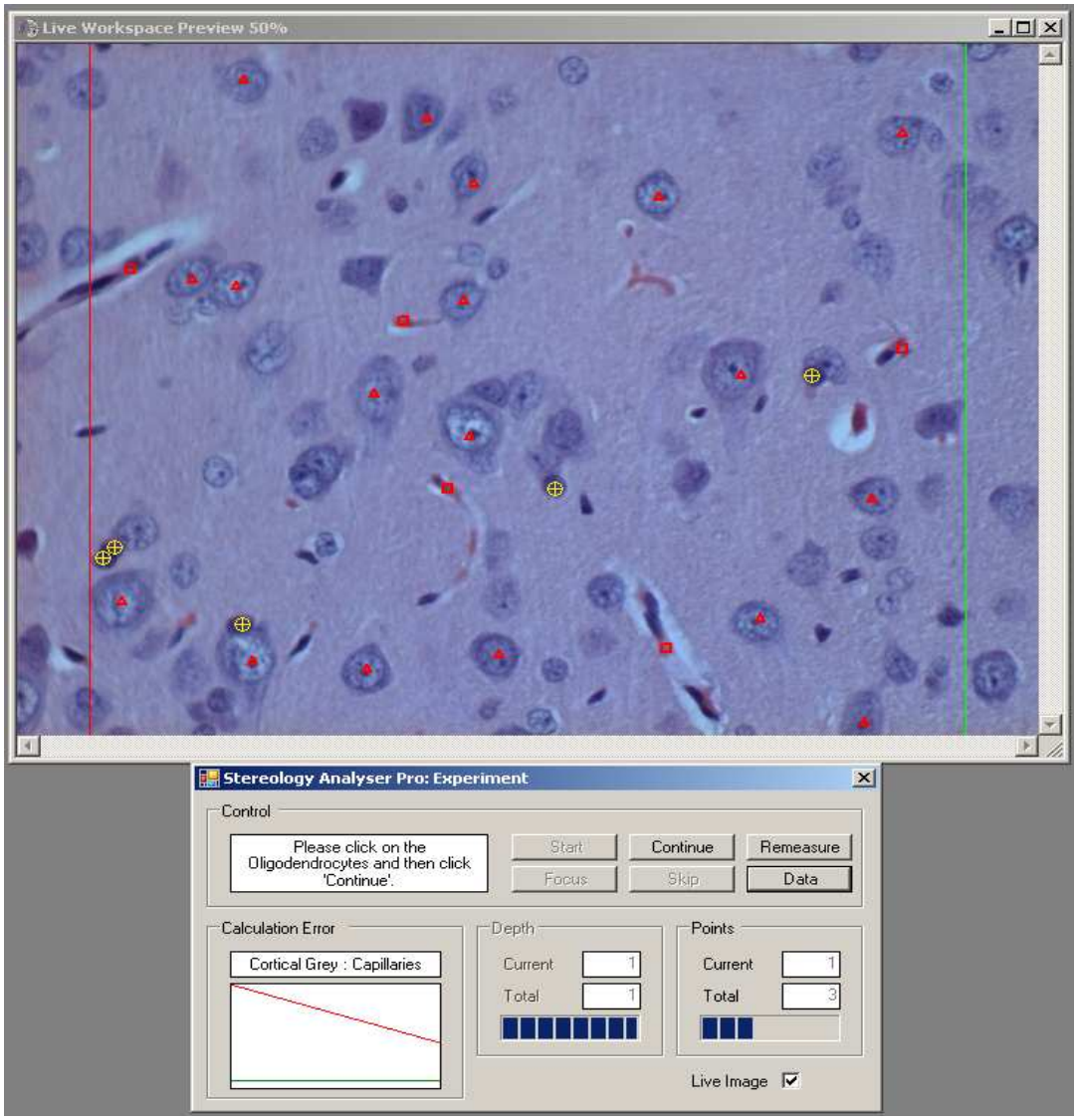

Figure 5.5. A screenshot from ImagePro™ showing the stereology experiment designed to perform counts of different cell types.

This particular shot is taken from a sampling point within the cortical grey matter of a mid coronal section at x20 objective. The red and green lines represent the boundary of the sampling point. Capillaries (red squares), neurons (red triangles) and oligodendrocytes (yellow circles with crosses) are highlighted here. For more information on how these structures were identified see chapter 6.

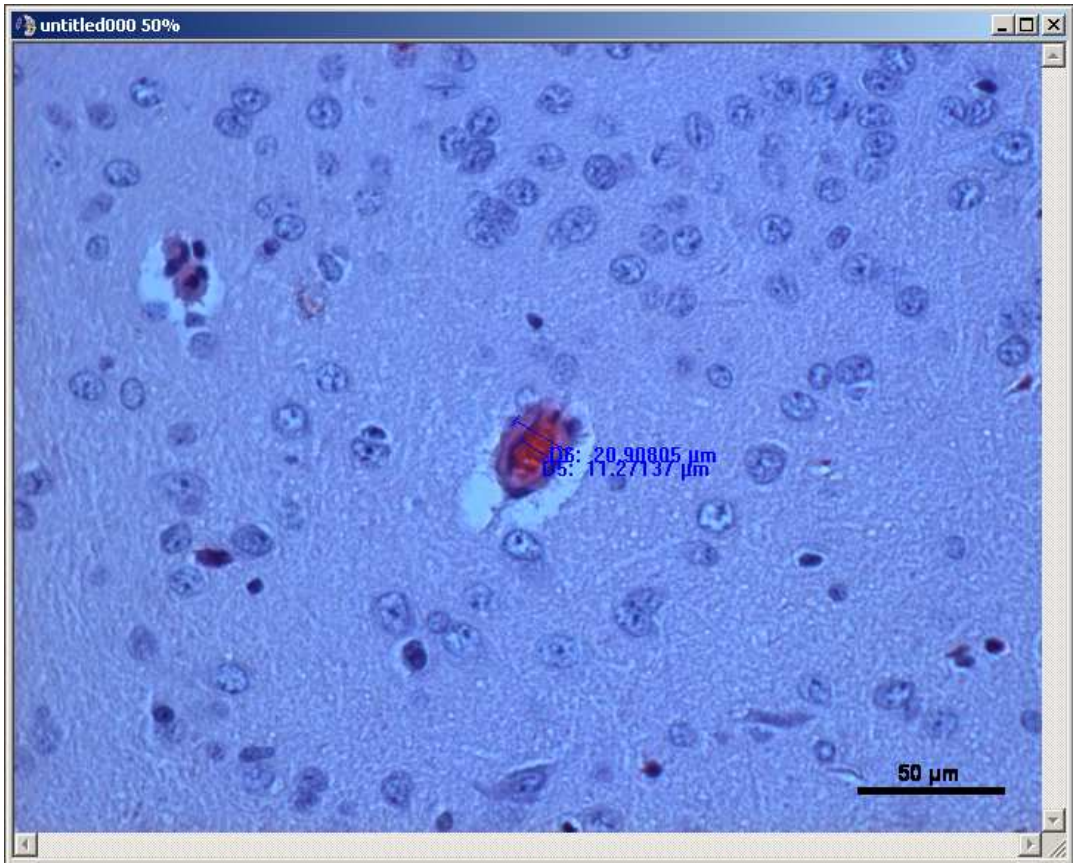

Figure 5.6. **Measurement of sclerotic ratio(Lammie et al. 1997) using the measurement tool on Image Pro™.**

Sections stained with H&E. Objective x20.

5.5 Immunohistochemistry

5.5.1 General principles of immunohistochemistry

Immunohistochemistry is used to localize antigens in cells of a tissue section using antibodies which bind specifically to the selected antigen. It is used to understand the distribution of a variety of cell types, proteins and enzymes in different parts of a tissue section(Bancroft and Cook 1994).

There are two methods of immunohistochemical staining; the direct method and the indirect method(Bancroft and Gamble 2002). The direct method is a one-step staining method, and involves an antibody labelled with a fluorescent tag or enzyme which reacts directly with the antigen. This method is fast and simple but does not amplify signal very well so is less commonly used(Ross and Pawlina 2005). In this study we used the indirect method of

immunohistochemistry. This uses an unlabelled primary antibody against the antigen being probed for and a second, labelled, antibody against the first(Bancroft and Cook 1994). The secondary antibody is raised against Immunoglobulin G (IgG) of the animal species in which the primary antibody has been developed. E.g. A mouse primary antibody must be coupled with an anti-mouse secondary antibody in order to prevent any immunoreactivity of the host species taking place. The indirect method is more sensitive because signal amplification occurs through several secondary antibody reactions with different antigenic sites on the primary antibody(Ross and Pawlina 2005). The secondary antibody is then labelled with a fluorescent dye or an enzyme. The indirect method is also advantageous because a labelled secondary antibody raised against mouse IgG, works well with any primary antibody raised in mouse. With the direct method, it would be necessary to make custom labeled antibodies against every antigen of interest.

For this study we used a biotinylated secondary antibody coupled with streptavidin-horseradish peroxidase, which we reacted with 3,3'-Diaminobenzidine (DAB) to produce a brown staining wherever primary and secondary antibodies are attached. We lightly counterstained with hematoxylin to highlight basic structures and neurons.

We applied the Avidin Biotin Complex (ABC) immunoperoxidase method (Vector Laboratories)(http://www.ihcworld.com/_protocols/general_IHC/standard_abc_method.htm) of indirect immunohistochemistry to all slides. All antibody dilutions and incubation times are available in table 5.2. We performed all incubations at room temperature unless specified. For the full ABC protocol see appendix G

For a list of all the antibodies used in this thesis see table 5.1.

5.5.2 Blocking and reducing background staining

We blocked all sections in 10% hydrogen peroxide for 10 minutes to prevent any endogenous peroxidase activity contributing to non-specific background staining. We also blocked endogenous biotin where necessary using the provided reagents within the ABC kit. Where necessary, blocking of cross reactive antigens within the tissue was also applied by choosing the correct secondary antibody. For example the monoclonal myelin basic protein (MBP) antibody we used was raised in rat and using this antibody in rat tissue meant any endogenous immunoglobulins would be detected by the antibody as well as those aimed at the exogenous antibody. To prevent this, a rabbit anti rat secondary antibody was applied to sections to remove any cross reactivity.

5.5.3 Heat mediated antigen retrieval

Fixation of tissue in formalin can create protein cross links which can cause antigenic sites to be masked and unable to bind to antibodies. By breaking these cross links, more antibody – antigen interactions can occur thereby increasing the overall signal obtained(Bancroft and Gamble 2002). Heat, in the form of a microwave, water bath or in our case, pressure cooker enables these cross links to be broken. We used a Menarini (A.Menarini Diagnostics) digital pressure cooker which heated the slides for 20 minutes before cooling gradually for a further 20 minutes. In most cases we immersed the slides in citric acid buffer (pH 6.0) which acted as the retrieval solution. For MBP staining we found TRIS-EDTA (pH 9.0) to be more effective.

5.5.4 Antibody optimization

We used human glioma tissue (for matrix metallopeptidase 9 (MMP9)) and rats donated from Prof. J. McCulloch's lab (all remaining antibodies) for the optimization of antibodies. Two rats (approximately 11 weeks old) underwent permanent bilateral carotid ligation and 2 were subjected to a sham procedure as part of the animal experiments for which they were being used. Bilateral carotid ligation is considered to be a model of low cerebral blood flow and rats develop white matter damage(Shibata et al. 2004). After a week of recovery we sacrificed the rats via cardiac perfusion with saline followed by paraformaldehyde for fixation. We transferred one hemisphere to PBS (Physiological Buffered Saline) for paraffin sectioning (see above) and froze the other hemisphere using isopentane to eventually be used for cryostat and laser microdissection training. We titrated all antibodies to values recommended by specification sheets from the supplier if the information was available. If no information was available trial and error was used to determine the optimal dilution, pre-treatment and incubation period used. Optimal dilution was reached when staining was clear, uniform and isolated to the appropriate structures across the section.

5.5.5 Image Analysis and reproducibility study

We measured percentage staining using ImagePro^{TM} software (version 6.3), blinded to species and age, in cortical, deep grey and white matter in the frontal and mid coronal sections as described earlier. We assessed intra-observer reliability using a randomly selected slide counted on 5 separate occasions (see chapter 6 for results). We used the same

standard sampling protocol developed for quantitative assessment of H&E slides described previously (see figure.5.3). We repeated the full image analysis protocol on both frontal and mid coronal sections in each animal blind to strain, age and diet. We then applied colour matched pixel counts to the entire hemisphere, counting each region of interest separately as described for the H&E stained slides. We converted counts into percentage areas of staining as a measure of immunoreactivity using ImagePro™, once each region had been defined by hand (figure 5.7).

Table 5.1. Descriptions and origins of primary antibodies used.

Antibody	Supplier	Clonality	Secondary Antibody (all 1:200 dilution)	Function
Collagen I	Abcam	Monoclonal	Rabbit anti Mouse (Dako)	Found in smooth muscle as a sign of scarring or repair.
Collagen IV	Abcam	Polyclonal	Swine anti Rabbit (Dako)	Indicates structural integrity of the basal lamina.
MMP9	Abcam	Monoclonal	Rabbit anti Mouse (Dako)	Expression indicates breakdown of the extracellular matrix.
Smooth Muscle Actin	Abcam	Monoclonal	Rabbit anti Mouse (Dako)	Cytoskeletal protein – indicator of basement membrane integrity.
Claudin 5	Lifespan Biosciences	Monoclonal	Rabbit anti Mouse (Dako)	Transmembrane protein present in the tight junctions of endothelial cells.
Iba-1	Abcam	Polyclonal	Rabbit anti Goat (Dako)	Activated microglial cells - inflammation
MBP	Abcam	Monoclonal	Rabbit anti Rat (Dako)	Myelin Basic protein – integrity of WM tracts
GFAP	Dako	Polyclonal	Swine anti Rabbit (Dako)	Indicator of astrocyte function.
Occludin	Lifespan Biosciences	Polyclonal	Swine anti Rabbit (Dako)	Tight junction protein within endothelial cells
Caspase 3	Abcam	Polyclonal	Swine anti Rabbit (Dako)	Indicator of cell death

Antibodies highlighted in red were intended for use but did not optimise well in brain tissue and were subsequently excluded from the panel. MMP9 = Matrix metallopeptidase 9. Iba-1 = ionized calcium binding adaptor molecule 1). MBP = Myelin Basic Protein. GFAP = Glial Fibrillary Acidic Protein.

5.5.6 Data Analysis

We performed statistical analysis in Minitab using a general linear model two-way ANOVA followed by Tukeys test for pairwise comparisons as the data consisted of mean percentages. For intra-observer reliability we used coefficient of variance analysis and measured the effect of day on staining count. For the assessment of antibodies we calculated the effects of strain and age. We assessed the effect of salt-loading and strain for the salt-loaded animals. For all of the statistical analysis, we analysed frontal and mid-coronal sections separately. We also analysed each region (cortical grey, white matter and deep grey) separately. P values of <0.05 were considered statistically significant.

Table 5.2. Dilutions and incubation periods used for primary antibodies.

Antibody	Dilution	Pretreatment	Incubation period (hrs)	Temperature
Collagen I	1:400	Heat mediated antigen retrieval in citric acid buffer.	24	4℃.
Collagen IV	1:200	Heat mediated antigen retrieval in citric acid buffer.	24	4℃.
MMP9	1:250	Heat mediated antigen retrieval in citric acid buffer.	1	Room temperature
Smooth Muscle Actin	1:400	Heat mediated antigen retrieval in citric acid buffer.	1	Room temperature.
Claudin 5	1:200	Heat mediated antigen retrieval in citric acid buffer.	24	4℃.
GFAP	1:800	Heat mediated antigen retrieval in citric acid buffer.	0.5	Room temperature.
MBP	1:150	Heat mediated antigen retrieval in EDTA buffer.	0.5	Room temperature
Iba-1	1:75	Heat mediated antigen retrieval in citric acid buffer.	0.5	Room temperature

Hrs = Hours. EDTA = ethylenediaminetetraacetic acid

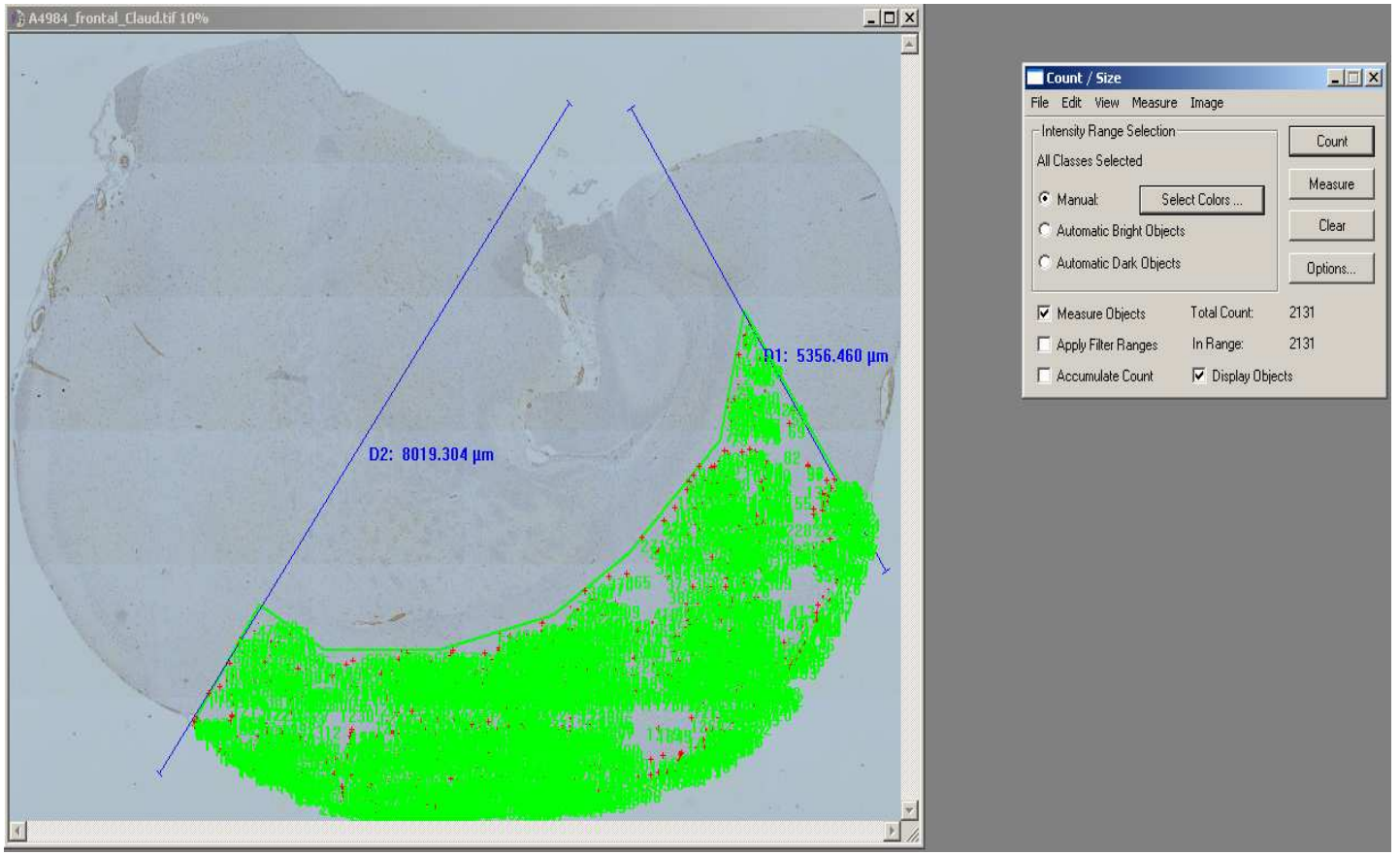

Figure 5.7. A screen shot taken from ImagePro (version 6.2) showing areas of immunoreactivity as highlighted pixels (red crosses).

This image is taken from a mid coronal section of a 5 week old WKY. The blue lines represent the boundaries of our standardised cross section (see figure 5.3).

5.6 RNA Microarray

The purpose of a microarray is to measure for each gene, the amount of message that was broadcast through the RNA. They are useful for measuring how much RNA was produced by each gene and the transcription levels of different genes in different cells / conditions. For a diagrammatical representation of the steps necessary to produce a RNA microarray see figure.5.8. For our particular array we used an Illumina platform and the RatRef12 array.

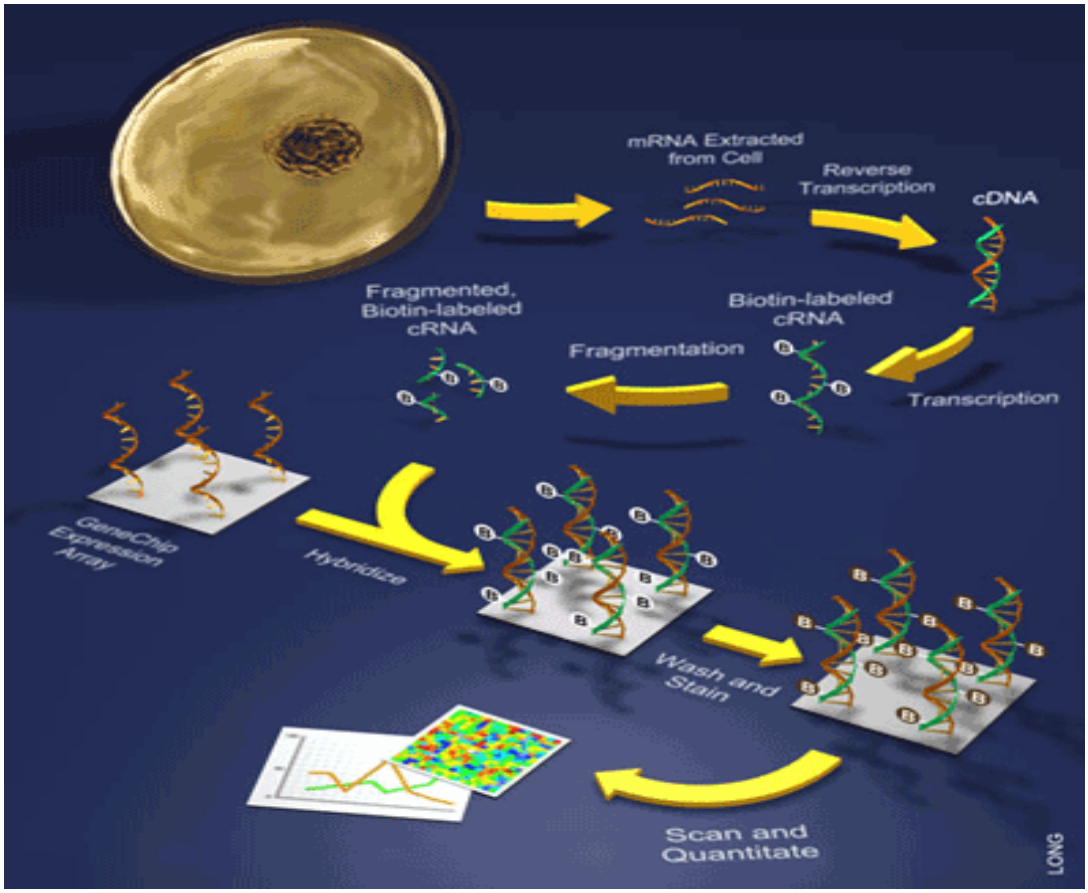

Figure 5.8. Schematic representation of the steps required to perform a microarray experiment.

Source: http://www.scq.ubc.ca/wp-content/eukaryoticexpressionsarra.gif. mRNA = messenger RNA. cRNA = complementary RNA.

5.7 Materials and methods

We used 4 hemispheres from each group of animals (5, 16, 21 week and 21 week salt-loaded from each strain) for total RNA extraction. Total animals n=32.

5.7.1 Laser capture microdissection- pilot study

We aimed to capture precise areas of the neurovascular unit so that changes in gene expression could be directly related to vascular pathology. To do this we employed laser capture microdissection. We removed each frozen hemisphere from -80°C freezer and placed it into a pestle and mortar containing liquid nitrogen. We treated all equipment mentioned in this section with RNAzap before use. We used the pestle to knock off a chunk of tissue that would have an edge suitable for mounting onto a cryostat. We mounted the tissue onto a chuck with Tissue-Tek® Optimal Cutting Temperature (OCT) compound and sectioned it coronally at a thickness of 6µm. We placed some sections straight into PCR tubes and kept them on dry ice for RNA quality assessment. We mounted the rest of the sections on slides which were kept on dry ice until all the required tissue was cut. We then incubated all of the sections in 70% ethanol for 1 minute, washed them in nuclease free water and incubated the sections in RNA later for 4 minutes before staining with cresyl violet. Simply, slides were hydrated in graded alcohols, stained with cresyl violet (by direct application of 300µl of cresyl violet to the slide) washed and dehydrated down the same grade of alcohols before being cleared in xylene.

Cresyl violet highlights nuclear structures blue. It has been shown to have no adverse effects in terms of RNA degeneration and is recommended along with Acridine Orange for laser capture microdissection(Roozen et al. 2010).

We used slides of both unstained and stained tissue for laser microdissection (LCM). On an Arcturus^{XT} ™ LCM instrument and using Capsure® LCM caps (Applied Biosystems) we took approximately 100 pulses per slide using the following settings; laser settings diameter 7µm, power ~ 60mW. We removed the film from the cap with tweezers and placed into 0.5ml Eppendorf containing 100µl lysis buffer (Qiazol) and kept the sample on ice for RNA extraction.

After numerous attempts at the above protocol it became clear that we could not obtain consistent samples of a high enough RNA quality to proceed to microarray analysis. We

therefore decided to use homogenized tissue slices (similar to those used in H&E and immunohistochemistry).

5.7.2 Homogenized tissue slices (frontal and mid coronal sections) for microarray analysis.

We removed each hemisphere from the -80°C freezer and immersed it in x10 volume of RNAlater®-ICE solution (Ambion) in a 20ml falcon. We left the hemisphere for 24 hours in a -20°C freezer to enable the RNA-later ice solution to penetrate the tissue completely.

The next day we mounted the hemisphere in a Zivic rat slicer matrix and cut 2mm coronal slices from a frontal and mid coronal region to correspond with the slices taken for immunohistochemistry and H&E staining. Therefore we had 64 samples in total (32 animals x 2 brain slices per animal). We weighed the slices and placed them in approximately 1.5ml (x10 volume) of lysis buffer in 7ml bijoux containers. We homogenized the tissue slices using a benchtop POLYTRON® homogenizer (Capitol Scientific Inc.) with an RNA blade attached for approximately 30 seconds or until no lumps of tissue remained. In between each sample the blade was washed once in nuclease free water, scraped with a 10µl pipette tip and washed twice more in nuclease free water to ensure any RNA from the previous sample was removed.

We then applied a Qiagen RNAeasy lipid tissue minikit (www.qiagen.com) for extraction of total RNA from fatty tissues to the homogenates. Briefly, the addition of chloroform produced a clear aqueous fraction to form which we transferred onto a microfilter cartridge. We added wash solutions and eluted the resulting RNA with nuclease free water (2x50µl). We placed half the elute into a second tube and treated it with turbo DNase. We then assessed yield and 260:280 ratio of the resulting RNA on a Nanodrop ND 1000 – a spectrophotometer (see figure 5.9 for a typical nanodrop RNA profile). Absorbance at 260nm was used for quantification of nucleic acids. Absorbance ratios (260/280nm) of approximately 2.0 for RNA indicated that the RNA preparation was sufficiently free from protein contamination. We took averages of duplicate or triplicate readings for samples requiring very precise quantification. Finally we extracted a 3µl sample of each RNA stock solution diluted to 300ng/µl to send to the Agilent bioanalyser for full assessment of RNA quality (see figure 5.10 for a typical RNA profile from the agilent bioanalyser).

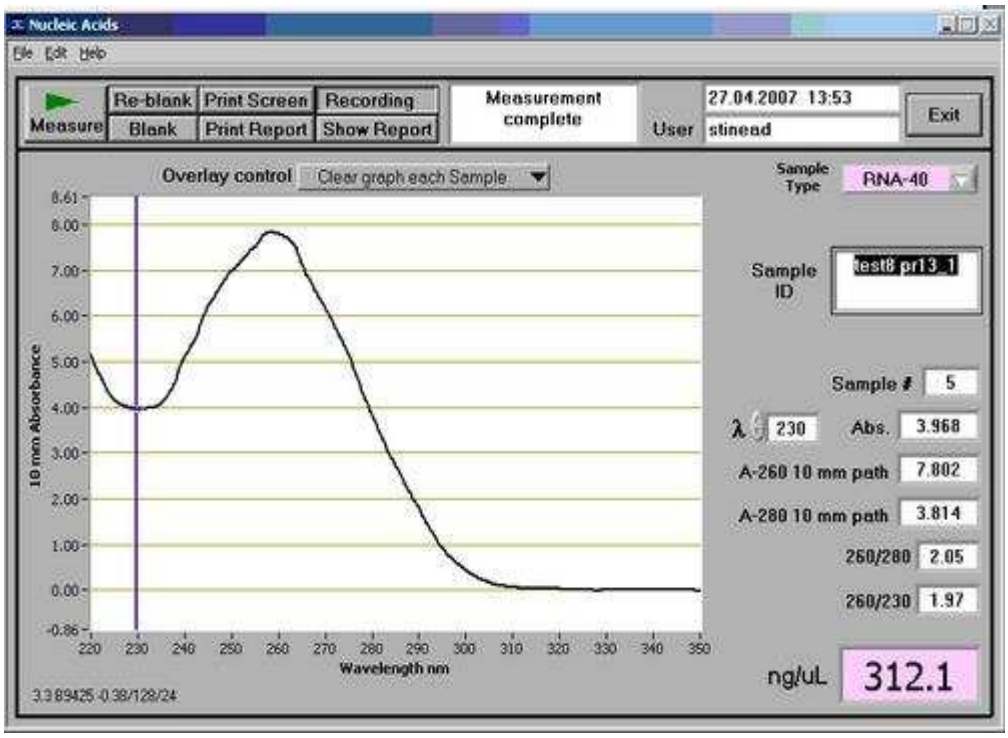

Figure 5.9. A typical good quality RNA profile from the nanodrop.

The 260/280 ratio of a good sample should be approximately 2.0 thereby indicating that genomic DNA has successfully been removed. The 260/230 ratio should be above 1.7 which indicates protein contamination is unlikely. The pink box in the bottom right hand corner represents the yield in ng/µl.

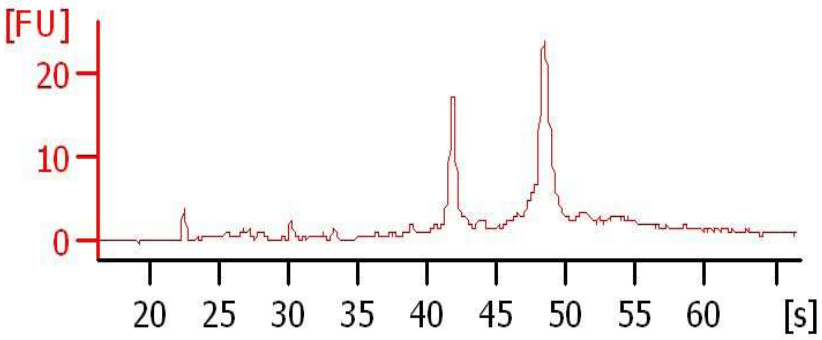

Figure 5.10 A typical total RNA profile obtained from the Agilent bioanalyzer.

FU = Fluorescence units. The peaks represent the 18S (the peak at ~ 42) and 28S (the peak at ~ 49) isomers of ribosomal RNA (rRNA) A perfect sample would have a 2:1 ratio (28S:18S). The RNA integrity (RIN) value for this particular sample was 9.5. We accepted samples with RIN values of ≥ 7.5.

5.7.3 RNA purification

We assessed the concentration of the samples of extracted RNA treated with DNase by running them on the nanodrop three times to determine a mean concentration. Optimum concentration for amplification is 500ng/11µl therefore we prepared the appropriate dilutions with nuclease free water. We prepared a 20µl sample so that the concentration could be checked again on the nanodrop. If necessary we made adjustments with either more stock sample or nuclease free water and once again the concentration checked.

5.7.4 In vitro transcriptions – amplification and formation of cRNA

We performed transcriptions from RNA to cRNA using an Ambion Illumina TotalPrep RNA amplification kit (www.ambion.com). Samples were done in batches of 12. 1 kit provides 24 samples worth of reagents.

We generated first strand complementary DNA (cDNA) by making up a first strand master mix containing an oligo (dT) tagged with a phage T7 promotor. We added 9µl of this master mix to 11µl of each RNA sample – a total solution of 20µl per 0.5ml Eppendorf. We incubated all the samples on a thermocycler at 42°C (with a heated lid of 50°C to prevent condensation forming within the tubes) for 2 hours. We then made a second strand cDNA master mix containing DNA polymerase and added 80µl to each sample. We returned the samples to the thermocycler for 2 hours this time at 16°C with no heated lid.

Meanwhile we heated 20µl of nuclease free water per sample to 55°C ready for the elution of cDNA. After removing the samples from the thermocycler we added 250µl of cDNA binding buffer to each sample and mixed by pipetting. We passed the solution over a column and spun it down for 1 minute at 10000g (g = rcf = relative centrifugal force). We discarded the flow through and added 500µl of wash buffer to the column and spun the column down at 10000g for 1 minute or until all the solution had passed through. In order to remove any excess wash solution from the column we discarded the flow through and spun the column down once more to dry the filter. Once dry we placed the filter into a new collection tube. We applied 20µl of 55°C water to the centre of the filter and incubated at room temperature for 2 minutes. We then spun the column down for 1 minute at 10000g to collect the eluted cDNA.

Meanwhile we prepared an in vitro master mix solution which amplifies and labels the cDNA with biotin UTP (deoxyuracil nucleotides) and added 7µl to a new 0.5ml Eppendorf.

We then transferred the elute (~20µl) from the collection tube over to the Eppendorf containing the IVT mix and mixed by pipetting up and down. We briefly spun down the samples on a centrifuge before incubating on the thermocycler (37°C with heated lid to 100°C) for 14 hours.

The following day we stopped the reaction by adding 75µl of nuclease free water at room temperature (to bring the solution to approximately 100µl). We set up a second set of columns and microfilters this time for cRNA extraction and heated 200µl of nuclease free water per sample to 55°C ready for elution. After removing samples from the thermocycler we added 250µl of cRNA binding buffer to each sample followed by 350µl of 100% 200 proof ethanol. We mixed the solution mixed by pipetting then loaded the total volume (~700µl) onto the column and spun it down at 10000g for 1 minute. We discarded the flow through and then added 650µl of wash buffer to each sample and spun down all the samples at 10000g until all the solution had passed through (approximately 1 minute). We again discarded the flow through and spun the column dry once more. We placed the filter into a new collection tube and applied 200µl of nuclease free water to the centre of each filter. We incubated the samples in a hybridisation oven at 55°C for 10 minutes before spinning the column down at 10000g for 1 minute. To increase the RNA concentration in the final eluted sample, we passed the elute over the same column and spun it down for a second time leaving a final cRNA elute of just less then 200µl. We checked the cRNA profiles of all samples by running them on the agilent bioanalyser (see figure 5.11 for a typical cRNA profile). We stored samples at -80°C until needed for hybridisation.

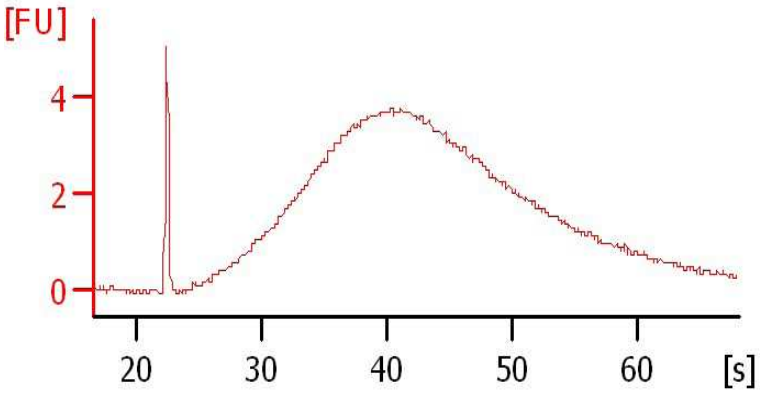

Figure 5.11. A typical cRNA profile obtained from the Agilent bioanalyzer.

FU = Fluorescence units. A good quality sample should be a smooth and equally distributed curve around a peak value of 40. Samples with peaks between 35 and 45 were generally accepted depending on the shape of the curve obtained. Samples shifted to the left indicate degradation. The height of the peak indicates cRNA yield.

5.7.5 Hybridisation to the chip

We performed the recommended Illumina protocol for hybridisation (www.illumina.com). We diluted each cRNA sample to 150ng/µl (as required by the protocol) with nuclease free water and nanodropped before hybridisation commenced. ((150/yield) x15 = 15µl total volume at 150ng/µl)

We heated a hybridization oven to 58°C and heated hybridisation buffer and humidity control buffer (HCB) to 58°C for 10 minutes prior to use to dissolve any salt crystals that may have formed during storage. Once ready we added 5µl of cRNA (~750ng) to 10µl of Hyb, mixed the solutions by pipetting and briefly spun them down. We placed 200µl of HCB into both top and bottom reservoirs of the hybridisation chamber to prevent the chips drying out.

Meanwhile we heated the cRNA samples for 5 minutes at 65°C and left them to cool to room temperature. Once at room temperature, we loaded 15µl of the sample/hyb mix onto the chip in the appropriate inlet port. We sealed the lid of the hybridisation chamber and the chambers were incubated at 58°C overnight (16hours). In preparation for washing the next day, we prepared 500ml of high-temp wash buffer (50ml of x10 stock to 450ml nuclease free water) and heated it in a Hybex water bath to 55°C overnight.

5.7.6 Washing and staining the bead chip (all incubations are performed at room temperature unless specified).

We removed the coverseals from the chips by submerging the chip face up in a beaker containing E1BC (Expression 1 Bead Chip) buffer (6mls of E1BC buffer in 2L of nuclease free water). We then transferred the chips to a slide rack and submerged them in a staining dish containing 250mls of wash E1BC solution. Once all chips were de-sealed we transferred the slide rack to the hybex water bath containing the preheated high-temp wash buffer and incubated for 10mins.

After incubation we transferred the slide rack back to the staining chamber containing E1BC wash buffer and plunged it in and out of the solution 5-10 times before placing it on an orbital shaker for 5 minutes at a medium speed.

We then moved the slide rack to a clean staining dish containing 250ml fresh 100% 200 proof ethanol and plunged it in and out 5-10 times before placing it on the orbital shaker for 10 minutes.

Once finished the rack we transferred the slide rack to a clean staining dish containing 250ml fresh E1BC wash buffer. Again we plunged it in and out of the solution 5-10 times and placed it on the orbital shaker for 2 minutes.

Meanwhile we prepared wash trays loaded with 4mls of block E1 (Expression 1) buffer in each tray. We transferred the chips from the slide rack to the wash trays with tweezers making sure that the chips were completely submerged in E1 buffer. We rocked the wash trays on the orbital shaker for 10mins at a medium speed.

We then prepared new wash trays containing 2ml per tray of block E1 buffer plus 1:1000 dilution of streptavidin-Cy3. We transferred the chips to these new trays with tweezers and covered them with a lid (streptavidin is photosensitive and produces a green signal when scanned). We rocked the trays for 10mins at a medium speed.

We prepared a third staining chamber containing 250ml of E1BC wash buffer. We transferred the chips back into a slide rack with tweezers and plunged the slide rack in and out of the wash solution 5-10times. We then shook the slide rack on the orbital shaker for 5 minutes at a medium to low speed.

In order to dry the chips we placed the slide rack into a centrifuge and spun them down at 280g at 25°C for 4 minutes. We stored the chips in the dark until they were ready to be scanned on the Illumina BeadArray Reader (www.illumina.com) (~ 1 hour per scan per

chip). The reader recorded the intensity of the green fluorescence signal produced by each well and if it reached a threshold value of 600 the sample was passed as being of good enough quality. Target sequences successfully bound to probe sequences generate a signal that depends on the strength of the hybridization (dependent on the number of paired bases, the hybridization conditions, and washing after hybridization). These intensity values were used as the basis for all the following data analysis.

5.7.7 Data analysis

All data exportation, normalization and statistical analysis performed with the help of Dr John McClure, University of Glasgow). The main challenge was to identify those genes whose expression is significantly different between the SHRSP and WKY. Fold change is the simplest and intuitive approach but this does not provide a significance estimate for any observed changes and the necessary cut off value is arbitrary and differs amongst researchers (Wit and McClure 2004). After we firstly normalised data from the Bead Array reader in Bead Studio (Illumina) and then exported it into third party software we ran a biologically motivated test for the detection of differentially expressed genes in replicated microarray experiments (Rank Products analysis)(Breitling et al. 2004).

5.7.7.1 Rank Products (RP) Analysis

Derived from biological reasoning, a non parametric RP analysis uses the following assumptions(Breitling et al. 2004);

- The relevant expression changes only affect a minority of genes
- Measurements are independent between replicate arrays
- Most changes are independent of each other
- Measurement variance is about equal for all genes

RP analysis does not depend on an estimate of the gene specific measurement variance and is particularly powerful where only a small number of replicates are available(Breitling et al. 2004).

RP values can be used to sort the genes according to the likelihood of observing them in a high position on lists of differentially expressed genes by chance. Genes with the smallest

RP values are the most interesting candidates. For our single channel array the RP values are calculated over all pairwise comparisons. To correct for the fact that pairwise comparisons between samples are not independent, the significance value has to be adjusted.

Instead of permuting the ranks of each replicate, we perform permutations of the expression values for each array and then calculate the corresponding fold changes for all pairwise comparisons. These fold changes are used to produce the RP values. The procedure is always performed separately for up and down regulation.

To determine a threshold for significant differential expression we used a nominal significance level of false discovery rate (FDR) $q<0.05$ to correct for multiple comparisons within the RP analysis. We based this on the Benjamini-Hochberg method(Bejamini and Hochberg 1995).

5.7.7.2 Approach to analysis using Ingenuity Pathway analysis (IPA) software.

As well as the above statistical methods, more sophisticated analysis techniques are available such as IPA which can be used to look at data from the perspective of interlinked metabolic pathways. IPA is a web based microarray and proteomic data analysis tool that utilises published data (Ingenuity® Knowledge Base) in order to identify whether multiple genes are involved in a particular pathway(s) or are differentially expressed in comparisons between experimental groups. It also uses statistical methods such as Fischers Exact Test to identify genes over represented in particular pathways. For more information on how IPA analyses uploaded data see appendix H. We used IPA to analyse our data using both candidate gene and genome wide approaches. For more information see chapter 8.

5.7.8 Quantitative real-time polymerase chain reaction (qRT-PCR)

In order to quantitatively validate any significant findings of interest from the microarray data we performed qRT-PCR. qRT-PCR can amplify any nucleic acid sequence present in a sample via a series of heating and cooling cycles(Kubista et al. 2004). Heating the sample to a high temperature firstly breaks the strands of the DNA helix (whether DNA or cDNA), then subsequent cooling enables the now isolated strands to bind to the DNA template. Finally reheating the reaction to approximately 72°C (the optimum temperature for polymerases) enables the primers to be extended by incorporating dNTPs (the four nucleotide triphosphates). The final amplified sequence can be used to generate a large

number of identical copies for quantitative analysis. Real time PCR is a modification of the original PCR methodology which allows for the detection and amplification of sequences simultaneously enabling the quantity of product formed to be monitored throughout the reaction(Higuchi et al. 1992). As the amount of product forms a fluorescent reporter signals its presence and subsequent accumulation. With each completed cycle the fluorescent signal exponentially increases until the reaction runs out of a critical component (e.g. the primers or polymerase) and the level stabilises(Bustin 2002). The number of cycles needed to reach this threshold is called the CT value. The CT value in gene expression analysis reflects the transcriptional activity within that particular sample(Kubista et al. 2004).

5.7.9 Materials

We used Applied Biosystems gene expression assays (Taqman®) for all qRT-PCRs in this thesis. If a pre-designed assay was not available, a custom assay was designed using Applied Biosystems software. Each Taqman® assay contained a x20 reaction mix containing template-specific forward and reverse primers and a probe that annealed between the two primers. Taqman® probes are hydrolysis probes and have two types of fluorescent dye. The probe DNA is fluorescently tagged at its 3' end, but fluorescence from intact probes is prevented by a quencher molecule that is bound to its 5' end(Holland et al. 1991).

During PCR amplification, the 5'-3' nucleolytic activity of the DNA polymerase cleaves the quencher from the probe, resulting in fluorescence levels proportional to the amount of PCR product present. All of the probes were designed to anneal across two exons in cDNA, guaranteeing that non-specific amplification did not occur from residual genomic DNA. Every effort was made to ensure that the amount of template cDNA was the same in each reaction of an experiment, however given the sensitivity of qRT-PCR, to allow for differences in the amount of cDNA obtained we normalized gene expression to a housekeeping gene. Ideally the housekeeping gene should be one whose expression is not expected to change over experimental groups or conditions and often beta actin is used. However as this gene is central to vascular structural integrity we used Glyceraldehyde-3-phosphate dehydrogenase (GAPDH) instead.

5.7.10 Protocol – Two step qRT-PCR (figure 5.12)

In order for levels of gene expression to be measured by qRT-PCR, extracted RNA samples need to be reverse transcribed to cDNA. All of the qRT-PCR reactions in this thesis were performed using the same DNase treated RNA extracted for assessment using the microarray technique as described previously in this chapter.

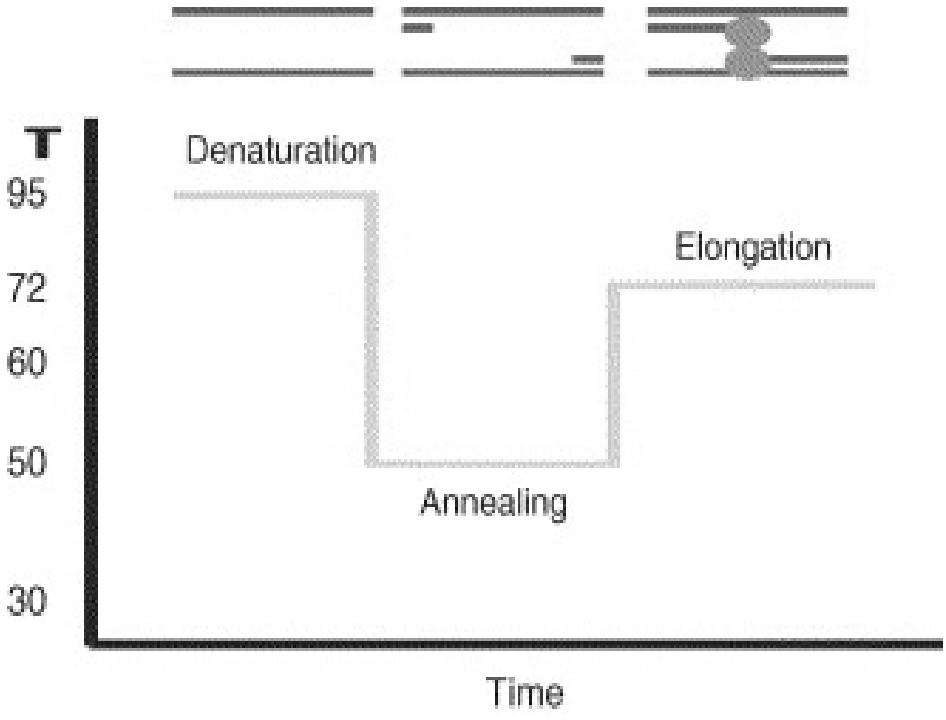

Figure 5.12. The three stages of PCR.

T = Temperature in degrees Celsius. Figure adapted from Kubista et al 2006. Denaturation – the sample is heated to approximately 95℃ to break the strands of either RNA or DNA. Annealing – the temperature is lowered to approximately 50℃ to enable the primers to anneal to the template. Elongation – the temperature is increased back up to approximately 72℃ – the optimum temperature for the polymerase to work to extend the primer by incorporating dNTPs. Each stage is diagrammatically represented at the top of the image.

5.7.10.1 First step – Reverse transcription (RT) to create cDNA

We firstly checked the concentration of each RNA sample (DNase treated) using the nanodrop then calculated how much of each sample was required (in µl) in order to ensure approximately 1µg of RNA in each 20µl reaction e.g. approximately 1.4µl of an RNA sample of concentration 700ng/µl would be required.

Each 20µl reaction contained 12.3µl of master mix, the required amount of RNA and the remaining volume was made up with nuclease free water (NFW). We used the Taqman® reverse transcription master mix (Applied Biosystems) which consisted of; RT buffer, Magnesium Chloride ($MgCl_2$) solution, RNase inhibitors, OligodT primers and Multiscribe™ reverse transcriptase enzyme.

On a 96 well plate we added the RNA, NFW and the master mix to each well in a systematic order labelling the wells appropriately. The plate was sealed with an adhesive clear plastic lid and placed onto the thermocycler. Once cDNA had been created we added 40µl of NFW to create enough stock cDNA from each sample (60µl) to be used to assess all our genes of interest. Spare cDNA was stored at -20°C.

5.7.10.2 Second step – qRT-PCR

We made up the qRT-PCR reaction mix using Taqman® universal master mix (Applied Biosystems) plus a probe for the housekeeping gene (GAPDH) and finally the Taqman® probe corresponding to our gene of interest. The housekeeping probe and the probe corresponding to our gene of interest were labelled with different reporter dyes. GAPDH was labelled with VIC® whereas our genes of interest were labelled with FAM®. The two dyes fluoresce at different wavelengths so can be easily distinguished on subsequent analyses. 3µl of the combined master mix and probe solution was added to 2ul of cDNA into each well of a 384 well plate and sealed with an adhesive optically clear plastic lid (total reaction volume 5µl in each well). We loaded all samples onto the plate in triplicates to produce reliable CT values. We then placed the plate into a 7900HT sequence detection system (Applied Biosciences) and programmed the platform to read the plate using Sequence Detection System (SDS) Software (version 2.4) (Applied Biosystems). The 7900HT system encompasses a heating block for thermal cycling and detectors to measure fluorescence in each well of a 384-well optical plate.

5.7.11 Data analysis

Fluorescence is measured after every amplification cycle to quantify the accumulation of PCR product. During the exponential phase of PCR cycling the rate of product accumulation is proportional to template concentration therefore relative template abundance can be quantified by monitoring increasing fluorescence in each well during temperature cycling.

We performed statistical analysis using CT values. The CT value is the cycle number at the threshold level of log-based fluorescence (the level at which fluorescence exceeds background noise). CT levels are inversely proportional to the amount of target nucleic acid in the sample (i.e. the lower the CT level the greater the amount of target nucleic acid in the sample).

Firstly we calculated dCT values for all replicates of all the samples, the dCT value is the difference in CT values between the gene of interest and the housekeeper (measured in the same sample). As we performed all of the PCR in triplicate, we took the mean dCT value from the 3 readings per biological replicate. We used this data to calculate the overall mean dCT plus the standard error of the mean for all 4 animals in each group and to perform a two-tailed T test to establish whether there was a significant difference in dCT values between the WKY and SHRSP.

We then used the overall mean dCT for each group to calculate the ddCT [delta-delta CT] value i.e. the difference between the mean dCT of SHRSP and the mean dCT value of WKY. This results in the mean ddCT for the "control" group equalling 0. As larger CT values mean lower gene expression, a negative ddCT will mean that a group has more gene expression on average than the "control" group. Also, an increase of 1 in a dCT value implies a halving of gene expression; an increase of 2 implies expression is one quarter of the value (reduction of 75%); a decrease of 1 implies a doubling of expression; a decrease of 2 implies a quadrupling of expression etc.

In order to correlate our data with the microarray findings we wished to express the PCR data in terms of fold change, however because differences in expression using CT values are on an negative exponential/power scale, in order to express the data as fold changes we converted ddCT values using the following formula;

RQ = 2^(-ddCT)

where RQ = relative quantification (this value is equivalent to fold change)and ^ means "to the power of", e.g. $2^0=1$.

We plotted the RQ numbers on a bar chart using excel. We calculated the error bars from ddCT values and exponentiated them using the 2^(-value) formula because the RQ scale is not symmetric (it is a ratio scale) therefore the lower end of an error bar will be nearer the RQ value than the upper end.

5.7.12 Gene sequencing

5.7.12.1 Standard (End point) PCR

All end point PCR and sequencing was performed by Miss Wendy Crawford (Centre for Cardiovascular Research, Glasgow University) and was performed on an MJ Research PTC Gradient Cycler in 96 well plates (ABgene).

Firstly we designed forward (n=4) and reverse (n=3) primers corresponding to the portion of the GUCY1a3 gene sequence covered by the Illumina microarray probe. All primers were designed by eye and all contained close to a 50% GC content to prevent a high melting temperature causing non specific bands to appear on electrophoresis. We purchased all primers from MWG Biotech.

To test for insertions or deletions within the sequence between strains we ran end point PCR using these primers, on DNA taken from the livers of SHRSP (n=4) and WKY (n=3). End point PCR (unlike qRT-PCR – see above) does not provide a quantitative assessment of the level of gene expression it simply provides a yes/no answer as to whether the gene is expressed. This was used to test for any changes within the length of sequence between the two strains such as the presence of an insertion or a deletion. We performed end point PCR on both cDNA and genomic DNA depending on the pairing of primers, for example AF when paired with CR covered the complete open reading frame and was therefore performed on genomic DNA.

Due to the need for absolute fidelity of DNA replication instead of using Taq DNA polymerases (as used in qRT-PCR see above) which are liable to incorporate incorrect nucleotides every 10,000 nucleotides, we used ‘Kod Hot Start’ DNA polymerase (Novagen). We performed Kod PCR’s using the designated kit and to manufacturer’s instructions. For full details of the reaction mixture and heat cycling protocol see appendix I. Briefly, the cycling conditions we used consisted of heating the PCR mixture to 95°C for 2 minutes to activate the polymerase, a denaturing step at the same temperature for 20 seconds, followed by a 30 second annealing phase at 52°C for all primers. Extension times depended on the length of sequence being created, for the forward primers we allowed 2.5 minutes whereas

for the reverse primers we allowed 10 minutes to ensure that all dNTP's were fixed (see www.novagen.com/protocol for a full version of the protocol). The MJ Research PTC Gradient Cycler then repeated this cycle 20-40 times and the results were analysed using agarose gel electrophoresis.

We used 1% agarose (Eurogentec) gels which were dissolved and electrophoresed at 6V per cm of gel in 1x Tris-Borate EDTA (TBE) buffer (Fisher Bioreagents) using BIO-RAD Power Pac 300 and BIO-RAD electrophoresis tanks. We added 1ng/100ml ethidium bromide (Sigma) to molten agarose before pouring gels and we loaded samples with 6x loading dye (50% glycerol, 0.05% bromophenol blue). We visualised gels using UV transillumination on a BIO-RAD Fluor-S Multimager. We assessed the size of PCR products using Promega 100bp or 1kb DNA ladders.

5.7.12.2 DNA Sequencing

We performed DNA sequencing by firstly purifying PCR products (WKY n=3, SHRSP n=2) to remove un-incorporated dNTPs, salts and / or primers using an Agencourt AMPure kit. This technique separates DNA products over 100bp in length via binding to paramagnetic beads (a full protocol is available in appendix J). We used the purified product (~8µl per 20µl PCR reaction) to conduct dideoxy sequencing.

We used Applied Biosystems BigDye Terminator n3.1 Cycle Sequencing kits for all sequencing reactions and reactions were performed in 96 well plates. All sequencing reactions included sequencing buffer (3.5µl), ready reaction (0.5µl), primer (3.2µl) and water (4.8µl). We used a temperature cycling program of 96°C for 45 seconds, 50°C for 25 seconds and 60°C for 4 minutes which was repeated 25 times.

We purified sequencing reactions to remove reaction constituents, un-incorporated nucleotides and / primers prior to electrophoresis using Agencourt CleanSeq reagent. We subsequently loaded 20µl of purified sequencing product into optically clear 96 well plates and filled any remaining wells on the plate with water to prevent drying of capillaries. We covered plates with Applied Biosystems Septa Seals which allow the entry of capillaries to the plate whilst preventing the evaporation of products.

We performed sequencing capillary electrophoresis on a 48-capillary Applied Biosystems 3730 Genetic Analyser with 36cm capillaries filled with POP-7 polymer (Applied Biosystems) and warmed to 60°C. We separated sequencing products by size using electrophoresis set to 8500V for 50 minutes.

5.7.13 Data analysis

We analysed sequencing using Applied Biosystems SeqScape software version 2.1. We aligned experimental sequences with known sequences derived from bioinformatic databases such as UCSC or ENSEMBL genome browser, or product sequences such as plasmid sequences.

CHAPTER 6 : QUALITATIVE AND QUANTITATIVE ASSESSMENT OF MICROVASCULAR AND PERIVASCULAR CHANGES WITH HEMATOXYLIN AND EOSIN STAIN.

6.1 Background

The cerebral pathology in the SHRSP was first assessed in the 1970's using conventional stains such as H&E along with light microscopy. The focus of this research was the end stage pathology therefore most papers describe changes in the brains of older animals which suffered a symptomatic 'stroke'. What the current literature lacks is a simple qualitative assessment of pathological changes in the brain from a young normotensive stage through to the end 'stroke' stage. This is important in order to establish the sequence of pathological changes in the brain and vessels. To our knowledge only one, Tagami et al, examined the perforating arterioles histologically every 4 weeks from 4 weeks to 52 weeks of age(Tagami et al. 1987). However, they did not compare SHRSP with a control strain (e.g. WKY or SHR), did not blind the analysis and provided few details on animals less than 12 weeks old(Tagami et al. 1987). Since then many studies focused on older ages and used salt-loading to accelerate pathological changes or induced large artery occlusion to test new stroke treatments, rather than trying to determine the spontaneous microvascular changes and possible mechanisms. The SHRSP literature also lacks quantitative assessments of features such as vessel and neuronal density and other changes to the neurovascular unit e.g. oligodendrocytes.

In the SHRSP, there is wide consensus that the arteries and arterioles display signs of arteriolar wall thickening and sclerosis which has been attributed to hypertension(Ogata et al. 1980;Fredriksson et al. 1985;Mies et al. 1999). However, there does not appear to have been any quantification of the scale of thickening although a sclerotic ratio for human small vessel disease (SVD) exists(Lammie et al. 1997).

Therefore in this study we aimed to;

A) Describe qualitatively the brain parenchymal and vascular histopathology in SHRSP animals compared with WKY controls, from a young normotensive age through to a stroke prone stage.

B) Quantify the pathological changes by performing density counts of neurovascular unit components.

C) Quantify the degree of vessel narrowing using a sclerotic index(Lammie et al. 1997)originally described in human microvascular disease.

6.2 Materials and Methods

6.2.1 Animals & Tissue preparation

As previously stated we assessed 5, 16 & 21 week old animals fed on a normal diet (n=30) and 21 week old WKY and SHRSP exposed to salt-loading (n=10). Hemispheres were fixed in formalin divided into 2mm slices and embedded in paraffin before being sectioned according to the standard sampling protocol described in chapter 5. We cut sections at 7µm from both a frontal and mid coronal section from each animal and mounted them on double frost slides for H&E staining.

6.2.2 Methods

H&E staining was conducted according to the protocol described in chapter 5. Briefly, we brought sections to water, incubated for 30mins in picric acid then stained them in hematoxylin for 7 minutes. Then we washed the sections in water, differentiated them in acid alcohol, washed them in water once more and dipped them in lithium carbonate before staining them in Eosin for 10 minutes. Sections were washed in water then dipped three times in the mordant potassium aluminate. After a final wash with water, we dehydrated slides via graded alcohols and finally cleared them in xylene.

6.2.3 Qualitative assessment of morphological changes

Three observers blinded to the animals age, strain and diet (EB, CS & JW) assessed all slides of both frontal and mid coronal sections for any gross pathology under a light microscope

(Olympus BX51). We recorded the presence of any vessel thickening, white matter rarefaction, and any other evidence of microinfarction or haemorrhage. We also examined the lining of the lateral ventricles for evidence of structural changes or leakage of cerebrospinal fluid (CSF) into the brain parenchyma.

6.2.4 Quantitative assessment of pathological changes

We performed two quantitative assessments on both frontal and mid coronal sections for each animal. Firstly we counted components of the neurovascular unit and secondly we assessed vessel wall thickening using the sclerotic index(Lammie et al. 1997) on three regions of interest (cortical grey, white matter and deep grey matter) using a standard sampling protocol that we described previously (see chapter 5).

6.2.4.1 Density counts of components of the neurovascular unit.

As described in more detail in chapter 5 of this thesis, using ImagePro™ (version 6.2), we designed a stereology protocol that generated three random sampling points of 300μm^2 at x20 objective within each region of interest for each slide – cortical grey, white matter and deep grey matter. Within each sampling point, we counted all capillaries, neurons and oligodendrocytes (‘objects’) within the same frame, in each sampling point in a random order. We exported the data for each region of interest to an excel spreadsheet for analysis.

The increase in size of the rat brain with advancing age would result in a different total area sampled at each age. To adjust for this, we adjusted the object counts for age by calculating ratios - 5:16 & 16:21 for all cross section areas and applying the ratio to the counts. The counts were not normally distributed so we calculated the median object count for each age, strain and brain section (frontal or mid coronal) for use in a general linear model.

6.2.4.2 Quantification of the presence / absence of vessel wall thickening using a sclerotic index.

To assess vessel wall thickening we used Lammie's sclerotic index(Lammie et al. 1997) where the following formula is applied;

Index = 1-(internal /external vessel diameter).

Normal vessels lie within the range of 0.2-0.3, and 0.3-0.5 constitutes moderate sclerosis, and severe sclerosis is anything over 0.5.

We sampled 5 vessels from each of the cortical and deep grey matter and three from the white matter for each section in each animal. Using the distance measurement tool on Image Pro™, we took the internal lumen diameter and the external diameter of the vessel. For more detail see chapter 5 of this thesis. We exported the data to an excel spreadsheet for calculation of the ratio and further statistical analyses.

6.2.5 Data analysis

The increase in size of the rat brain with advancing age would result in a different total area sampled at each age. To adjust for this, we adjusted the object counts for age by calculating ratios - 5:16 & 16:21 for all cross section areas and applying the ratio to the counts. The counts were not normally distributed so we calculated the median object count for each age, strain and brain section (frontal or mid coronal) for use in a general linear model (GLM).

We performed statistical analysis using R software. We performed a GLM using either the median counts or the mean ratio of all vessels sampled within a region of interest per strain per age. We analysed the effect of age, strain and salt-loading on both sets of data. P values of <0.05 were considered statistically significant. Error bars represent 95% confidence intervals.

6.3 Results

6.3.1 Qualitative assessment of morphological changes

6.3.1.1 Animals fed on a normal diet – ages 5, 16 and 21 weeks;

5 week old **–** no differences were noted on H&E staining in 5 week old SHRSP compared with WKY. In SHRSP there was one area of endothelial proliferation in a frontal meningeal vessel (figure 6.1).

16 week old **–** no differences were noted between strains at age 16 weeks in the frontal or mid coronal sections.

21 week old animals – in the WKY animals there were a few areas of vessel wall thickening and endothelial proliferation (figure 6.2). In the SHRSP there were many thickened vessel walls and we saw hyalinization in a wide variety of vessels across all regions in meningeal arteries to the small perforating arterioles in the deep grey matter in both frontal and mid coronal sections (figure 6.3).

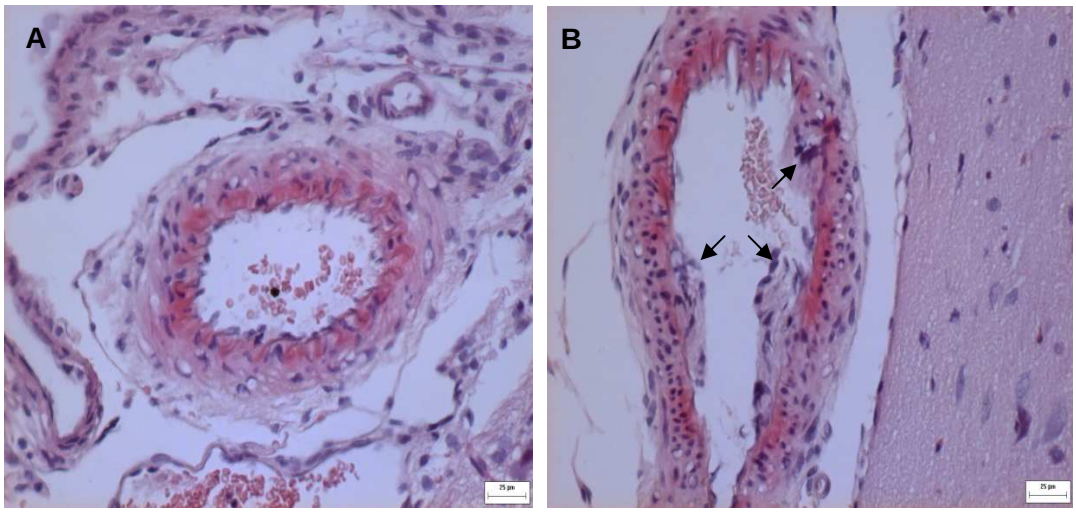

Figure 6.1. H&E stained frontal sections.

Taken from 5 week old A) WKY and B) SHRSP rat. The leptomeningeal vessel in the SHRSP rat shows evidence of endothelial cell proliferation (↙). Images x20 objective. Scale bar = 25µm

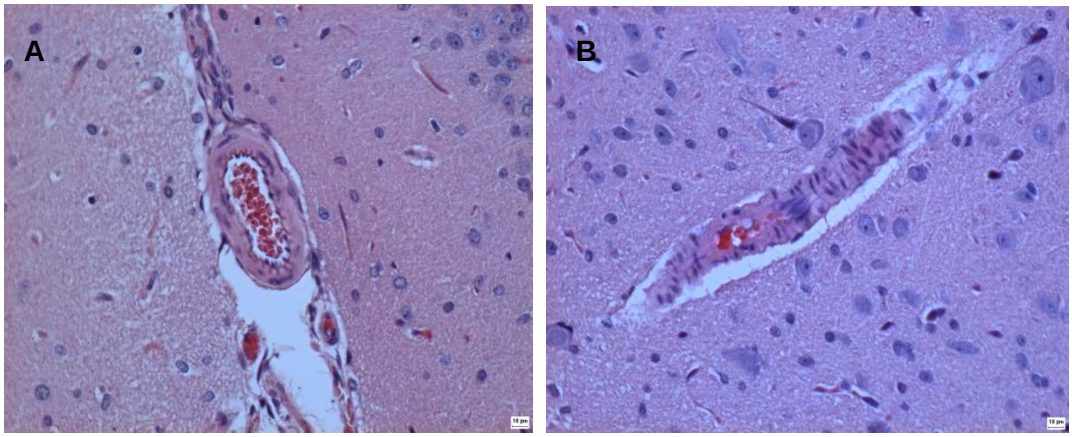

Figure 6.2. H&E staining of cortical arterioles taken from 21 week old A) WKY and B) SHRSP animals raised on a normal diet.

Both images taken at x20 objective. The vessel from the WKY rat has an even wall with a clearly visible lumen and endothelial cell layer. The vessel from the SHRSP rat in contrast has unevenly thick walls in places obscuring the lumen and lacks a defined internal elastic lamina and endothelial cell layer.

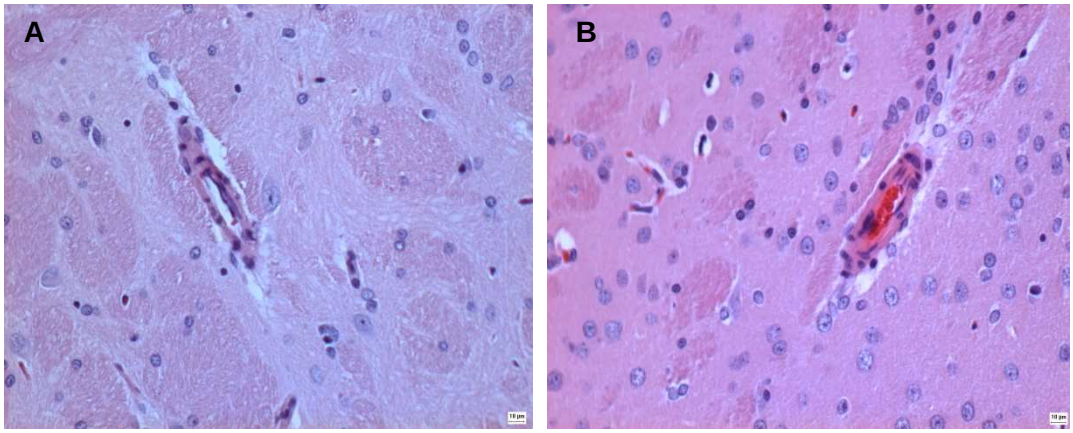

Figure 6.3. H&E staining of arterioles taken from the deep grey matter of 21 week old A) WKY and B) SHRSP animals raised on a normal diet.

Both images taken at x20 objective. The vessel from the WKY rat once again has an even wall with a clearly visible lumen. In contrast the SHRSP vessel has a visibly thickened wall.

Salt-loaded (+NaCl) animals (21 weeks) – Both strains showed more morphological changes when salt-loaded than when fed on a normal diet. Two WKY+NaCl rats showed vacuolated white matter and others showed vessel hyalinization (figure 6.4). Thickening of vessels due to smooth muscle and endothelial proliferation was common in all sections. Additionally, there was an area of white matter rarefaction and cavitation in the internal capsule of one SHRSP+NaCl rat consistent with an established lacunar infarct (figure 6.5).

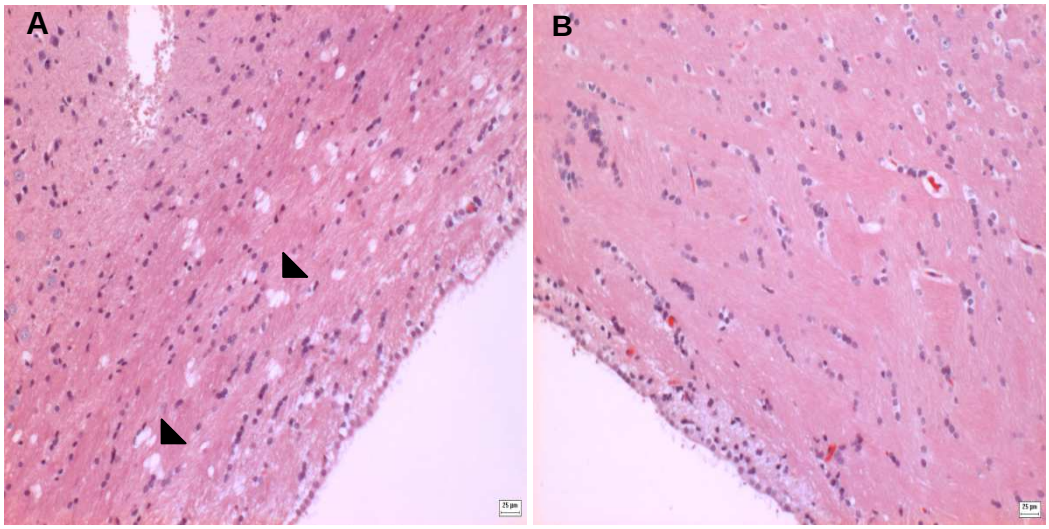

Figure 6.4. H&E staining of A) a 21 week WKY+NaCl versus B) a 21 week WKY.

Both images taken at x10 objective. Scale bar = 25µm. In two WKY+NaCl animals we saw potential vacuolation (black triangles) in the white matter surrounding the lateral ventricle. Despite all tissue being fixed and processed in exactly the same way we did not encounter this in any other group of animals.

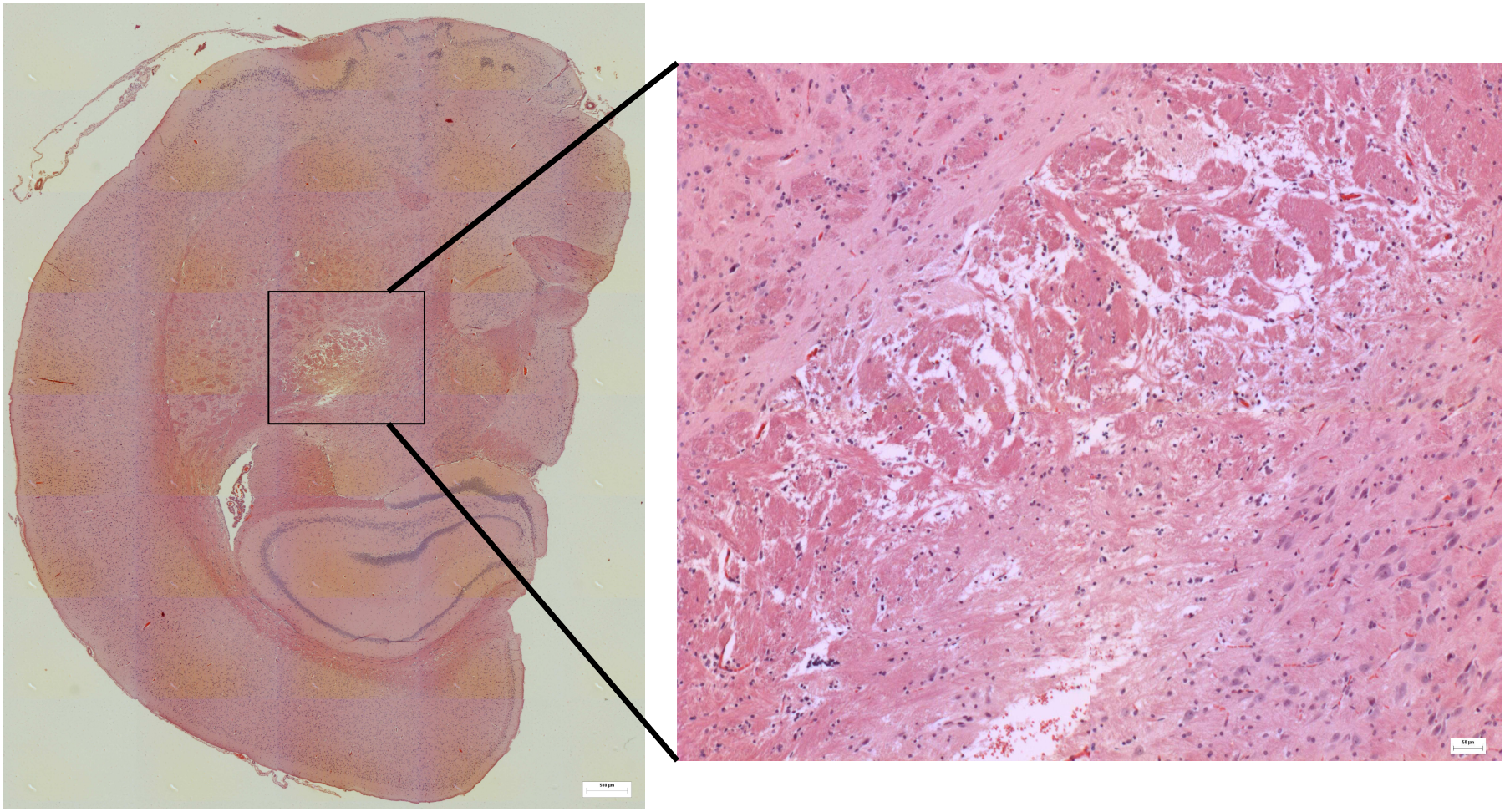

Figure 6.5. H&E staining of a mid coronal section taken from a 21 week SHRSP+NaCl showing an area of white matter cavitation in the internal capsule. Left image is a tiled image taken at x4 objective.

Right image taken at x10 objective. This area of rarefaction enveloped approximately half the length of the internal capsule in this section. Calcified neurons were also found close to the site.

6.3.2 Quantitative assessment of pathological changes

6.3.2.1 Density counts of components of the neurovascular unit.

All median count data and the results of statistical analysis can be seen in table 6.1.

6.3.2.2 Animals fed on a normal diet – ages 5, 16 and 21 weeks

Capillaries (figure 6.6) – There were no strain or age differences in capillary counts in the white matter of either brain section. In the frontal section there were significantly higher counts at ages 16 & 21 weeks in both cortical grey ($p<0.001$) and deep grey matter ($p<0.001$) compared to 5 week olds.

Neurons (figure 6.7) – There were no strain or age differences in neuronal cell counts in the frontal or mid coronal white matter. In the frontal section, the neuronal cell count was significantly higher in the cortical grey matter at 21 weeks than at 5 weeks ($p=0.02$) and significantly higher in the deep grey matter at 16 weeks than at 5 weeks ($p=0.01$). In mid coronal sections there were no strain or age differences in the cortical grey matter. In the deep grey matter neuronal cell counts were significantly higher at 16 weeks compared to 5 weeks ($p=0.02$).

Oligodendrocytes (figure 6.8) – There were no differences in oligodendrocyte counts in the white matter of either brain section or in the frontal cortical grey matter. In the frontal deep grey matter both species showed a trend towards a higher count of oligodendrocytes at age 16 weeks compared to 5 weeks ($p=0.07$). In the mid coronal cortical grey matter the oligodendrocyte counts were higher in SHRSP than WKY at all ages ($p=0.03$).

Table 6.1. Median count data ± 95% confidence intervals for capillaries, neurons and oligodendrocytes in 5, 16 and 21 week old WKY and SHRSP.

	AGE	5 weeks (median ± 95% CI)			16 weeks (median ± 95% CI)			21 weeks (median ± 95% CI)		
	REGION	Cortex	White Matter	Deep Grey	Cortex	White Matter	Deep Grey	Cortex	White Matter	Deep Grey
Capillaries Frontal	WKY	26 (24-33)	27 (26-42)	34 (22-34)	64 (54-67)	30 (29-33)	51 (47-67)	38 (31-42)	27 (26-27)	32 (31-33)
	SHRSP	27 (21-33)	30 (30-33)	24 (14-28)	67 (46-68)	31 (24-40)	50 (42-63)	53 (48-57)	36 (22-39)	42 (40-44)
	P for strain	Cortex = NS			White Matter = NS			Deep Grey = NS		
	P for age	Cortex p<0.001			White Matter = NS			Deep Grey = NS		
Capillaries Mid Coronal	WKY	33 (30-40)	30 (24-36)	35 (29-41)	69 (60-76)	27 (23-32)	49 (38-54)	31 (26-34)	25 (24-28)	24 (22-29)
	SHRSP	38 (35-50)	23 (23-24)	31 (29-32)	42 (41-52)	20 (19-23)	30 (25-39)	46 (31-46)	25 (18-27)	35 (28-44)
	P for strain	Cortex = NS			White Matter = NS			Deep Grey = NS		
	P for age	Cortex = NS			White Matter = NS			Deep Grey = NS		
Neurons Frontal	WKY	99 (89-160)	225 (223-239)	168 (164-182)	208 (192-266)	223 (216-311)	208 (205-272)	163 (157-200)	264 (257-295)	172 (155-173)
	SHRSP	156 (124-158)	272 (222-306)	168 (164-188)	212 (148-213)	297 (257-386)	234 (198-325)	246 (223-274)	249 (227-282)	205 (194-205)
	P for strain	Cortex = NS			White Matter = NS			Deep Grey = NS		
	P for age	Cortex p<0.05			White Matter = NS			Deep Grey p<0.05		
Neurons Mid Coronal	WKY	185 (177-201)	252 (214-257)	155 (138-221)	286 (278-296)	285 (261-296)	245 (211-333)	188 (177-208)	288 (278-361)	151 (124-208)
	SHRSP	229 (161-235)	263 (154-365)	166 (146-178)	237 (182-240)	315 (300-346)	270 (254-315)	267 (182-276)	318 (305-318)	244 (240-262)
	P for strain	Cortex = NS			White Matter = NS			Deep Grey = NS		
	P for age	Cortex = NS			White Matter = NS			Deep Grey p<0.05		
Oligodendrocytes Frontal	WKY	16 (12-21)	24 (22-31)	17 (14-17)	15 (14-15)	36 (33-38)	23 (14-28)	9 (7-10)	13 (11-18)	12 (12-16)
	SHRSP	16 (15-23)	23 (22-24)	12 (11-21)	19 (16-24)	25 (25-28)	24 (23-26)	17 (14-18)	18 (17-20)	12 (9-14)
	P for strain	Cortex = NS			White Matter = NS			Deep Grey = NS		
	P for age	Cortex = NS			White Matter = NS			Deep Grey = NS		
Oligodendrocytes Mid Coronal	WKY	16 (15-18)	28 (20-34)	17 (16-20)	26 (22-28)	31 (27-38)	28 (20-52)	12 (12-17)	16 (15-21)	13 (9-14)
	SHRSP	24 (23-26)	29 (26-41)	21 (21-28)	17 (14-17)	26 (19-26)	17 (17-22)	19 (19-23)	19 (18-35)	19 (15-20)
	P for strain	Cortex p<0.05			White Matter = NS			Deep Grey = NS		
	P for age	Cortex = NS			White Matter = NS			Deep Grey = NS		

Each value represents n=5 animals. NS = No significant difference.

CAPILLARIES

A) Frontal Section

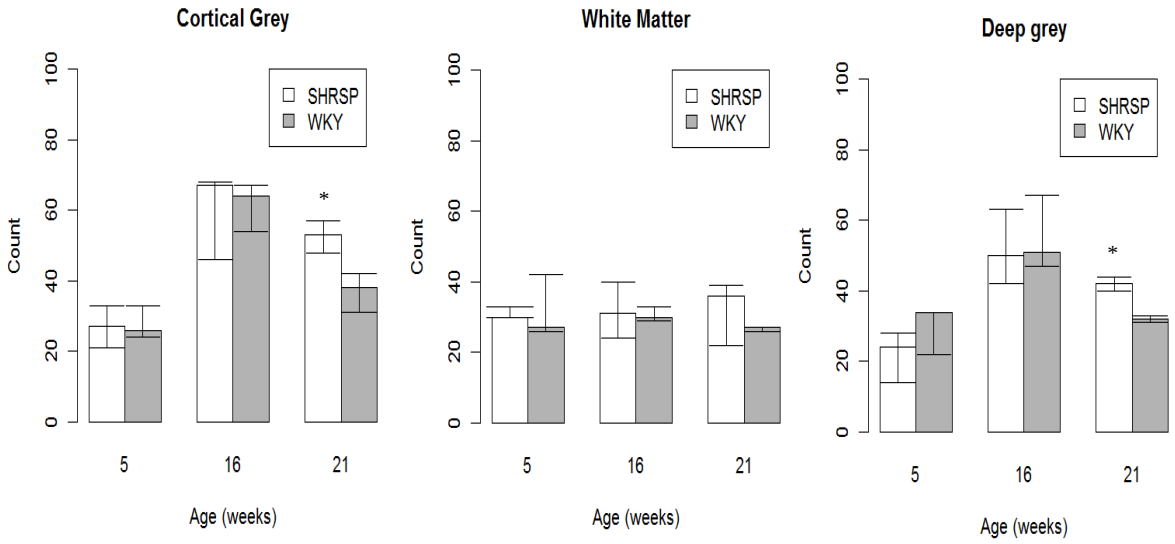

B) Mid Coronal Section

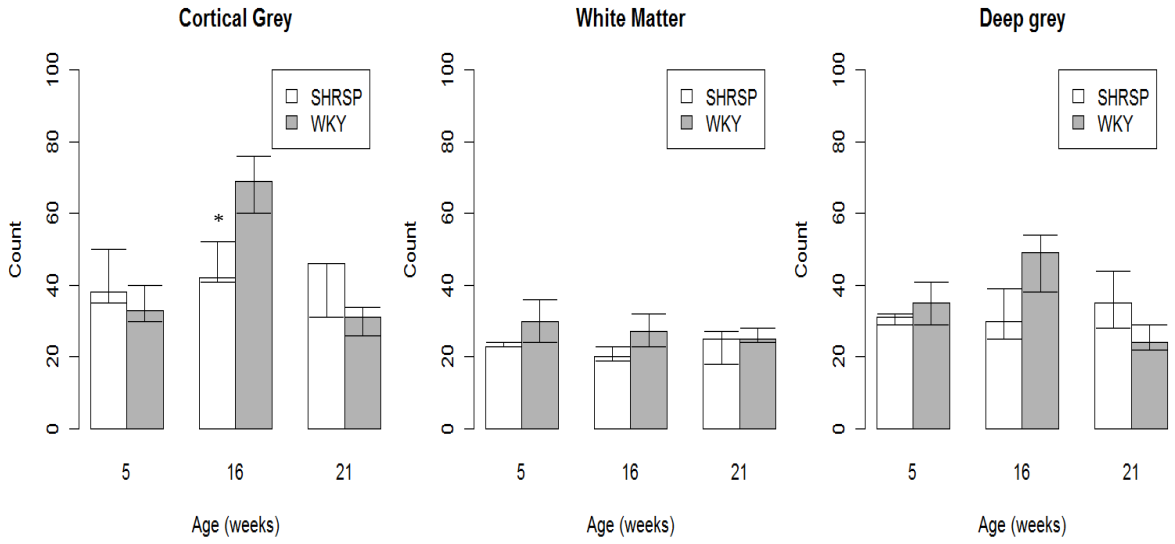

Figure 6.6. Bar graphs showing the median number of capillaries (y axis) counted in 3x300μm^2 frames in n=5 rats per group at ages 5, 16 and 21 weeks.

A) frontal and B) mid coronal brain sections. Error bars represent 95% confidence intervals. We found no overall significant differences between the two strains however the capillary count in the cortical grey matter of the frontal section significantly increased with age ($p<0.001$) in both strains.

NEURONS

A) Frontal Section

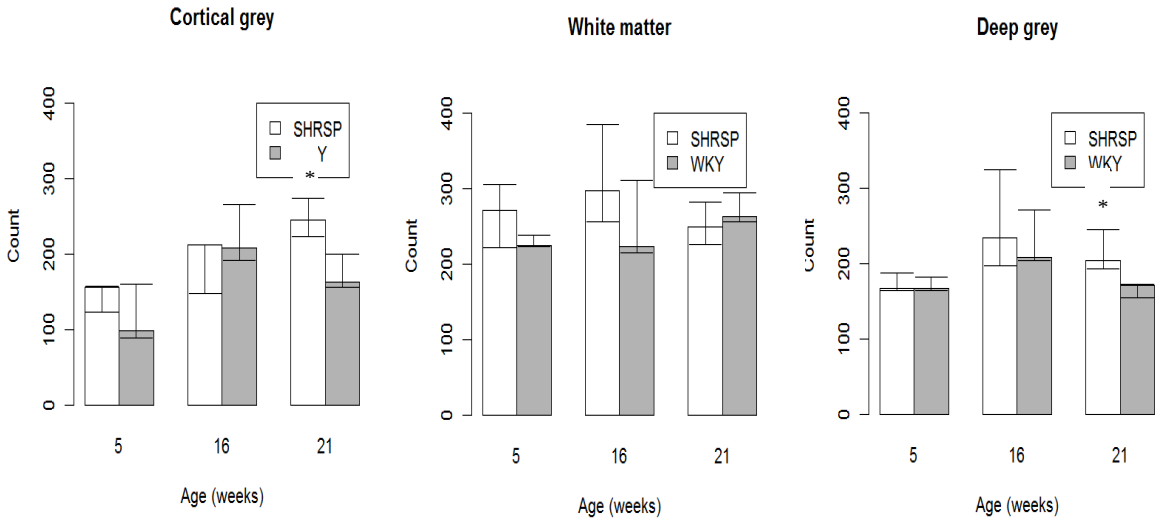

B) Mid Coronal Section

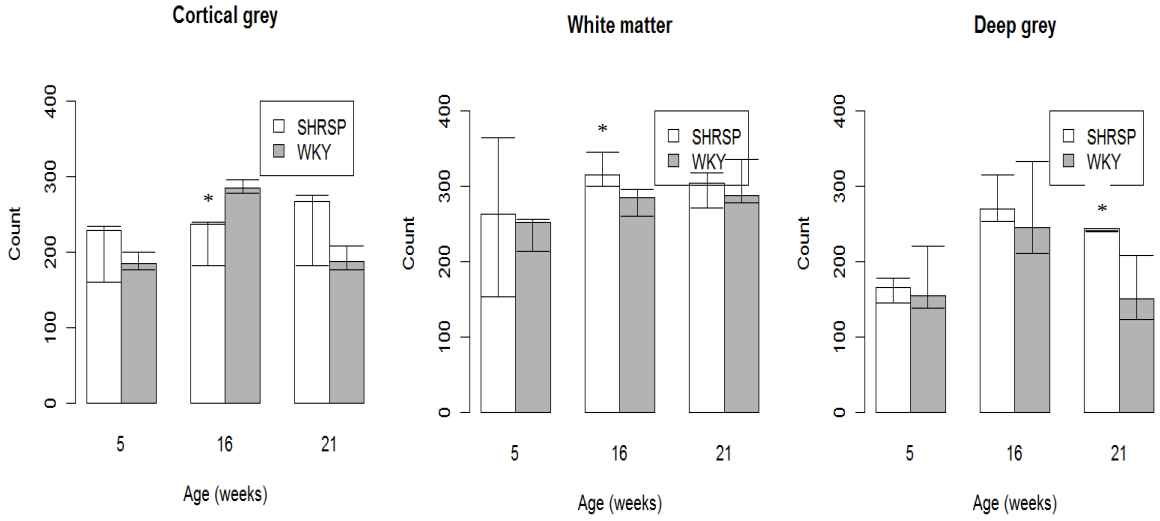

Figure 6.7. **Bar graphs showing the median number of neurons (y axis) counted in 3x300µm^2 frames in n=5 rats per group at ages 5, 16 and 21 weeks**.

A) frontal and B) mid coronal brain sections. Error bars represent 95% confidence intervals. We found no significant differences in neuronal count between the strains. We did find a significant increase in neuronal count with age in the cortical grey and deep grey matter of the frontal section as well as the cortical grey matter of the mid coronal section ($p<0.05$).

OLIGODENDROCYTES

A) Frontal Section

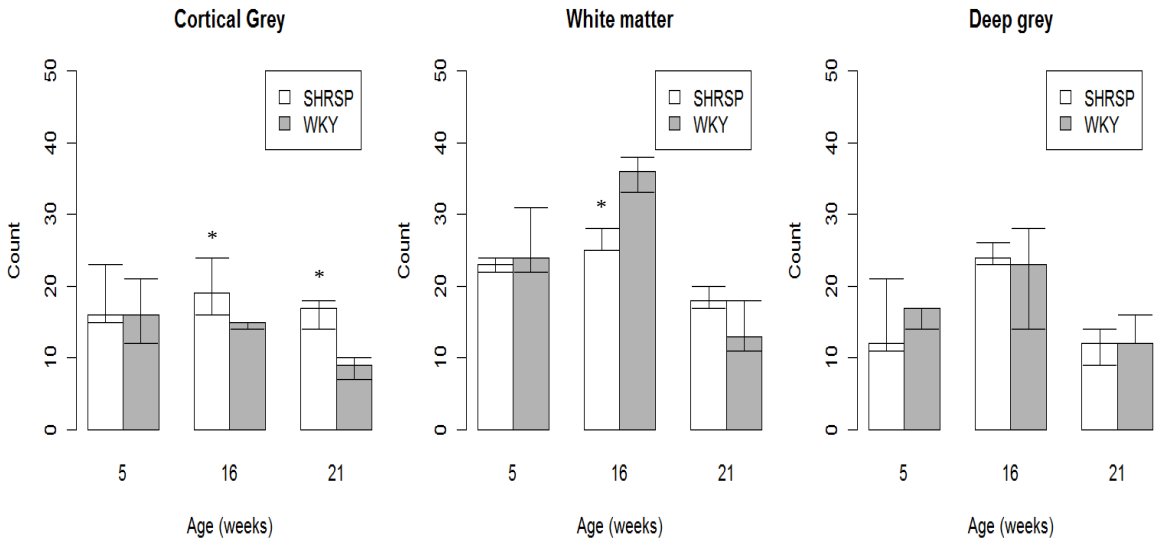

B) Mid Coronal Section

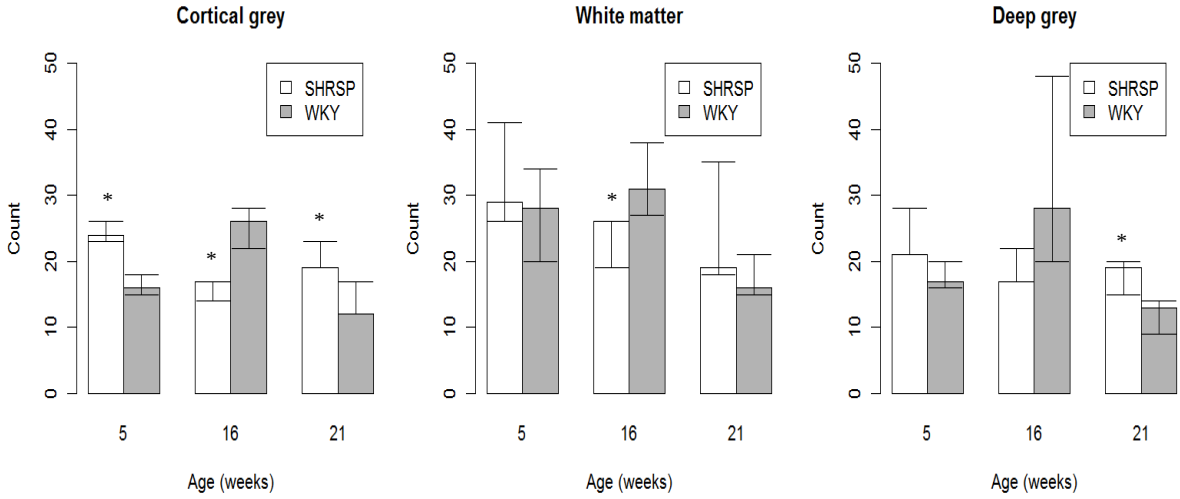

Figure 6.8. Bar graphs showing the median number of oligodendrocytes (y axis) counted in 3x300µm^2 frames in n=5 rats per group at ages 5, 16 and 21 weeks.

A) frontal and B) mid coronal brain sections. Error bars represent 95% confidence intervals. We found significantly more oligodendrocytes in the cortical grey matter of the mid coronal section in SHRSP rats versus WKY aged 5 and 21 weeks ($p<0.05$).

6.3.2.3 Salt-loaded (+NaCl) animals (aged 21 weeks)

For all count data and results of statistical analysis see table 6.2.

Salt was associated with a decrease in capillary count (figure 6.9) in the white matter of the mid coronal section in WKY+NaCl versus SHRSP+NaCl ($p=0.02$).

Salt had no significant effect on any of the neuronal cell counts (figure 6.10) or oligodendrocyte counts (figure 6.11) in any region of either brain section.

Table 6.2. Median count data ± 95% confidence intervals for capillaries, neurons and oligodendrocytes in 21 week old WKY and SHRSP fed either standard rat chow or exposed to 1% salt-loading from the age of 18 weeks.

COUNT	SALT	No Salt (median ± 95% CI)			Salt (median ± 95% CI)		
	REGION	Cortex	White Matter	Deep Grey	Cortex	White Matter	Deep Grey
Capillaries Frontal	WKY	17 (16-18)	7 (6-9)	14 (12-17)	15 (13-17)	9 (7-12)	15 (14-16)
	SHRSP	18 (17-22)	13 (9-15)	19 (17-19)	16 (13-22)	12 (10-12)	16 (15-17)
	P for salt		WKY:WKY+NaCl No significant differences	WKY+NaCl :SHRSP+NaCl No significant differences		SHRSP:SHRSP+ NaCl No significant differences	
Capillaries Mid Coronal	WKY	12 (11-16)	8 (8-9)	14 (9-17)	15 (11-16)	4 (2-5)	13 (12-13)
	SHRSP	16 (16-18)	9 (8-9)	14 (13-15)	16 (13-18)	9 (8-11)	11 (10-18)
	P for salt		WKY:WKY+NaCl No significant differences	WKY+NaCl :SHRSP+ NaCl Cortex = NS White Matter p=0.02 Deep Grey = NS		SHRSP:SHRSP+NaCl No significant differences	
Neurons Frontal	WKY	72 (66-89)	102 (97-103)	80 (80-108)	76 (74-85)	95 (78-100)	72 (72-83)
	SHRSP	91 (79-105)	98 (84-102)	91 (89-92)	79 (68-86)	112 (91-114)	94 (83-95)
	P for salt		WKY:WKY+NaCl No significant differences	WKY+salt:SHRSP+NaCl No significant differences		SHRSP:SHRSP+NaCl No significant differences	
Neurons Mid Coronal	WKY	75 (70-77)	102 (98-103)	76 (65-92)	86 (82-98)	95 (78-100)	90 (61-91)
	SHRSP	83 (78-97)	98 (84-102)	94 (85-94)	98 (64-106)	112 (91-114)	96 (94-108)
	P for salt		WKY:WKY+NaCl No significant differences	WKY+salt:SHRSP+NaCl Cortex = NS White matter = NS Deep grey p=0.04		SHRSP:SHRSP+NaCl No significant differences	
Oligodendrocytes Frontal	WKY	5 (3-6)	5 (4-9)	5 (5-6)	3 (3-3)	4 (4-5)	6 (5-7)
	SHRSP	7 (5-8)	7 (6-7)	4 (4-5)	5 (4-5)	5 (5-8)	4 (3-6)
	P for salt		WKY:WKY+NaCl No significant differences	WKY+NaCl:SHRSP+NaCl No significant differences		SHRSP:SHRSP+NaCl No significant differences	
Oligodendrocytes Mid Coronal	WKY	5 (4-7)	6 (4-7)	5 (5-6)	4 (3-6)	8 (8-9)	5 (5-5)
	SHRSP	7 (6-9)	11 (6-12)	6 (6-7)	7 (6-7)	7 (5-10)	6 (6-7)
	P for salt		WKY:WKY+NaCl No significant differences	WKY+NaCl:SHRSP+NaCl No significant differences		SHRSP:SHRSP+salt No significant differences	

Each value represents n=5 animals. NS = no significant difference.

CAPILLARIES

A) Frontal Section

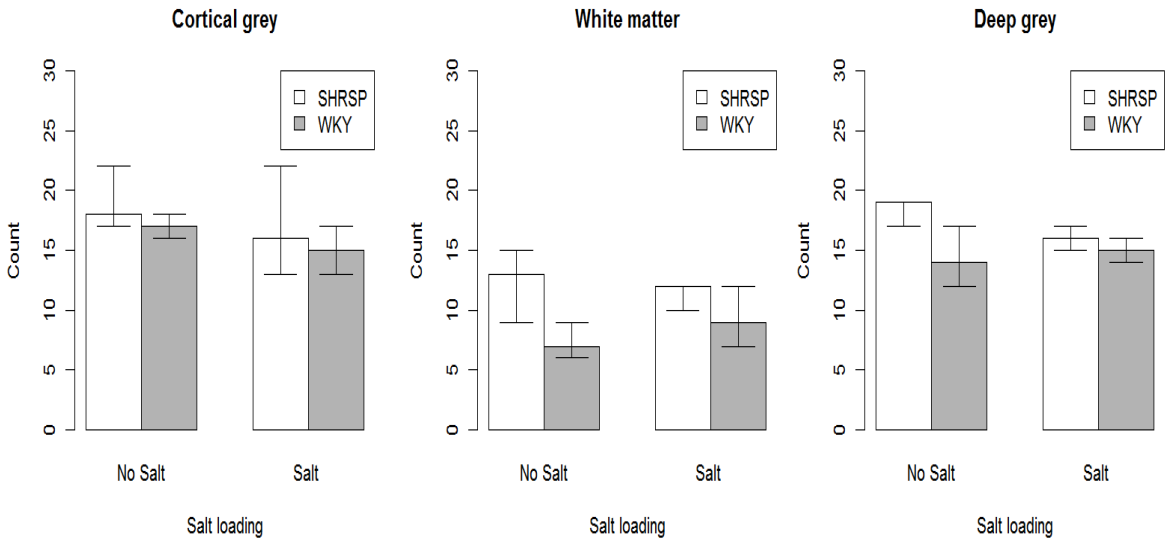

B) Mid Coronal Section

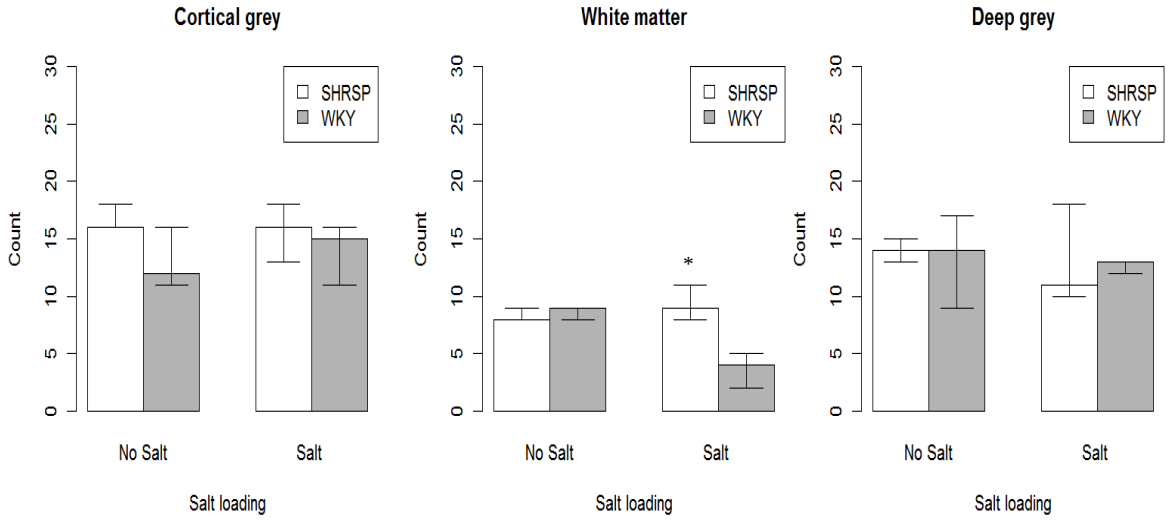

Figure 6.9. Bar graphs showing the median number of capillaries (y axis) counted in 3x300µm^2 frames.

Counts taken from the cortical grey matter, white matter and deep grey matter of in both A) frontal and B) mid coronal brain sections in salt-loaded rats of both strains versus rats fed standard rat chow (n=5 rats per bar). Error bars represent 95% confidence intervals. We found no effect of salt loading on capillary count in the frontal section. In the mid coronal section we found significantly more capillaries in the white matter in SHRSP+NaCl versus WKY+NaCl ($p<0.05$).

NEURONS

A) Frontal Section

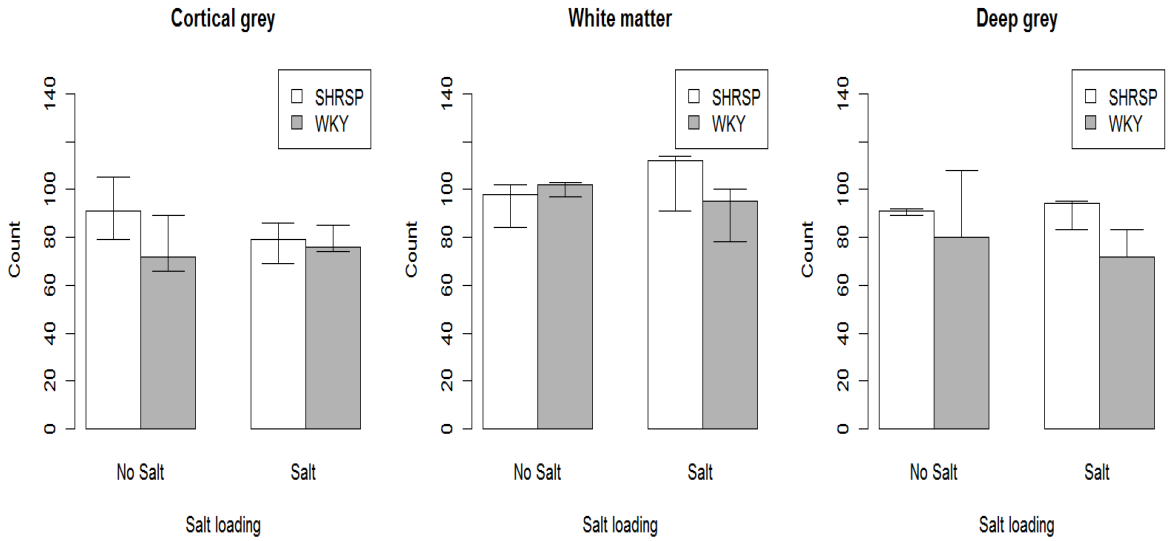

B) Mid Coronal Section

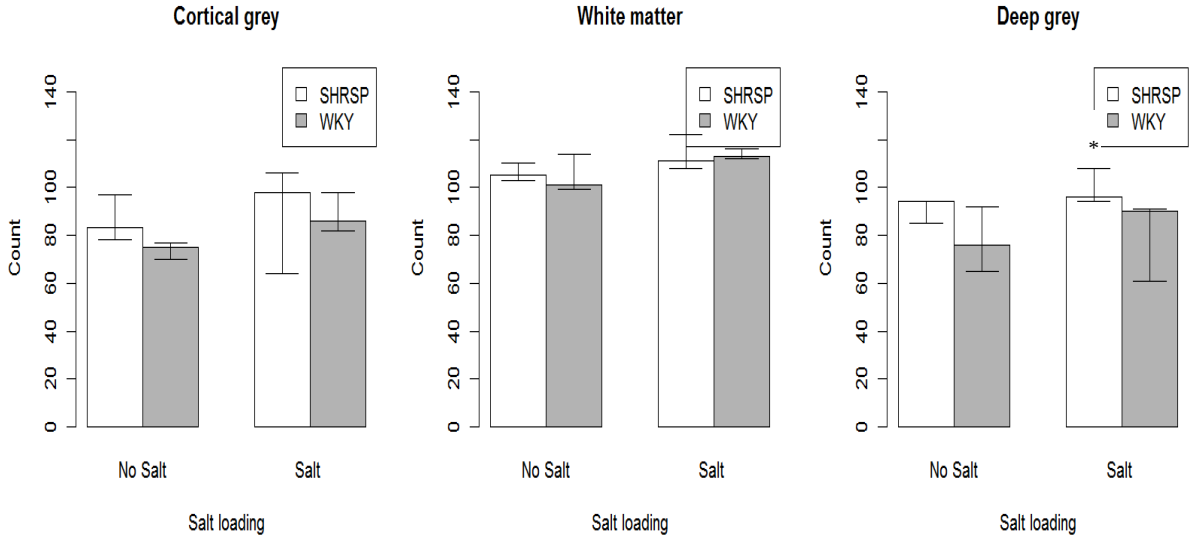

Figure 6.10. Bar graphs showing the median number of neurons (y axis) counted in 3x300µm^2 frames.

Counts taken from the cortical grey matter, white matter and deep grey matter of in both A) frontal and B) mid coronal brain sections in salt-loaded rats of both strains versus rats fed standard rat chow (n=5 rats per bar). Error bars represent 95% confidence intervals. We found no difference in neuronal count in the frontal section. In the deep grey matter of the frontal section we found significantly more neurons in SHRSP+NaCl versus WKY+NaCl ($p<0.05$).

OLIGODENDROCYTES

A) Frontal Section

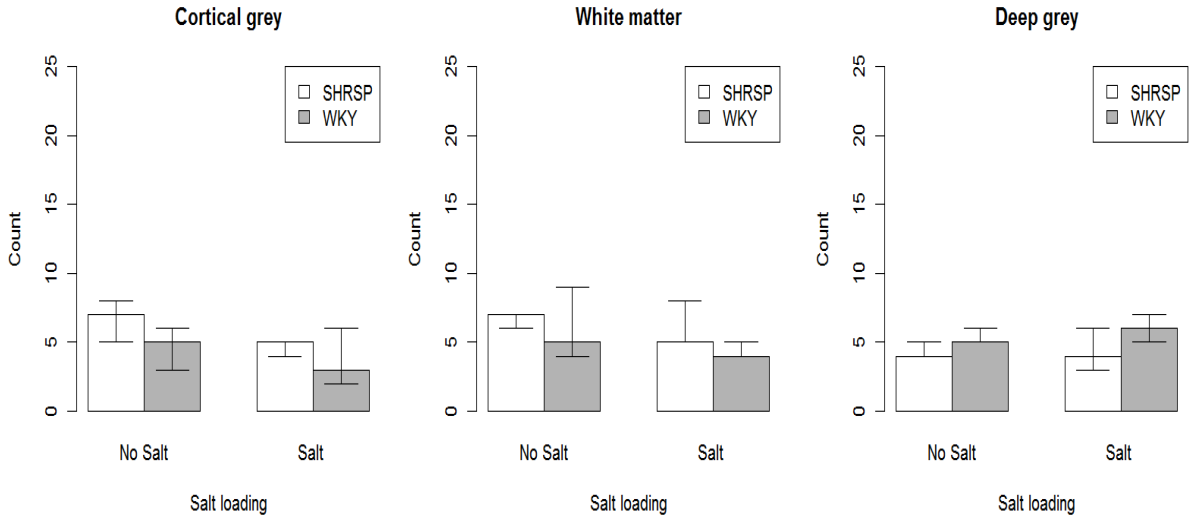

B) Mid Coronal Section

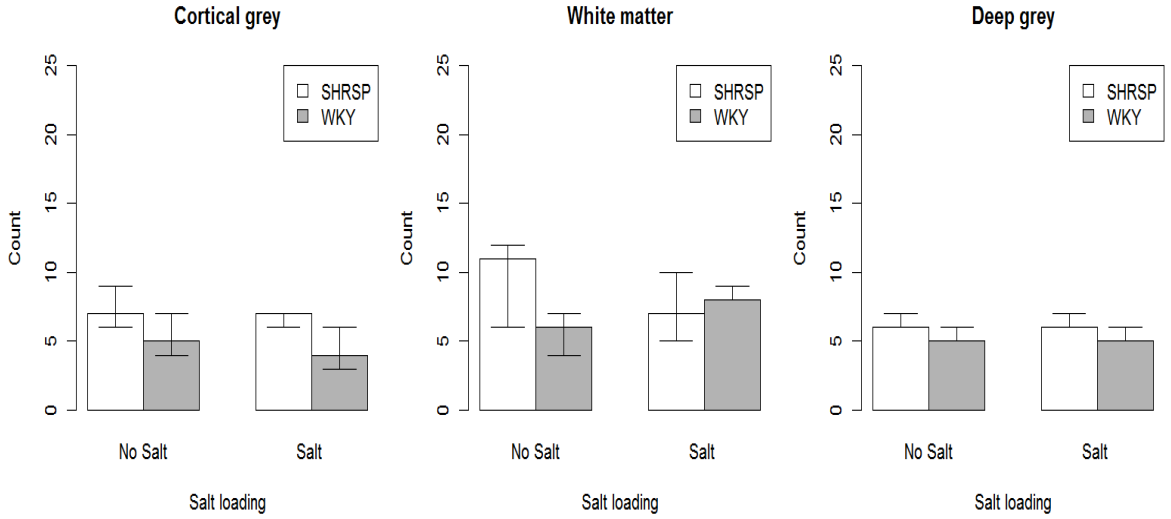

Figure 6.11. Bar graphs showing the median number of oligodendrocytes (y axis) counted in 3x300µm^2 frames.

Counts taken from the cortical grey matter, white matter and deep grey matter of in both A) frontal and B) mid coronal brain sections in salt-loaded rats of both strains versus rats fed standard rat chow (n=5 rats per bar). Error bars represent 95% confidence intervals. We found no significant difference in oligodendrocyte count in either brain section due to salt loading in both strains.

6.3.3 Quantitative assessment of vessel wall thickening.

6.3.3.1 General observation

All the index values were equal to or above 0.45 (range 0.45-0.68), indicating that all vessels measured, regardless of age, strain and salt diet were classified as showing moderate to severe sclerosis according to Lammie's scale(Lammie et al. 1997).

6.3.3.2 Animals fed on a normal diet – ages 5, 16 and 21 weeks (figure 6.12)

For all data and the results of two way ANOVA analysis see table 6.3.

In the cortical grey matter of the frontal section we found a significantly higher sclerotic index in 21 week old SHRSP versus 21 week WKY ($p=0.03$). Otherwise we found no effect of age on the sclerotic index of vessels in the frontal sections of either strain.

In the mid coronal sections there was a significant increase in the sclerotic index with age in the cortical grey and deep grey matter in both strains. In the cortical grey matter these occurred between 5 and 16 weeks ($p=0.02$) and 5 and 21 weeks ($p=0.04$). In the deep grey matter the increase was also significant between 5 and 21 weeks ($p=0.03$). This gradual increase in sclerotic index was not seen in the white matter of the section in any strain.

6.3.3.3 Salt-loaded (+NaCl) animals (aged 21 weeks) (figure 6.13).

For all data and the results of two way ANOVA analysis see table 6.4.

We found no difference in sclerotic ratio between salt-loaded and non salt-loaded animals of the same strain and no significant difference in sclerotic ratio between SHRSP+NaCl and WKY+NaCl.

Table 6.3. Measurements of sclerotic ratio according to Lammie's equation (Lammie et al. 1997) in 5, 16 and 21 week old WKY and SHRSP.

SECTION	**FRONTAL SECTION**								
AGE	**5 weeks (**±S.E.M)			**16 weeks (**±S.E.M)			**21 weeks (**±S.E.M)		
REGION	**Cortex**	**White Matter**	**Deep Grey**	**Cortex**	**White Matter**	**Deep Grey**	**Cortex**	**White Matter**	**Deep Grey**
WKY	0.602±0.055	0.614±0.060	0.610±0.035	0.588±0.052	0.558±0.039	0.593±0.058	0.583±0.072	0.568±0.072	0. 599±0.049
SHRSP	0.580±0.040	0.596±0.048	0.596±0.087	0.604±0.0 28	0.602±0.038	0.607±0.036	0.654±0.023	0.655±0.041	0.643±0.023
P for strain	Cortex = NS			White Matter = NS			Deep Grey = NS		
P for age	Cortex = NS			White Matter = NS			Deep Grey = NS		
SECTION	**MID CORONAL SECTION**								
AGE	**5 weeks (**±S.E.M)			**16 weeks (**±S.E.M)			**21 weeks (**±S.E.M)		
REGION	**Cortex**	**White Matter**	**Deep Grey**	**Cortex**	**White Matter**	**Deep Grey**	**Cortex**	**White Matter**	**Deep Grey**
WKY	0.587±0.037	0.630±0.027	0.607±0.018	0.624±0.034	0.611±0.067	0.624±0.048	0.639±0.030	0.678±0.016	0. 661±0.019
SHRSP	0.595±0.023	0.560±0.042	0.645±0.026	0.655±0.0 27	0.648±0.039	0.636±0.047	0.632±0.044	0.643±0.036	0.681±0.026
P for strain	Cortex = NS			White Matter = NS			Deep Grey = NS		
P for age	Cortex $p<0.05$			White Matter = NS			Deep Grey $p<0.05$		

Each value represents the mean of 5 animals. NS = No significance.

Table 6.4. Measurements of sclerotic ratio according to Lammie's equation (Lammie et al. 1997) in 21 week old WKY and SHRSP animals fed standard rat chow ± 1% NaCl salt-loading from the age of 18 weeks.

SECTION	**FRONTAL SECTION**					
SALT	**No Salt (**±S.E.M)			**Salt (**±S.E.M)		
REGION	**Cortex**	**White Matter**	**Deep Grey**	**Cortex**	**White Matter**	**Deep Grey**
WKY	0.583±0.052	0.568±0.072	0.599±0.038	0.615±0.037	0.646±0.043	0.619±0.035
SHRSP	0.654±0.028	0.655±0.041	0.643±0.040	0.640±0.039	0.659±0.018	0.617±0.044
P for salt	WKY:WKY+NaCl No significant differences		WKY+salt:SHRSP+NaCl No significant differences		SHRSP:SHRSP+NaCl No significant differences	
SECTION	**MID CORONAL SECTION**					
SALT	**No Salt (**±S.E.M)			**Salt (**±S.E.M)		
REGION	**Cortex**	**White Matter**	**Deep Grey**	**Cortex**	**White Matter**	**Deep Grey**
WKY	0.639±0.030	0.678±0.016	0.661±0.019	0.639±0.021	0.654±0.026	0.645±0.023
SHRSP	0.632±0.044	0.643±0.036	0.681±0.026	0.643±0.055	0.661±0.038	0.665±0.025
P for salt	WKY:WKY+NaCl No significant differences		WKY+NaCl:SHRSP+NaCl No significant differences		SHRSP:SHRSP+NaCl No significant differences	

Each value represents the mean of 5 animals. NS = No significance.

SCLEROTIC INDEX

A) Frontal Section

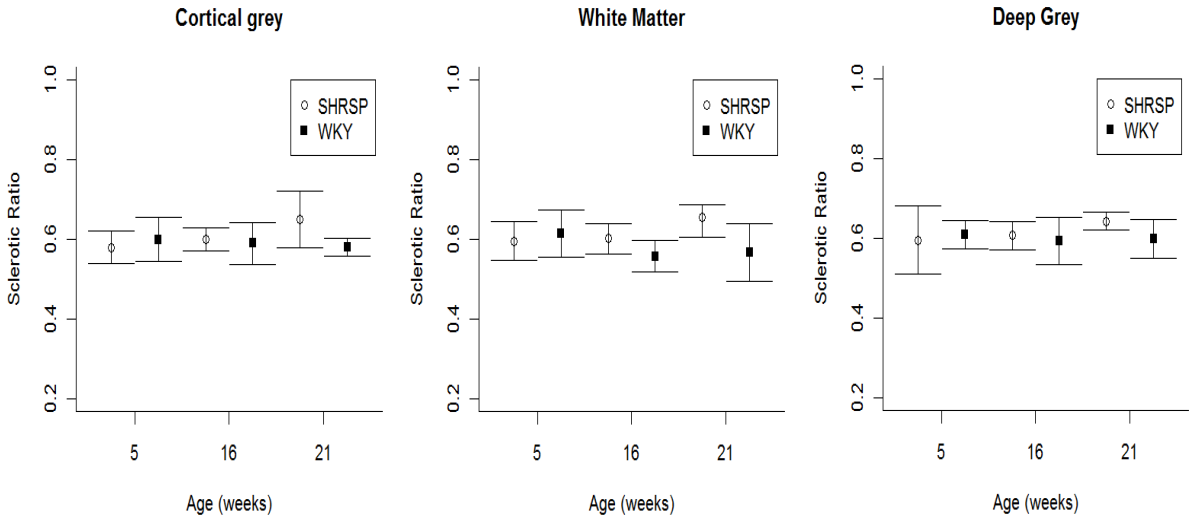

B) Mid Coronal Section

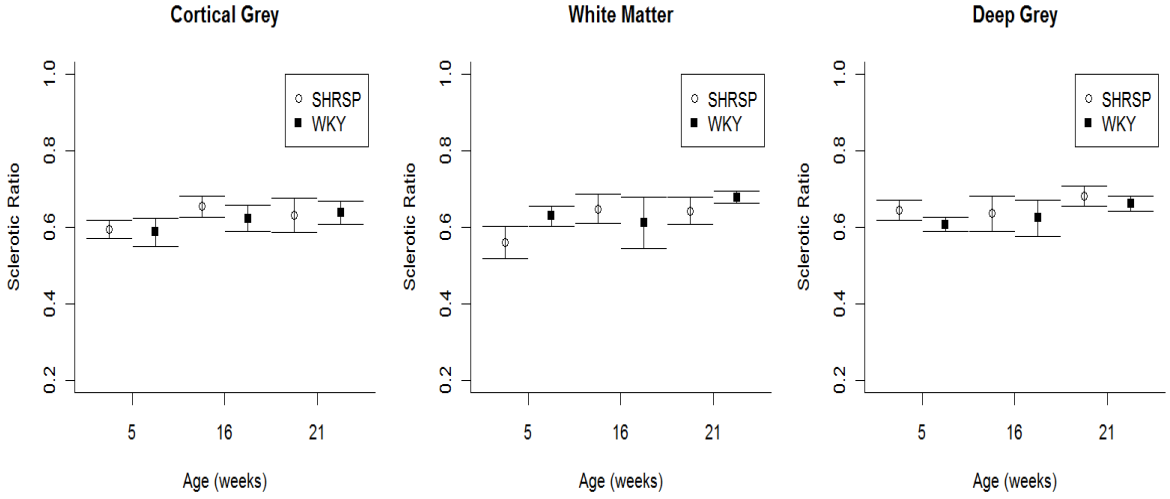

Figure 6.12. Plots showing the mean sclerotic ratio (y axis) calculated from vessels in the cortical grey, white matter and deep grey matter.

A) frontal and B) mid coronal brain sections. N=5 rats per group at ages 5, 16 and 21 weeks. Error bars represent ± the standard error of the mean. We found no significant difference in sclerotic ratio between the strains at any age.

SALT-LOADED ANIMALS

A) Frontal Section

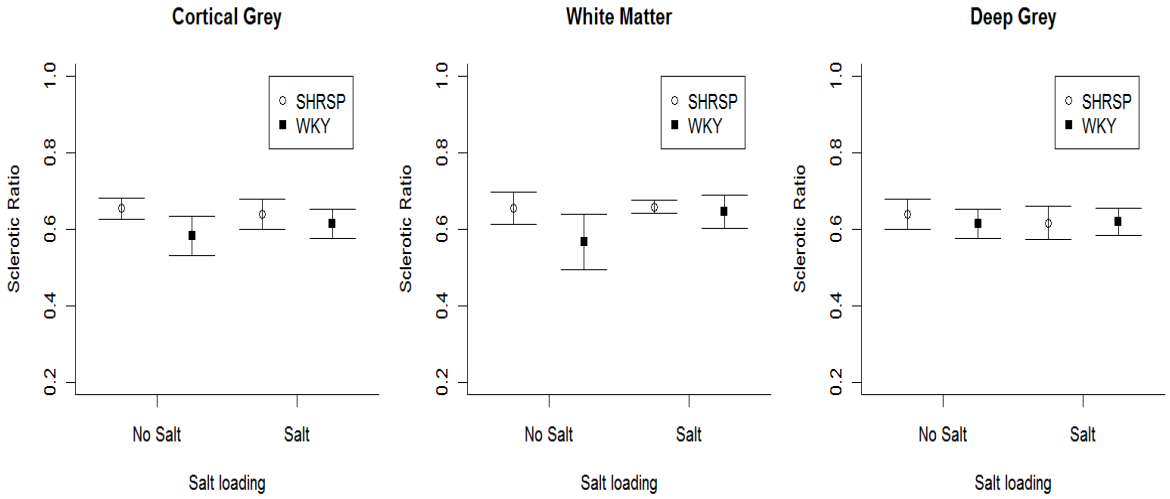

B) Mid Coronal Section

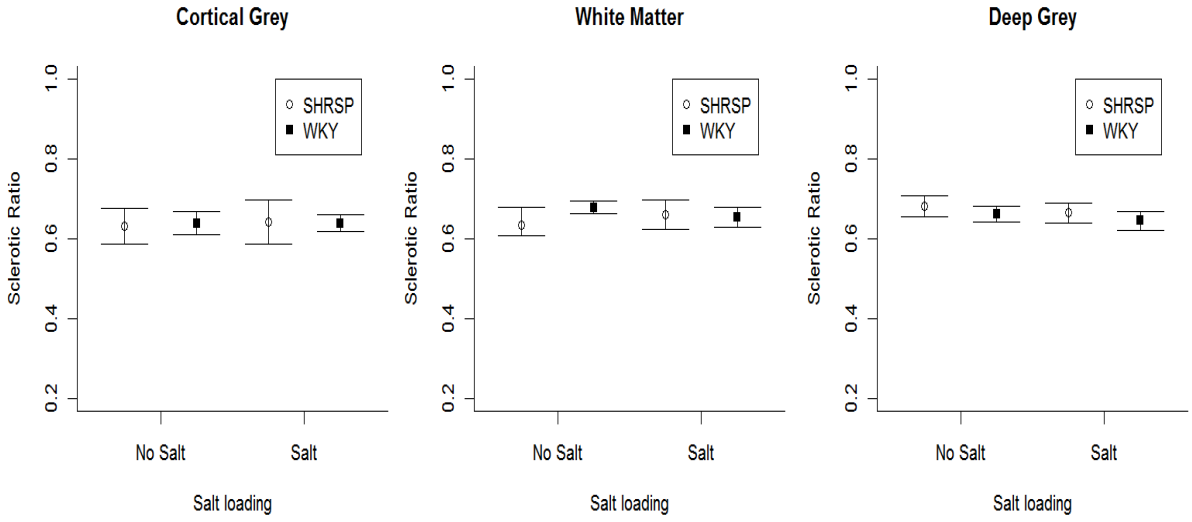

Figure 6.13. Plots showing the mean sclerotic ratio (y axis) calculated from vessels in the cortical grey, white matter and deep grey matter.

A) frontal and B) mid coronal brain sections in 21 week old rats. No salt indicates rat fed standard rat chow. Salt represents rats exposed to 1% NaCl salt-loading in drinking water from the age of 18 weeks. N=5 rats per group. Error bars represent ± the standard error of the mean. We found salt loading had no effect on sclerotic ratio in both strains.

6.4 Discussion

6.4.1 Summary of main findings

6.4.1.1 Qualitative assessments

Our assessment of H&E stained slides taken from 5 week, 16 week and 21 week old WKY and SHRSP found that most morphological changes were in general not visible until 21 weeks of age in SHRSP. However we also found evidence of endothelial cell proliferation in SHRSP at 5 weeks of age. This finding needs further validation but could indicate that not all vascular changes in the SHRSP are purely a consequence of hypertension.

Finding evidence of endothelial proliferation in young SHRSP is not unexpected. The few studies that have looked for evidence of vascular impairments in young SHRSP devoid of hypertension have found disturbances in vasoreactivity(Hirafuji et al. 2002) and the structure of the vascular tree(Coyle 1987) as well as tight junction protein expression (see chapter 7) and polarity(Lippoldt et al. 2000). However this does not mean that hypertension is not accountable for changes seen at older ages.

By 21 weeks vessel wall thickening in the SHRSP was more evident in the deep grey vessels and very obvious in the larger (e.g. meningeal) vessels. These changes are common in hypertensive animal strains(Yamori et al. 1976b;Ogata et al. 1980) and in hypertensive human patients(Lammie 2002b) and are at least in part, a response to the raised blood pressure in the SHRSP which by 16 weeks is fully established at a malignant level(Yamori and Horie 1977).

In salt-loaded animals, the vascular changes of 21 week old WKY+NaCl were exacerbated compared to age matched WKY. More striking was the appearance of vacuolated whiter matter in 40% of the WKY+NaCl especially as salt has no effect on the blood pressure of WKY animals at this age (see chapter 7). SHRSP+NaCl displayed heightened degrees of vessel wall thickening to SHRSP fed standard rat chow but additionally there was an area of white matter rarefaction and cavitation in the internal capsule of one 21 week old SHRSP+NaCl. It is unclear how prevalent these infarcts are in animals of this age as most studies sacrifice only after recorded symptomatic episodes.

6.4.1.2 Quantitative assessments

In general we found no differences in the density counts of capillaries and neurons between WKY and SHRSP rats. We did however find that capillary and neuron density increased with age in both strains of rat. This would be expected due to the growth and development of more neurovascular connections with age but goes against findings in some vascular dementia and small vessel disease patients which show a decrease in vessel and neuronal densities(Roman et al. 2002;Schuff et al. 2003;Moody et al. 2004). This discrepancy could simply be because our rats were biologically younger than the aged humans in these studies. Unlike the capillary and neuron counts we found no evidence of an increase in oligodendrocyte numbers with age in either strain. In salt-loaded animals, only the white matter of the mid coronal section showed a significantly lower oligodendrocyte density in WKY+NaCl compared to WKY. Therefore, whilst striking differences in cell densities due to salt were not seen, we cannot rule out that even relatively mild salt-loading could impact on cell densities even in WKY animals and larger studies are needed. A previous study has already highlighted the impact of salt-loading on proteins relating to the vascular unit in both SHRSP and WKY animals (see chapter 7) and the impact of salt on vascular pathology in particular needs to be fully assessed in both strains.

Our assessment of sclerotic ratio using Lammie's index(Lammie et al. 1997) did not reveal any significant differences between the two strains, although both strains showed an increase in vessel wall thickness with increasing age. More surprisingly we found that every measurement we took regardless of age or strain or salt intake fell within the range of moderate to severe sclerosis (>0.5). This suggests that the sclerotic index for humans needs to be modified if it is to be applied to other species. Our animals underwent exsanguination before the brains were fixed as they were primarily being used for genetic studies. Perfusion prior to fixation might preserve the vascular structure and make the human ranges of the index more relevant to rats. We would advise caution when applying this scale to other species.

6.4.1.3 Study methodology

Our qualitative assessment of morphological changes was performed by three observers so we are confident that we did not miss any although all studies have limitations. Pathology is by its nature, a static assessment of a dynamic process. However, by selecting age groups covering a pre-hypertensive stage, an established hypertensive stage and a stroke-prone stage we have tried to asses the sequence of changes. Having access to an age between 5 and 16 weeks and an older possibly symptomatic animal would have made the study more complete, however we were restricted by animal availability. We did, however use a standardised method to reduce bias and assess the two regions most likely to display damage, as defined by previous studies(Ogata et al. 1980;Fredriksson et al. 1988)). However, by restricting ourselves to these regions we may have missed focal pathology at other levels.

This study was performed blind to age, strain and diet of the rats and used randomly generated sampling points. We also performed each of the assessments separately so density counts and sclerotic ratio measurements were not influenced by qualitative findings. As well as using these methods to reduce bias, it is important to use control strains and to test the effect of salt when looking at the SHRSP. There is a need for future experiments to methods which can detect more subtle changes e.g. immunohistochemistry on targeted regions (see chapter 7) rather than simple macroscopic examinations of coronal brain slices. Using standardised protocols and sampling methods such as ours can also enable more quantitative assessments such as lesion frequency and number to be conducted in ways more comparable to those used in human imaging studies.

6.5 Conclusion

Most morphological changes in SHRSP rats are not visible until after the development of hypertension and are characteristic of vascular remodelling, however endothelial cell proliferation at 5 weeks was also evident and warrants a larger investigation of young SHRSP. Salt-loading caused heightened remodelling in the SHRSP and an old infarct. Evidence of white matter damage in WKY+NaCl was also evident. More studies are needed on the effects of salt on control strains. Vessel and neuronal densities are unaltered in SHRSP compared to age matched WKY. Finally clear evidence of vessel hypertrophy in SHRSP could not be quantified using a sclerotic ratio designed for human vessels. This may be due to our method of fixation or species differences. Future studies should use a method of fixation optimized for preserving vessel structure.

CHAPTER 7 : CEREBRAL SMALL VESSEL ENDOTHELIAL STRUCTURAL CHANGES PREDATE HYPERTENSION IN STROKE PRONE SPONTANEOUSLY HYPERTENSIVE RATS: A BLINDED, CONTROLLED IMMUNOHISTOCHEMICAL STUDY OF 5-21 WEEK OLD RATS.

7.1 Background

While there is an association between the severity of arteriolosclerosis and the number of lacunar lesions(Dozono et al. 1991b), a causal relationship has never been demonstrated. In SVD the chronic arteriolar damage affects all areas of the vascular unit including vessel wall and basement membrane thickening(Jellinger 2007), luminal narrowing, collagen deposition(Zhang et al. 2010), degeneration of smooth muscle cells, loss of activated astrocytes and vascular leakage(Wardlaw 2005).

As previously noted, pathological descriptions from autopsy material provide static information about a dynamic process, and have limitations in describing the underlying mechanisms of the vessel damage. Consequently, appropriate animal models such as the SHRSP may have a role in determining the dynamic processes underlying the development of vessel pathology seen in conditions such as vascular dementia and lacunar stroke.

A number of studies have assessed parenchymal and vessel damage in SHRSP retrospectively after spontaneous strokes have occurred (see chapter 4). However, few studies have looked at the progressive development of pathology over the rat's life(Bailey et al. 2011a). Additionally, there is little information regarding the cerebral small vessels in young animals before hypertension develops.

Many groups now use a Japanese diet or salt-loading in order to quicken the development of the cerebral pathology in SHRSP(DiNicolantonio and Silvapulle 1988). The direct effect of this diet on the vascular changes of SHRSP rats and WKY rats has not been properly compared with rats fed standard rat chow (see chapter 4).

With this background the aims of this study were to use immunohistochemical techniques to a) assess changes in the neurovascular unit and their time sequence, in SHRSP fed standard rat chow versus WKY controls at 5, 16 and 21 weeks and b) to compare salt-loaded WKY and SHRSP aged 21 weeks with age matched animals of both strains.

7.2 Materials and methods

7.2.1 Animals & tissue preparation

See chapter 5 for detailed descriptions of animal maintenance, sacrifice, and subsequent tissue preparation.

We used n=5 male rats aged 5, 16 & 21 week rats fed a normal diet (total n=30) plus n=5 salt-loaded 21 week old rats from each strain (total n=10). Salt-loaded animals had 1% NaCl added to their drinking water at the age of 18 weeks, which continued until sacrifice at 21 weeks.

7.2.2 The use of antibodies to assess the structural integrity of the vascular unit.

We selected antibodies which would assess the integrity of vascular unit right from the endothelial layer on the inside out via the basal lamina and vessel wall. Therefore we chose a major structural protein of the endothelial tight junctions (Claudin-5), Collagen IV to assess basal lamina integrity, the major cellular component of the vessel wall media (Smooth Muscle Actin), and Collagen I to assess evidence of vessel wall scarring.

7.2.3 The use of antibodies to assess the presence / absence of vessel disease

As well as assessing the vascular unit we wanted to assess changes in the surrounding extracellular domain including astrocyte activation (glial fibrillary acidic protein [GFAP]) and matrix remodelling (matrix metalloproteinase 9 [MMP9]). We also wanted to assess any response to vascular disease so we looked for the presence of inflammation (Iba-1) and any myelin loss (myelin basic protein (MBP)).

For a full list of antibodies, suppliers and dilutions see chapter 5.

7.2.4 Protocol

We used the ABC immunoperoxidase method (Vector Laboratories) briefly described in chapter 5 and available in full in appendix G of this thesis. Antigen heat retrieval using a pressure cooker (with slides immersed in citric acid buffer) was used as a pre-treatment for all antibodies. Slides were blocked against non-specific binding in hydrogen peroxide for 10mins followed by either rabbit or swine serum. We used 3.3'-diaminobenzidine (DAB)

tetrahydrochloride to reveal immunoreactivity. Sections were lightly counterstained in Harris' haematoxylin. TBS

7.2.5 Image analysis

We measured percentage staining using ImagePro™ software (version 6.3), blinded to species and age, in cortical, deep grey and white matter. We developed a standard sampling protocol to assess the same 3 areas (and therefore vessels) of interest across all animals (see chapter 5), by identifying standard cross sections using landmarks such as the rhinal fissure and piriform cortex. We divided the cross section into cortical grey matter, white matter and deep grey matter using the freehand tool on ImagePro™. We applied the full image analysis protocol to both frontal cortex and mid coronal sections in each animal. To determine the amount of positive immunostaining present we used the count tool in ImagePro to determine the colour which best represented positive staining. This involved moving the cursor over an area of the section strongly stained for our antibody of interest and clicking on a strongly highly stained pixel. ImagePro subsequently highlights all pixels within the region of interest that match the colour specified by the observer. If any positive staining remained one of these pixels was clicked on next and any other pixels corresponding to the next hue where cumultively highlighted until the observer felt all the positive immunostaining was accounted for. For reproducibility we performed all immunostaining for each antibody on the same day (i.e. all Claudin-5 staining performed in the same run). We then applied colour matched pixel counts, counting each region of interest separately. We converted counts into percentage areas of staining as a measure of immunoreactivity using ImagePro™, once each region had been defined by hand.

7.2.6 Image analysis intra-observer reliability study

To assess the viability of our image analysis protocol before applying it to all slides, we assessed intra-observer reliability using a randomly selected slide counted on 5 separate occasions. Each slide photographed on the same day using the same microscope and software settings (x4 lens, 4ms exposure) in ImagePro™ 6.3.

We assessed all regions of interest on the slide. The observer was blinded to the age, strain and antibody used on the slide. We obtained the area of immunoreactivity by colour thresholding segmentation (pixel counts). From this value the percentage of the region of

interest stained was calculated. We analysed the data using a coefficient of variance analysis to assess the effect of day on the percentage staining count.

7.2.7 Data Analysis

We performed statistical analysis in Minitab using a general linear model (two-way ANOVA) followed by Tukeys test for pairwise comparisons. For the assessment of antibodies we calculated the effects of strain and age. We assessed the effect of salt diet and strain for the salt loaded animals. For all of the statistical analysis, we analysed frontal cortex and mid-coronal sections separately as there were significant differences in the distribution of grey and white matter within the regions. We also assessed the effect of brain territory on the expression of the different vascular markers. We considered values of $p<0.05$ to be statistically significant. All data are shown as mean ± SEM.

7.3 Results

7.3.1 Image analysis intra-observer reliability study

Our reliability study to assess the reproducibility of our image analysis protocol found that less than 10% of the variance within the counts was due to the effect of day (cortical grey – C*v* = 0.03, white matter – C*v* = 0.06 and deep grey – C*v* = 0.09). We therefore concluded that our protocol was reproducible and the observer was consistent in assessing percentage staining values. See figure 7.1.

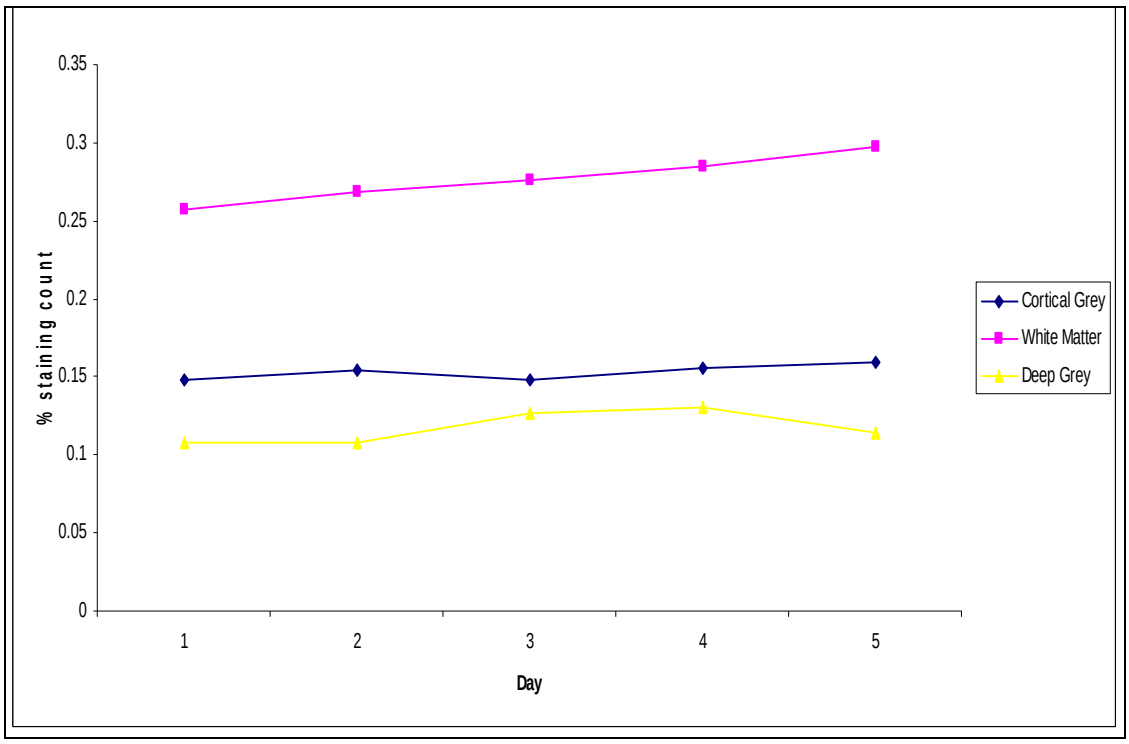

Figure 7.1. The results of a one way ANOVA assessing the impact of day (replicate) on percentage staining counts of smooth muscle actin (SMA) immunoreactivity by the same observer.

A coefficient of variance analysis revealed that less than 10% of the variance within the counts was due to the effect of day (cortical grey – C*v* = 0.03, white matter – C*v* = 0.06 and deep grey – C*v* = 0.09).

7.3.2 Antibodies used to assess the structural integrity of the vascular unit.

7.3.2.1 Animals fed on a normal diet (standard rat chow) aged 5, 16 and 21 weeks.

A summary of the results for the frontal cortex and the mid coronal sections for all regions and all antibodies are shown in Tables 7.1 and 7.2 which summarise the results from 2 way ANOVA analysis. Figure 7.2 shows the appearance of immunoreactivity for each antibody. For pictures of the immunostaining of each antibody at each age see appendix K.

Claudin-5 (Figure 7.3).

Claudin-5 immunoreactivity was significantly lower in SHRSP rats compared to age matched WKY rats across the cortical grey, white matter and deep grey matter in both frontal and mid-coronal sections ($p<0.01$ for all regions). This decrease in Claudin-5 immunoreactivity was present even in 5 week old rats in the deep grey matter of the frontal sections (($p<0.001$). Claudin-5 expression in WKY rats tended to increase with age although this was only significant in the cortical grey matter of the frontal sections ($p<0.01$). We found no increase in Claudin-5 immunoreactivity with age in the SHRSP rats.

SMA: (Figure 7.4).

In SHRSP versus WKY, there was more SMA staining in the cortical grey and white matter of the frontal sections ($p<0.05$ for both regions) and in the deep grey matter of the mid coronal sections ($p<0.05$). We saw a significant increase of SMA staining with age particularly between the ages of 5 and 16 weeks in all regions of the frontal section ($p<0.001$). In the mid-coronal sections we also saw a progressive increase in SMA expression with age which was significant in the deep grey and white matter ($p<0.01$ for both regions).

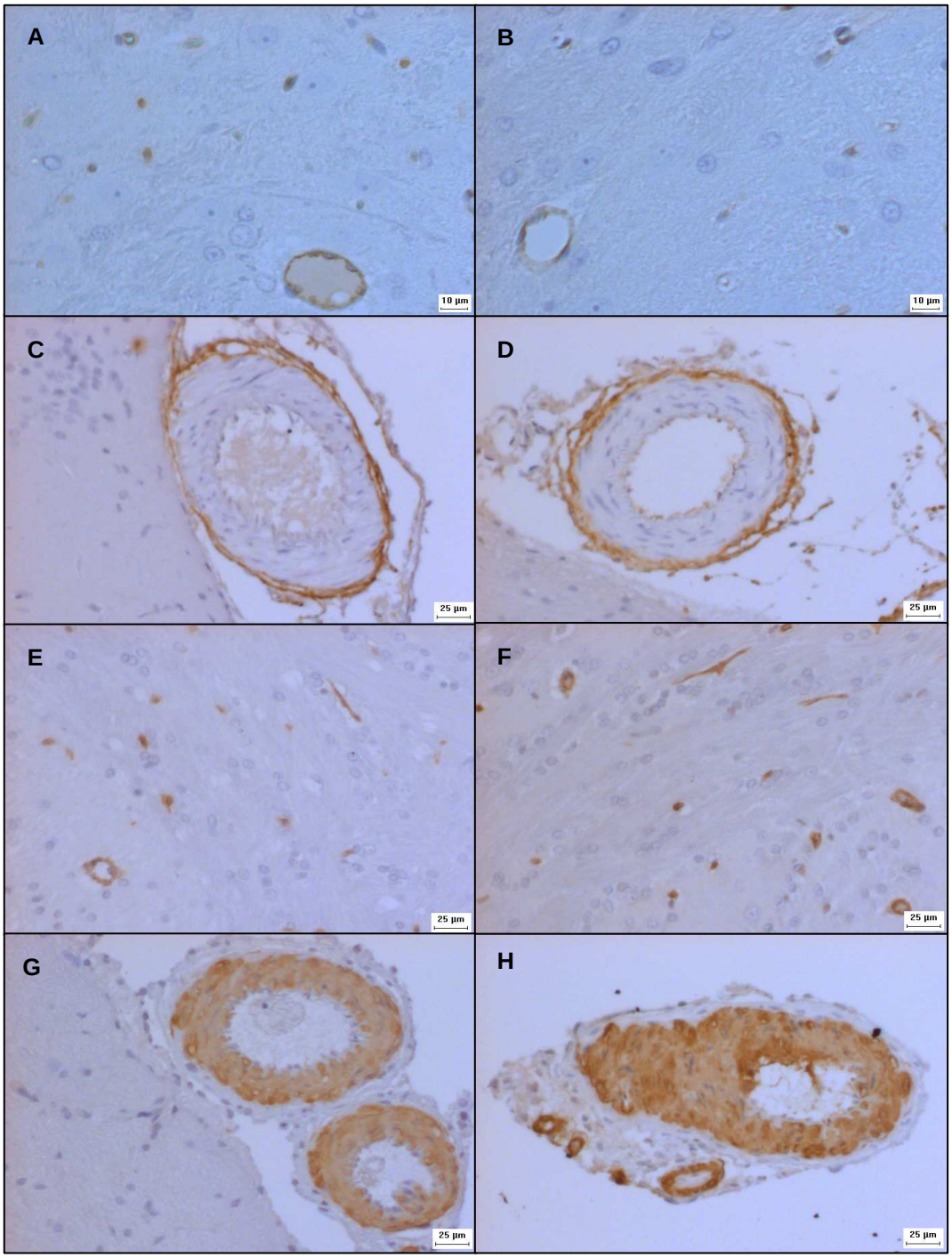

Figure 7.2. Immunohistochemical staining of Claudin-5 (A&B), Collagen I (C&D), Collagen IV (E&F) and Smooth muscle actin (G&H).

In all images WKY is on the left and SHRSP is on the right. Claudin images taken at x20 objective from the deep grey matter of 5 week old animals. Note the decrease in the intensity of Claudin-5 staining in SHRSP (panel B). Collagen I images taken at x10 objective from leptomeningeal vessels of 16 week old animals. Collagen IV images taken at x10 objective from the white matter of 21 week old animals. Note the more intense staining in SHRSP (panel F). Smooth muscle actin images taken at x10 objective from the leptomeningeal vessels of 21 week old animals. Note the increased thickness of the vessel wall in SHRSP (panel H).

Collagen I:(Figure 7.5)

In SHRSP rats, there was significantly less collagen I immunoreactivity in the white matter of the frontal sections compared with WKY ($p<0.05$). There were no significant differences between the strains in the mid coronal sections. In WKY rats, collagen I expression was low at 5 weeks, increased by 16 weeks and reduced slightly by 21 weeks. This increase with age was particularly apparent in the deep grey matter of the mid-coronal sections, where there was a large increase in collagen I immunoreactivity in both SHRSP and WKY rats from 5 to 16 weeks ($p<0.01$), with at least twice as much staining here than in any other region.

Collagen IV: (Figure 7.6)

We found no significant difference between the strains in frontal or mid-coronal sections. Collagen IV increased with advancing age in both strains, significantly in the white matter of both the frontal section and mid coronal section ($p<0.05$). In mid coronal sections, collagen IV immunoreactivity also significantly increased between 5 and 16 weeks in the cortical grey matter.

Table 7.1. Results of two way ANOVA analysis on the effect of strain and/or age on the percentage staining of 4 antibodies assessing the structural integrity of vessels.

	SECTION	FRONTAL SECTION								
	AGE	5 weeks			16 weeks			21 weeks		
	REGION	Cortex	White Matter	Deep Grey	Cortex	White Matter	Deep Grey	Cortex	White Matter	Deep Grey
Claudin5	WKY	0.107±0.049	0.116±0.006	0.135±0.061	0.225±0.027	0.191±0.091	0.118±0.069	0.280±0.124	0.268±0.127	0. 231±0.162
	SHRSP	0.090±0.042	0.101±0.061	0.045±0.024	0.113±0.0 50	0.090±0.016	0.083±0.24	0.132±0.027	0.073±0.045	0 .047±0.033
	P for strain	Cortex p<0.001			White Matter p<0.01			Deep Grey p<0.001		
	P for age	Cortex p<0.01			White Matter = NS			Deep Grey = NS		
Collagen I	WKY	0.040±0.017	0.052±0.035	0.067±0.026	0.260±0.147	0.356±0.288	0.145±0.101	0.172±0.047	0.134±0.079	0. 119±0.074
	SHRSP	0.041±0.017	0.015±0.006	0.047±0.034	0.168±0.0 85	0.131±0.090	0.081±0.057	0.138±0.100	0.066±0.032	0.030±0.014
	P for strain	Cortex = NS			White Matter p<0.05			Deep Grey = NS		
	P for age	Cortex p<0.001			White Matter p<0.001			Deep Grey = NS		
Collagen IV	WKY	0.151±0.107	0.073±0.035	0.145±0.091	0.293±0.178	0.140±0.075	0.179±0.100	0.183±0.120	0.234±0.016	0. 062±0.017
	SHRSP	0.141±0.073	0.063±0.017	0.110±0.095	0.410±0.2 37	0.102±0.057	0.119±0.079	0.361±0.075	120±0.032	0. 100±0.044
	P for strain	Cortex = NS			White Matter = NS			Deep Grey = NS		
	P for age	Cortex = NS			White Matter p<0.05			Deep Grey = NS		
SMA	WKY	0.111±0.062	0.108±0.060	0.094±0.057	0.427±0.091	0.287±0.104	0.280±0.087	0.189±0.075	0.100±0.049	0. 139±0.044
	SHRSP	0.129±0.048	0.108±0.041	0.082±0.030	0.583±0.2 40	0.328±0.061	0.421±0.072	0.356±0.121	0.260±0.136	0.199±0.088
	P for strain	Cortex p<0.05			White Matter p<0.05			Deep Grey = NS		
	P for age	Cortex p<0.001			White Matter p<0.001			Deep Grey p<0.001		

Data taken from frontal section tissue in SHRSP versus WKY rats fed a normal diet. Numbers indicate percentage staining ± the standard error of the mean from n=5 animals. NS = No significant difference.

Table 7.2. Results of two way ANOVA analysis on the effect of strain and/or age on the percentage staining of 4 antibodies assessing the structural integrity of vessels.

	SECTION	MID CORONAL SECTION								
	AGE	5 weeks			16 weeks			21 weeks		
	REGION	Cortex	White Matter	Deep Grey	Cortex	White Matter	Deep Grey	Cortex	White Matter	Deep Grey
Claudin5	WKY	0.173±0.043	0.130±0.055	0.132±0.050	0.156±0.047	0.169±0.044	0.345±0.106	0.200±0.025	0.261±0.140	0. 415±0.125
	SHRSP	0.067±0.027	0.081±0.077	0.078±0.025	0.114±0.0 82	0.076±0.038	0.344±0.172	0.080±0.070	0.129±0.058	0.113±0.084
	P for strain	Cortex p<0.001			White Matter p<0.01			Deep Grey p<0.01		
	P for age	Cortex = NS			White Matter = NS			Deep Grey p<0.001		
Collagen I	WKY	0.071±0.011	0.079±0.047	0.050±0.029	0.113±0.071	0.144±0.081	0.446±0.164	0.088±0.064	0.060±0.012	0. 732±0.190
	SHRSP	0.043±0.019	0.025±0.012	0.041±0.031	0.090±0.0 73	0.096±0.074	0.536±0.172	0.307±0.135	0.147±0.081	0.356±0.187
	P for strain	Cortex = NS			White Matter = NS			Deep Grey = NS		
	P for age	Cortex p<0.01			White Matter p<0.05			Deep Grey p=0.001		
Collagen IV	WKY	0.234±0.075	0.066±0.032	0.080±0.016	0.218±0.061	0.361±0.095	0.313±0.133	0.240±0.089	0.265±0.121	0. 152±0.018
	SHRSP	0.373±0.109	0.253±0.110	0.253±0.084	0.129±0.0 47	0.166±0.062	0.143±0.053	0.183±0.082	0.054±0.033	0.146±0.044
	P for strain	Cortex = NS			White Matter = NS			Deep Grey = NS		
	P for age	Cortex p<0.05			White Matter p=0.01			Deep Grey = NS		
SMA	WKY	0.265±0.114	0.153±0.073	0.199±0.106	0.286±0.042	0.235±0.075	0.335±0.066	0.292±0.043	0.385±0.183	0. 291±0.087
	SHRSP	0.250±0.109	0.144±0.059	0.179±0.068	0.281±0.0 90	0.310±0.107	0.514±0.218	0.529±0.237	0.517±0.231	0.704±0.225
	P for strain	Cortex = NS			White Matter = NS			Deep Grey p<0.05		
	P for age	Cortex = NS			White Matter p<0.01			Deep Grey p<0.01		

Data taken from mid coronal tissue in SHRSP versus WKY rats fed a normal diet. Numbers indicate percentage staining ± the standard error of the mean from n=5 animals. NS = No significant difference.

CLAUDIN-5

A) Frontal Section

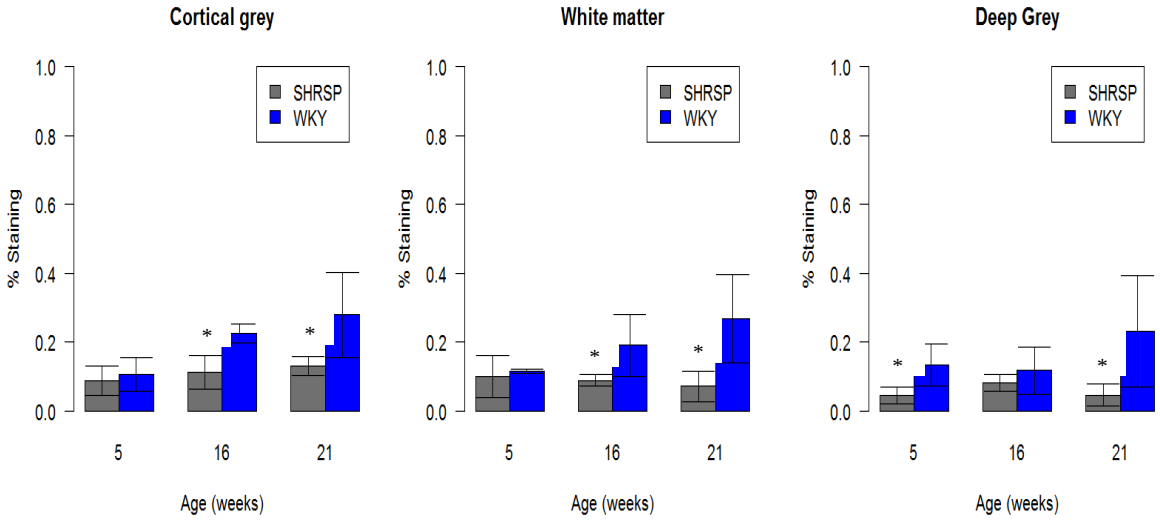

B) Mid Coronal Section

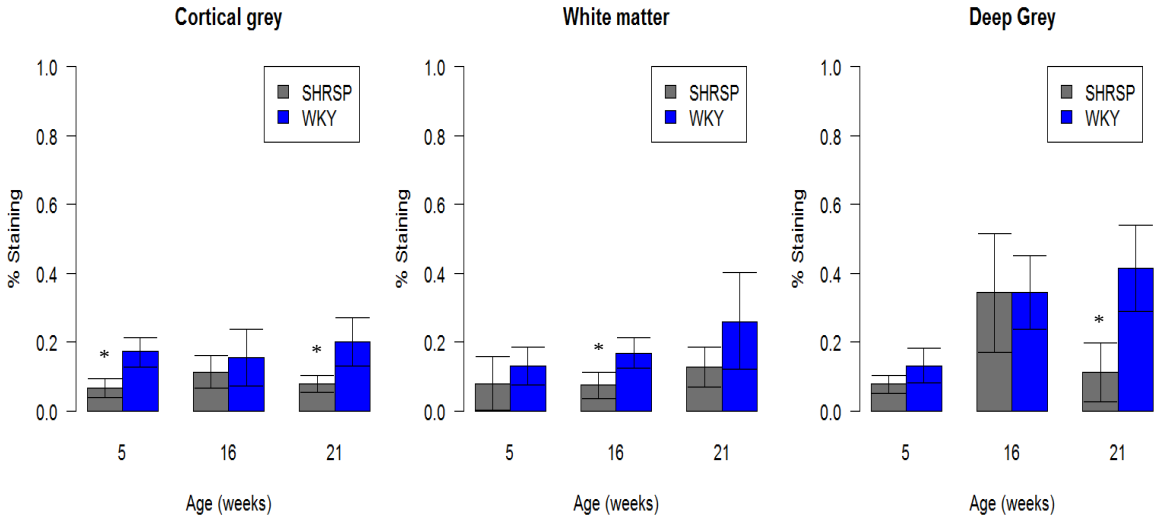

Figure 7.3. Claudin-5 staining in both A) frontal and B) mid coronal sections of 5, 16 and 21wk old WKY and SHRSP rats.

N=5 rats per group. Error bars represent the standard error of the mean. Overall SHRSP had less Claudin-5 immunoreactivity in the cortical grey, white matter and deep grey matter of both the frontal and mid coronal sections ($p<0.01$).

SMOOTH MUSCLE ACTIN

A) Frontal Section

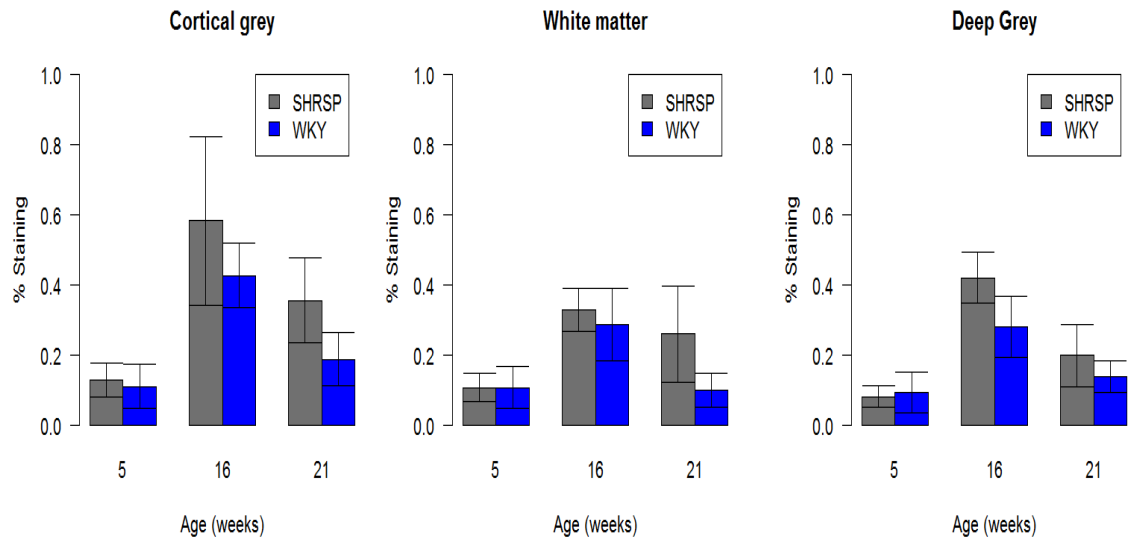

B) Mid Coronal Section

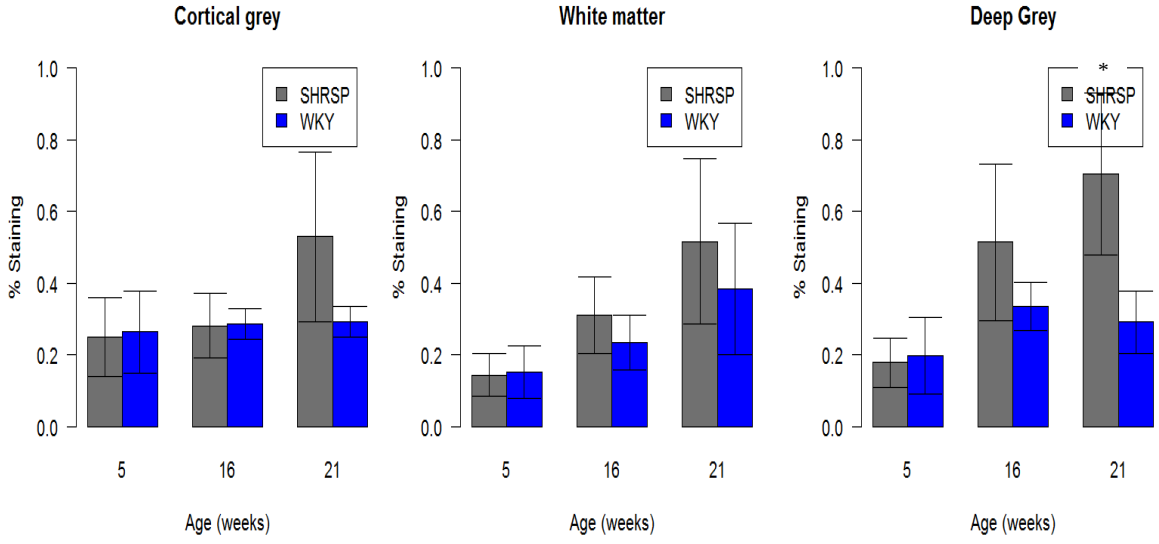

Figure 7.4. Smooth muscle actin staining in both A) frontal and mid coronal sections of 5, 16 and 21wk old WKY and SHRSP rats.

N=5 rats per group. Error bars represent the standard error of the mean. SHRSP had significantly more SMA immunoreactivity in the cortical grey and white matter of the frontal section ($p<0.05$) and in the deep grey matter of the mid coronal section ($p<0.05$).

COLLAGEN I

A) Frontal Section

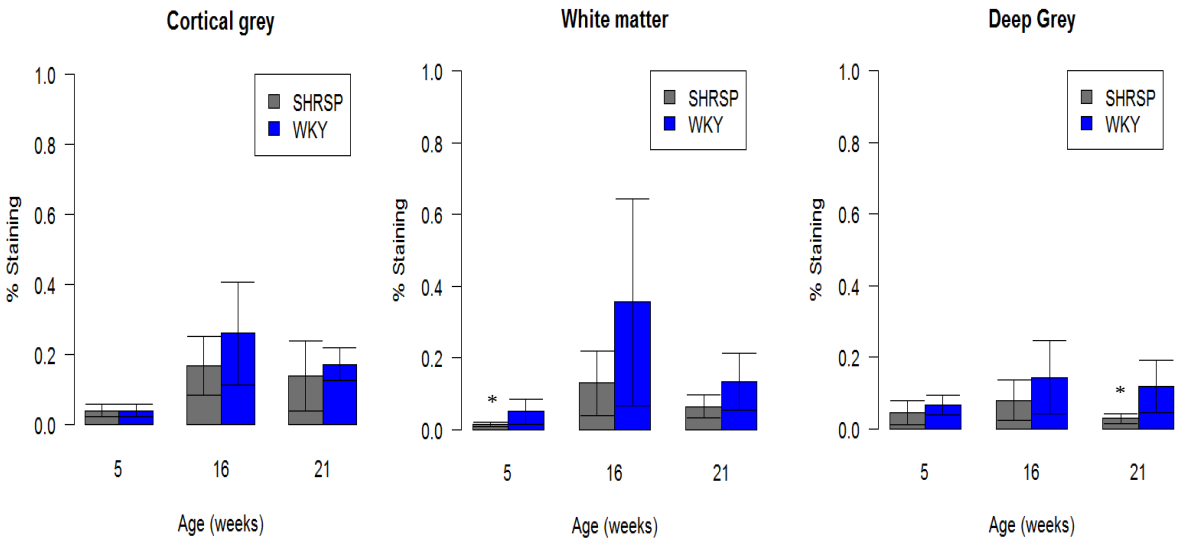

B) Mid Coronal Section

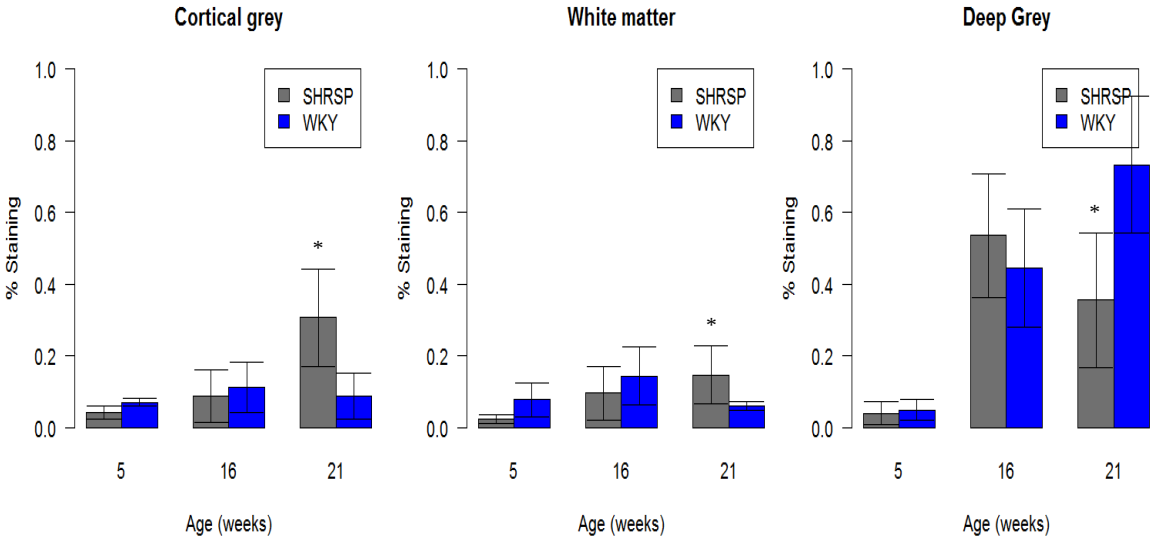

Figure 7.5. Collagen I staining profiles of both a frontal (A) and mid coronal section (B) in WKY versus SHRSP.

Each bar represents N=5. Error bars represent the standard error of the mean. No significant difference in immunoreactivity was found between the strains overall. A significant increase in Col I was found with increasing age in both strains and in both brain sections ($p<0.05$).

COLLAGEN IV

A) Frontal Section

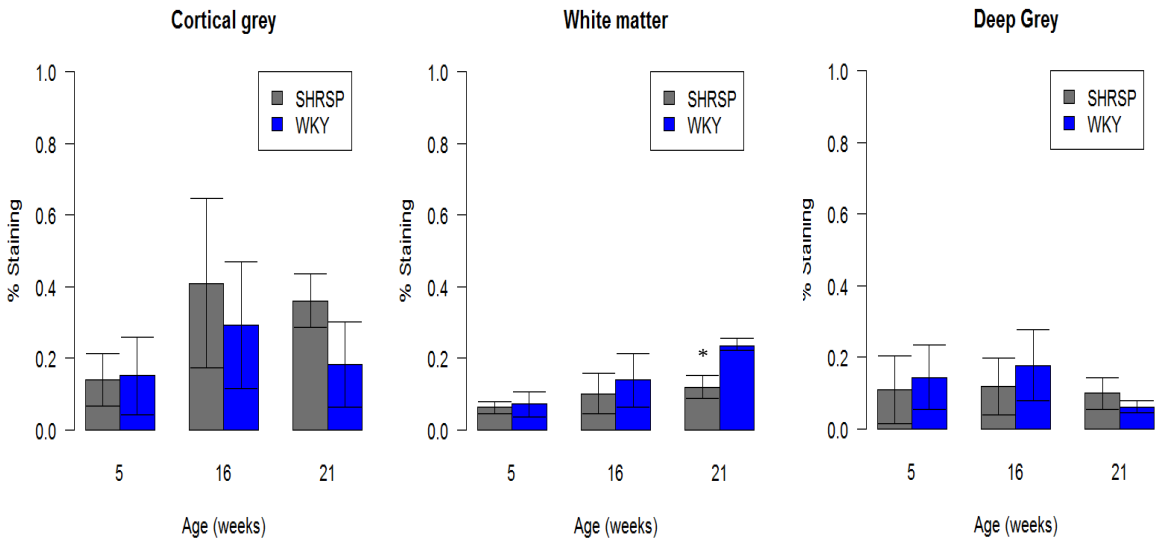

B) Mid Coronal

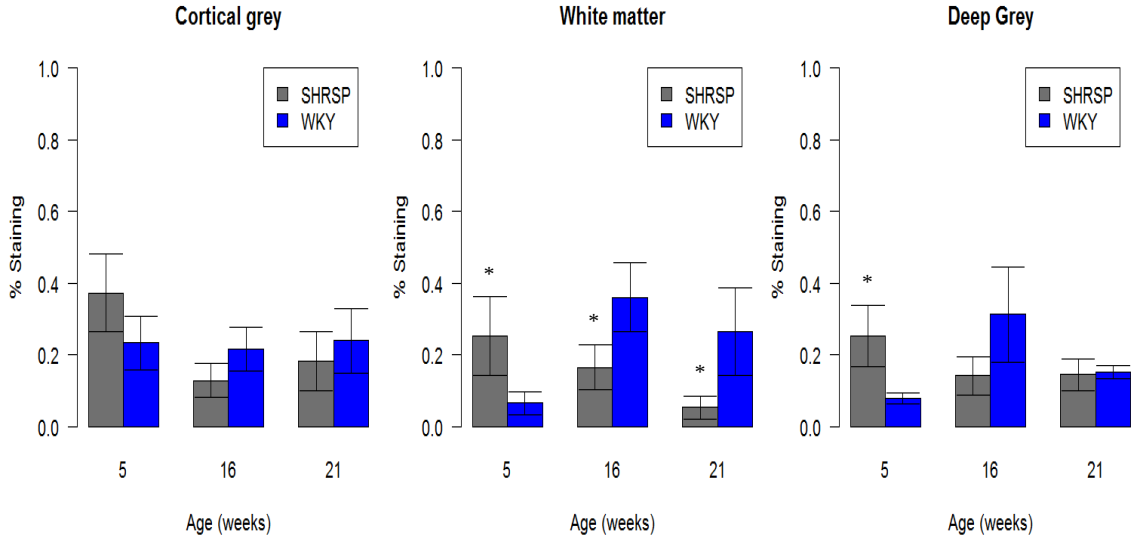

Figure 7.6. Collagen IV staining profiles of both a frontal (A) and a mid-coronal section (B) in WKY and SHRSP.

Each bar represents N=5. Error bars represent standard error of the mean. Overall no significant difference in immunoreactivity was found between WKY and SHRSP, however a significant decrease with age was found in the SHRSP ($p<0.05$).

7.3.3 Antibodies used to assess the presence / absence of vessel disease

7.3.3.1 Animals fed on a normal diet (standard rat chow) aged 5, 16 and 21 weeks.

A table of the results for the frontal cortex and the mid coronal sections for all regions and all antibodies are shown in Tables 7.3 and 7.4 which summarise the results from 2 way ANOVA analysis. Figure 7.7 shows the appearance of immunoreactivity for each antibody. For pictures of the immunostaining of each antibody at each age see appendix K.

MMP9: (Figure 7.8)

There was no significant difference between strains at any age except in the cortical grey matter of the mid coronal section ($p<0.05$). In both strains, cortical grey matter displayed the highest levels of immunoreactivity in both frontal and mid-coronal sections. We found a significant increase in MMP9 immunoreactivity with age in the cortical grey matter of the frontal section ($p<0.05$) and also in the deep grey matter of the mid coronal section ($p<0.001$).

GFAP: (Figure 7.9).

In the frontal sections we saw significantly more GFAP staining in the cortical grey and white matter of SHRSP rats ($p<0.01$ & $p<0.001$ respectively) than WKY. There was no difference between strains in the mid-coronal section.

In the frontal section we also found that GFAP increased with age in all three tissue regions ($p<0.001$). In mid coronal sections we found a similar significant increase with age across all three regions ($p<0.01$).

Iba-1: (Figure 7.10)

SHRSP showed higher levels of Iba-1 immunoreactivity than WKY rats in the cortical grey matter of both the frontal and mid coronal sections ($p=0.05$ & $p<0.01$ respectively), as well as the deep grey matter of the mid coronal section ($p<0.01$).There was a significant increase in Iba-1 immunoreactivity with age in the white matter of the frontal sections ($p<0.05$). This was repeated in the cortical grey matter of the mid coronal sections where there was a significant increase in Iba-1 immunoreactivity between ages 5 and 16 weeks ($p<0.01$). There was no significant effect of age on Iba-1 in the white matter or deep grey matter.

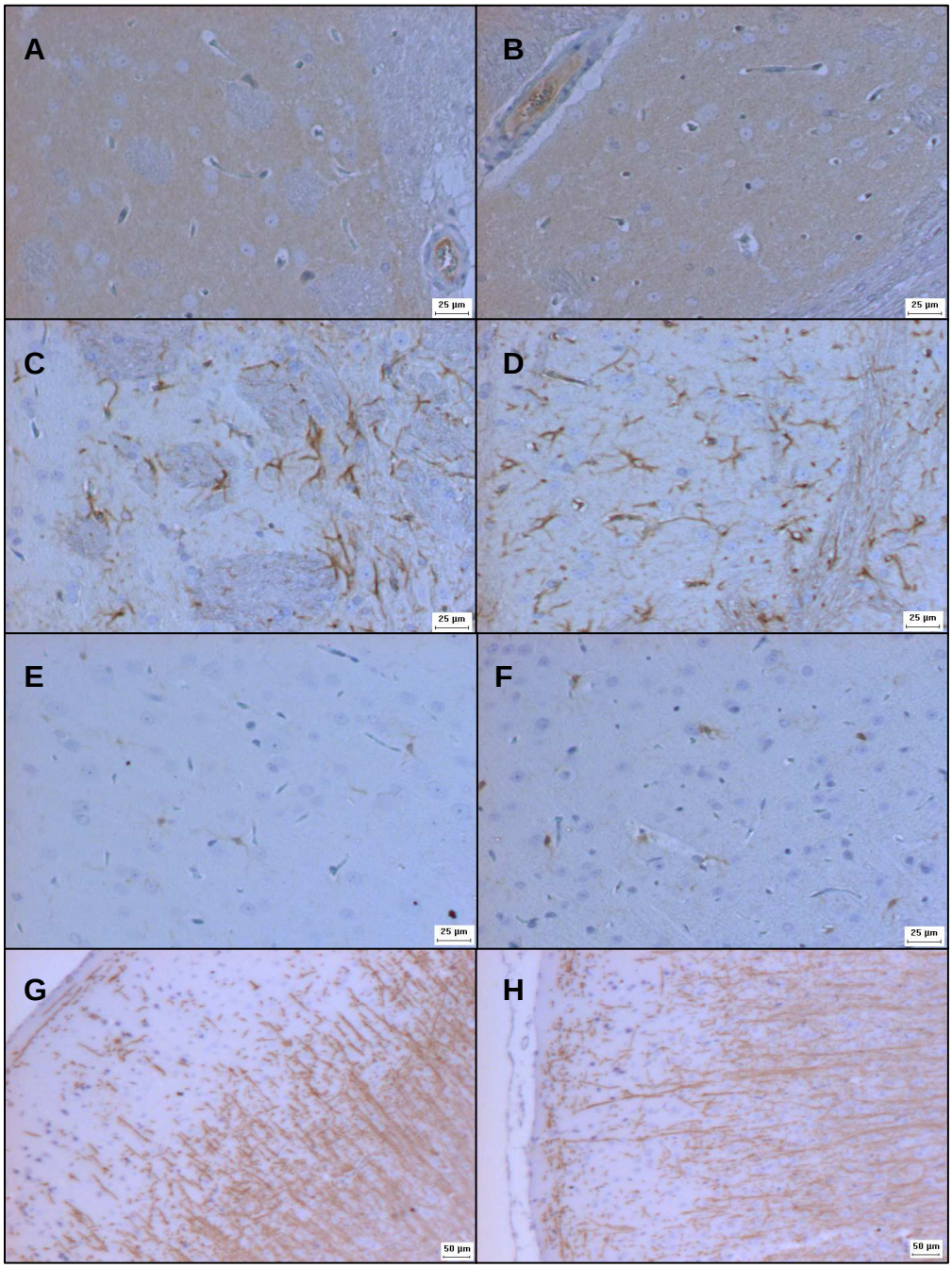

Figure 7.7. Immunohistochemical staining of MMP9 (A&B), GFAP (C&D), Iba-1 (E&F) and MBP (G&H).

In all images WKY is on the left and SHRSP is on the right. MMP9 images taken at x10 objective from the deep grey matter of 21 week old animals. GFAP images taken at x10 objective from the deep grey matter of 16 week old animals where GFAP staining was quantitatively higher (panel D). Iba-1 images taken at x10 objective from the cortex of 21 week old animals. MBP images taken at x4 objective from the cortex of 5 week old animals. Note the decrease in MBP staining intensity in SHRSP (panel H).

*MBP: (*Figure 7.11).

We found significantly less MBP staining in both the cortical grey and white matter of both frontal and mid coronal sections of SHRSP compared to WKY (all p values < 0.01). This decrease was also significant in the deep grey matter of the frontal section ($p<0.01$). The strain difference was particularly evident at the earlier ages of 5 & 16 weeks. The effect of age on MBP immunoreactivity varied widely between regions. In the white matter and deep grey matter of the frontal section along with the cortical grey matter of the mid coronal section there was an increase in MBP expression with age (although this only reached significance in the white matter of the frontal section where $p<0.01$). In the cortical grey matter of the frontal section in both strains there was a dramatic decrease in MBP immunoreactivity at 21 weeks ($p<0.001$). This trend was similar in the white matter and deep grey matter of the mid coronal section (both p values <0.01).

Table7.3. Results of two way ANOVA analysis on the effect of strain and/or age on the percentage staining of 4 antibodies assessing the presence/absence of vascular disease.

	SECTION	FRONTAL SECTION								
	AGE	5 weeks			16 weeks			21 weeks		
	REGION	Cortex	White Matter	Deep Grey	Cortex	White Matter	Deep Grey	Cortex	White Matter	Deep Grey
MMP9	WKY	0.167±0.087	0.035±0.018	0.150±0.080	0.319±0.145	0.478±0.315	0.119±0.078	0.349±0.301	0.154±0.101	0.096±0.065
	SHRSP	0.232±0.200	0.438±0.225	0.321±0.180	0.581±0.283	0.164±0.125	0.151±0.101	0.148±0.077	0.143±0.081	0.030±0.020
	P for strain	Cortex = NS			White Matter = NS			Deep Grey = NS		
	P for age	Cortex p<0.05			White Matter = NS			Deep Grey = NS		
GFAP	WKY	0.125±0.023	1.615±0.166	1.359±0.198	0.711±0.158	2.198±0.573	0.863±0.283	0.914±0.199	1.387±0.254	1.490±0.567
	SHRSP	0.343±0.119	7.170±1.188	3.588±0.643	0.152±0.041	2.152±0.547	0.507±0.138	0.715±0.169	2.420±0.758	1.034±0.304
	P for strain	Cortex p<0.01			White matter p<0.001			Deep Grey = NS		
	P for age	Cortex p<0.001			White Matter p<0.001			Deep Grey p<0.001		
IBA-1	WKY	0.032±0.017	0.024±0.015	0.043±0.016	0.039±0.006	0.033±0.011	0.036±0.028	0.063±0.012	0.110±0.042	0.048±0.013
	SHRSP	0.038±0.016	0.064±0.017	0.033±0.014	0.084±0.023	0.071±0.029	0.068±0.027	0.071±0.034	0.084±0.048	0.052±0.028
	P for strain	Cortex p<0.05			White Matter = NS			Deep Grey = NS		
	P for age	Cortex p=0.01			White Matter p=0.01			Deep Grey = NS		
MBP	WKY	2.132±0.653	0.490±0.155	0.681±0.161	2.502±0.921	0.609±0.293	1.518±0.421	0.462±0.205	1.403±0.611	1.690±0.797
	SHRSP	1.215±0.469	0.213±0.080	0.340±0.439	1.147±0.524	0.174±0.070	0.237±0.062	0.477±0.191	0.632±0.324	0.472±0.186
	P for strain	Cortex p<0.01			White matter p<0.01			Deep Grey p<0.01		
	P for age	Cortex p<0.01			White Matter p<0.01			Deep Grey = NS		

Data taken from frontal section tissue in SHRSP versus WKY rats fed a normal diet. Numbers indicate percentage staining ± the standard error of the mean from n=5 animals. NS = No significant difference.

Table7.4. Results of two way ANOVA analysis on the effect of strain and/or age on the percentage staining of 4 antibodies assessing the presence/absence of vascular disease

	SECTION	MID CORONAL SECTION								
	AGE	5 weeks			16 weeks			21 weeks		
	REGION	Cortex	White Matter	Deep Grey	Cortex	White Matter	Deep Grey	Cortex	White Matter	Deep Grey
MMP9	WKY	0.279±0.102	0.148±0.042	0.103±0.035	0.351±0.105	0.181±0.095	0.088±0.032	0.141±0.058	0.023±0.012	0.520±0.171
	SHRSP	0.367±0.107	0.074±0.032	0.066±0.013	0.367±0.109	0.099±0.062	0.121±0.050	0.452±0.133	0.207±0.102	0.380±0.106
	P for strain	Cortex p<0.05			White Matter = NS			Deep Grey = NS		
	P for age	Cortex = NS			White Matter = NS			Deep Grey p<0.001		
GFAP	WKY	0.346±0.102	2.399±0.600	2.170±0.477	0.694±0.327	0.966±0.338	1.616±0.377	0.638±0.353	2.388±0.529	1.898±0.496
	SHRSP	0.214±0.065	2.415±0.650	1.745±0.498	0.332±0.127	1.206±0.512	0.894±0.253	0.702±0.172	2.093±0.501	2.246±0.515
	P for strain	Cortex = NS			White matter = NS			Deep Grey = NS		
	P for age	Cortex p<0.01			White Matter p<0.001			Deep Grey p=0.001		
IBA-1	WKY	0.022±0.007	0.024±0.012	0.023±0.008	0.033±0.007	0.037±0.026	0.038±0.015	0.032±0.020	0.022±0.011	0.013±0.006
	SHRSP	0.030±0.020	0.042±0.022	0.050±0.032	0.094±0.044	0.039±0.017	0.041±0.025	0.045±0.015	0.036±0.019	0.036±0.020
	P for strain	Cortex p<0.01			White Matter = NS			Deep Grey p<0.01		
	P for age	Cortex p<0.01			White Matter = NS			Deep Grey = NS		
MBP	WKY	1.742±0.544	0.861±0.206	0.266±0.095	2.425±0.921	2.337±0.921	1.374±0.777	3.922±1.252	1.659±0.633	0.583±0.228
	SHRSP	1.457±0.362	0.298±0.089	0.613±0.102	1.465±0.694	1.134±0.183	0.910±0.091	1.570±0.786	1.098±0.661	0.383±0.235
	P for strain	Cortex p<0.01			White matter p<0.05			Deep Grey = NS		
	P for age	Cortex = NS			White Matter p<0.05			Deep Grey p<0.01		

Data taken from mid coronal tissue in SHRSP versus WKY rats. Numbers indicate percentage staining ± the standard error of the mean from n=5 animals. NS = No significant difference.

MMP9

A) Frontal Section

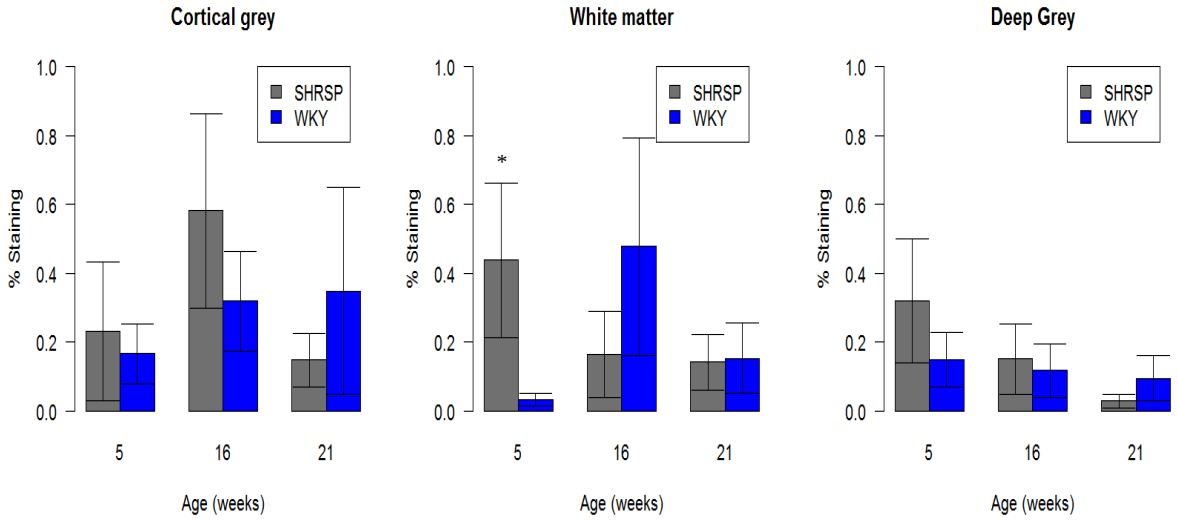

B) Mid Coronal Section

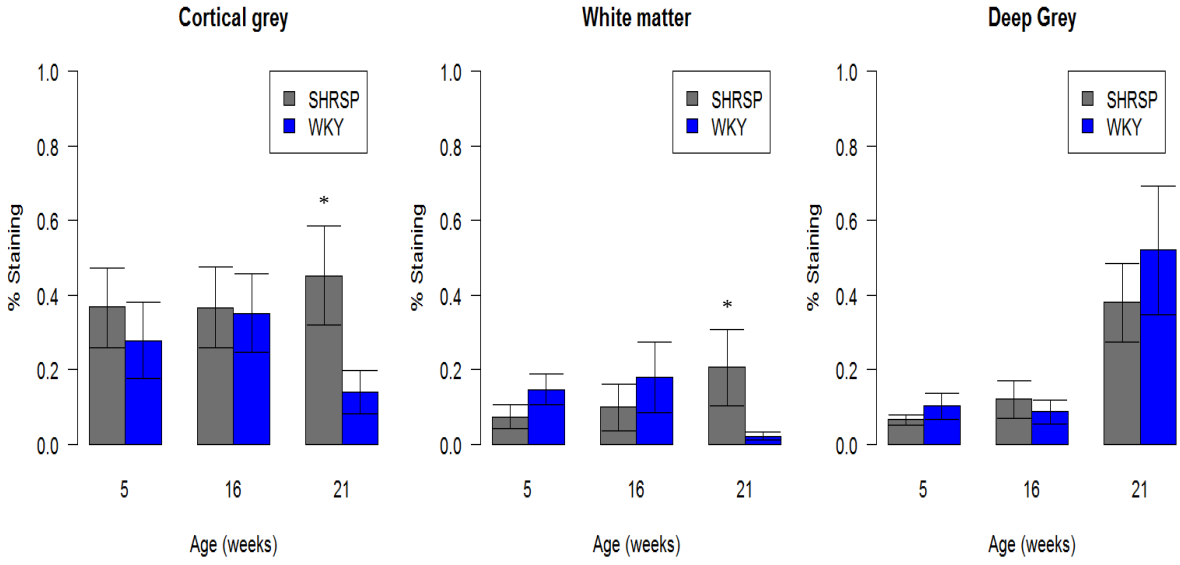

Figure 7.8. MMP9 staining profiles of both a frontal (A) and mid coronal (B) section of WKY and SHRSP.

Each bar represents N=5. Error bars represent the standard error of the mean. We found that SHRSP had significantly more MMP9 immunoreactivity in the cortical grey matter of the mid coronal section ($p<0.05$). We also found a significant increase in immunoreactivity with age in the cortical grey matter of the frontal section ($p<0.05$) and the deep grey matter of the mid coronal section ($p<0.001$).

GFAP

A) Frontal section

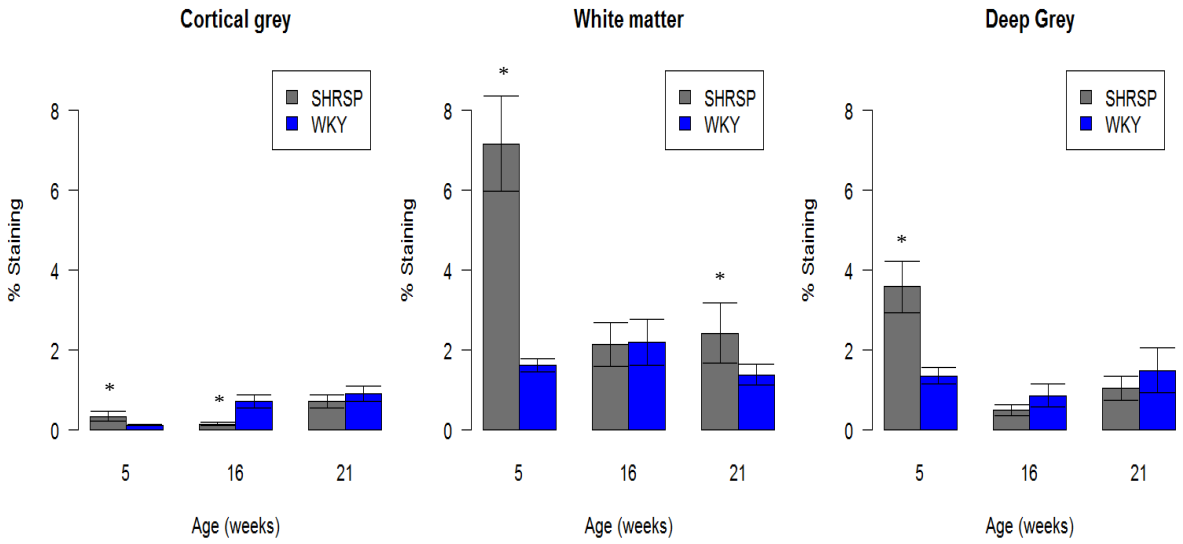

B) Mid Coronal Section

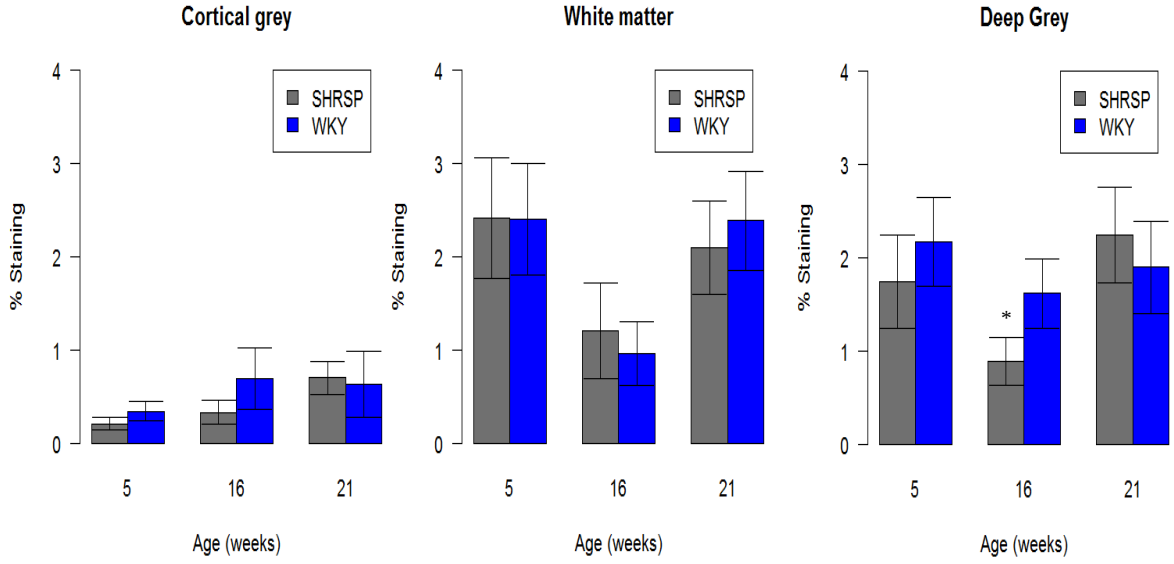

Figure 7.9. GFAP staining profiles of both frontal (A) and mid coronal (B) sections of WKY versus SHRSP.

Each bar represents n=5. Error bars represent the standard error of the mean. We found a significant increase in GFAP immunoreactivity in the SHRSP in the cortical grey and white matter of the frontal section ($p<0.01$). We also found a significant increase with age in both strains in all regions of both the frontal and mid coronal section ($p<0.01$).

IBA-1

A) Frontal Section

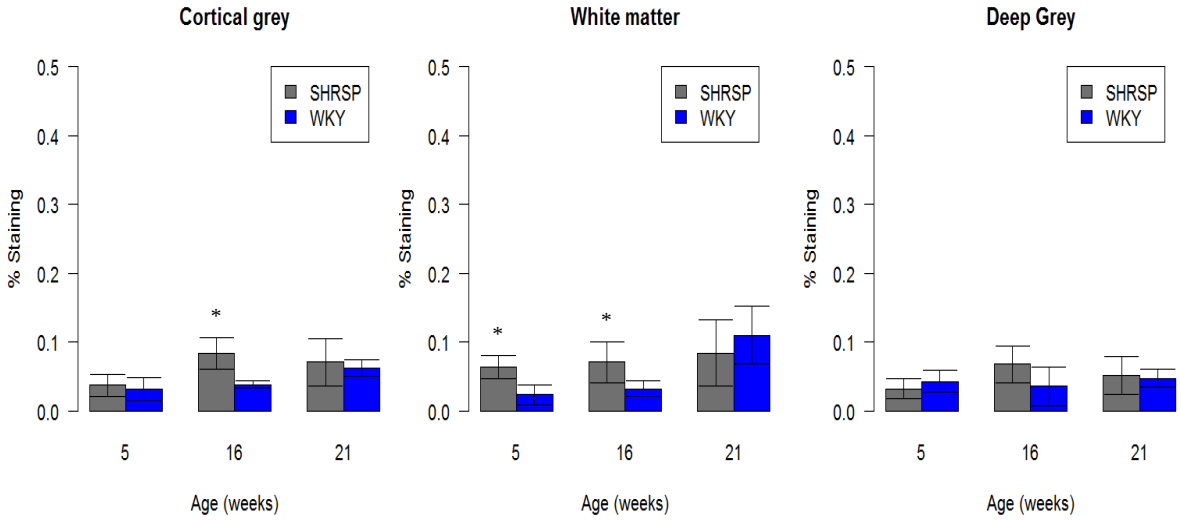

B) Mid Coronal Section

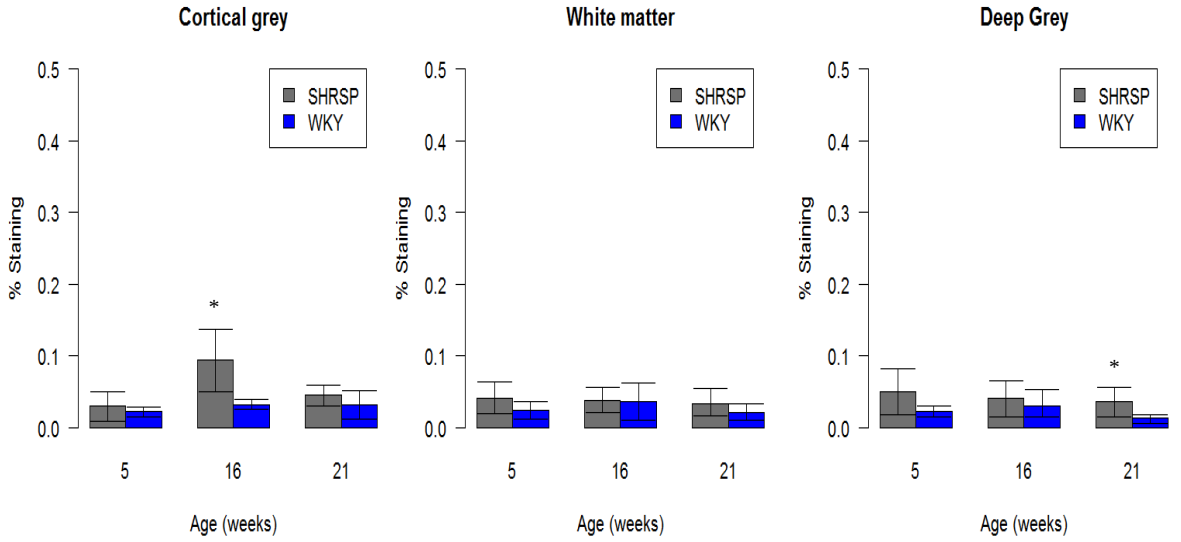

Figure 7.10. Iba-1 staining profiles of both frontal (A) and mid coronal sections (B) in WKY and SHRSP.

Each bar represents N=5. Error bars represent standard error of the mean. SHRSP had significantly higher immunoreactivity in the cortical grey matter of the frontal and mid coronal sections ($p<0.05$) as well as the deep grey matter of the mid coronal section ($p<0.01$). We also found an effect of age in the cortical grey matter of both sections ($p<0.01$).

MBP

A) Frontal Section

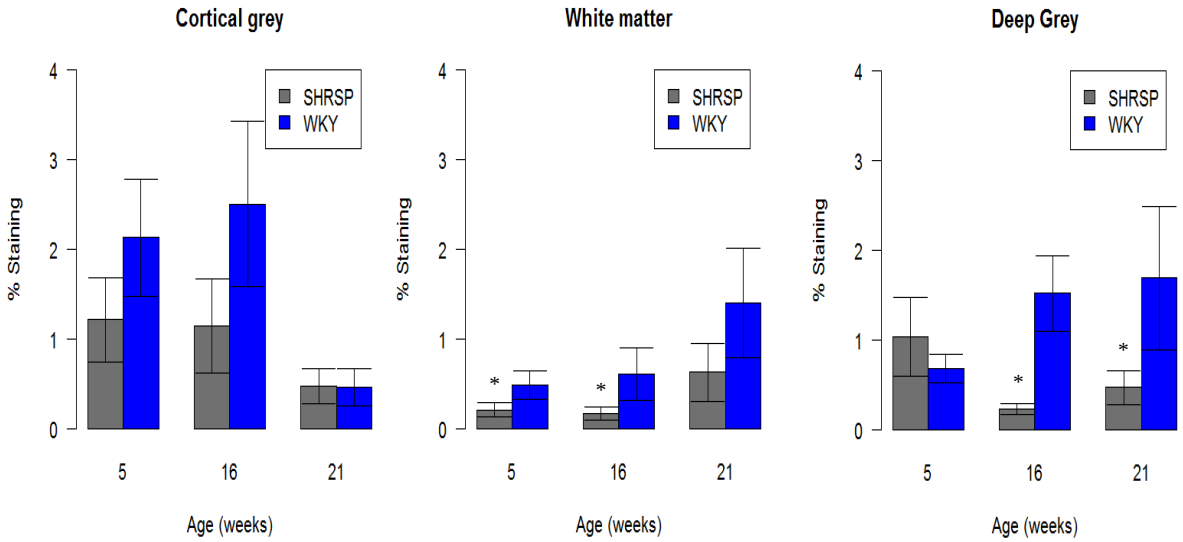

B) Mid Coronal Section

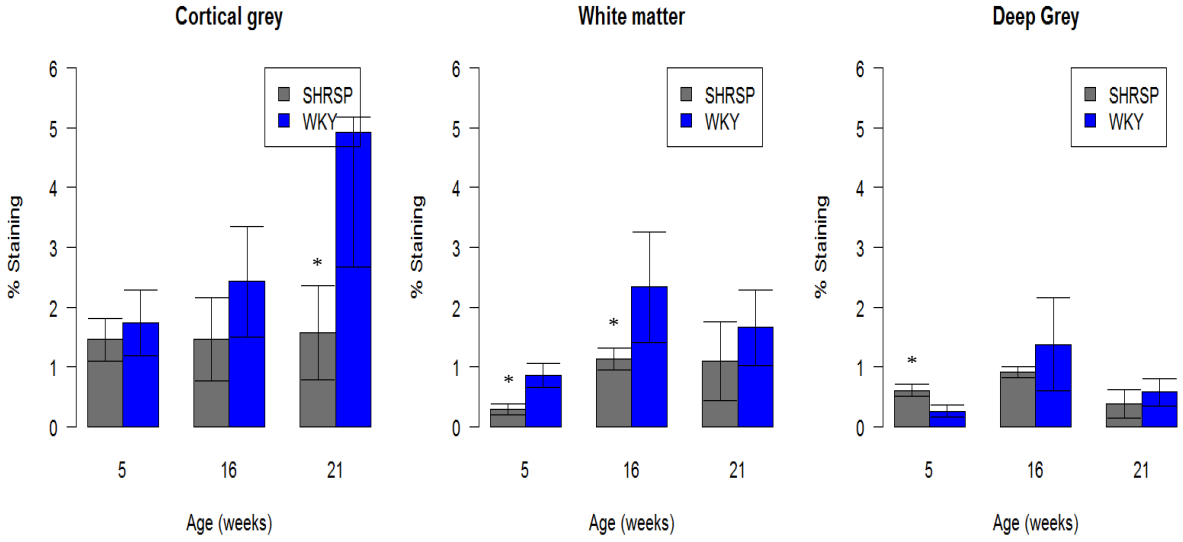

Figure 7.11. MBP staining profiles of both a frontal (A) and mid coronal (B) section of WKY versus SHRSP.

Each bar represents N=5. Error bars represent the standard error of the mean. We found significantly less MBP immunoreactivity in the SHRSP in all regions of both brain sections except the deep grey matter of the mid coronal section ($p<0.01$). We also found an increase with age in both strains in the cortical grey and white matter of the frontal section ($p<0.01$), as well as the white matter and deep grey of the mid coronal section ($p<0.05$).

7.3.4 Animals with salt-loading (+NaCl) (all rats aged 21 weeks)

7.3.4.1 All Antibodies

A summary of the results for the frontal cortex and the mid coronal sections for all regions and all antibodies are shown in Tables 7.5–7.8 which summarise the results from 2 way ANOVA analysis. Figures 7.15-7.22 are graphical representations of this data for each antibody. For pictures of the immunostaining of each antibody in both non salt-loaded and salt-loaded animals see appendix L.

Weekly systolic blood pressure readings of 21 week old SHRSP+NaCl were significantly higher than SHRSP (236.9±4.22mmHg versus 200.1±6.7mmHg, p=<0.05) We found no difference between systolic blood pressure readings of WKY+NaCl rats versus WKY - 154.4±2.97mmHg salt versus 151.8±4.47 mmHg normal rat chow.

7.3.4.2 WKY+NaCl versus WKY:

In WKY+NaCl versus WKY, we found GFAP immunoreactivity (figure 7.13 & 7.20) was significantly reduced in the frontal section cortical grey matter ($p<0.05$), claudin-5 immunoreactivity was reduced in all areas particularly in the frontal cortex, although this did not reach statistical significance (figure 7.12 & 7.15). Also in WKY+NaCl MBP immunoreactivity (figure 7.14 & 7.22) was significantly increased in the cortical grey matter of the frontal section ($p=0.01$), whilst significantly decreased in the white matter of the same section ($p<0.05$). MBP in the white matter of the mid coronal section was significantly increased ($p<0.05$) in WKY+NaCl.

7.3.4.3 SHRSP+NaCl versus SHRSP:

In SHRSP+NaCl versus SHRSP, we found Collagen IV was significantly decreased in the cortical grey matter of the frontal section ($p<0.05$) (figure 7.18). Iba-1 expression varied greatly within the cortical grey matter of the two brain sections in SHRSP+NaCl (figure 7.21). It was significantly lower in the cortical grey matter of the frontal section ($p<0.01$), however it was significantly higher in the same region of the mid coronal section ($p=0.01$). GFAP immunoreactivity (figure 7.20) was significantly increased in the mid-coronal section white matter ($p<0.01$), SHRSP+NaCl tended to have less SMA immunoreactivity across all regions in both frontal and mid coronal sections (although this did not reach statistical

significance) (figure 7.16). Finally MBP immunoreactivity (figure 7.22) was significantly decreased in SHRSP+NaCl the white matter of the mid coronal section (p=0.006).

7.3.4.4 WKY+NaCl versus SHRSP+NaCl:

Salt-loading obscured some between-strain differences seen in rats fed normal chow, and exaggerated others. For example, we did not we see the difference in claudin-5 immunoreactivity between WKY and SHRSP rats fed a normal diet repeated in the salt-loaded animals, as the amount of claudin-5 immunoreactivity in salt-loaded WKY rats had decreased (figure 7.15). We found more GFAP immunoreactivity in mid coronal white matter ($p<0.05$) than WKY+NaCl rats (figure 7.20). Iba-1 immunoreactivity (figure 7.21) was no difference between salt-loaded animals in the frontal brain section, however, in the mid coronal section SHRSP+NaCl had significantly increased Iba-1 immunoreactivity in the cortical grey and deep matter ($p<0.05$ and $p=0.01$ respectively).

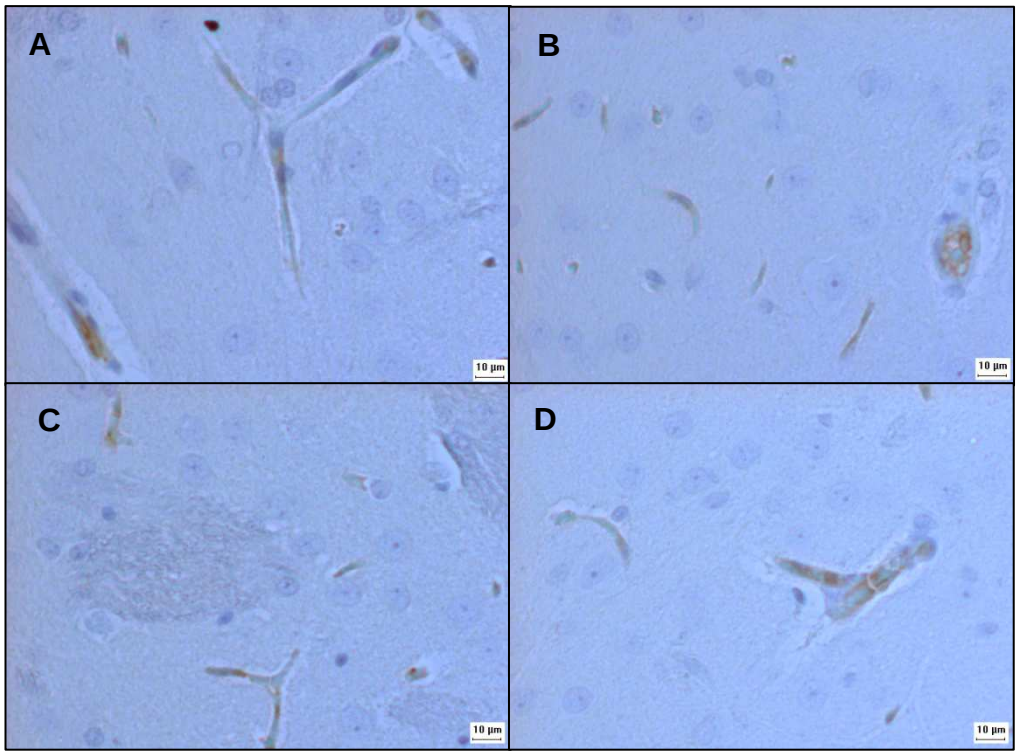

Figure 7.12. Immunoreactivity of Claudin-5 in 21 week old animals A) WKY B) WKY+NaCl C) SHRSP D) SHRSP+NaCl.

All images taken at x20 objective in the deep grey matter of a frontal section. In WKY+NaCl we saw a trend towards a decrease in immunopositive staining versus WKY (B versus A). There was no difference between SHRSP+NaCl and SHRSP (C versus D). The reduction in staining in C vs A is a strain difference (SHRSP vs WKY aged 21 weeks) quantitatively displayed previously in figure 7.3.

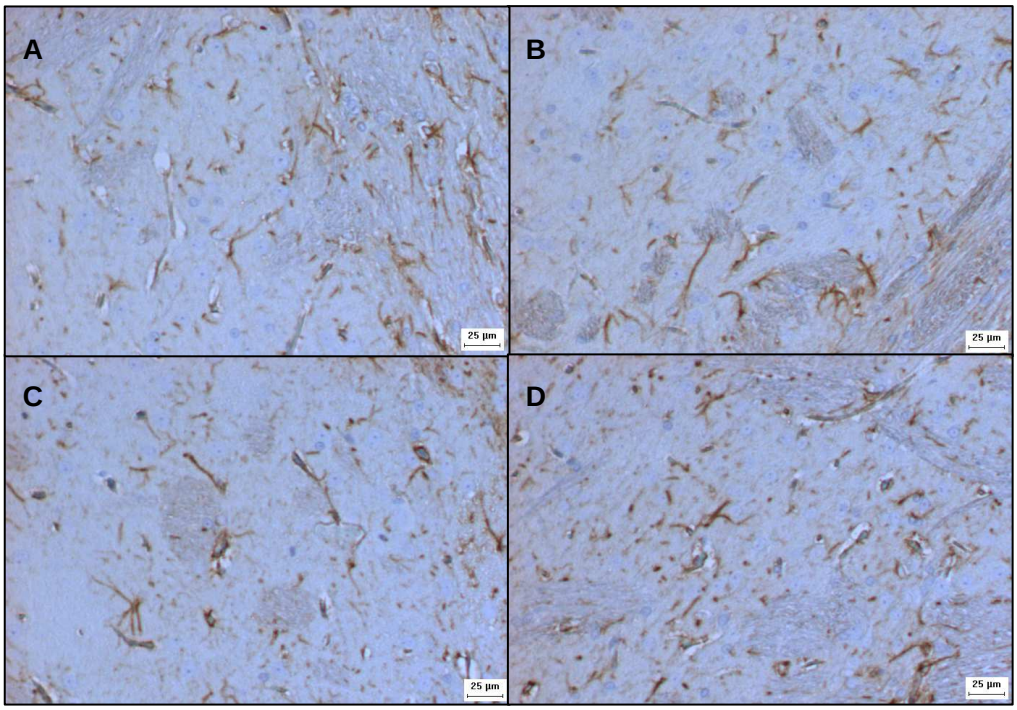

Figure 7.13. **Immunoreactivity of GFAP in 21 week old animals A) WKY B) WKY+NaCl C) SHRSP D) SHRSP+NaCl.**

All images taken at x10 objective in the deep grey matter of a frontal section. Note the increase in GFAP positive staining in SHRSP+NaCl versus SHRSP (panel D vs C).

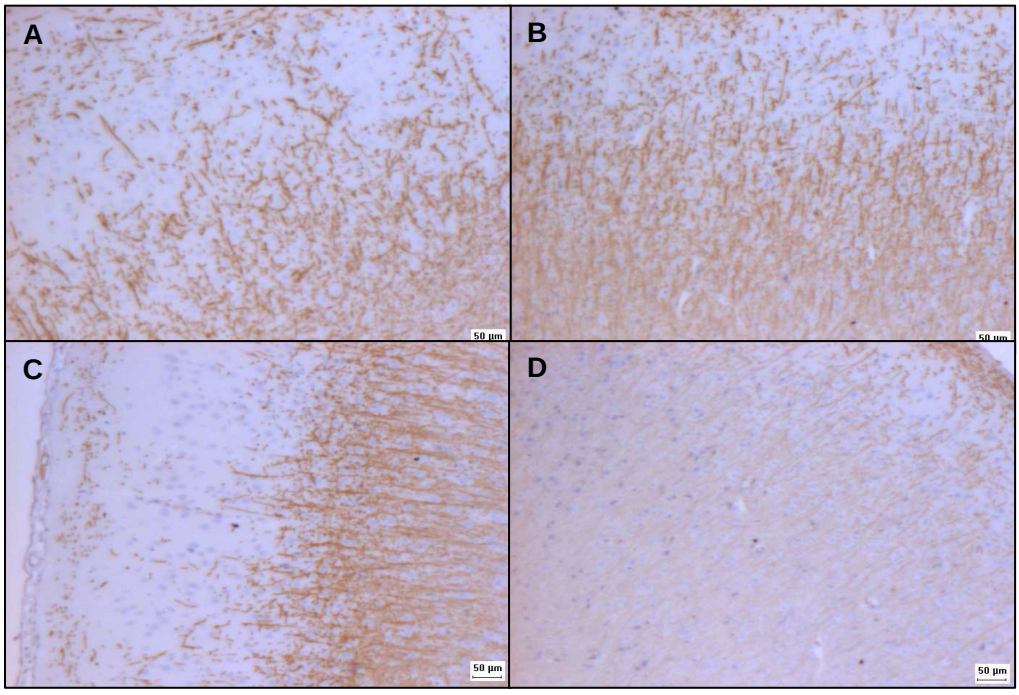

Figure 7.14. Immunoreactivity of MBP in 21 week old animals A) WKY B) WKY+NaCl C) SHRSP D) SHRSP+NaCl.

All images taken at x4 objective in the cortical grey matter of a frontal section. Note the decrease in MBP staining in SHRSP+NaCl versus SHRSP (panel D vs B). Also note the decrease in MBP staining in WKY+NaCl versus WKY (panel C vs A).

Table 7.5. Results of ANOVA analysis on the effect of salt on the percentage staining of 4 antibodies assessing vascular structure.

	SECTION	FRONTAL SECTION					
	SALT	No Salt			Salt		
	REGION	Cortex	White Matter	Deep Grey	Cortex	White Matter	Deep Grey
Claudin5	WKY	0.280±0.123	0.268±0.127	0.231±0.162	0.160±0.063	0.112±0.057	0.085±0.049
	SHRSP	0.132±0.027	0.073±0.045	0.048±0.033	0.104±0.029	0.126±0.048	0.117±0.087
	P for salt	WKY:WKY+NaCl No significant differences		WKY+NaCl:SHRSP+NaCl No significant differences		SHRSP:SHRSP+NaCl No significant differences	
Collagen I	WKY	0.172±0.047	0.134±0.079	0.120±0.072	0.094±0.050	0.080±0.039	0.077±0.051
	SHRSP	0.138±0.100	0.066±0.032	0.030±0.014	0.097±0.064	0.099±0.067	0.030±0.014
	P for salt	WKY:WKY+NaCl No significant differences		WKY+NaCl:SHRSP+NaCl No significant differences		SHRSP:SHRSP+NaCl No significant differences	
Collagen IV	WKY	0.183±0.120	0.234±0.162	0.062±0.017	0.203±0.142	0.106±0.062	0.089±0.025
	SHRSP	0.361±0.074	0.120±0.032	0.100±0.044	0.113±0.053	0.041±0.028	0.098±0.049
	P for salt	WKY:WKY+NaCl No significant differences		WKY+NaCl:SHRSP+NaCl No significant differences		SHRSP:SHRSP+NaCl Cortex p=0.02 White = NS Deep Grey = NS	
SMA	WKY	0.189±0.075	0.100±0.049	0.139±0.043	0.298±0.161	0.087±0.025	0.146±0.056
	SHRSP	0.356±0.121	0.260±0.136	0.199±0.087	0.231±0.027	0.171±0.094	0.139±0.067
	P for salt	WKY:WKY+NaCl No significant differences		WKY+NaCl:SHRSP+NaCl No significant differences		SHRSP:SHRSP+NaCl No significant differences	

Data taken from frontal section tissue in 21 week old SHRSP versus WKY rats fed either a normal diet or salt-loaded with 1% NaCl from the age of 18 weeks. Numbers indicate percentage staining ± the standard error of the mean from n=5 animals. NS = No significant difference.

Table 7.6. Results of ANOVA analysis on the effect of salt on the percentage staining of 4 antibodies assessing vascular structure.

	SECTION	MID CORONAL SECTION					
	SALT	No Salt			Salt		
	REGION	Cortex	White Matter	Deep Grey	Cortex	White Matter	Deep Grey
Claudin5	WKY	0.200±0.025	0.261±0.140	0.414±0.125	0.233±0.122	0.144±0.084	0.439±0.222
	SHRSP	0.080±0.070	0.129±0.058	0.113±0.084	0.177±0.103	0.233±0.054	0.223±0.085
	P for salt	WKY:WKY+NaCl No significant differences		WKY+NaCl:SHRSP+NaCl No significant differences		SHRSP:SHRSP+NaCl No significant differences	
Collagen I	WKY	0.088±0.064	0.060±0.012	0.732±0.381	0.242±0.150	0.131±0.080	0.475±0.202
	SHRSP	0.308±0.135	0.147±0.081	0.356±0.237	0.154±0.050	0.171±0.138	0.349±0.135
	P for salt	WKY:WKY+NaCl No significant differences		WKY+NaCl:SHRSP+NaCl No significant differences		SHRSP:SHRSP+NaCl No significant differences	
Collagen IV	WKY	0.239±0.089	0.265±0.121	0.151±0.018	0.311±0.100	0.116±0.068	0.230±0.153
	SHRSP	0.183±0.112	0.054±0.033	0.146±0.044	0.413±0.198	0.229±0.143	0.239±0.085
	P for salt	WKY:WKY+NaCl No significant differences		WKY+NaCl:SHRSP+NaCl No significant differences		SHRSP:SHRSP+NaCl No significant differences	
SMA	WKY	0.292±0.044	0.385±0.183	0.291±0.087	0.262±0.076	0.219±0.092	0.649±0.187
	SHRSP	0.530±0.237	0.517±0.231	0.704±0.352	0.426±0.200	0.403±0.118	0.398±0.252
	P for salt	WKY:WKY+NaCl Cortex = NS White = NS Deep Grey p<0.05		WKY+NaCl:SHRSP+NaCl No significant differences		SHRSP:SHRSP+NaCl No significant differences	

Data taken from mid coronal tissue in 21 week old SHRSP versus WKY rats fed either a normal diet or salt-loaded with 1% NaCl from the age of 18 weeks. Numbers indicate percentage staining ± the standard error of the mean from n=5 animals. NS = No significant difference.

Table 7.7. Results of ANOVA analysis on the effect of salt on the percentage staining of 4 antibodies assessing the presence / absence of vascular disease.

	SECTION	FRONTAL SECTION					
	SALT	No Salt			Salt		
	REGION	Cortex	White Matter	Deep Grey	Cortex	White Matter	Deep Grey
MMP9	WKY	0.349±0.211	0.154±0.101	0.096±0.065	0.132±0.098	0.112±0.073	0.087±0.057
	SHRSP	0.148±0.077	0.143±0.081	0.030±0.023	0.264±0.106	0.248±0.174	0.158±0.132
	P for salt	WKY:WKY+NaCl No significant differences		WKY+NaCl:SHRSP+NaCl No significant differences		SHRSP:SHRSP+NaCl No significant differences	
GFAP	WKY	0.914±0.199	1.387±0.254	1.490±0.567	0.493±0.136	1.991±0.230	0.835±0.161
	SHRSP	0.715±0.169	2.419±0.758	1.034±0.304	1.046±0.299	1.840±0.314	1.190±0.139
	P for salt	WKY:WKY+NaCl Cortex p<0.05 White = NS Deep Grey = NS		WKY+NaCl:SHRSP+NaCl Cortex p<0.01 White = NS Deep Grey = NS		SHRSP:SHRSP+NaCl No significant differences	
IBA-1	WKY	0.063+0.013	0.109+0.042	0.048+0.013	0.031+0.011	0.054+0.016	0.027+0.010
	SHRSP	0.071+0.035	0.084+0.048	0.052+0.028	0.014+0.002	0.030+0.013	0.051+0.026
	P for salt	WKY:WKY+NaCl No significant differences		WKY+NaCl:SHRSP+NaCl No significant differences		SHRSP:SHRSP+NaCl Cortex p<0.01 White = NS Deep Grey = NS	
MBP	WKY	0.477±0.191	1.402±0.611	1.690±0.697	1.990±0.794	0.346±0.117	1.165±0.092
	SHRSP	0.462±0.204	0.632±0.224	0.472±0.286	0.427±0.237	0.561±0.294	1.189±0.290
	P for salt	WKY:WKY+NaCl Cortex p=0.01 White p<0.05 Deep Grey = NS		WKY+NaCl:SHRSP+NaCl Cortex p<0.01 White = NS Deep Grey = NS		SHRSP:SHRSP+NaCl No significant differences	

Data taken from frontal section tissue in 21 week old SHRSP versus WKY rats fed either a normal diet or salt-loaded with 1% NaCl from the age of 18 weeks. Numbers indicate percentage staining ± the standard error of the mean from n=5 animals. NS = No significant difference.

Table 7.8. Results of ANOVA analysis on the effect of salt on the percentage staining of 4 antibodies assessing the presence / absence of vascular disease.

	SECTION	MID CORONAL SECTION					
	SALT	No Salt			Salt		
	REGION	Cortex	White Matter	Deep Grey	Cortex	White Matter	Deep Grey
MMP9	WKY	0.141±0.058	0.217±0.013	0.521±0.171	0.162±0.115	0.367±0.225	0.717±0.346
	SHRSP	0.452±0.232	0.207±0.102	0.380±0.196	0.350±0.225	0.119±0.056	0.375±0.182
	P for salt	WKY:WKY+NaCl No significant differences		WKY+NaCl:SHRSP+NaCl No significant differences		SHRSP:SHRSP+NaCl No significant differences	
GFAP	WKY	0.683±0.302	2.388±0.529	1.898±0.496	0.615±0.174	2.439±0.382	2.551±0.382
	SHRSP	0.702±0.172	2.093±0.500	2.246±0.515	0.504±0.162	3.965±0.766	2.552±0.702
	P for salt	WKY:WKY+NaCl No significant differences		WKY+NaCl:SHRSP+NaCl Cortex = NS White p<0.05 Deep Grey = NS		SHRSP:SHRSP+NaCl Cortex = NS White p<0.01 Deep Grey = NS	
IBA-1	WKY	0.032+0.020	0.022+0.011	0.013+0.006	0.055+0.020	0.034+0.021	0.019+0.009
	SHRSP	0.045+0.015	0.034+0.019	0.036+0.020	0.112+0.033	0.109+0.099	0.063+0.026
	P for salt	WKY:WKY+NaCl No significant differences		WKY+NaCl:SHRSP+NaCl Cortex p<0.05 White = NS Deep Grey p=0.01		SHRSP:SHRSP+NaCl Cortex p=0.01 White = NS Deep Grey = NS	
MBP	WKY	4.622±2.152	1.659±0.634	0.582±0.228	3.834±1.410	0.521±0.150	0.292±0.107
	SHRSP	1.570±0.786	1.098±0.761	0.383±0.233	1.944±0.886	0.063±0.046	0.130±0.105
	P for salt	WKY:WKY+NaCl No significant differences		WKY+NaCl:SHRSP+NaCl Cortex p<0.05 White = NS Deep Grey p=0.01		SHRSP:SHRSP+NaCl Cortex p=0.01 White = NS Deep Grey = NS	

Data taken from mid coronal tissue in 21 week old SHRSP versus WKY rats fed either a normal diet or salt-loaded with 1% NaCl from the age of 18 weeks. Numbers indicate percentage staining ± the standard error of the mean from n=5 animals. NS = No significant difference.

CLAUDIN-5

A) Frontal Section

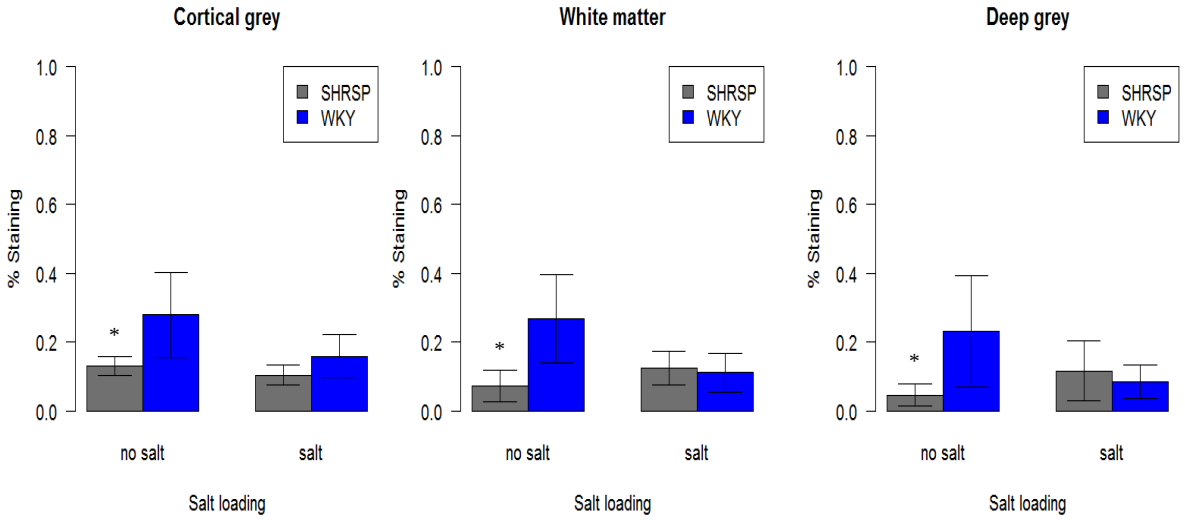

B) Mid Coronal Section

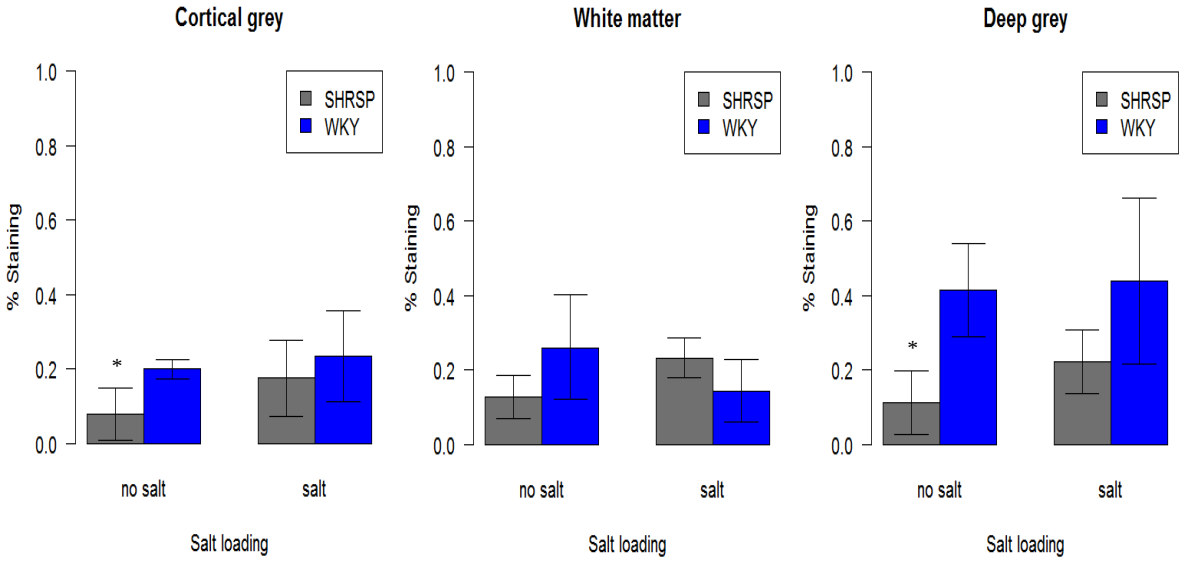

Figure 7.15. Claudin-5 staining profiles of both a frontal (A) and a mid-coronal section (B) taken from 21 week old rats either salt-loaded from 18 weeks of age or raised or standard rat chow.

Each bar represents N=5. Error bars represent standard error of the mean. We found no significant effect of salt loading on Claudin-5 staining with salt loading in either strain. However note the reduction in staining in the frontal section of WKY+NaCl versus WKY rats.

SMOOTH MUSCLE ACTIN

A) Frontal Section

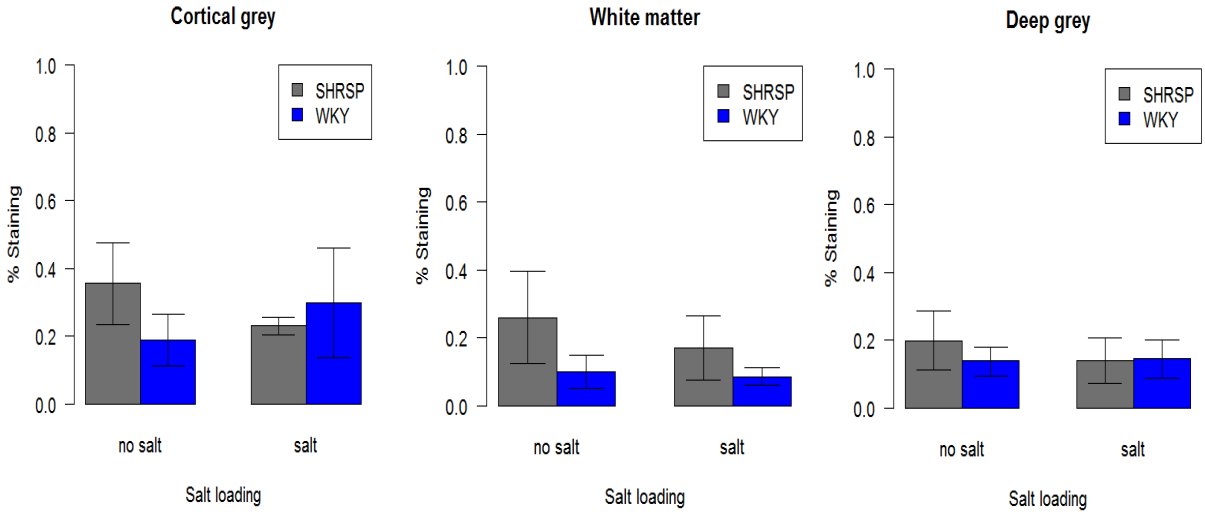

B) Mid Coronal Section

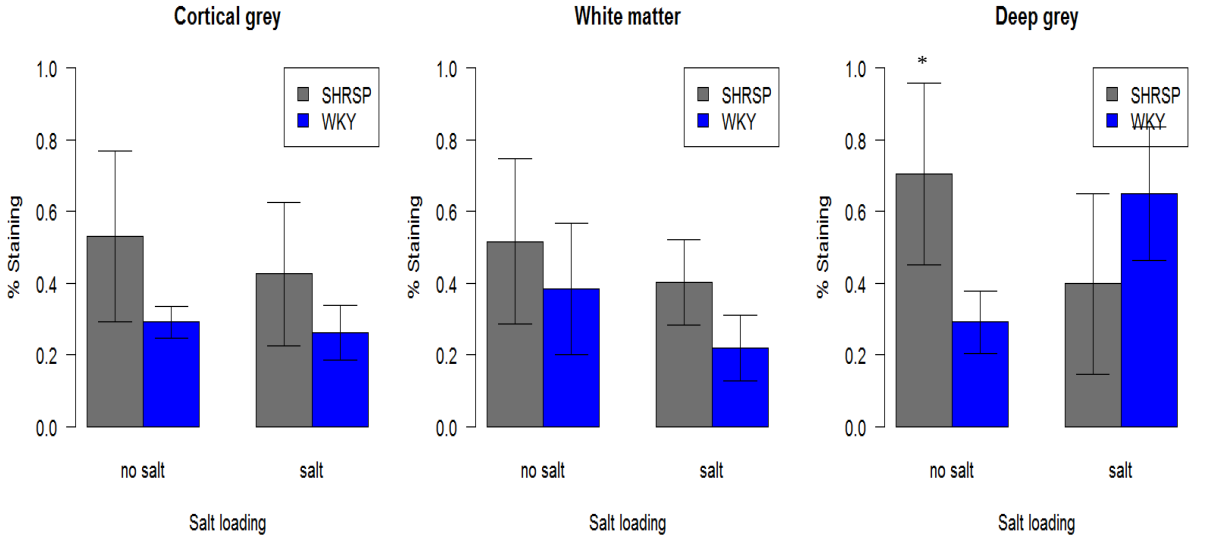

Figure 7.16. Smooth Muscle Actin staining profiles of both a frontal (A) and a mid-coronal section (B) taken from 21 week old rats either salt-loaded from 18 weeks of age or raised or standard rat chow.

Each bar represents N=5. Error bars represent standard error of the mean. We found no significant effect of salt on SMA staining in the frontal section. In the mid coronal section WKY+NaCl had more SMA staining in the deep grey matter than WKY ($p<0.05$).

COLLAGEN I

A) Frontal Section

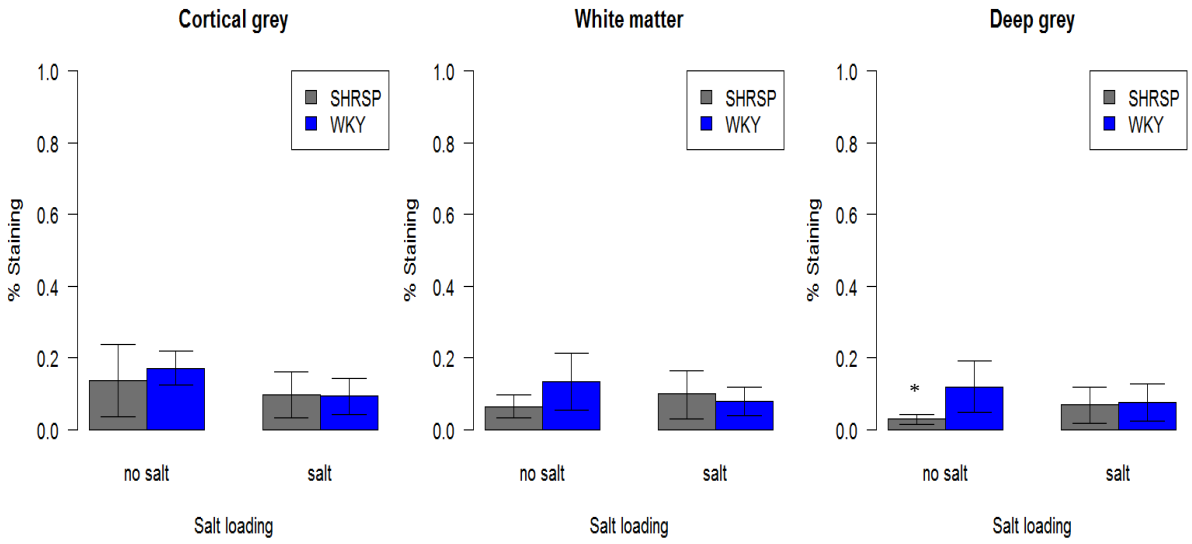

B) Mid Coronal Section

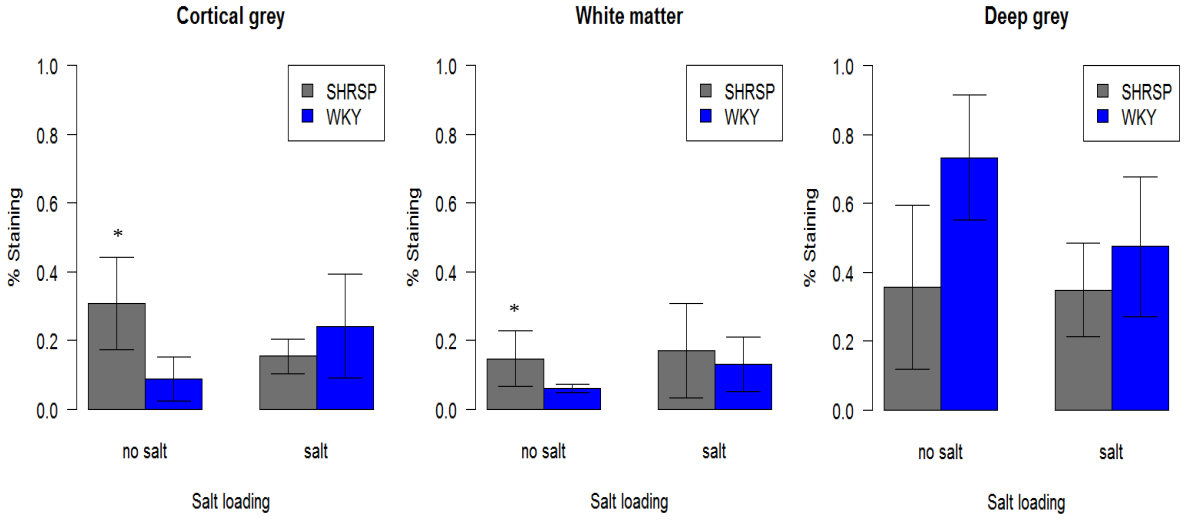

Figure 7.17. Collagen I staining profiles of both a frontal (A) and a mid-coronal section (B) taken from 21 week old rats either salt-loaded from 18 weeks of age or raised or standard rat chow.

Each bar represents N=5. Error bars represent standard error of the mean. We found no significant effect of salt loading on either strain in both brain sections.

COLLAGEN IV

A) Frontal Section

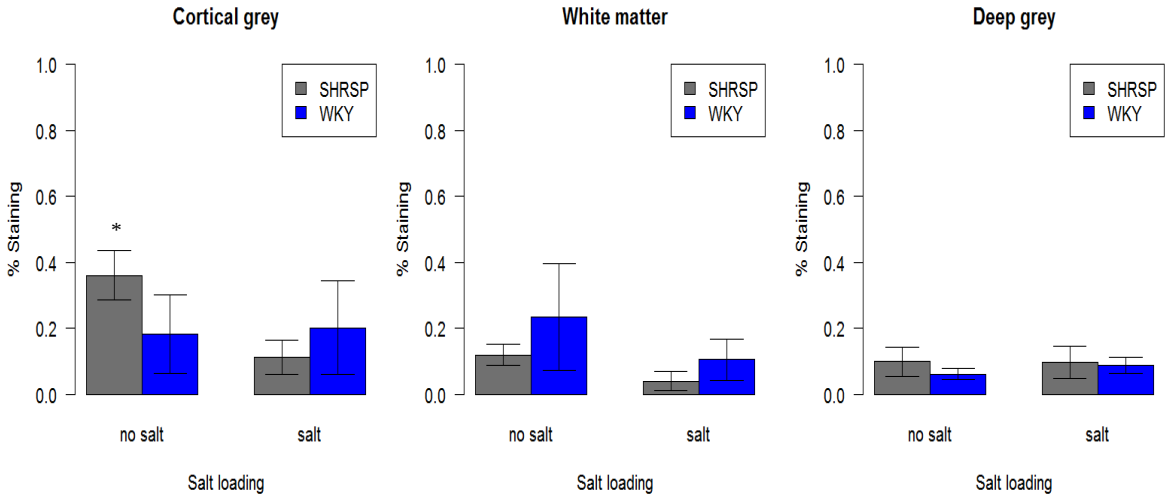

B) Mid Coronal Section

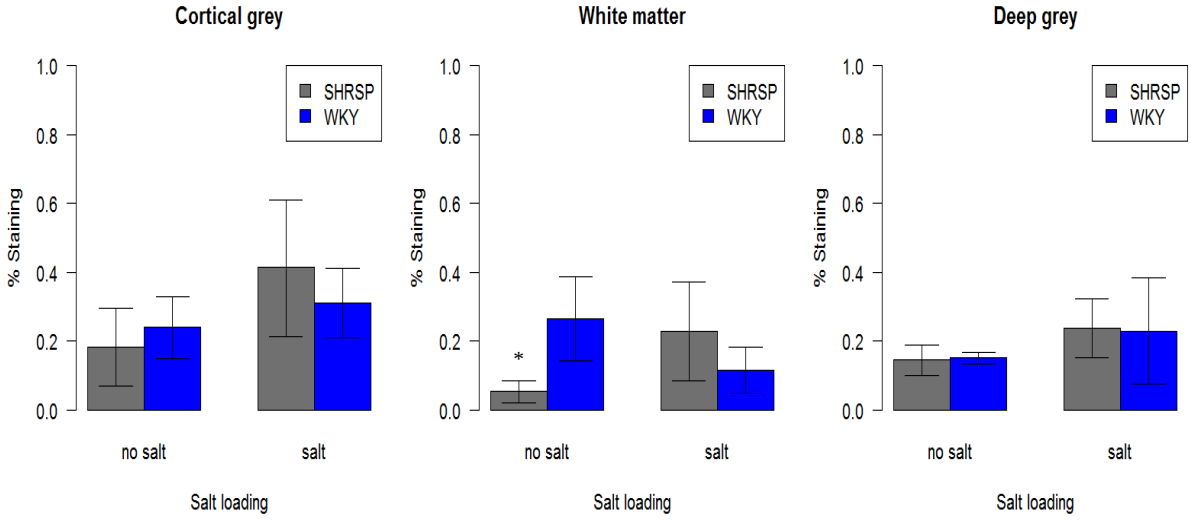

Figure 7.18. Collagen IV staining profiles of both a frontal (A) and a mid-coronal section (B) taken from 21 week old rats either salt-loaded from 18 weeks of age or raised or standard rat chow.

Each bar represents N=5. Error bars represent standard error of the mean.We found significantly less Collagen IV staining in the cortical grey matter of SHRSP+NaCl versus SHRSP ($p<0.05$) in the frontal section. In the mid coronal section no significant differences were found due to salt loading.

MMP9

A) Frontal Section

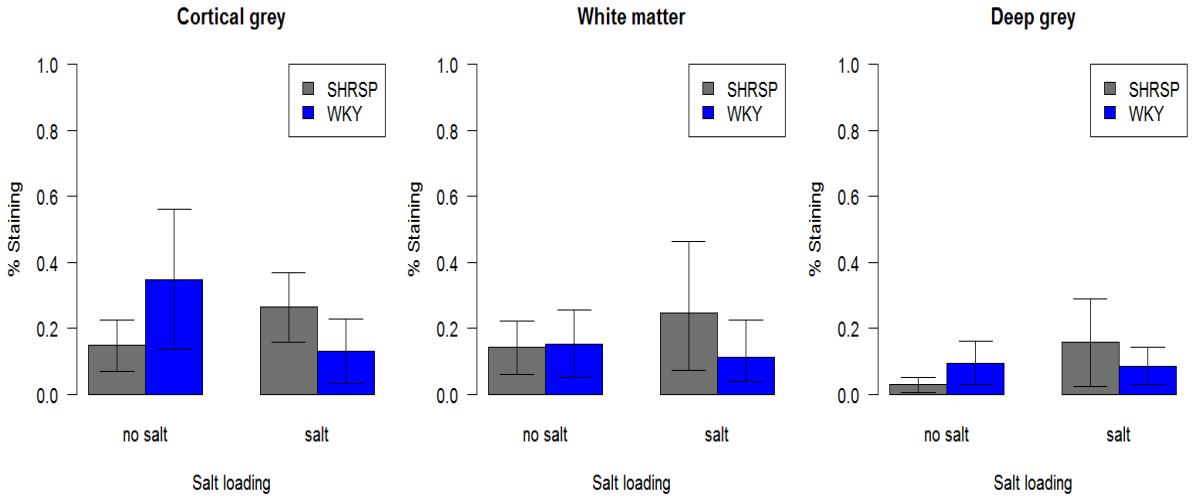

B) Mid Coronal Section

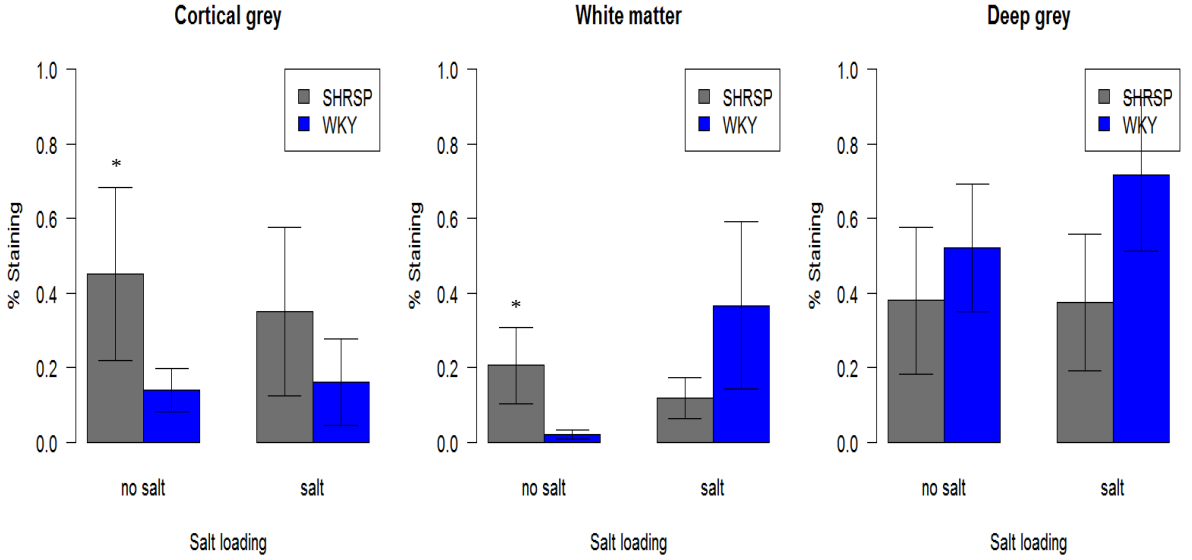

Figure 7.19. MMP9 expression in 21 week old salt-loaded versus 21 week old rats fed a normal diet.

Note the reversal in MMP9 expression between the salt-loaded and non-salt loaded animals. Each bar represents N=5. Error bars represent the standard error of the mean. We found no significant differences in MMP9 staining with salt in the frontal section or mid coronal section in either strain.

GFAP

A) Frontal Section

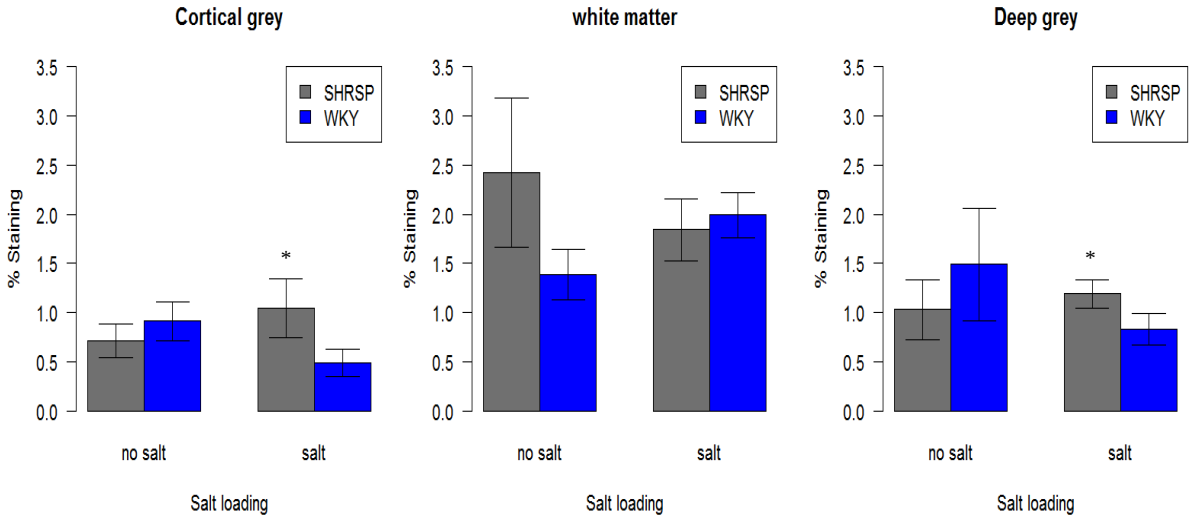

B) Mid Coronal Section

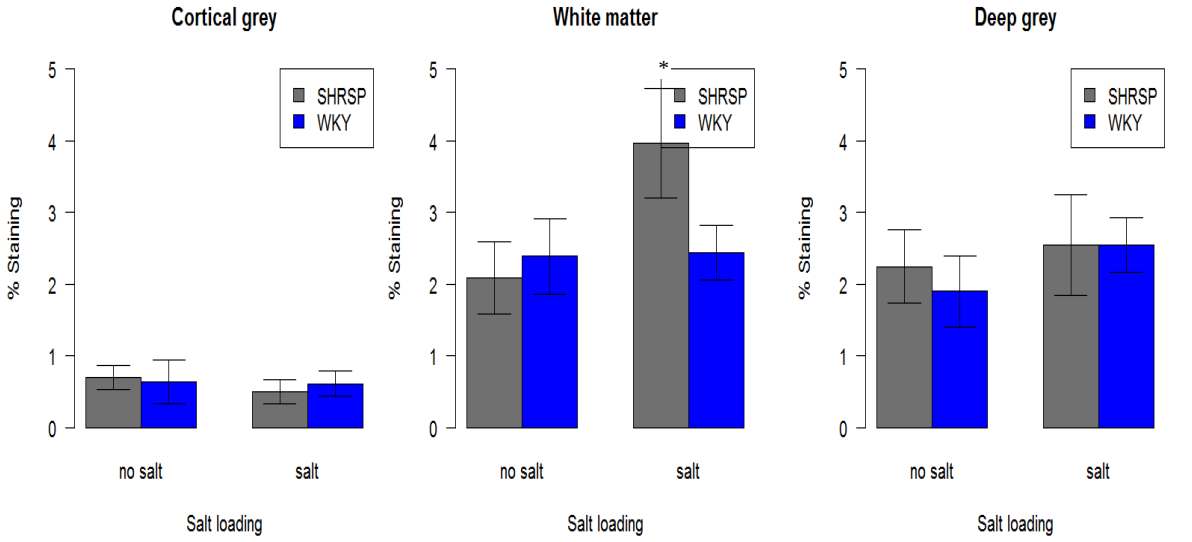

Figure 7.20. GFAP staining profiles of both a frontal (A) and a mid-coronal section (B) taken from 21 week old rats either salt-loaded from 18 weeks of age or raised or standard rat chow.

Each bar represents N=5. Error bars represent standard error of the mean. We found WKY+NaCl had significantly less GFAP staining in the cortical grey matter of the frontal section versus WKY ($p<0.05$). In turn SHRSP+NaCl had significantly more GFAP than WKY+NaCl in the same region ($p<0.01$). In the mid coronal section SHRSP+NaCl had significantly more GFAP staining in the white matter than both SHRSP ($p<0.01$) and WKY+NaCl ($p<0.05$).

IBA-1

A) Frontal Section

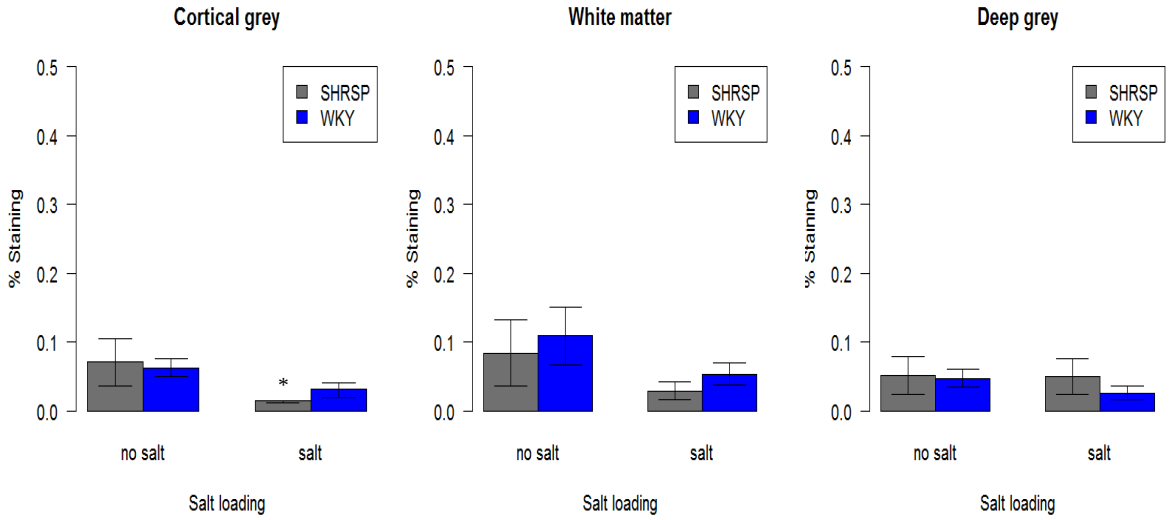

B) Mid Coronal Section

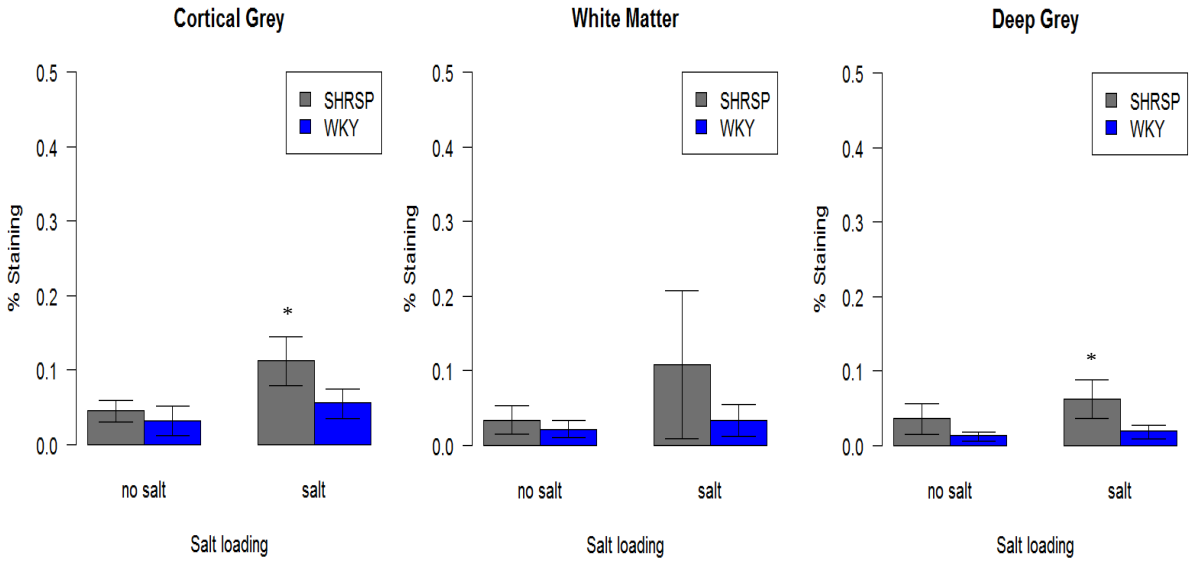

Figure 7.21. Iba-1 staining profiles of both a frontal (A) and a mid-coronal section (B) taken from 21 week old rats either salt-loaded from 18 weeks of age or raised or standard rat chow.

Each bar represents N=5. Error bars represent standard error of the mean. We found SHRSP+NaCl had significantly less Iba-1 staining in the cortical grey matter of the frontal section ($p<0.01$). In the mid coronal section SHRSP+NaCl had significantly more Iba-1 staining in the cortical grey matter than both WKY+NaCl ($p<0.05$) and SHRSP ($p<0.01$). SHRSP+NaCl also had significantly more Iba-1 staining in the deep grey matter of the mid coronal section versus WKY+NaCl ($p<0.01$).

MBP

A) Frontal Section

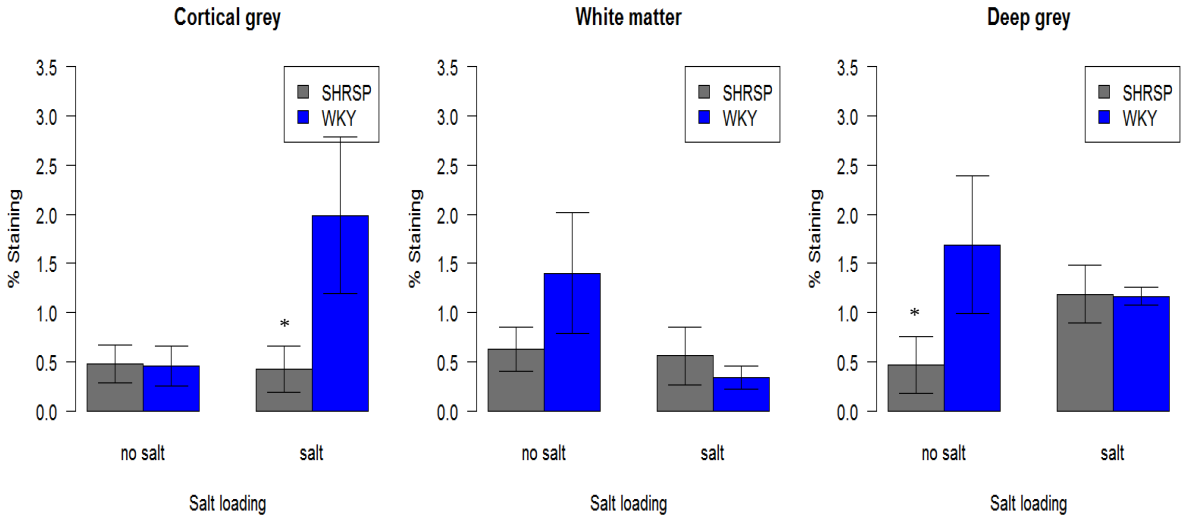

B) Mid Coronal Section

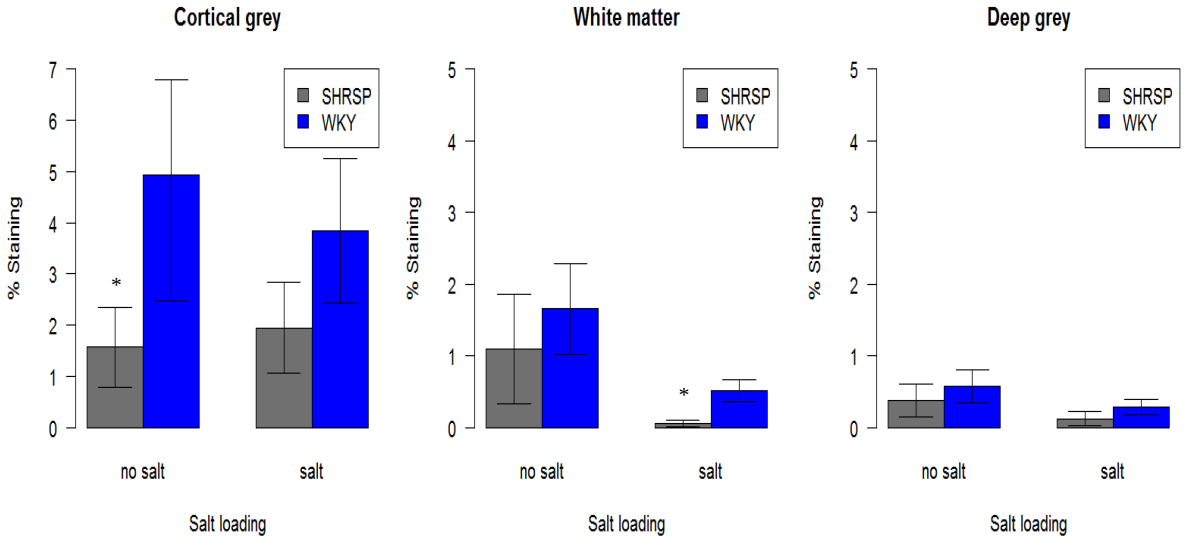

Figure 7.22. MBP staining profiles of both a frontal (A) and a mid-coronal section (B) taken from 21 week old rats either salt-loaded from 18 weeks of age or raised or standard rat chow.

Each bar represents N=5. Error bars represent standard error of the mean. We found WKY+NaCl had significantly more MBP staining than both WKY ($p<0.01$) and SHRSP+NaCl ($p<0.01$) in the cortical grey matter of the frontal section. However, WKY+NaCl had significantly less MBP staining in the white matter versus WKY ($p<0.05$). In the mid coronal section SHRSP+NaCl had significantly less MBP staining in the cortical grey and deep grey matter than WKY+NaCl ($p<0.05$).

7.4 Discussion

7.4.1 Summary of main findings

For a summary of all the significant differences in immunostaining found with age in this chapter see table 7.9. We found a significant reduction in a major neural tight junction protein (Claudin-5) in SHRSP from the earliest ages. We saw increased immunoreactivity for SMA at 16 weeks – but not at 5 weeks in SHRSP, which would reflect smooth muscle hyperplasia or hypertrophy in response to hypertension. We found increased immunoreactivity for Iba-1 in the cortical grey matter of SHRSP in both the frontal and mid coronal sections which suggests increased activation of microglia in these regions. Finally salt-loading affected the expression of neurovascular markers in both the control animals (WKY) and SHRSP.

The difference in Claudin-5, a major endothelial tight junction protein, was seen in SHRSP from 5 weeks of age, before the development of hypertension, adding further evidence to the hypothesis that not all small vessel and brain tissue changes are due to hypertension alone(Wardlaw et al. 2001;Jackson and Sudlow 2005a). Cerebral endothelial cell tight junctions are complex structures involving the interactions of multiple proteins, and are a key component in maintenance of the blood brain barrier. Claudin-5 functionally contributes towards the sealing of tight junctions(Nitta et al. 2003). It is tempting to postulate that a decrease in Claudin-5 as early as 5 weeks of age, possibly from birth, may predispose to disruption of the blood brain barrier and thence the affected vessels to subsequent arteriopathy. Increasing evidence from the human literature tends to support this hypothesis.

The increase in SMA immunoreactivity at 16 weeks in SHRSP versus WKY agrees with previous findings(Lin et al. 2001;Fujita et al. 2008) and may represent smooth muscle hypertrophy compensating for the steady increase in blood pressure in SHRSP. The increase in collagen I immunoreactivity in SHRSP in all regions of the mid coronal section by the age of 16 weeks, suggests focal medial scarring, possibly secondary to hypertensive damage to smooth muscle cells. Our results agree with previous findings which indicate that the effects of hypertension in this rat show similarities with human small vessel disease(Nabika et al. 2004). Vessel wall hypertrophy and scarring are common observations from hypertensive patients(Laurent 1995).

The increased Iba-1 immunoreactivity in the grey matter of SHRSP in both the frontal and mid coronal sections increased activation of microglia. We did not find any significant changes in the immunoreactivity of MMP9 in SHRSP versus WKY rats suggesting that, at the ages we studied there was little matrix remodelling in the perivascular tissues. We found no difference in collagen IV immunoreactivity between the strains implying that the basal lamina

was mostly intact in SHRSP or at least no different to WKY, or that any changes were too small to be detected by immunohistochemistry and image analysis.

Table 7.9. A summary table of all the significant differences in immunoreactivity with age in the SHRSP and WKY.

ANTIBODY	Significant differences in immunostaining due to strain across all ages			
	Direction of effect in SHRSP	Level of significance*	Brain section and region of interest	
			Frontal	Mid Coronal
Claudin-5	Decrease	p<0.01	All ROI	All ROI
SMA	Increase	p<0.05	CG & WM	DG
Collagen I	N/A	N/A	N/A	N/A
Collagen IV	N/A	N/A	N/A	N/A
GFAP	Increase	p<0.01	CG & WM	N/A
MMP9	N/A	N/A	N/A	N/A
Iba-1	Increase	p<0.01	CG	CG & DG
MBP	Decrease	p<0.05	All ROI	CG &WM

Data represents the results of ANOVA analysis comparing the mean percentage staining within a region of interest. * Level of significance quoted is the lowest value across all comparisons therefore if p<0.01 is stated then significance reached a minimum of this level in all regions quoted -some regions may have been more highly significant. CG = cortical grey. WM = white matter. DG = deep grey. ROI = region of interest. N/A = not applicable – no significant results.

7.4.1.1 The effects of salt-loading:

For a summary of all the significant differences found in response to salt loading in this chapter see table 7.10. We also found that a salt diet has effects on the structure of the blood brain barrier - decreased immunoreactivity of claudin-5 and increased microglial activation (Iba-1) in SHRSP and WKY rats, although not all changes reached significance. Additionally, SHRSP+NaCl have increased levels of GFAP immunoreactivity indicating more reactive gliosis than in non salt-loaded animals. These effects were observed without any increase in blood pressure in the WKY strain, while salt-loading significantly increased the already raised blood pressure in the SHRSP. SHRSP+NaCl develop high levels of hypertension and end stage pathology sooner than those left to have 'spontaneous' strokes(DiNicolantonio and Silvapulle 1988) and rarely live beyond 28 weeks of age. We found the difference in the immunoreactivity of claudin-5 between the strains at 21 weeks of age was absent in salt-loaded animals because the WKY rats also had lower levels of claudin-5. We found some evidence that salt-loading causes activation of microglial cells particularly in the mid coronal sections of SHRSP when compared to salt loaded WKY. This could suggest an increased inflammatory response to salt-loading in the SHRSP. MBP immunoreactivity was also affected by salt-loading in the cortical grey (frontal section) and white matter (both sections) of the WKY rats, although the changes were somewhat erratic with expression both increasing and decreasing. An increase in MBP may not be seen as harmful an event as a decrease but MBP is directly involved in T lymphocyte mediated inflammatory pathways and can therefore lead to increased permeability of the BBB(Cserr and Knopf 1992).

Many studies have suggested an inflammatory mechanism in salt loaded rats which in turn compromises the blood brain barrier(Blezer et al. 1998;Guerrini et al. 2002;Sironi et al. 2004). However, our results using animals reared on a normal diet show that the SHRSP has changes occurring at the endothelial tight junctions *without* the need for salt-loading. Therefore previous studies may have been confounded in their assessment of blood brain barrier integrity by routine use of salt-loading. The SHRSP in its spontaneous state is advantageous when trying to model human small vessel stroke as, although high salt intake is a recognised risk factor for all ischaemic stroke, it has not specifically been associated with a small vessel subtype(Jackson et al. 2010).

Table 7.10. A summary table of all the significant differences in immunoreactivity in response to mild salt loading in SHRSP and WKY aged 21 weeks.

ANTIBODY	Strain	Significant differences in immunostaining due to salt loading			
		Direction of effect in salt loaded animals	Level of significance*	Brain section and region of interest	
				Frontal	Mid Coronal
Claudin-5	**WKY**	N/A	N/A	N/A	N/A
	SHRSP	N/A	N/A	N/A	N/A
SMA	**WKY**	Decrease	p<0.05	N/A	WM
	SHRSP	Decrease	p<0.01	N/A	WM
Collagen I	**WKY**	N/A	N/A	N/A	N/A
	SHRSP	N/A	N/A	N/A	N/A
Collagen IV	**WKY**	N/A	N/A	N/A	N/A
	SHRSP	Decrease	p<0.05	CG	N/A
GFAP	**WKY**	Decrease	p<0.05	CG	N/A
	SHRSP	Increase	p<0.05	N/A	WM
MMP9	**WKY**	N/A	N/A	N/A	N/A
	SHRSP	N/A	N/A	N/A	N/A
Iba-1	**WKY**	N/A	N/A	N/A	N/A
	SHRSP	Increase	p<0.01	CG	CG
MBP	**WKY**	Decrease	p<0.05	CG & WM	N/A
	SHRSP	Decrease	p<0.01	N/A	WM

Data represents the results of ANOVA analysis comparing the mean percentage staining within a region of interest. *Level of significance quoted is the minimum value across all comparisons therefore if p<0.01 is stated then significance reached a minimum of this level in all regions quoted - some regions may have been more highly significant. CG = cortical grey. WM = white matter. DG = deep grey. ROI = region of interest. N/A = not applicable – no significant results.

7.4.2 Aspects of study methodology

This study has limitations. Firstly the SHRSP is inbred. The animals we used have been bred in a colony separately from the original source for over 15 years. Thus there may be subtle genetic differences between our colony and other SHRSP colonies, so our findings may differ qualitatively or quantitatively from other colonies. Secondly, we found some strong trends in our data that did not achieve statistical significance. This may reflect the small number of animals studied (5 rats per group) and a larger study would make the data more robust. Some antibodies produced larger errors due to their diffuse immunoreactivity (e.g. MMP9). This made colour threshold assessment using pixel counts inherently more difficult, increasing the likelihood of human error.

However, this study also has several strengths, particularly as few studies have described the changes in the small vessels and surrounding tissue in young SHRSP rats. We selected young rats still at a normotensive stage, an established hypertensive stage (16 weeks) and a stroke-prone stage (21 weeks). Further advantages are that we sourced all animals from the same colony where both the control WKY and the SHRSP are kept in the same conditions and fed exactly the same diet. Additionally, the observer was blinded to the age and strain of the rats throughout the immunohistochemistry and image analysis protocols. We used a standardised sampling protocol to standardise anatomical areas of cortical grey, white matter and deep grey matter to ensure sampling from consistent regions despite the challenge of differences in brain size at different ages. The importance of this is demonstrated in the differences we have found between regions within the same brain sections and the differences between frontal and coronal sections. For example a significant increase in collagen I with age was evident in all regions of the mid coronal section but only the cortical grey matter of the frontal section. Likewise the increase in SMA immunoreactivity was more evident in the mid coronal section. Frontal and mid coronal sections of the brain have differing ratios of cortical grey, white matter and in particular deep grey matter – the mid coronal section has a much larger area of deep grey matter. The vascular beds feeding cortical structures are very different from those feeding subcortical structures. Cortical vessels anastomose efficiently with surrounding vessels whereas arterioles of the deep grey structures are end arterioles with no access to collateral flow. This difference is also important as the SHRSP has been suggested as a model of subcortical diseases such as vascular dementia(Kimura et al. 2000) but few studies have looked at the vasculature in the deep grey or white matter in great detail.

7.5 Conclusion

In conclusion we have shown that from a pre-hypertensive age, the SHRSP has less of the tight junction protein claudin-5. We have also confirmed that prolonged hypertension causes vessel wall hypertrophy (due to an increase in SMA) and an accumulation of collagen 1 within the vessel wall. Salt decreases tight junction proteins not only in the SHRSP rats but also in the WKY animals. The changes in vascular endothelium tight junctions are then exacerbated by both an increase in blood pressure and a high salt intake. However in the WKY+NaCl, these changes occurred without any measurable change in blood pressure, suggesting that the effects of salt may be mediated through direct action on the endothelium rather than simply through raised blood pressure. Therefore a high salt diet in people, with or without hypertension, may compromise the structure of the blood brain barrier and increase the risk of cerebrovascular disease, cognitive decline and dementia. This effect would be particularly relevant in conditions such as lacunar stroke where there is already evidence indicating that blood brain barrier failure is a causative mechanism(Wardlaw et al. 2003).

Future experiments should focus on examining the SHRSP endothelium in more detail in young rats, at narrower age intervals, in larger numbers and look for the potential genetic differences in the SHRSP rat that could account for endothelial tight junction structural differences. The structure of the vascular endothelium outside of the brain (e.g. in the kidney) should also be investigated to assess whether the alteration in tight junction proteins within the brain endothelium are repeated elsewhere.

CHAPTER 8 : TIME COURSE AND SALT SPECIFIC MICROARRAY ANALYSIS OF GENE EXPRESSION IN BRAIN REGIONS SUSCEPTIBLE TO SPONTANEOUS STROKES AND VASCULAR PATHOLOGY IN THE SPONTANEOUSLY HYPERTENSIVE STROKE PRONE RAT (SHRSP).

8.1 Background

The SHRSP was originally considered to be (and still is) a model of malignant hypertension and cardiovascular disease as it displays left ventricular hypertrophy, however only a few microarray studies of hypertensive (SHR, SHRSP) and salt sensitive (Dahl salt sensitive) rat strains have been performed to identify the genetics underlying cardiovascular disease (e.g.(Garrett et al. 2002;McBride et al. 2003;Garrett et al. 2005)). However these studies were performed in adult rats when hypertension is fully established, meaning that any changes in gene expression could simply have been secondary to increased blood pressure. Few studies have assessed the SHRSP at more than one time point over the development of hypertension in order to separate candidate genes for hypertension from those which might contribute to other disease states the SHRSP is used to model – kidney disease, attention deficit hyperactive disorder and in our case stroke. Whilst a couple of microarray studies of temporal mRNA expression in the SHRSP kidney have been performed (Seubert et al. 2005;Clemitson et al. 2007;Polke 2008) there have not been any studies on brain tissue to correlate changes in mRNA expression with the cerebral vascular and parenchymal pathology. Therefore the question of what makes the SHRSP 'stroke prone' (Hinojos et al. 2005) upon exposure to levels of hypertension the SHR experiences is still unanswered(Bailey et al. 2011a).

The STR1 (stroke related -1) locus on chromosome 1 in the SHRSP was originally suggested as the 'stroke-prone' locus despite containing no obvious candidate genes(Rubattu et al. 1999) as it affected latency to stroke in SHRSP crossed with stroke resistant SHR in a study designed to eliminate the influence of blood pressure(Rubattu et al. 1996). The polygenic nature of stroke makes it unlikely that this one locus would be the only genetic factor conferring stroke-proneness in SHRSP and soon afterwards another locus on chromosome 5 was also proposed as a contributing factor to stroke sensitivity(Jeffs et al. 1997b). This locus surrounds Atrial and Brain Naturetic Peptides and SHRSP and is also blood pressure independent. Indeed SHRSP sampled from a range of ages (4-36 weeks), have been shown to have multiple genetic differences (all compared to WKY) considered to have a direct influence on the incidence or timing of stroke, independently of hypertension including: decreased endothelial nitric oxide (NO) and increased superoxide species(Grunfeld et al. 1995;McBride et al. 2005), impaired endothelial dependent vasorelaxation(Negishi et al.

1999), irregular Na^+ exchange in vascular smooth muscle cells(Thompson et al. 1988;Kobayashi et al. 1990) and impaired activation and decreased aggregation of platelets(Tomita et al. 1984;Umegaki et al. 1986;Klee et al. 1993;Ikeda et al. 1996).

Although the above are considered independent of hypertension, longitudinal study of the brain (including young animals) is necessary to identify sequential changes in brain parenchymal and/or cerebrovascular mRNA expression to distinguish secondary effects of hypertension from underlying susceptibility to tissue damage. In this thesis we have already shown that SHRSP have features indicating susceptibility to brain vascular and parenchymal damage at 5 weeks of age, prior to the onset of hypertension including: impaired endothelial tight junctions, perivascular inflammation and glial damage (see chapter 7).

However, whilst the study of young SHRSP is not confounded by hypertension the study of older age groups is confounded not just by exposure to hypertension but invariably to dietary interventions too. Over the last 20 years the use of salt administered either as a 'Japanese Diet' or as salt added to drinking water, has been used increasingly in research using SHRSP (Bailey et al Int J Stroke in press) as a means to quicken the onset of pathological changes and create a more severe phenotype of cardiovascular and cerebrovascular disease (DiNicolantonio and Silvapulle 1988;Schmidlin et al. 2005;Yamamoto et al. 2008). The effect of salt sensitivity on cerebrovascular gene expression in the SHRSP has not been fully determined. Perhaps more importantly, the effect of salt on the cerebrovascular pathology of control strains such as the Wistar Kyoto rat (WKY) - the parent strain of the SHRSP and SHR, has also not been assessed

8.1.1 Aims of the study

In light of the unanswered questions raised above we used a microarray approach to measure mRNA expression in order to assess two aims; Firstly, to assess differences in cerebral gene expression between the WKY and SHRSP from weanling to maturity (5, 16 and 21 weeks) and secondly, to determine the impact of salt loading on cerebral gene expression in both WKY and SHRSP.

8.2 Methods

8.2.1.1 Animals and tissue

For our serial timepoint study we used male WKY and SHRSP animals from three age groups (5 week, 16 week and 21 week old animals) with four WKY and four SHRSP animals per age group (total animals n=24). To study the effect of salt loading (+NaCl) we used WKY and SHRSP animals all aged 21 weeks (n=4 of each strain) at time of sacrifice. All rats were fed standard rat chow throughout, however in half of the 21 week old WKY and SHRSP we added 1%NaCl to their drinking water at 18 weeks, producing 3 weeks of salt loading. We kept all animals in identical conditions. We preserved one brain hemisphere from each animal in liquid nitrogen. We then immersed the entire hemisphere in x10 volume of RNAlater®-ICE solution (Ambion) and incubated for 24 hours at -20°C to enable full penetration of the solution. The next day we mounted the hemisphere in a Zivic rat slicer matrix and cut a 2mm coronal slice from a frontal and a mid coronal region based on a previously described protocol (see chapter 5) to capture standardised brain areas matched for age. These areas captured the frontal cortex, thalamus, internal capsule and basal ganglia – areas susceptible to cerebral and vascular pathology in the SHRSP.

8.2.1.2 RNA extraction

We placed the slices in approximately 1.5ml (x10 volume) of lysis buffer (Qiazol (Qiagen)) and homogenized the tissue using a POLYTRON® homogenizer (Capitol Scientific Inc.). We then applied a Qiagen RNAeasy lipid tissue minikit (www.qiagen.com) for the extraction of RNA from fatty tissues to the homogenates. We eluted the resulting RNA with nuclease free water (2x50µl). We treated half the elute with turbo DNase to remove any remaining genomic DNA. We then assessed the quality of the resulting RNA on a Nanodrop ND 1000 and Agilent bioanalyser 2100.

8.2.1.3 RNA amplification and purification

We performed transcriptions from RNA to cRNA using an Ambion Illumina Total Prep RNA amplification kit (www.ambion.com). We generated first strand cDNA with a first strand master mix containing an oligo (dT) tagged with a phage T7 promotor. Second strand cDNA was generated with a master mix containing DNA polymerase. To the elute we added the in vitro master mix solution according to kit instructions which amplifies and labels the cDNA with biotin UTP. We obtained a final cRNA elute of just less then 200µl. We checked the

cRNA profiles of all samples by running them on the Agilent bioanalyser. We added 5µl of cRNA (~750ng) to 10µl of hybridisation buffer and loaded the resulting 15µl onto a RatRef12 chip (www.illumina.com) in the appropriate inlet port. We incubated chips at 58°C overnight, washed them with E1BC solution, incubated chips in E1 buffer for 10 minutes and stained them in a solution of E1 buffer plus 1:1000 dilution of streptavidin-Cy3. We performed a final wash with E1BC wash buffer on the orbital shaker then dried the chips by centrifuging.

For analysis if mRNA expression we used RatRef12 microarray chips (www.illumina.com) which contain a total of 22,519 gene and probe sets. This is the one of the most comprehensive rat chips commercially available. We scanned chips on an Illumina Bead Reader and recorded the intensity of the green fluorescent signal emitted. Samples with a signal intensity of >600 passed the bead array reader's quality control.

8.2.1.4 Quantitative real time polymerase chain reaction (qRT-PCR)

We performed qRT-PCR to quantitatively confirm differential expression measured in the microarray experiment. We used the same DNase-treated RNA from the microarray experiment as the template for the synthesis of cDNA. We performed qRT-PCR reactions using Applied Biosystems Taqman® Gene Expression Assay. Probes were obtained from Applied Biosystems. Briefly we reverse transcribed 20 µl reactions on a 96 well plate containing approximately 1µg of RNA using the Taqman® reverse transcription master mix (Applied Biosystems) which included OligodT primers and Multiscribe™ reverse transcriptase enzyme. We performed qRT-PCR on the cDNA by creating a reaction mix in the same Eppendorf containing Taqman® universal master mix (Applied Biosystems) plus a probe for a housekeeping (control) gene e.g. GAPDH (VIC® labelled) and the Taqman® probe corresponding to our gene of interest (FAM® labelled) (See table 8.1 for a list of all Taqman® probes used). The samples were run on a 384 well plate on a 7900HT Sequence detector (Applied Biosystems).

Table 8.1. Taqman® probes used to validate candidate genes of interest using qRT-PCR.

GENE	ASSAY ID	AMPLICON LENGTH	LOCATION	EXON BOUNDARY
ACTB	Rn00667869_m1	91	Ch12 13452437 - 13456026	4-5
ALB	Rn00592480_m1	96	Ch14 19126935 - 19142214	6-7
AVP	Rn00566449_m1	66	Ch3 118205007 - 118206985	1-2
GFAP	Rn00566603_m1	76	Ch10 92059881 – 92068555	7-8
GPR98	Rn01757838_m1	54	Ch2 9575038 – 9704399	32-33
GUCY1a3	Rn00567252_m1	77	Ch2 173756824 - 173818316	6-7
GUCY1b3	Rn00562775_m1	135	Ch2 173683153 - 173735298	3-4
MBP	Rn01399619_m1	80	Ch18 78943608 – 79057329	3-4
MMP14	Rn00579172_m1	62	Ch15 32493852 – 32503077	1-2
SLC24a2	Rn00582020_m1	72	Ch5 106295254 - 106537714	7-8

Properties of each of the 10 Taqman probes used to validate candidate genes of interest including length of the probe and section of the gene covered. ACTB = Beta Actin. ALB = Albumin, AVP = Arginine Vasopressin, GFAP = Glial Fibrillary Acidic Protein, GPR98 = G-Protein Coupled Receptor 98, GUCY1a3 = Guanylate Cyclase 1 alpha 3 subunit, GUCY1b3 = Guanylate Cyclase 1 beta 3 subunit, MBP = Myelin Basic Protein, MMP14 = Matrix Metallopeptidase 14 and SLC24a2 = Sodium/Potassium/Calcium exchanger 2. Ch = Chromosome.

8.2.1.5 Standard PCR

We designed forward and reverse primers corresponding to the portion of the GUCY1a3 gene sequence covered by the Illumina microarray probe. For a full list of probes see table 8.2. To test for insertions or deletions within the sequence between strains we ran end point PCR using these primers, on DNA taken from the livers of SHRSP (n=4) and WKY (n=3). We used a proofreading 'Kod Hot Start' DNA polymerase (Novagen) and performed PCR's using the designated kit and to manufacturer's instructions. Extension times depended on the length of sequence being created. We performed all PCR's on a MJ Research PTC Gradient Cycler using 96 well plates. Results were analysed using agarose gel electrophoresis. We visualised gels on a BIO-RAD Fluor-S Multimager and assessed the size of PCR products using Promega 100bp or 1kb DNA ladders.

Table 8.2. **Characteristics of the primers designed for sequencing GUCY1a3.**

Oligo Name	**Sequence (5'->3')**	**Yield (µg)**	**Tm (ºC)**	**GC content (%)**
GUCY1a3_AF	GTTCTCACACACAGCCTTC (19)	345	56.7	52.6
GUCY1a3_Ex6_BF	GTCAAATGAATCTACATCGTTGA (23)	229	55.3	34.8
GUCY1a3_3pr_CF	GTAGTTCAGTAAGTGTCAAAG (21)	207	54.0	38.1
GUCY1a3_3pr_DF	GACAACTAAACCACCCAA (18)	291	51.4	44.4
GUCY1a3_3pr_AR	CTTCTGCAATCCTAAAGTCA (20)	232	53.2	40.0
GUCY1a3_3pr_BR	GATACAGTTCCTCCATTTGC (20)	246	55.3	45.0
GUCY1a3_3pr_CR	CCAAAACACCCACAATCA (18)	163	51.4	44.4

Within the name of each probe GUCY1a3 = Guanylate cyclase 1 alpha subunit 3, 3pr = 3' prime UTR, A/B/C/D refers to the order the probes were designed in, the letters F/R refer to either 'forward' or 'reverse'. Tm = melting temperature.

8.2.1.6 DNA Sequencing

We used Applied Biosystems BigDye Terminator n3.1 Cycle Sequencing kits for all sequencing reactions and performed reactions in 96 well plates (WKY n=3, SHRSP n=2). A reaction solution of sequencing buffer, ready reaction, primer, purified PCR product and water was loaded into each well. To sequence, we used a temperature cycling program of 96°C for 45 seconds, 50°C for 25 seconds and 60°C for 4 minutes, repeated 25 times. We subsequently loaded 20µl of purified sequencing product into optically clear 96 well plates covered with Applied Biosystems Septa Seals. We performed sequencing capillary electrophoresis on a 48-capillary Applied Biosystems 3730 Genetic Analyser with 36cm capillaries filled with POP-7 polymer (Applied Biosystems) and warmed to 60°C. We separated sequencing products by size using electrophoresis set to 8500V for 50 minutes.

8.2.2 Data and statistical analysis

8.2.2.1 Microarray data

We firstly normalised data from the Bead Array reader in Bead Studio (Illumina) and then exported it into third party software (R). Rank Products (RP) analysis is a non parametric test that compares the ranks of the fold changes of differentially expressed genes in replicated microarray experiments. A nominal significance level of false discovery rate (FDR) $q<0.05$ determined using the Bejamini-Hochberg method (Bejamini and Hochberg 1995) was taken as the threshold for significant differential expression. We did not set a minimum fold change for significance or signal intensity. We uploaded all data from RP analysis onto Ingenuity Pathway Analysis (IPA) (Ingenuity® Systems www.ingenuity.com) and analysed both sets of data using both a candidate gene approach (looking for changes in genes and pathways of interest) and a genome wide approach (to generate new hypotheses). IPA uses an extensive peer previewed literature base to assess whether genes are directly functionally connected as well as using statistical methods (e.g. Fischer's exact test) to identify over represented genes within functional groups (for more detail see chapter 5 and appendix H).

8.2.2.2 qRT-PCR data

Cycle threshold (CT) values were exported from sequence detection system (SDS) software into an Excel spreadsheet where the mean delta cycle threshold (dCT) values and standard errors versus the housekeeper gene were calculated (Students T Test). From these values the

delta delta CT (ddCT) values and relative quantification of mRNA expression changes (2^ddCT) values were calculated and plotted using functions in Excel.

8.2.2.3 Sequencing data

We analysed sequencing using Applied Biosystems SeqScape software and aligned experimental sequences with known sequences derived from bioinformatic databases such as ENSEMBL genome browser.

8.3 Results

8.3.1 mRNA expression data

After analyzing the microarray data using rank products (RP) analysis we generated Venn diagrams in order to visualize the results in terms of age groups, brain sections and +/- NaCl. These diagrams were then used to upload gene lists of interest onto IPA for further analysis. All significant fold changes reported = $q<0.05$.

8.3.2 Animals aged 5, 16 and 21 weeks.

8.3.2.1 The genome wide approach

i) Analysis of Venn diagrams

RP data used to generate the following Venn diagrams can be accessed in Appendix M.

In the frontal brain section we found 62 genes from RP analysis were differentially expressed between WKY and SHRSP across all ages, whilst in the mid coronal section we found 55 common to all ages (figure 8.1). Of these, 49 genes were common to both frontal and mid coronal brain sections. However, we found no direct functional connections between these genes using IPA.

.

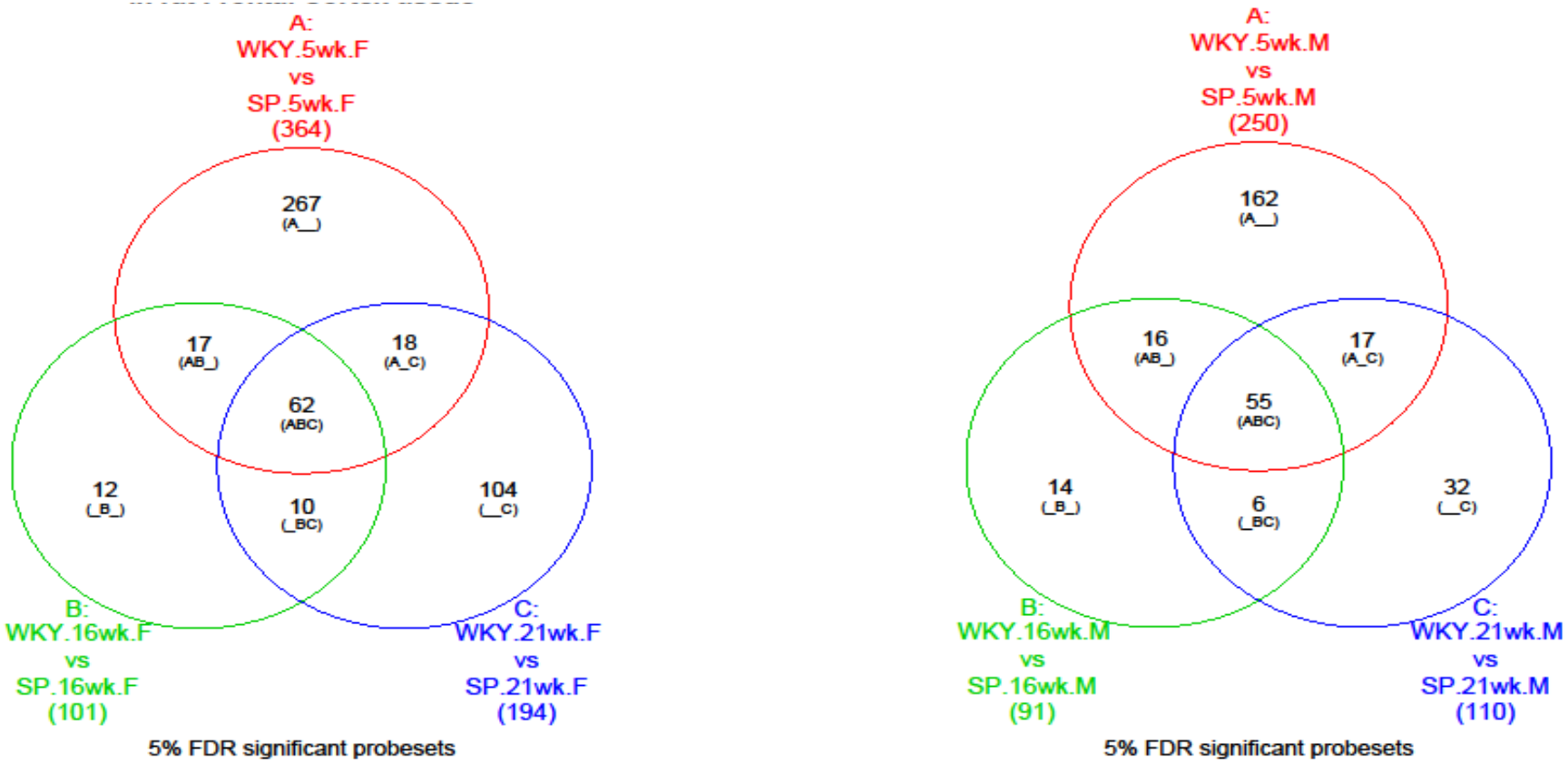

Figure 8.1. 3 way Venn diagrams of RP significant Illumina probes for WKY versus SHRSP at ages 5, 16 and 21 weeks.

A) Genes differentially expressed in frontal brain sections and **B**) Genes differentially expressed in mid coronal brain sections. The centre values (ABC) in both figures represent genes which were commonly significantly differentially expressed in SHRSP versus WKY at all ages. 49 genes were found to be commonly differentially expressed across all ages and in both brain sections.

After looking across all age groups we focused on 5 week old animals as we found there to be over double the number of significantly differentially expressed genes at this age common to both brain sections compared to 16 and 21 weeks (162 versus 71 at 16 weeks and 63 at 21 weeks). We also focused on this age group in order to identify changes in gene expression prior to the onset of hypertension. Here RP analysis showed that there were 162 genes differentially expressed between WKY and SHRSP at 5 weeks of age that were common to both brain sections (figure 8.2) (For RP data see Appendix N). These genes generated numerous significant interactions, in particular a cluster of early growth response genes involved in cell proliferation were significantly up regulated in SHRSP by approximately ~1.5 fold change (figure 8.3). A heatmap displaying genes of interest from this comparison can be seen in appendix P.

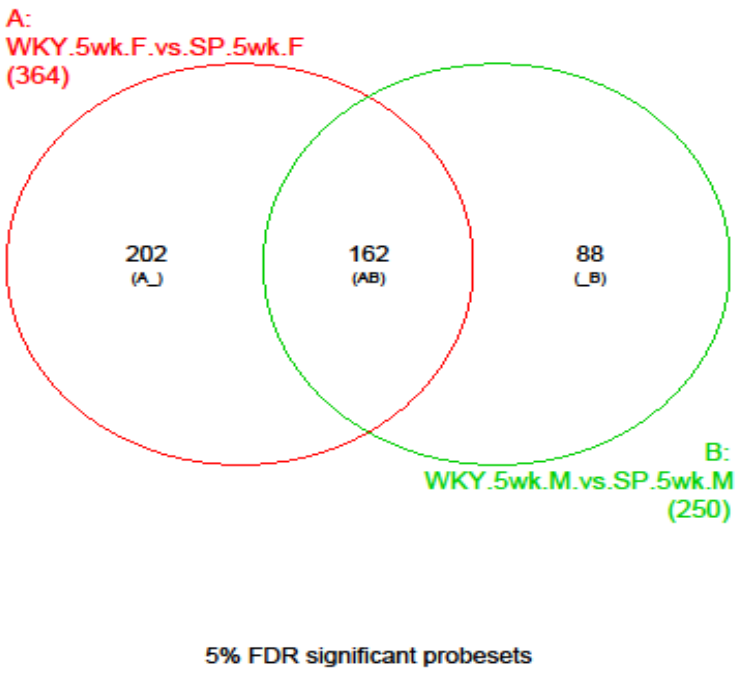

Figure 8.2. A 2 way Venn diagram representing the number of significantly differentially expressed genes in both sections of 5 week old SHRSP versus age matched WKY.

The red circle represents genes differentially expressed within the frontal section alone. The green circle represents genes differentially expressed within the mid coronal section alone. The intersection represents genes commonly differentially expressed in both brain sections.

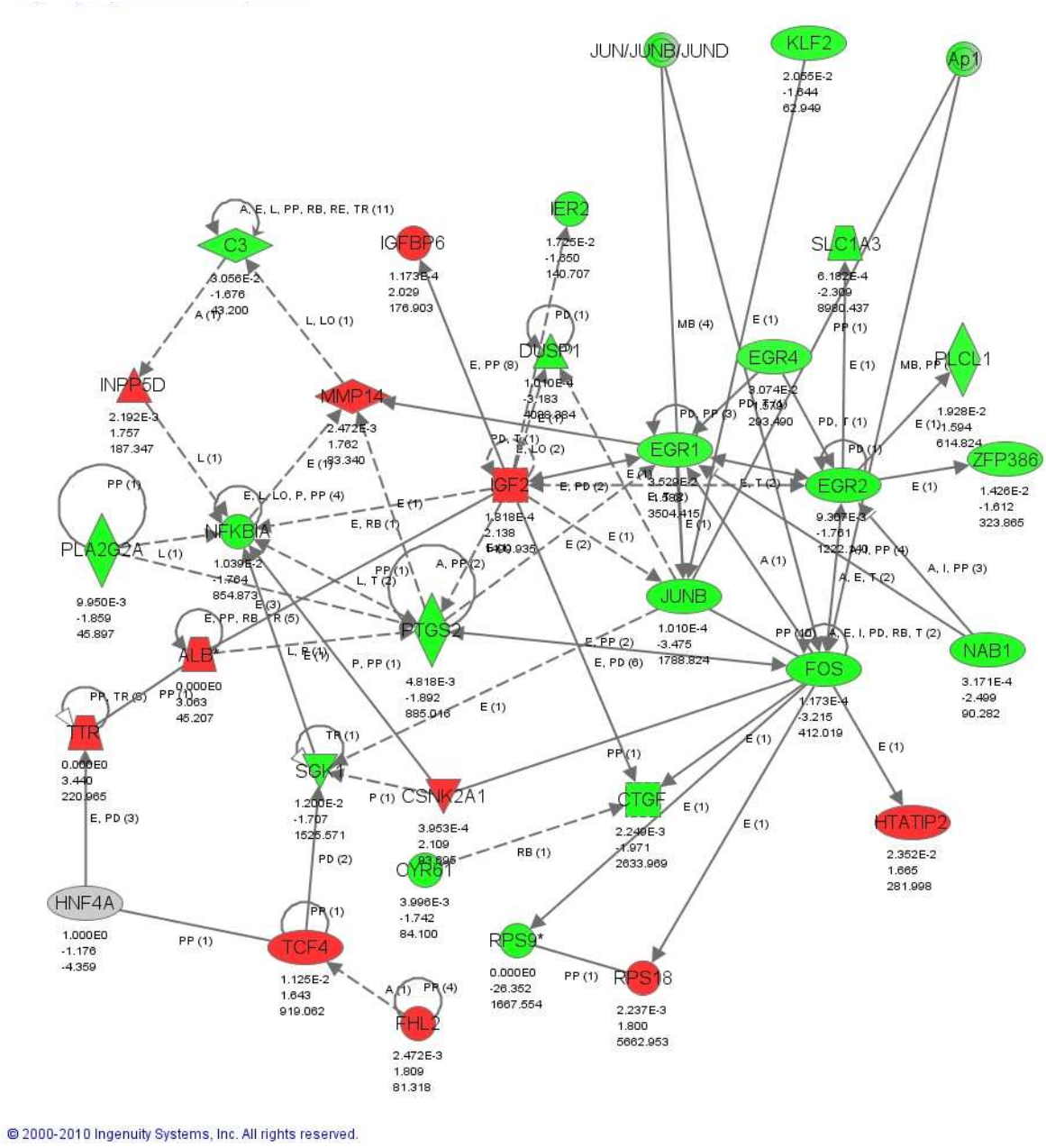

Figure 8.3. A network generated by IPA software representing interactions between differentially expressed genes at 5 weeks of age.

Genes highlighted red were down regulated in SHRSP. Genes highlighted in green are up regulated in SHRSP. Statistics quoted are from top to bottom – p value, fold change and intensity of fluorescence generated by the probe when scanned by the array reader. Solid lines indicate direct interactions. Dotted lines indicate indirect interactions. The purple box highlights a cluster of genes all up regulated in SHRSP which could signal a cell proliferation phenotype.

ii) The top 10 most up and down regulated genes in terms of fold change (all significant q<0.05) at ages 5, 16 and 21 weeks

When looking at the most up and down regulated genes we focused on the top 10 in each direction as we found a strong consistency across all age groups (see table 8.3). One gene of interest which appeared in the top 10 up-regulated genes was Guanylate cyclase soluble subunit alpha-3 (GUCY1a3) – the intracellular receptor for nitric oxide in vascular smooth muscle cells (Kloss et al. 2003). This gene was up regulated in SHRSP by a fold change of ~ 20 in both sections at all ages. Interestingly its corresponding heterodimer subunit - GUCY1b3 showed no changes in gene expression at any age or in any brain section.

G-protein receptor 98 (GPR98) a g protein coupled receptor with a role in neuropeptide signalling was consistently down-regulated in SHRSP by a fold change of ~3 in both sections. Albumin (ALB) was also down regulated in SHRSP by ~3-4 fold change in at least one brain section at all ages. Genes which were highly differentially expressed only at specific age groups included Arginine vasopressin (AVP) which was down regulated by a fold change of 4 in the mid coronal section of 5 week old SHRSP, guanine nucleotide binding protein, alpha inhibiting 1 (GNAI1) which was down by a 3 fold change in the frontal section of 16 week old SHRSP and Beta Actin (ACTB) which was down-regulated in the frontal section of 21 week old SHRSP.

iii) Analysis of over-represented biological pathways determined by IPA

IPA uses Fischers exact test to identify biological pathways (known as canonical pathways in IPA) which contain the largest proportion of significantly differentially expressed genes in given conditions. From this we found that the acute phase response signalling pathway (figure 8.4), consistently appeared within the top five over represented pathways in at least one brain section of the SHRSP at all ages. Tight junction signalling featured highly within the top five pathways affected in the frontal sections of 16 and 21 week old SHRSP.

Table 8.3. **The top 10 up and down regulated genes in SHRSP versus WKY in each brain section and for each age group.**

	FRONTAL SECTION				MID CORONAL SECTION			
Age	**Up regulated**	**Fold change**	**Down regulated**	**Fold change**	**Up regulated**	**Fold change**	**Down regulated**	**Fold change**
5	RGD1564649	x48.1	MRPL18	x27.7	RGD1564649	x59.7	MRPL18	x29.1
	RPS9	x26.4	HCG 2004593	x16.4	RPS9	x25.6	HCG 2004593	x13.2
	GUCY1A3	x21.8	RGD1565336	x5.3	GUCY1A3	x23.0	RGD1565336	x4.6
	FAM151B	x8.3	TTR	x3.4	FAM151B	x6.7	AVP	x4.3
	RGD1311103	x4.9	GPR98	x3.3	RGD1311103	x4.9	LOC100125697	x3.5
	ARC	x4.4	LOC100125697	x3.2	ZNF597	x4.2	GPR98	x3.2
	ZNF597	x4.1	ALB	x3.1	RNF149	x4.1	PXMP4	x3.1
	RNF149	x3.9	COLQ	x2.9	ARC	x3.9	CSNK2A1	x2.6
	JUNB	x3.5	PXMP4	x2.8	DUSP1	x3.1	VPS13C	x2.6
	ZNF317	x3.4	HLA-C	x2.6	RPS16	x3.0	C20ORF7	x2.5
16	RGD1564649	x46.7	MRPL18	x25.4	RGD1564649	x54.5	MRPL18	x31.4
	RPS9	x24.0	HCG 2004593	x12.3	RPS9	x27.2	HCG 2004593	x12.9
	GUCY1A3	x19.8	RGD1565336	x4.7	GUCY1A3	x14.5	RGD1565336	x5.4
	FAM151B	x8.8	LOC100125697	x4.0	FAM151B	x7.9	GPR98	x3.7
	RGD1311103	x5.4	PXMP4	x3.9	RGD1311103	x6.6	ALB	x3.7
	ZNF597	x4.0	ALB	x3.7	ZNF597	x4.0	LOC100125697	x3.6
	RPS16	x3.1	GPR98	x3.2	AVP	x3.8	VPS13C	x3.3
	RGD1566136	x2.8	GNAI1	x3.0	RGD1566136	x3.0	CSNK2A1	x3.3
	HLA-C	x2.8	C7ORF23	x2.9	RSP16	x2.9	PXMP4	x3.1
	ADPGK	x2.7	RGD1564078	x2.8	HLA-C	x2.8	C7ORF23	x3.0
21	RGD1564649	x46.9	MRPL18	x30.7	RGD1564649	x45.6	MRPL18	x25.9
	GUCY1A3	x20.3	HCG 2004593	x11.3	GUCY1A3	x20.7	HCG 2004593	x14.1
	RSP9	x18.8	TTR	x7.4	RSP9	x18.9	RGD1565336	x4.7
	FAM151B	x7.3	RGD1565336	x3.9	FAM151B	x7.3	GPR98	x4.3
	RGD1311103	x6.6	ALB	x3.8	RGD1311103	x4.8	OXT	x3.4
	ZNF597	x4.8	GPR98	x3.8	ZNF597	x4.5	ALB	x3.3
	RGD1566136	x3.7	PXMP4	x3.6	TTR	x3.7	MOBP	x3.2
	RNF149	x3.4	OPCML	x3.6	RNF149	x3.4	LOC100125697	x3.1
	RPS16	x3.2	ACTB	x3.4	ADPGK	x3.4	PXMP4	x3.0
	HLA-C	x2.8	LOC100125697	x3.2	HLA-C	x3.3	VPS13C	x2.8

All genes listed are significantly expressed FDR <0.05 is applied. RGD = Rat genome database. RPS9 = Ribosomal protein S9. GUCY1A3 = guanylate cyclase 1, soluble, alpha 3. FAM151B = family with sequence similarity 151, member B. ARC = activity-regulated cytoskeleton-associated protein. ZNF = Zinc finger protein. RNF149 = Ring finger protein 149. JUNB = jun B proto-oncogene. MRPL18 = mitochondrial ribosomal protein L18. HCG = Human chorionic gonadotrophin. AVP = Arginine vasopressin. LOC = Location. GPR = G-protein coupled receptor. ALB = Albumin. COLQ = collagen-like tail subunit of asymmetric acetylcholinesterase. PXMP4 = peroxisomal membrane protein 4. CSNK2A1 = casein kinase 2, alpha 1 polypeptide. VPS13C = vacuolar protein sorting 13 homolog C. C20ORF7 = Chromosome 20 open reading frame 7. HLA-C = Myosin heavy chain class 1 receptor C. ADPGK = ADP-dependent glucokinase. C7ORF23 = Chromosome 7 open reading frame 23. GNAI1 = guanine nucleotide binding protein, alpha inhibiting 1. OPCML = opioid binding protein/cell adhesion molecule-like. ACTB = Beta actin. OXT = Oxytocin. MOBP = myelin-associated oligodendrocyte basic protein.

8.3.2.2 Candidate gene approach

i) Identifying differentially expressed genes within biological pathways of interest.

As well as looking for pathways which contained an over representation of genes, we also looked for genes which were differentially expressed in the SHRSP within pathways considered from the literature to be relevant to cerebral small vessel disease e.g. Nitric Oxide signalling, Renin-angiotensin signalling.

Within nitric oxide signalling in the cardiovascular system, we found more significantly differentially expressed genes at the age of 5 weeks in the SHRSP compared to the older ages. GUCY1a3 was highly up-regulated in the SHRSP and this gene also occurs in the endothelin-1 vasoconstriction pathway within which GNAI1 (guanine nucleotide binding protein, alpha inhibiting 1) was down regulated with a fold change ranging from 1.6-3.0, in 5 and 16 week old SHRSP.

Several genes functionally associated with tight junctions had significantly altered expression, some across all ages (e.g. PPP2R1A, (protein phosphatase 2 regulatory subunit A, alpha isoform), up regulated by ~1.5 fold in SHRSP)) whilst others just in 5 week old SHRSP (e.g. FBJ murine osteosarcoma viral oncogene homolog (FOS) up regulated 3 fold). We found several acute phase response signalling pathway genes were significantly differentially expressed, in some cases across all ages and others just in 5 week old SHRSP. In this pathway, the most consistently down regulated genes were transcription factor 4 (TCF4) (~2.0 fold change) and albumin (ALB) (~3.5 fold change). Within the renin-angiotensin signalling pathway, two protein kinases (PRKAR2B and PRKCD) and cFOS were significantly differentially expressed in SHRSP however, these genes have multiple functions and are not pivotal to this pathway. In the atherosclerosis pathway, the only genes significantly differentially expressed were at 5 weeks of age in both brain sections; PLA2G2A (a member of the phospholipase A2 family) was up regulated in SHRSP (1.9 fold change), and COL3A1 was significantly down regulated in SHRSP (1.7 fold change). Due to its role in vascular wall structure, humans deficient in Col3a1 protein exhibit increased arterial fragility and vascular rupture (Pope et al. 1996).

Figure 8.4. **Biological pathways in IPA containing an over representation of significantly differentially expressed genes in the frontal section of 5, 16 and 21 week old SHRSP versus WKY.**

The blue bar represents how significant the uploaded data set is to the pathway (log p value) and the orange line represents the number of genes differentially expressed as a proportion of the total genes within that pathway.

ii) Gene expression versus protein immunoreactivity assessed in chapter 7 (Bailey et al. 2011b)

We compared the mRNA expression analysis directly to proteins assessed previously in the same animals using immunohistochemistry and found the following results. Glial fibrillary acidic protein (GFAP) mRNA expression was significantly down-regulated in the frontal section of 5 week old SHRSP versus WKY (1.5 fold change) which contradicted the significant increase in GFAP immunoreactivity we have previously described. Meanwhile in 21 week old SHRSP, we found myelin basic protein (MBP) to be significantly down-regulated in the frontal section of SHRSP versus WKY (2.6 fold change) and this agreed with our immunohistochemistry data (chapter 7 figure 7.11 table 7.4). We saw no significant differences in the mRNA expression of Claudin-5, Collagen I, Collagen IV, SMA, MMP9 or Iba-1 between the strains despite finding significant reductions in the immunoreactivity of Claudin-5 at all ages, Collagen I at 5 and 16 weeks and increases in the immunoreactivity of SMA and Iba-1 at 16 weeks and beyond (chapter 7). We did however find that MMP14 in the microarray analysis was significantly down-regulated in SHRSP in the frontal section of 5 week old animals and this gene has direct influences upon Claudins, Collagens and other matrix metalloproteinases such as MMP9.

8.3.3 qRT-PCR of candidate genes

From the results above we chose the following genes for quantitative validation with qRT-PCR; GUCY1a3, GUCY1b3, MMP14, GFAP, ALB, MBP, GPR98 and AVP (see table 8.2 for details of Taqman probes and table 8.4 for reasons as to why these particular genes were chosen). For full statistical data see table 8.5.

Table 8.4. **Genes from the microarray analysis which were chosen for quantitative validation with qRT-PCR and the reasons they were chosen as genes of interest.**

Gene	Reason chosen for qRT-PCR
GUCY1a3	Due to its consistent up regulation of over x15 fold change at all ages in both sections.
GUCY1b3	Due to its coexistence with GUCY1a3 as a heterodimer.
MMP14	Due to its direct interactions with other genes of interest and down regulation at 5 weeks of age. At 5 weeks in the frontal section there was significantly less MMP14 gene expression in the SHRSP rats.
GFAP	To validate findings from a previous immunohistochemistry study (chapter 7) and significant microarray data at 5 weeks.
ALB	Due to consistent findings of down regulation at all ages and in both sections
MBP	Due to significant microarray findings at 21 weeks and significant differences in protein expression at 21 weeks in a previous immunohistochemistry study (chapter 7).
GPR98	Due to significant down regulation across all ages.
AVP	Due to significant finding at 5 weeks and relevant to vasoactive mechanisms.

ALB = Albumin, AVP = Arginine Vasopressin, GFAP = Glial Fibrillary Acidic Protein, GPR98 = G-Protein Coupled Receptor 98, GUCY1a3 = Guanylate Cyclase 1 alpha 3 subunit, GUCY1b3 = Guanylate Cyclase 1 beta 3 subunit, MMP14 = Matrix Metallopeptidase 14 and SLC24a2 = Sodium/Potassium/Calcium exchanger 2.

GFAP (protein) was increased in the frontal section of 5 week old SHRSP on immunohistochemistry compared with WKY (chapter 7). However, the microarray data showed GFAP mRNA expression to be significantly down-regulated in SHRSP in the same brain section at the same age. qRT-PCR replicated the microarray data by showing that SHRSP had a 2-fold down-regulation in GFAP mRNA expression compared to WKY rats ($p=0.01$) (figure 8.5a).

MMP14 in the microarray analysis was significantly down-regulated in SHRSP in the frontal section of 5 week old animals. qRT-PCR showed a 5 fold decrease in MMP14 mRNA expression in the frontal section of SHRSP versus WKY ($p<0.01$) see figure 8.5b.

AVP, according to the mRNA analysis, was significantly down-regulated in the mid coronal section of 5 week old SHRSP. qRT-PCR showed a similar result, where only a quarter of the gene expression was seen in SHRSP in this section ($p<0.001$) versus WKY (figure 8.5c)

GUCY1a3, despite being consistently up-regulated by >15 fold change in SHRSP at all ages and in both brain sections on the microarray, showed no significant differences in mRNA expression at any age or in any brain section using qRT-PCR. Similarly qRT-PCR did not validate the findings of ALB, MBP or GPR98 by showing no significant difference in gene expression between WKY and SHRSP at any age. qRT-PCR did however validate the microarray findings of MMP14, GFAP, AVP and GUCY1b3 (no significant difference).

Table 8.5. Data obtained from qRT-PCR analysis for each gene of interest.

Probe/Gene		RQ values ± standard error					
Age & Section		5F	5M	16F	16M	21F	21M
GUCY1a3	WKY	1.47 ± 0.26	1.00 ± 0.18	0.72 ± 0.03	1.00 ± 0.39	**1.68** ± 0.22	1.00 ± 0.43
	SHRSP	1.00 ± 0.50	0.33 ± 0.78	1.00 ± 0.34	0.84 ± 0.29	**1.00** ± 0.19	1.48 ± 0.30
	p value	NS	NS	NS	NS	**0.05**	NS
GUCY1b3	WKY	1.49 ± 0.98	1.00 ± 0.21	1.17 ± 0.16	1.00 ± 1.03	1.43 ± 0.23	1.00 ± 0.24
	SHRSP	1.00 ± 0.48	1.26 ± 0.11	1.00 ± 0.45	1.45 ± 0.71	1.00 ± 0.32	1.24 ± 0.44
	p value	NS	NS	NS	NS	NS	NS
MMP14	WKY	**5.45 ± 0.45**	**1.00 ± 0.26**	0.27 ± 0.12	1.00 ± 0.62	2.22 ± 1.38	1.00 ± 0.42
	SHRSP	**1.00 ± 0.31**	**2.22 ± 0.48**	1.00 ± 0.54	1.14 ± 1.05	1.00 ± 0.60	1.57 ± 0.20
	p value	**<0.01**	**<0.05**	NS	NS	NS	NS
GFAP	WKY	**2.33 ± 0.47**	1.00 ± 0.24	0.87 ± 0.24	1.00 ± 0.36	1.59 ± 0.45	1.00 ± 0.13
	SHRSP	**1.00 ± 0.20**	0.69 ± 0.09	1.00 ± 0.42	1.15 ± 0.46	1.00 ± 0.25	0.98 ± 0.23
	p value	**<0.05**	NS	NS	NS	NS	NS
ALB	WKY	**4.39 ± 0.07**	**1.00 ± 0.64**	0.30 ± 0.14	1.00 ± 1.06	2.22. ± 0.21	1.00 ± 1.16
	SHRSP	**1.00 ± 1.23**	**-23.2 ± 20.35**	1.00 ± 0.87	1.04 ± 0.68	1.00 ± 1.12	1.56 ± 1.16
	p value	**<0.05**	**<0.05**	NS	NS	NS	NS
AVP	WKY	1.49 ± 0.76	**1.00 ± 0.26**	N/A			
	SHRSP	1.00 ± 0.43	**0.26 + 0.08**				
	p value	NS	**<0.01**				
GPR98	WKY	N/A		0.48 ± 0.33	1.00 ± 1.00	N/A	
	SHRSP			1.00 ± 1.28	1.26 ± 1.12		
	p value			NS	NS		
MBP	WKY	N/A				1.68 ± 1.13	1.00 ± 0.54
	SHRSP					1.00 ± 0.68	1.03 ± 0.18
	p value					NS	NS

Data represents the relative quantity (RQ) values (± the standard error of the mean) between the gene of interest and the house keeper gene GAPDH for WKY and SHRSP at ages 5-21 weeks and from both frontal (F) and mid coronal (M) brain sections. Green highlights significant results which agreed with mRNA expression data. Red indicates significant results which did not agree with mRNA expression data. Some genes were only tested at ages of interest. N/A corresponds to ages where gene expression was not validated with qRT-PCR.

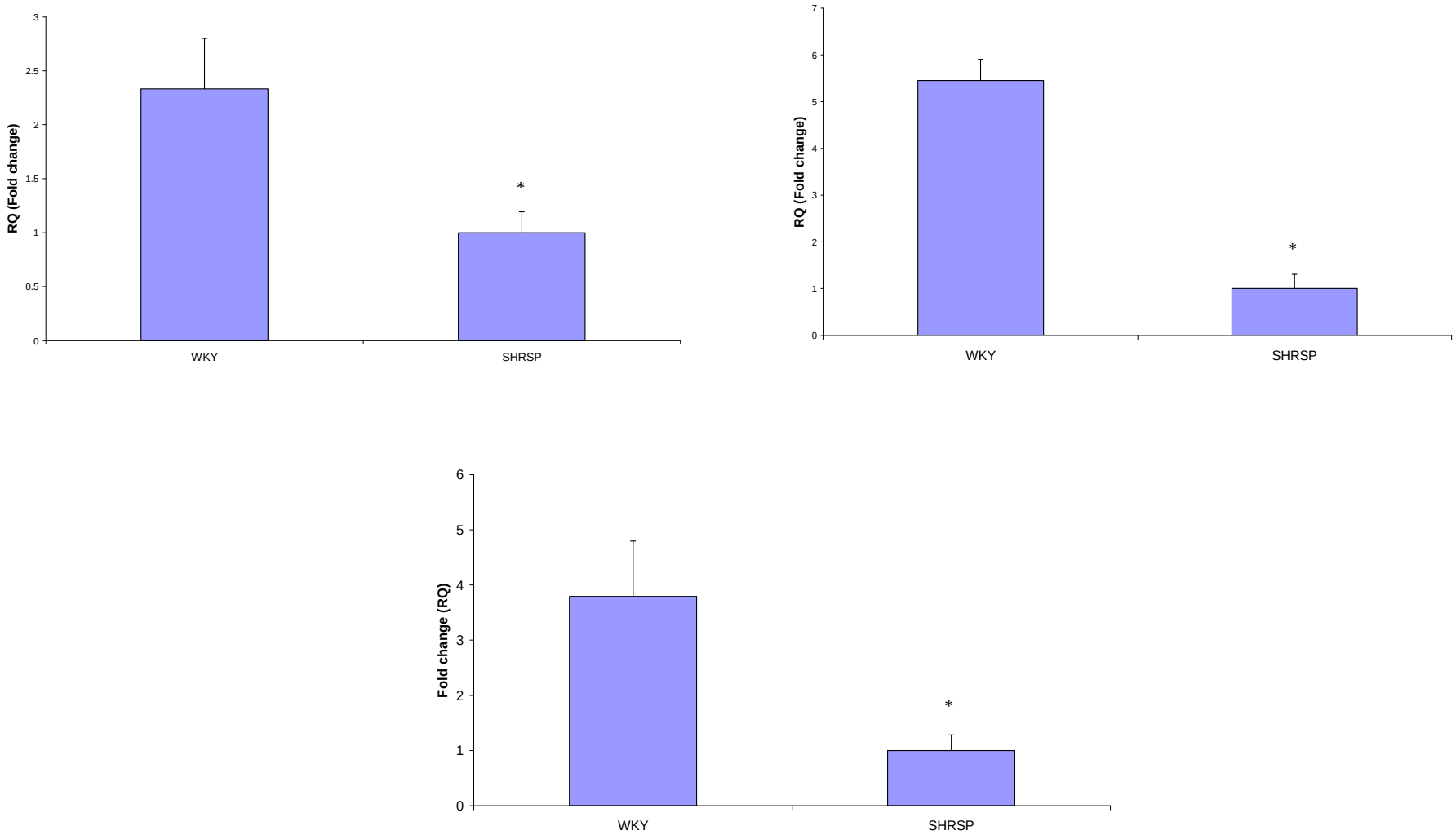

Figure 8.5. Validation of significant changes in gene expression of A) GFAP, B) MMP14 and C) AVP in 5 week old rats.

Figures A & B display data from analysis of the frontal brain section only. Figure C displays data from analysis of the mid coronal section only. Bars represent the difference in fold change between WKY and SHRSP. Error bars represent the standard error of the mean. Each bar represents n=4 rats. * = significant at $p<0.05$. ** significant at $p<0.01$.

8.3.4 DNA sequencing of GUCY1a3

In order to determine why the microarray findings relating to GUCY1a3 did not correlate with qRT-PCR we performed end point PCR and DNA sequencing using primers designed to capture the area of the gene covered by the GUCY1a3 Illumina microarray probe. Using PCR we found that the signal from both WKY DNA and SHRSP DNA was the same meaning that no large scale insertion or deletions were present in the area of the Illumina probe in the SHRSP (see Appendix R for an image of the electrophoresis gel). Knowing this we then sequenced the gene and found a single nucleotide polymorphism in the 3'UTR (untranslated region) of the GUCY1a3 gene at position 4379. This is a known SNP in this strain (RS13457820 – www.ensembl.org). In Norwegian Brown rats and in WKY a cytosine (C) resides at this position whereas in the SHRSP a thymine (T) is present (see figure 8.6).

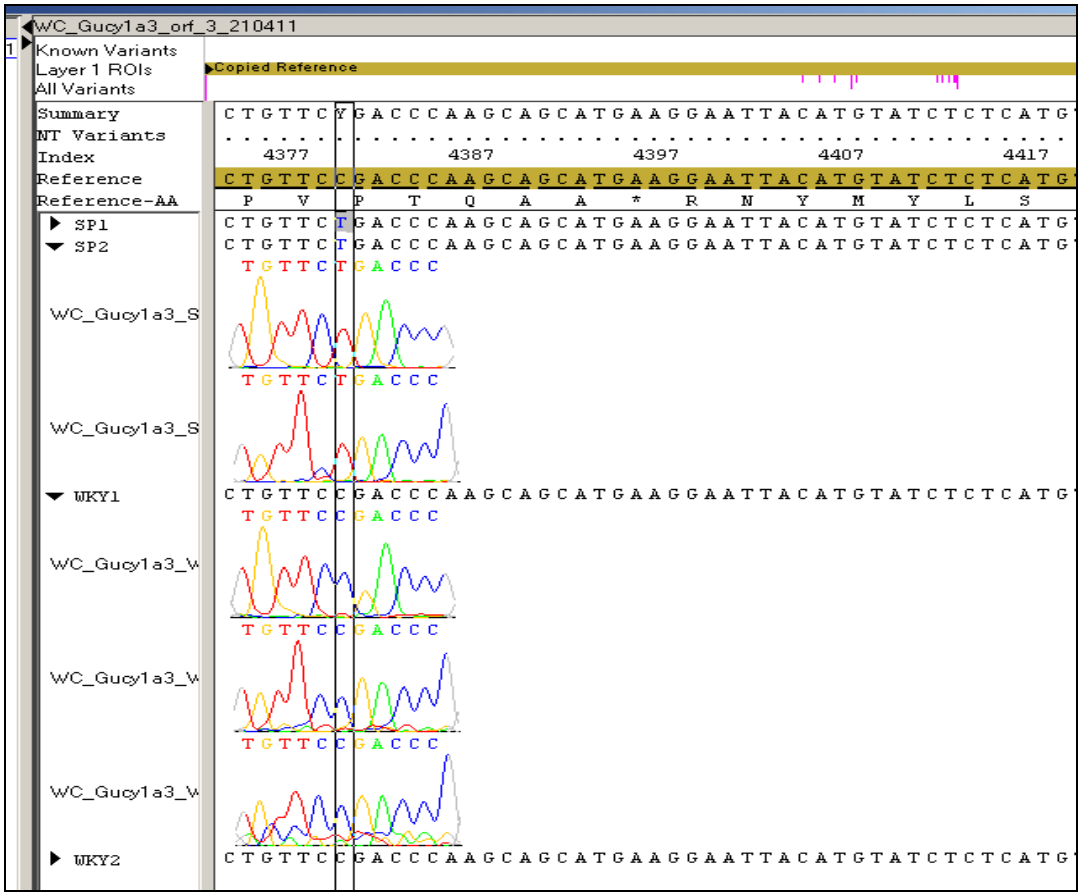

Figure 8.6. Identification of a SNP found in SHRSP within the 3'UTR of the GUCY1a3 gene.

Image taken from Applied Biosystems SeqScape software version 2.1 and shows sequences from WKY and SHRSP (n=2 for each strain). The black box highlights position 4379 where the C in WKY is replaced by a T in SHRSP.

8.3.5 B) Salt-loaded animals (+NaCl) versus age matched animals fed standard rat chow

8.3.5.1 The genome wide approach

i) Analysis of Venn diagrams

To assess the influence of NaCl we generated Venn diagrams to identify the effect on salt across 3 comparisons, WKY+NaCl versus WKY, SHRSP+NaCl versus SHRSP and WKY+NaCl versus SHRSP+NaCl. RP data used to generate Venn diagrams can be accessed in Appendix O

WKY+NaCl versus WKY (see figure 8.7).

As there were few genes (n=9) which were differentially expressed in both brain sections of WKY+NaCl versus WKY we focussed on the frontal section alone. In this section, RP analysis idenified 31 genes which were differentially expressed and within these genes we found a small network of 11 genes which were directly functionally connected (according to IPA's Knowledge Base), centred around amyloid precursor protein (APP). Most of the genes in this network were down-regulated in WKY+NaCl (figure1a). Interestingly when the RP analysis of SHRSP+NaCl versus SHRSP was overlaid onto this network, all of the genes surrounding APP (except albumin and APP itself) were once again found to be differentially expressed but this time they were all significantly up-regulated rather than down-regulated in the salt loaded animal suggesting a different response to salt loading in the two strains (figure 8.8b).

SHRSP+NaCl versus SHRSP

We found no significantly differentially expressed genes which were common to both brain sections in SHRSP+NaCl versus SHRSP. Therefore, as with WKY+NaCl versus WKY we focussed on genes significantly differentially expressed within the frontal section where there were over 10 times as many expressed versus the mid coronal section 83 versus 7) Within these 83 genes, we found a small network of 13 genes (figure 8.9) centered around beta actin (ACTB) including genes functionally related to maintaining the structural integrity of the vascular cytoskeleton (e.g. ACTB, Destrin (DSTN) and beta-catenin (CTNNB1)).

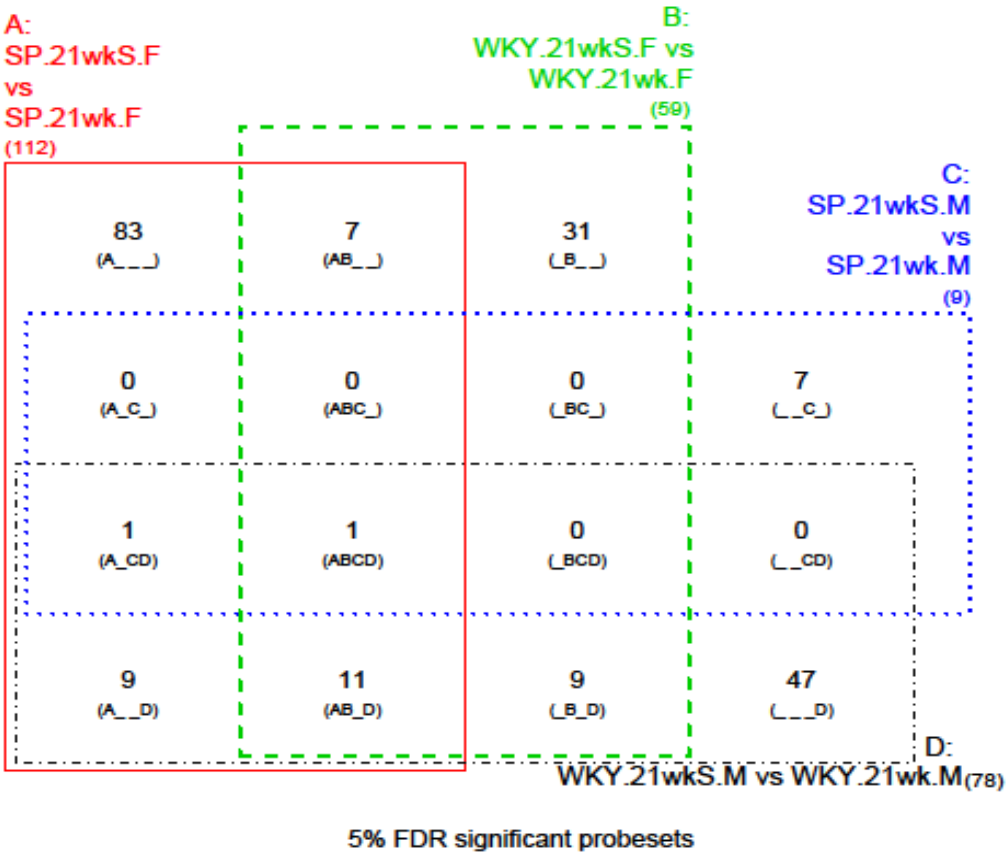

Figure 8.7. A four way Venn diagram from rank products analysis representing genes which were significantly differentially expressed in all comparisons of all WKY and SHRSP (+/-NaCl) in both frontal (F) and mid coronal (M) brain sections.

The violet circle represents the number of genes differentially expressed in the frontal section of WKY+NaCl versus WKY. These genes were used to generate the network seen in figure 8.9. The orange circle represents the number of differentially expressed genes in both brain sections in salt loaded SHRSP versus non salt loaded SHRSP (in this case 0). The green circle represents genes which were differentially expressed between salt loaded SHRSP versus non salt loaded SHRSP in the frontal section only. These genes were used to generate the network seen in figure 8.10. This diagram also shows that very few genes were significantly differentially expressed between WKY+NaCl and SHRSP+NaCl.

WKY+NaCl versus SHRSP+NaCl

We found only 1 gene (Mitochondrial ribosomal protein L18 - MRPL18) which was differentially expressed in WKY+NaCl versus SHRSP+NaCl which was common to both brain sections. We found only 7 which were differentially expressed in the frontal section alone (Albumin (ALB), (Peroxisomal membrane protein 4 (PXMP4), Family with sequence similarity 151 B (FAM151B), Zinc finger protein 597 (ZNF597), Ribosomal protein S9 (RPS9), Ribosomal protein L17 pseudogene 39 (RPL17P39), Transthyretin (TTR) and none were differentially expressed in the mid coronal section. Incidently no networks of interest could be generated from this data in IPA.

Heatmaps displaying the genes of interest from all 3 salt comparisons can be seen in appendix Q.

ii) The top 10 up and down-regulated genes in terms of fold change in salt loaded animals versus non salt loaded animals of the same strain and between strains (table 8.6).

In stark contrast to the previous data on age-related changes, the addition of NaCl produced very inconsistent and often small (albeit significant) fold changes in both WKY+NaCl versus WKY and SHRSP+NaCl versus SHRSP.

WKY+NaCl versus WKY

The only gene to appear in the 10 most highly up-regulated genes of both brain sections in this comparison was Albumin (up 2 fold). A cluster of genes involved in the acute phase response pathway and closely associated with albumin were up-regulated in the frontal section: Alpha-1-microglobulin/bikunin precursor (AMBP), Apolipoprotein H (APOH) and Alpha-2-HS-glycoprotein (AHSG) were all up-regulated by 2.2-2.5 fold.

The most down-regulated gene in salt loaded versus non-salt loaded WKY was MBP in the frontal section (2.6 fold). Only three genes were highly down-regulated in both sections. Beta actin (ACTB) was down 2.3 fold, whilst N-ethylmaleimide-sensitive factor (NSF) and M2-pyruvate kinase (PKM2) were down 2 fold.

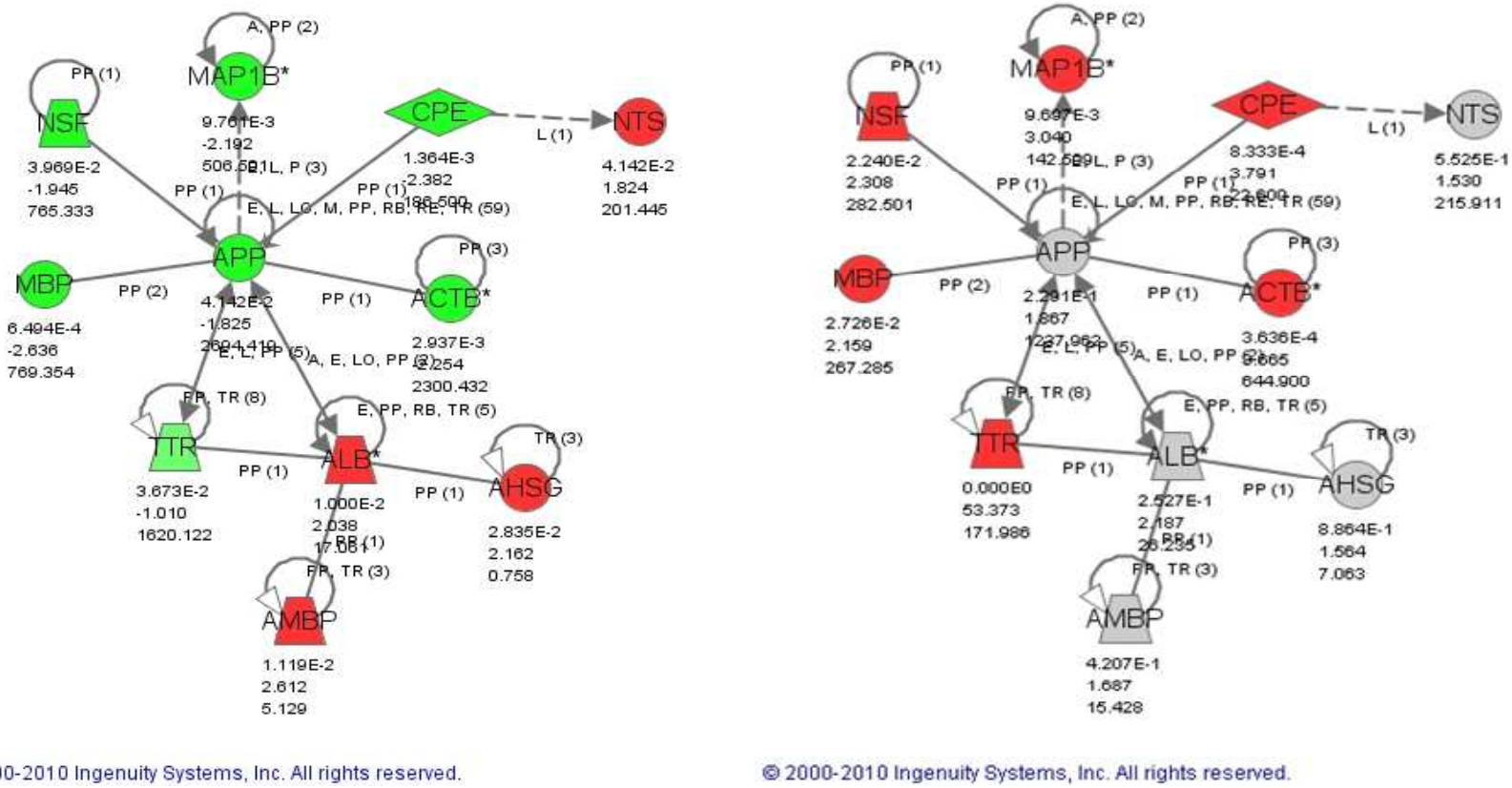

Figure 8.8. A) A network generated by IPA software representing interactions between differentially expressed genes within the frontal sections of age matched WKY versus salt loaded WKY.

All genes highlighted in green are down regulated in salt loaded WKY. Genes highlighted red are up regulated in salt loaded WKY. Statistics quoted are from top to bottom – p value, fold change and signal intensity. Solid lines indicate direct interactions. Dotted lines indicate indirect interactions. B) The same network with salt loaded SHRSP versus non salt loaded SHRSP data over laid. In this network genes highlighted in red indicate genes up regulated in salt loaded SHRSP when compared to non salt loaded SHRSP

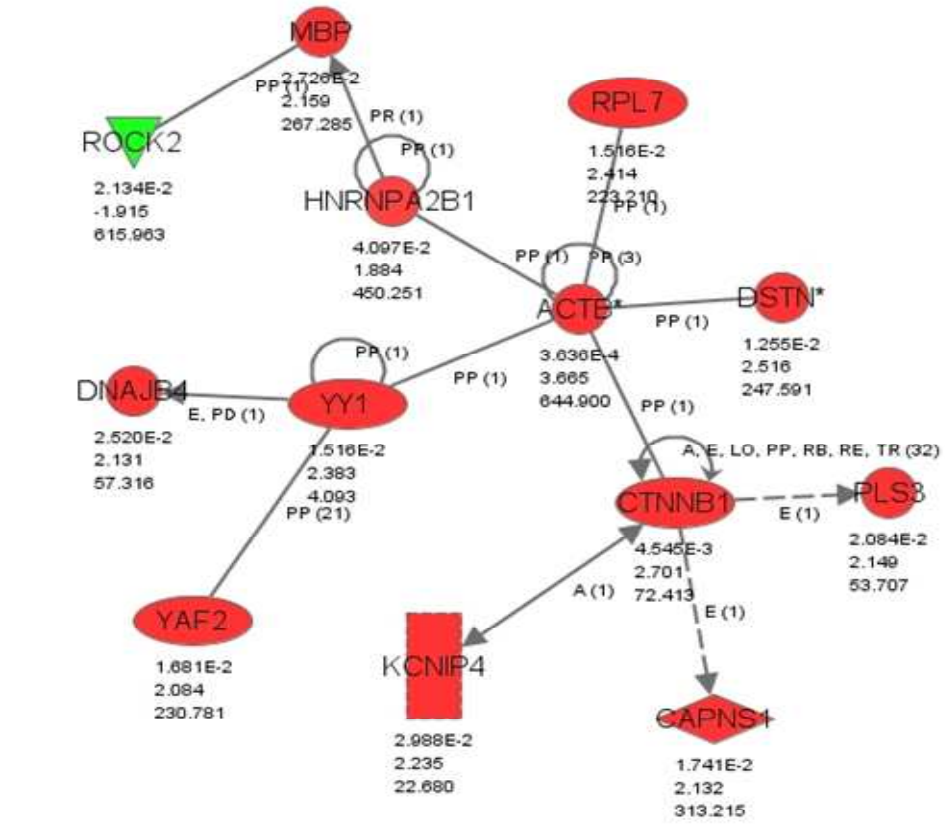

Figure 8.9. A network generated by IPA software representing interactions between differentially expressed genes within the frontal sections of age matched SHRSP versus salt loaded SHRSP.

All genes highlighted in green are down regulated in salt loaded SHRSP. Genes highlighted red are up regulated in salt loaded SHRSP. Statistics quoted are from top to bottom – p value, fold change and signal intensity. Solid lines indicate direct interactions. Dotted lines indicate indirect interactions.

SHRSP+NaCl versus SHRSP

Genes highly up-regulated in the frontal section included, carboxypeptidase E (CPE) (3.8 fold change) and ACTB (3.7 fold change). In the mid coronal section two solute carriers (SLC17a6 - fold change of 2.2 and SLC24a2 - fold change of 2.0) were up-regulated in the mid coronal section. Albumin was also within the top 10 up-regulated genes with a fold change of 1.7 in the mid coronal section.

In the frontal section there were several genes that differed by approximately a 2 fold change, including VOPP1 (vesicular, overexpressed in cancer, prosurvival protein 1) with a fold change of 2.7. CYR61 – an angiogenic inducer was down-regulated by a fold change of 1.9. Only 8 genes in the mid coronal section were significantly down-regulated in the salt loaded versus non-salt loaded SHRSP, of which Transthyretin (TTR) came top with a fold change of 3.1 (table 8.4). Von Willebrand factor (VWF) and vascular growth factor (VGF) were down-regulated in the mid coronal section (down 2.3 and 1.9 fold respectively) in SHRSP+NaCl.

WKY+NaCl versus SHRSP+NaCl

The most highly differentially expressed genes between salt loaded WKY and salt loaded SHRSP matched previous observations from 5 and 16 week old non-salt loaded WKY and SHRSP (unpublished observations) (see table 8.3) indicating the effect of strain on gene expression was more substantial than the effect of salt (see table 8.6).

iii) Analysis of over-represented biological pathways determined by IPA

Using RP data, we found the acute phase response signalling pathway contained the most differentially expressed genes in all salt versus no salt comparisons consistently appearing within the top five pathways in IPA (figure 8.10). Salt-loading in both rat strains was associated with changes within the tight junction signalling pathway of frontal brain sections (figure 8.4). Pathways pertaining to oxidative stress and leukocyte extravasation also contained a high proportion of differentially expressed genes in both salt-loaded versus non salt-loaded strains particularly in the frontal section (figure 8.10).

8.3.5.2 Candidate gene approach

i) Identifying differentially expressed genes within biological pathways of interest.

As with the age-related data above we looked for genes which were significantly differentially expressed within biological pathways of interest available on IPA.

In the acute phase response pathway ALB was consistently down-regulated across all salt comparisons, although in WKY+NaCl in the frontal section a group of closely associated genes, AMBP (alpha-1-microglobulin/bikunin precursor), AHSG (alpha-2-HS-glycoprotein) and APOH (Apolipoprotein H) were down-regulated by approximately 2 fold change (see figure 8.8).

In the frontal section of salt loaded versus non salt loaded SHRSP we found Claudin-11 to be down-regulated 2.3 fold within the tight junction signalling pathway. However, we also found Claudin-11 to be up-regulated in salt loaded SHRSP when compared to salt loaded WKY (1.8 fold change) again indicating a difference in response to salt between the strains.

Table 8.6. The top 10 up and down regulated genes within and between strain salt comparisons

	FRONTAL SECTION				MID CORONAL SECTION			
Salt	**Up regulated**	**Fold change**	**Down regulated**	**Fold change**	**Up regulated**	**Fold change**	**Down regulated**	**Fold change**
WKY+ NaCl versus WKY	LOC100129193	x16.3	MBP	x2.6	LOC100129193	x4.2	PRKCD	x2.5
	AMBP	x2.6	CPE	x2.4	TMEM27	x2.6	ACTB	x2.3
	APOH	x2.2	ACTB	x2.3	SLCO1A5	x2.3	WSF1	x2.3
	ALDOB	x2.2	TSPAN7	x2.2	GPM6A	x2.2	VWF	x2.3
	AHSG	x2.2	MAP1B	x2.1	MCTP1	x2.1	NSF	x2.2
	GC	x2.0	PPP3CB	x2.0	TAC1	x2.1	PKM2	x2.1
	ALB	x2.0	TPI1	x1.9	GPR88	x2.0	SLC24A2	x2.1
	GPM6A	x1.9	NSF	x1.9	TTR	x2.0	OXT	x2.1
	TCEB1	x1.9	PKM2	x1.9	LRRC7	x1.9	VGF	x1.9
	NTS	x1.8	SETD3	x1.9	ALB	x1.9	PRKCG	x1.9
SHRSP+NaCl versus SHRSP	TTR	x53.4	VOPP1	x2.7	LOC100129193	x3.3	TTR	x3.1
	SOSTDC1	x10	RPS13	x2.1	SLC17A6	x2.2	SOSTDC1	x2.8
	SLCO1A5	x5.2	TPI1	x2.1	SLC24A2	x2.0	ADORA2A	x2.4
	OTX2	x3.9	SEC61G	x1.9	HBB	x1.9	AQP1	x2.3
	CPE	x3.8	ROCK2	x1.9	OPCML	x1.9	SCN4B	x2.1
	ACTB	x3.7	CYR61	x1.9	SEPT7	x1.9	SLC32A1	x2.0
	F5	x3.6	HBXIP	x1.8	AMBP	x1.8	RASD2	x2.0
	GDI1	x3.4	MYEF2	x1.8	CABP7	x1.7	DLX5	x1.9
	SNURF	x3.4	GSK3B	x1.8	ALB	x1.7	No further	-
	TSPAN7	x3.3	IL11	x1.7	ANXA1	x1.7	significant	-
WKY+NaCl versus SHRSP+NaCl	RGD1564649	x46.1	MRPL18	x39.4	RGD1564649	x43.9	MRPL18	x41.7
	RSP9	x19.5	HCG 2004593	x18.3	RSP9	x16.8	HCG 2004593	x16.1
	GUCY1A3	x15.3	LOC100125697	x5.3	GUCY1A3	x14.5	RGD1565336	x5.2
	TTR	x7.2	PXMP4	x4.7	FAM151B	x8.0	LOC100125697	x4.8
	FAM151B	x5.8	RGD1565336	x4.5	RGD1311103	x6.1	GPR18	x4.6
	RGD1311103	x5.6	GPR18	x4.1	ZNF597	x4.7	PXMP4	x3.6
	SOSTDC1	x5.0	ALB	x4.0	AVP	x3.5	ALB	x3.6
	ZNF597	x4.4	C20ORF7	x3.6	PMCH	x3.3	HLA-C	x3.3
	OXT	x3.2	CSNK2A1	x3.5	SIPA1L2	x2.9	VPS13C	x3.2
	RGD1566136	x3.0	RGD1564078	x3.5	RGD1566136	x2.8	CSNK2A1	x3.0

Results are for each brain section and age matched animals. N=4 for all groups. All genes listed are significantly expressed when a FDR of q<0.05 is applied. For gene names PTO.

LOC = Location. AMBP = alpha-1-microglobulin/bikunin precursor. APOH = Apolipoprotein H. ALDOB = aldolase B, fructose-bisphosphate. AHSG = alpha-2-HS-glycoprotein. GC = group specific component. GPM6A = glycoprotein m6a. TCEB1 = transcription elongation factor B (SIII), polypeptide 1. NTS = neurotensin. CPE = carboxypeptidase E. ACTB = Beta Actin. TSPAN7 = tetraspanin 7. MAP1B = microtubule-associated protein 1B. PPP3CB = protein phosphatase 3, catalytic subunit, beta isoform. TPI1 = triosephosphate isomerase 1. NSF = N-ethylmaleimide-sensitive factor. PKM2 = pyruvate kinase, muscle. SETD3 = SET domain containing 3. TMEM27 = transmembrane protein 27. SLCO1A5 = solute carrier organic anion transporter family, member 1a5. MCTP1 = multiple C2 domains, transmembrane 1. TAC1 = tachykinin 1. GPR88 = G Protein coupled receptor 88. TTR = Transthyretin. LRRC7 = leucine rich repeat containing 7. SLC17A6 = solute carrier family 17 member 6. SLC24A2 = solute carrier family 24 member 2. OPCML = opioid binding protein/cell adhesion molecule-like. VGF = Vascular growth factor. PRKCG = protein kinase C, gamma. SOSTDC1 = sclerostin domain containing 1. OTX2 = orthodenticle homeobox 2. F5 = coagulation factor V. GDI1 = GDP dissociation inhibitor 1. SNURF = SNRPN upstream reading frame. VOPP1 = vesicular, over expressed in cancer, prosurvival protein 1. SEC61G = SEC61, gamma subunit. ROCK2 = Rho-associated coiled-coil containing protein kinase 2. CYR61 = cysteine-rich, angiogenic inducer, 61. HBXIP = hepatitis B virus x interacting protein. MYEF2 = myelin expression factor 2. GSK3B = glycogen synthase kinase 3 beta. IL11 = Interleukin 11. HBB = hemoglobin, beta. SEPT7 = septin 7. CABP7 = calcium binding protein 7. ANXA1 = annexin A1. ADORA2A = adenosine A2a receptor. AQP1 = aquaporin 1. SCN4B = sodium channel, voltage-gated, type IV, beta. SLC32A1 – solute carrier family 32 member 1. RASD2 = RASD family, member 2. DLX5 = distal-less homeobox 5. PMCH = pro-melanin-concentrating hormone. SIPA1L2 = signal-induced proliferation-associated 1 like 2. RGD = Rat genome database. RSP9 = Ribosomal protein 9. GUCY1a3 = Guanylate cyclase alpha subunit 3. FAM151B = family with sequence similarity 151, member B. ZNF597 = Zinc finger protein 597. OXT = Oxytocin. MRPL18 = Mitochondrial ribosomal protein L18.PXPM4 = peroxisomal membrane protein 4. GPR18 = G protein coupled receptor 18. CSNK2A1 = casein kinase 2, alpha 1 polypeptide. AVP = Arginine vasopressin. HLA-C = major histocompatibility complex, class C. VPS13C = vacuolar protein sorting 13 homologue.

Figure 8.10. The top 5 biological pathways in IPA containing an over representation of significantly differentially expressed genes in the frontal sections of A) WKY+NaCl versus WKY, B) WKY+NaCl versus SHRSP+NaCl and C) SHRSP+NaCl versus SHRSP.

The blue bar represents how significant the uploaded data set is to the pathway (log p value) and the orange line represents the number of genes differentially expressed as a proportion of the total genes within that pathway.

ii) A comparison of gene expression versus protein expression, of biomarkers assessed in the same animals using immunohistochemistry (chapter 7).

When comparing gene expression of proteins we assessed in the same animals using immunohistochemistry, we found only MBP was differentially expressed. In WKY versus salt loaded WKY, MBP was down regulated in the frontal section (2.6 fold change). This was also consistent between SHRSP and salt loaded SHRSP with a 2.2 fold down regulation in the frontal section. MBP was not differentially expressed between salt loaded WKY and salt loaded SHRSP.

8.3.6 qRT-PCR of candidate genes

From the microarray results above, we chose the following genes for quantitative validation with qRT-PCR: MBP, ACTB and SLC24a2. For all statistical data see table 8.7.

MBP - In salt loaded WKY versus non salt loaded WKY, the microarray showed that MBP was significantly down regulated in the frontal section in the salt loaded animals (2.6 fold change). This was also consistent in salt loaded SHRSP versus non salt loaded SHRSP (salt loaded SHRSP had ~2.2 fold less MBP in the frontal section versus non-salt loaded SHRSP. No significant differences in gene expression were detected with qRT-PCR.

ACTB – The microarray showed ACTB to be significantly down regulated in WKY+NaCl versus WKY in both brain sections (fold change 2.3). The microarray data also showed a significant up regulation of ACTB in the frontal section of SHRSP+NaCl versus SHRSP (fold change 3.7). These results indicated a possible salt specific effect. qRT-PCR however, did not validate this finding with no significant differences in gene expression found between any of the salt / no salt comparisons.

SLC24a2 – was chosen for validation because, like ACTB, the microarray data showed two significant results. Firstly we found SLC24a2 to be significantly down regulated in both sections of WKY+NaCl versus WKY (~2 fold change). Secondly we found SLC24a2 to be significantly up regulated in the mid coronal section of SHRSP+NaCl (2 fold change) versus SHRSP. Unfortunately qRT-PCR did not validate these findings with no significant changes in the gene expression of SLC24a2 with salt-loading in any strain.

Table 8.7. **Data obtained from qRT-PCR analysis for each gene of interest.**

Probe/Gene		RQ (relative fold change) ± standard error			
Age / Salt / Section		21 no salt F	21 no salt M	21 salt F	21 salt M
MBP	WKY	1.65 ± 0.36	1.00 ± 0.34	1.07 ± 0.40	1.00 ± 0.86
	SHRSP	1.00 ± 0.71	1.10 ± 0.10	1.00 ± 0.28	1.74 ± 1.13
	p value	NS	NS	NS	NS
ACTB	WKY	1.57 ± 0.44	1.00 ± 0.14	0.87 ± 0.15	1.00 ± 0.21
	SHRSP	1.00 ± 0.35	1.00 ± 0.30	1.00 ± 0.13	1.29 ± 0.15
	p value	NS	NS	NS	NS
SLC24a2	WKY	1.68 ± 1.13	1.00 ± 0.54	0.91 ± 0.41	1.00 ± 0.70
	SHRSP	1.00 ± 0.68	1.02 ± 0.18	1.00 ± 0.31	0.75 ± 0.52
	p value	NS	NS	NS	NS

Data represents the relative fold change (RQ value) ± the standard error between the gene of interest and the house keeper gene GAPDH for non salt-loaded and salt loaded WKY and SHRSP at age 21 weeks and from both frontal (F) and mid coronal (M) brain sections. NS = No significant difference.

8.4 Discussion

8.4.1 Summary of results – animals aged 5, 16 & 21 weeks

In this study we have found differential gene expression in several key pathways in the SHRSP at 5 weeks prior to the onset of hypertension which together, contribute towards the SHRSP having heightened susceptibility to small vessel disease and cerebral pathology via dysfunction of; the structural integrity of astrocytes (GFAP – decreased mRNA expression validated by qRT-PCR), components of the extracellular matrix (MMP14 – decreased mRNA expression validated by qRT-PCR), tight junction signalling (pathway contained a significant number of significantly differentially expressed genes), fluid transport (ALB – decreased mRNA expression) and defects in nitric oxide signalling / vasoreactivity (AVP – decreased mRNA expression validated by qRT-PCR, GUCY1a3 – increased mRNA expression, GNAI1 – decreased mRNA expression). In addition we found a network of early growth response genes which were up-regulated in SHRSP at 5 weeks which supports our observations of endothelial proliferation on H&E sections (chapter 6). Our results also showed that an inflammatory pathway (the acute phase response) contained many up-regulated genes, at all ages in the SHRSP, indicating a chronically challenged immune system across the SHRSP life course. We also found evidence that myelination is disrupted at 21 weeks (reduced MBP(Bailey et al. 2011b)).

Direct comparison of mRNA expression with proteins we assessed using immunohistochemistry in the same animals (chapter 7) produced 2 significant results (GFAP and MBP). GFAP mRNA levels were down-regulated in the frontal section of 5 week old SHRSP. This is the opposite finding to our immunohistochemistry data which showed significantly more GFAP in this section at the same age (chapter 7) (Bailey et al. 2011b). This discrepancy could be explained by post-transcriptional modification, which directly determines how much of the mRNA is translated into protein. Post-transcriptional modification can be influenced by simple changes such as over exposure to a neurotransmitter or increased levels of reactive oxygen species (Adachi 2010). Further investigation into the structure and function of astrocytes in young SHRSP is needed. The mRNA expression of MBP at 21 weeks in the SHRSP mirrored our immunohistochemsitry findings with a significant reduction in MBP expression in SHRSP in both sections versus WKY. This finding indicates that the SHRSP suffers axonal pathology most likely secondary to microvascular pathology.

Additionally we also found a down-regulation of MMP14 in the frontal section of 5 week old SHRSP. This could suggest changes in the extra cellular matrix existing as early as 5 weeks of age in the frontal brain region. MMP14 directly influences collagens and claudins thereby

influencing vascular integrity (Sounni et al. 2010). This is consistent with our previous finding of significantly reduced immunoreactivity of Claudin-5 at the same age (Bailey et al. 2011b). Further investigation of both mRNA expression and protein levels of MMP14 in young animals will be necessary in order to fully establish its influence on the structure of both tight junctions and the vascular cytoskeleton.

Using a genome wide approach, we found that the most highly differentially expressed genes (both up-regulated and down-regulated) were mostly conserved across all ages. In particular we found that GUCY1a3 (an intracellular nitric oxide receptor) was highly up-regulated in both brain sections of SHRSP by >15 fold change at all ages. Through sequencing we subsequently found a SNP in the 3'UTR end of the gene in SHRSP. Whilst this may in part explain the discrepancy between our microarray and PCR data it may not be the sole reason for seeing such a significant difference (x20 fold change) between the SHRSP and WKY on the microarray as 1 SNP in a 77 amplicon sequence would not affect the binding ability of the probe enough to produce a 20 fold change. SHRSP from the same colony have been shown to have a 5 fold up-regulation of GUCY1a3 in the heart at 5 weeks of age (unpublished observations). Further work addressing the role of microRNAs in this region and studies to look for evidence of alternate splicing are currently underway. Validation of this result via the assessment of corresponding protein expression is also needed; however, suitable antibodies for immunohistochemistry are currently unavailable for paraffin sections.

However despite this, our finding for GUCY1a3 coupled with the significant decrease in expression of AVP at 5 weeks suggests that SHRSP have impaired vasoreactivity from birth. This hypothesis is supported by previous data which has shown young SHRSP to have impairments in vasodilation (Volpe et al. 1996), impairments in the renin-angiotensin system (Unger 2002;Racasan et al. 2005), heightened responses of the vasculature to sympathetic stimulation (Luft et al. 1986) and significantly lower bioavailability of nitric oxide - attributed to the increased presence of superoxide species (Grunfeld et al. 1995;Gotoh et al. 1996;McBride et al. 2005). Therefore the up-regulation of this intracellular receptor could be a compensatory mechanism trying to capture as much as the available nitric oxide as possible before it is degraded.

In the opposite direction, albumin was consistently down-regulated in SHRSP across all ages by ~3 fold change however the signal intensity was very low and subsequently this finding was not validated at all ages by qRT-PCR. Albumin is a very ubiquitous protein but it is a regulator of osmotic pressure and can signal changes in endothelial permeability (Menzies et al. 1993). Recently it has been shown that 10 week old SHRSP have a significantly reduced level of oxidised albumin in the serum (Michihara et al. 2010), low albumin could enhance

fluid transport across the BBB leading to an increase in perivascular edema and we believe the contribution of albumin to a 'stroke-prone' state needs to be investigated further.

Using the predetermined biological pathways within IPA software we found acute phase response signalling and tight junction signalling featured most often within the top 5 pathways over represented by changes in gene expression. Elements of these pathways have been investigated in SHRSP using various assays but never using microarray technology on brain tissue (Lippoldt et al. 2000;Sironi et al. 2001;Uehara 2003). In relation to the acute phase response, previous studies have shown an increase in proteinuria and inflammatory proteins in serum at ages both prior to the onset of hypertension and 'stroke prone' ages (Sironi et al. 2001;Ballerio et al. 2007). Differences in gene expression within the tight junction pathway indicate that the blood brain barrier in SHRSP could be compromised from a young age which also agrees with previous findings (Lippoldt et al. 2000;Bailey et al. 2011b). One possible reason for the inflammatory response, high levels of oxidative stress and impaired vasoreactivity seen in 5 week old SHRSP could be the levels of hypertension SHRSP foetus' are exposed to in the womb – i.e. the Barker Hypothesis which correlates fetal adaptation to adverse environmental conditions in the perinatal period with the manifestation of cardiovascular disease in adult life (Barker 2002). There is already evidence in SHR that this is the case (see Racasan 2005 for a review (Racasan et al. 2005)) with an imbalance in nitric oxide and reactive oxygen species playing a pivotal role. As the SHR does not 'stroke' this suggests that alongside this imbalance there are other factors which contribute to the 'stroke-proneness' of the SHRSP.

8.4.2 Summary of results – salt-loaded versus non salt-loaded animals (all aged 21 weeks)

Through conducting mRNA expression analysis and qRT-PCR on WKY+NaCl and SHRSP+NaCl versus non salt-loaded age matched animals we found the majority of changes in gene expression due to salt-loading occurred in the frontal brain section. Within this frontal brain region salt induced differential expression of genes associated with myelin integrity and solute carriers in WKY rats. In SHRSP+NaCl a whole network of genes integral to vascular structure was down-regulated and components of the tight junction signalling pathway were also significantly differentially expressed. Pathways pertaining to oxidative stress and inflammation were affected by changes in gene expression due to salt-loading in both strains. Finally the differences in gene expression between WKY+NaCl versus SHRSP+NaCl were almost identical to those in non salt-loaded animals (see table 8.3), suggesting that inherent

strain differences have more of an effect on gene expression than salt. However, the fact that we found differences due to salt-loading in both strains cannot be ignored.

In WKY rats, salt-loading resulted in several genes in a network centered around APP and MBP being up-regulated, indicating increased expression of myelin associated proteins. The same group of genes were down-regulated in SHRSP+NaCl versus SHRSP. This indicates a very different response to salt in the two different strains of rat or perhaps a different stage in disease and requires further investigation.

In the SHRSP, salt-loading resulted in a down-regulation of a gene network involved in maintaining vascular structure. In addition, tight junction signalling featured within the top 5 pathways affected in the frontal section of WKY+NaCl versus SHRSP+NaCl, as well as SHRSP+NaCl versus SHRSP. Within the tight junction signalling pathway we found Claudin-11 to be significantly down-regulated in SHRSP+NaCl versus SHRSP in the frontal section and conversely up-regulated in the same section in SHRSP+NaCl when compared to WKY+NaCl. As the SHRSP already has reduced Claudin-5 protein expression independently of salt-loading (Bailey et al. 2011b) the difference in Claudin-11 could indicate problems within tight junctions and increased leakiness of blood vessels particularly when coupled with changes in the expression of albumin.

This is not to say that the WKY is immune to vascular damage due to salt-loading. The changes in APP and MBP could be a response to self-inflicted vascular damage. Also Von Willebrand factor (VWF) and vascular growth factor (VGF) were both down-regulated in the mid coronal section (2.3 and 1.9 fold respectively) of WKY+NaCl versus WKY.

We found the acute phase response signalling pathway contained the most differentially expressed genes in all salt versus no salt comparisons indicating that the inflammatory response is significantly affected by salt-loading.

Pathways pertaining to oxidative stress and leukocyte extravasation contained a significant proportion of differentially expressed genes in salt versus no salt comparisons in both strains. These results agree with previous data which showed increased levels of oxidative stress and an increased inflammatory response to be systemic responses to high salt intake in SHRSP (McBride et al. 2005;Kim-Mitsuyama et al. 2005;Kobayashi et al. 2009;Michihara et al. 2010).

Previous studies have linked a systemic inflammatory condition to stroke susceptibility in the SHRSP (Sironi et al. 2004) and the network of genes we found to be up-regulated in WKY+NaCl versus WKY (including MBP and APP) contained many genes involved in the acute phase response as well as myelin formation and maintenance. This inflammatory pathway could be detrimental to myelin integrity and cause white matter damage and could

explain why we encountered evidence of white matter vacuolation in WKY+NaCl seen in H&E sections of the same animals (chapter 6 of this thesis) and saw a significant reduction in the expression of MBP protein using immunohistochemistry on the same animals (chapter 7 of this thesis).

Genes within the two networks mentioned above (e.g. MBP, ALB and ACTB) were also amongst the top 10 up or down-regulated genes in the salt-loaded animals making their presence very significant. Few genes were differentially expressed by over 3 fold change and those that were, were mostly pseudogenes whose function is still undetermined or are essentially 'dead' genes i.e. genes that are still subject to regulation by transcriptions factors or other agents and not functional themselves. In the SHRSP, solute carriers such as SLC24a2 were frequently within the top 10 up or down-regulated genes. SLC24a2 is a sodium/potassium/calcium exchanger therefore its presence in response to increased sodium was not unexpected. The fact that it was affected in SHRSP and not WKY may be consistent with previous findings that show the SHRSP to be salt sensitive as a strain (Rothermund et al. 2001;Graham et al. 2007).

8.4.3 Overall

There were more genes differentially expressed in the frontal section than the mid coronal section and we often found genes which were consistently differentially expressed in one section but not the other. The reason for this is unclear. It could be due to the differences in tissue type distribution within the two sections (i.e. the frontal section will have a larger proportion of cortical grey matter, whilst the mid coronal section will have a larger proportion of white and deep grey matter). It could also be due to the differences in brain functions located within the two sections. A larger study would have to be performed to establish the reason for these differences.

None of the significantly expressed genes we found were located in or around the STR1 locus on chromosome 1 – the so called 'stroke-prone' locus. Our study is not the first to find genes or other loci aside from the STR1 locus which are believed to contribute to stroke development in the SHRSP and act independently of hypertension. Jeffs et al (Jeffs et al. 1997a) found a quantitative trait locus on chromosome 5 which co localises with the genes encoding atrial and brain natriuretic factor, which along with the differential expression of albumin we found in this study, highlights the importance in fluid transport and blood pressure regulation as a precursor to stroke development. Stroke is a polygenic condition in humans and we believe that even in an inbred strain of rat, the genetic cause of stroke is unlikely to be monogenic or related to a single quantitative trait locus.

This study has limitations. Whilst using one of the most comprehensive chips commercially available the entire rat genome is not faithfully represented. Over 22,000 probes are on a RatRef12 chip but some genes are over represented due to the presence of multiple transcriptomes. Some genes of interest were absent from the chip in particular smooth muscle actin. Therefore we cannot directly compare protein expression of SMA with RNA expression. Gene expression does not always mimic protein expression and this could explain why our previous finding of increased GFAP at 5 weeks on immunohistochemistry (see chapter 7) was completely reversed in the microarray. Whilst qRT-PCR validated the findings of GFAP, MMP14, AVP and GUCY1b3 it did not verify the differential expression of GUCY1a3, MBP, SLC24a2, ACTB, GPR98 and ALB as mentioned above. There are several possible reasons for the disparity between microarray and PCR data. The probe used for PCR (Taqman®) and the probe for the same gene on the microarray chip could map to different sections of the gene sequence. For example the GUCY1a3 probe on the microarray maps to a region downstream of the 3'UTR (all Illumina probes are biased towards the 3' end), in contrast the Taqman® probe crosses exons 6 and 7 of the gene. A separation of more than 1000 nucleotides between the PCR primer location and the microarray probe lowers the likelihood of agreement between the two techniques (Etienne et al. 2004). Additionally, we did not measure microRNAs which directly effect mRNA levels(Ambros 2004).

We used an unbiased and randomised approach and used a candidate gene and genome wide evaluation of transcription. No microarray of SHRSP brain tissue has been performed on animals as young as 5 weeks of age and therefore by doing this we have looked at an age group which is prior to the influence of hypertension as well as ages that are. All tissue was taken from the same brains used for our previous immunohistochemistry study (chapter 7) albeit the opposite cerebral hemisphere of the brain. Therefore when comparing the two separate techniques we are directly comparing the same animals. We randomized samples throughout the entire microarray protocol and were careful to use the same batch of IVT kits and RNA extraction kits where possible. The quality of every sample (both RNA and cRNA) was checked prior to loading onto the microarray on both a nanodrop and Agilent bioanalyzer and all samples were hybridized to the chips and scanned at the same time. We did not set a cut off level for fold change. Some studies set a fold change of 2 as a minimum for significance however we believe that a cluster of genes all significantly altered by a 1.7 fold change, for example, could still indicate a biologically significant finding.

Studies of salt-loaded animals should always have salt-loaded controls to establish salt specific changes in gene expression and avoid confounding due to salt. Studies using the SHRSP as a model of cerebral small vessel disease should refrain from salt-loading their animals as it only serves to complicate an already complex pattern of pathological changes.

Studies to assess salt-loading in younger animals are urgently required and salt intake should be assessed in studies of human cerebrovascular disease.

8.5 Conclusions

Our microarray and qRT-PCR data have revealed a significant proportion of genes which are differentially expressed in biological pathways which indicate impairments in vasoreactivity, the structural integrity of astrocytes and changes in the extra cellular matrix and the inflammatory response, all before the onset of hypertension in the SHRSP. Future work should focus on looking for changes in gene expression in more targeted areas e.g. extracting vessels using laser capture microdissection. Congenic strains and / or the SHR should also be tested in this way to enable genetic differences due solely to hypertension to be distinguished from those which could reveal more about the 'stroke-proneness' of the SHRSP.

Whilst a microarray approach is not able to distinguish the underlying pathogenic insult from secondary changes in cellular function and pathophysiology, it is able to highlight changes in gene expression which could contribute to the development of pathology or highlight potential genetic susceptibilities or pre disposing factors. We have used a time series to monitor initial changes at a young age which may cause effects later and tracked these changes over time. Finally, many genes that we found to be differentially expressed are of unknown function – however new information is constantly becoming available and the entire WKY and SHRSP genomes are nearing completion meaning our microarray data can be reanalysed in the future to incorporate new knowledge in the context of genome-wide SNPs that may help us differentiate between cis-acting and trans-acting effects.

CHAPTER 9 : GENERAL DISCUSSION

9.1 Main findings of this thesis

There has been widespread investigation into the potential causes of lacunar stroke pathology. However the majority of these studies have been performed in post mortem human tissue which is not optimal for addressing causative mechanisms. In order to find an alternative approach, in this thesis we have systematically assessed all the available potential experimental models of lacunar stroke, identified the most pertinent (the spontaneous pathology of the SHRSP rat) and discovered significant gaps in knowledge pertaining to the primary cause of highly relevant cerebral pathology in this model. We also discovered experimental manipulations (e.g. salt-loading) which only serve to hinder our understanding of the causative mechanisms in this model. Through our experimental work we have tried to address the relevant gaps in knowledge by assessing pathological changes within the cerebral vasculature of the SHRSP across a variety of ages (particularly young pre-hypertensive animals), as well as looking at the effects of salt loading on both the SHRSP and its control strain. This experimental work revealed that the presence of inflammation, as well as alterations in vascular reactivity, the nitric oxide signalling pathway and the structural integrity of the blood brain barrier are all evident before the onset of hypertension and perhaps more importantly, in the absence of salt loading. We also confirmed previous findings of vessel remodelling at older ages as a secondary response to hypertension. Furthermore, salt loading in control animals may induce some of these features without exposure to raised blood pressure. Therefore the findings from this thesis provide additional support for a non-ischaemic primary causative[i] mechanism for small vessel disease and lacunar stroke, with, in addition, the possibility that some species forebrains are particularly disposed to developing the features of SVD.

9.2 Human pathology – is the reliance on a few retrospective pathology studies coupled with disparate terminology hampering our understanding?

Lacunar stroke is considered to have a distinct clinical picture compared to large artery stroke due to growing evidence of distinct differences in risk factor profiles(Jackson and Sudlow 2005a) and well recognised differences in arteriopathy(Wardlaw 2005;Jackson et al. 2010). The original descriptions of this arteriopathy by Fisher are widely accepted despite his retrospective pathological material collectively coming from less than 20 patients(Fisher 1965;Fisher 1968;Fisher 1978). This population is restricted and may represent only a small

proportion of lesions which are now seen on imaging, especially now we know that only approximately 20% of lacunar lesions actually cavitate(Potter et al. 2010b)). This reliance on a few core studies and the pathological presumptions engrained from these studies are not conducive to advancing our knowledge of lacunar stroke etiology, especially when there are several other relevant pathology studies available in the current literature.

Our systematic review of human lacunar stroke pathology (chapter 2) found almost 40 pathology studies describing over 4000 relevant lesions. However over half of these lesions came from only one study and only 15 studies addressed the pathology of patients with a clinically verified lacunar syndrome. Studies of lacunar lesions in general were dogged by mixed terminology, non-standardised pathological assessment, and a lack of in depth histology targeting specific biomarkers (e.g. markers of inflammation, vascular structural integrity, axonal pathology etc).

Neurologists, Neuropathologists and Neuroradiologists should preferably work together in studies but will have to harmonise the differing terminology used in their respective fields in order to advance our knowledge in this area more rapidly.

All pathological investigations of lacunar stroke and associated conditions (e.g. vascular dementia, leukoaraiosis etc) need to be wary of artefacts. Early studies from Marie(Marie P 1901), Ferrand(Ferrand J 1902) and Dechambre(Dechambre 1838) described findings particularly in the white matter which, from examination of the images provided were more than likely an artifact of fixation – something possibly not appreciated at the time. Whilst observers now are much more aware of these artifacts, our reliance on these earlier works may inadvertently have diverted us to look for pathology that is not there or relevant.

Within studies of lacunar stroke or SVD a Neuropathologist is the ideal observer for examination of histopathological data in order to avoid such artifacts or unrelated pathology. However, it is important to blind the pathologist to appropriate data. For example, knowledge of clinical data may influence examination or interpretation of the specimen. This can mean either an excess of ‘relevant’ findings or failure to notice other pathology which could be relevant to the cause.

9.2.1 Future directions for human pathology studies

Put simply, more autopsy specimens are needed and whilst specimens assessed for SVD are available, they are usually contained within an Alzheimer's disease, other dementia, general aging or possibly sudden death (in older people) cohort banks. These brain banks could utilise this tissue resource to focus on SVD. Failing that brain banks need to be established in order to truly separate SVD etiology from related disorders. However, brains from patients who have died suddenly from non neurological disease both with and without risk factors for SVD may also be a valuable resource with which to study very early signs of SVD.

Like experimental animal studies, work conducted on human brain tissue needs to be conducted blind to clinical records and any in vivo imaging data. Preferably the imaging data should also be blindly assessed by at least one radiologist, if not more, so that a consensus view is established. In this context, sample size is also of paramount importance in pathology studies of both human and animal tissue. Not having a large enough sample size can result in finding non significant differences from quantitative assessments that may not reflect visual difference(s). Therefore, whilst we recommend the use of standardised quantitative methods in future studies, they must be performed to a high standard as outlined by guidelines available on the equator network (www.equator-network.org).

The terminology applied to lacunar stroke and cerebral small vessel disease must be standardised in pathology and on imaging. Thankfully the issue is increasingly coming to the fore(Pantoni et al. 2006;Potter et al. 2011) and hopefully a defined set of terms will soon follow. Preferably, separate terms should be used for imaging and pathology as transient lesions are not the same as an established infarct and appearances on imaging are very different to those under a microscope. However, there should be a common frame within clinical, imaging and pathology settings from which to devise appropriate terminology.

Multiple pathological abnormalities occur in vessels of different sizes and furthermore vessels at different sites in the brain show different pathologies under the same conditions (e.g. the medullary arteries display more severe thickening and dilatation than other arteries of comparable size)(Dozono et al. 1991a). More targeted approaches which segregate different vascular territories and brain regions are needed.

Therefore to summarise, more, well characterised autopsy material, backed by detailed clinical, imaging and risk factor data plus a more open-minded approach is needed in order to advance our knowledge of the pathogenesis of lacunar lesions and related SVD.

9.3 The SHRSP – its relevance as a model of SVD and lacunar stroke.

Our systematic review of potential animal models of lacunar stroke identified a variety of models claiming to produce infarcts pertinent to lacunar stroke, however most of these produced infarcts which were too large or affected the wrong brain / vascular territory to be fully relevant (chapter 3). Whilst a few models produced infarcts of a relevant size and situation their method of induction was not pertinent and little / no vascular pathology was achieved. Representing both parenchymal and vascular pathology is vital in order for an animal model to be truly useful for investigating the cause of lacunar stroke and SVD. In conclusion, our review found only the spontaneous pathology of the SHRSP rat could satisfy these requirements (chapter 3).

Unfortunately, in the current research climate, the SHRSP is being used to model a wide range of disorders and is now rarely used in its 'spontaneous' state. Furthermore, our systematic review of the cerebral pathology of the SHRSP (chapter 4) revealed a distinct lack of studies describing changes in the small vessels and at young ages despite this strain being highlighted as the most relevant model of small vessel disease(Hainsworth and Markus 2008) and vascular dementia(Saito et al. 1995) by others as well as being, in our opinion, the most pertinent model of lacunar stroke (chapter 3)(Bailey et al. 2009;Bailey et al. 2011a).

The use of high salt diets and / or salt-loading has increased over the last 20 years. This in turn means that both the scale and the evolution of relevant vascular pathology is artificially hastened and exaggerated(Schmidlin et al. 2005). Most studies of SHRSP which described a systemic inflammatory condition salt-loaded their animals. This makes it hard to dissect whether inflammatory changes are a direct response to salt or a heightened response to a pre existing condition, as there is at least one study which describes vasoactive edema in relatively young SHRSP in the absence of salt loading(Fredriksson et al. 1985). Also salt, whilst being a risk factor for all subtypes of stroke considered to act through raising blood pressure(Warlow et al. 2008b), has not been proven as a specific risk factor for small vessel disease or lacunar stroke. Therefore we feel the use of salt only serves to complicate a picture that is already complex. In order to be used effectively to study small vessel changes, the SHRSP (and any control strain) should not be exposed to any dietary, pharmacological or artifical experimental manipulation. The effects of salt should be tested separately.

In its 'spontaneous state' the SHRSP provides a model which incorporates both vascular and parenchymal lesions which develop over a timescale relevant to human pathology and harbours a pertinent risk factor in the form of hypertension. It is not a transgenic animal and therefore has no solitary genetic mutation which can be held solely to blame for the pathological changes seen. On the contrary the SHRSP probably has many genetic differences

which have yet to be identified. We are fully aware that this species is highly inbred and may therefore be of limited relevance to the average human, but the microvascular and brain morphological features are so similar to those described in humans that it is hard to ignore. To truly rule out a genetic disorder as a primary cause of the cerebral pathology seen in the SHRSP congenic strain analyses and correlative human tissue studies are needed.

Laboratories using the SHRSP must be aware that their findings should only be extrapolated to other SHRSP colonies with caution. This is because the selection processes for maintaining colonies differ between countries and colonies within those countries. For example, Japanese rat colonies are selectively bred to have higher systolic blood pressure than the Glasgow colony (230mmHg versus 190mmHg average systolic blood pressure respectively(Davidson et al. 1995;Kato et al. 2003). The reason for this is unclear.

Researchers who use the SHRSP often select the WKY as their control animal of choice as it is the parent strain of the SHRSP and SHR. However, there is evidence that the genetic background of the WKY is more heterogeneous than previously thought(Kurtz and Morris, Jr. 1987;Kurtz et al. 1989) which could potentially influence genetic studies and could explain some seemingly erroneous results between colonies. However lots of other methodological factors could also be to blame, such as the lack of blinding and / or randomisation as well as small sample sizes. Also the presence of heterogeneity within a model may be useful when trying to translate findings from experimental models into the heterogeneous human population, as long as the experimental design accounts for the variation.

9.3.1 The gaps in SHRSP knowledge – future directions

We identified 100 studies reflecting over 30 years of cerebral pathological investigation of the SHRSP. Despite this we found only one potential sequential histopathological investigation of vascular and tissue changes throughout the life of the SHRSP(Tagami et al. 1987). Additionally, the relationship of these changes to spontaneous strokes (particularly concerning the small vessels and prior to the development of hypertension) has not been specifically studied, despite much agreement that the small vessels suffer the major impact of the vascular changes(Mies et al. 1999). In addition the venular system has been overlooked.

Future studies in this area should include more targeted sensitive studies of pathological changes in young SHRSP, such as profiling inflammatory markers in SHRSP rats who have not been raised on a high salt intake, or where a direct salt / no salt comparison is conducted, are required. Detailed analysis of the differences in separate vascular structures such as the arteriolar walls and endothelium, plus how changes in the arterioles and venules relate to the sequence of spontaneous tissue pathological changes, are also needed. Larger sample sizes

assessing a wider range of age groups plus further genetic characterisation, particularly with the use of congenic strains, will hopefully be able to shed more light on the 'stroke proneness' of the SHRSP. Our microarray and PCR data (see below) have already highlighted abnormalities pertaining to instabilities in the BBB and vascular structure plus impairments in the vasoactive response from very early ages in the SHRSP. These are the type of findings which could give clues as to why some people are more susceptible than others to SVD and lacunar stroke.

9.4 Experimental data

From the experimental studies conducted in this thesis (chapters 6-8) we made several significant findings.

9.4.1 Normotensive animals – 5 weeks of age

Firstly, we had several important results at 5 weeks of age when SHRSP are still normotensive.

In chapter 6 we discovered evidence of endothelial cell proliferation in 5 week old SHRSP on H&E staining, which supported the discovery of a network of early growth response genes that were significantly up regulated in the frontal section of SHRSP at the same age (microarray data see chapter 8).

We found the immunoreactivity of the tight junction protein Claudin-5 to be significantly decreased in 5 week old SHRSP in all the areas of the brain analysed (chapter 7). Our microarray data did not specifically highlight any changes in the gene expression of BBB components but did reveal a significant decrease in MMP14 expression at the same young age. MMP14 directly influences the collagen family (degrading collagen I, II and III) as well as laminin and fibronectin which are substrates(Bini et al. 1999). A decrease in MMP14 gene expression could therefore have implications for the integrity of the vascular structure including that of the BBB as MMP14 is produced by endothelial cells(Lafleur et al. 2003) and directly interacts with tight junction proteins(Bar-Or et al. 2003). This is not the first evidence for a potential structural BBB impairment in SHRSP prior to stroke. Lippoldt et al showed that a loss of polarity across the BBB exists in cerebral vascular endothelial cells at 13 weeks just after hypertension is fully established(Lippoldt et al. 2000).

Also in relation to the BBB, our microarray data demonstrated a significant and consistent decrease in the gene expression of Albumin (ALB). Coupled with this was a significant

decrease in arginine vasopressin (AVP) expression in the mid coronal section at 5 weeks. ALB is a plasma protein with many functions. However, one of the most fundamental is to regulate blood volume(Menzies et al. 1993). AVP regulates water reabsorption(Miller 2006) from interstitial tissues to blood meaning a decrease in the level of both of these proteins could cause an increase in edema due to a decrease in oncotic pressure(Menzies et al. 1993) which in turn would make the BBB appear more permeable. This, plus any pre existing structural deficits in the BBB, could add up to resulting BBB leakage.

In the tissue surrounding the cerebral vessels we found increased microglial activation (Iba-1) increased astrocytosis (GFAP) (both from IHC – chapter 7 and the microarray data – chapter 8) along with altered gene expression within an inflammatory signalling pathway receptive to acute injury in the SHRSP at 5 weeks (chapter 8). These data combined suggest a heightened inflammatory response and / or the presence of inflammation at a young age. Previous studies showed an 'atypical inflammatory response' in young SHRSP(Sironi et al. 2004) although this was after salt loading. Our observations are independent of the effect of salt and hypertension (at 5 weeks SHRSP are still normotensive) therefore both of these risk factors could simply be exacerbating a pre-existing condition within the SHRSP.

Our microarray study (chapter 8) highlighted a major difference in gene expression of an intracellular nitric oxide (NO) receptor (GUCY1a3) in the SHRSP at 5 weeks of age (~20 fold change) right through to 21 weeks (~15 fold change). This suggests that SHRSP have an altered NO signalling pathway from birth, which may in turn compromise vascular reactivity. This evidence adds to previous data which described a lack of NO bioavailability in the SHRSP(Gotoh et al. 1996;Ma et al. 2001;Hirafuji et al. 2002), attributed to a heightened presence of reactive oxygen species which remove NO faster than usual, rather than to a change in the gene expression of nitric oxide synthases(Grunfeld et al. 1995;Gotoh et al. 1996;Michihara et al. 2010). Our data suggest that the NO pathway is abnormal from the start rather than, as previously suggested, damaged by the consequences of hypertension.

9.4.2 Hypertensive animals- 16 and 21 weeks

As well as reporting novel findings in very young SHRSP, we also confirmed the presence of vascular alterations directly attributable to hypertension in animals aged 16 and 21 weeks. Increased vessel wall thickening due to the accumulation of SMA (IHC study chapter 7) confirmed previous findings(Lin et al. 2001;Fujita et al. 2008) and supported our morphological observations in H&E sections (see chapter 6) which showed thickened vessels of a variety of sizes in all brain regions. In our IHC study, we also saw increased immunoreactivity of collagen I in 16 week SHRSP in all regions of the mid coronal section indicating focal medial scarring. This is most likely to be a secondary response to damage incurred in smooth muscle cells brought on by exposure to high blood pressure. We found that our study was too small to reveal significant changes in relevant cell or vessel densities and using a sclerotic index developed for human vasculature was too insensitive to quantify increases in vascular smooth muscle hypertrophy in rats. However, we would encourage larger studies which enable the quantification of pathological changes wherever possible.

9.4.3 The effects of salt

9.4.3.1 WKY animals aged 21 weeks

In 21 week old WKY given 1% NaCl in their drinking water from the age of 18 weeks, we found white matter vacuolation on H&E sections (chapter 6), increased astrocytosis (GFAP) and decreased MBP, VGF and vWF gene expression (chapters 7 and 8) compared with WKY, indicating that even the vasculature and white matter of the control strain is susceptible to salt. In the case of the cerebral white matter, a network of genes centred round MBP and APP was significantly down regulated in WKY+NaCl (chapter 8) indicating axonal pathology, which was confirmed by the appearance of MBP immunostaining (chapter 7).

Genes within the acute phase response signalling pathway were the most affected by salt loading as determined by IPA analysis (chapter 8). An inflammatory response to salt in the SHRSP has been demonstrated by several studies(Blezer et al. 1998;Sironi et al. 2001;Guerrini et al. 2002;Sironi et al. 2004) but importantly they did not try to quantify the effect of salt specifically. Furthermore the specific effect of salt on WKY rats or other 'control' strains has not been addressed.

Finally, a down regulation of SLC24a2- a sodium/potassium/calcium channel - was seen in salt loaded WKY versus WKY fed a normal diet (chapter 8). This finding comes in response to what was a short period of mild salt exposure in the adult rat and without a significant change in blood pressure. Therefore, changes in the control strain like this cannot be ignored

when trying to address the impact of salt loading on the SHRSP. Animals exposed to salt from birth may be much more affected.

9.4.3.2 SHRSP animals aged 21 weeks

SHRSP+NaCl rats displayed the most severe vascular pathology on H&E sections and we found an established internal capsule infarct in one salt loaded SHRSP rat (chapter 6). Like the WKY animals, salt loading caused significant changes in gene expression within the acute phase signalling response pathway indicating an inflammatory response to salt (chapter 8). As mentioned above, an inflammatory response to salt loading in the SHRSP is well described using imaging and proteomics in SHRSP given salt from 6 weeks of age and was supported by the increase in microglial activation seen in the salt loaded SHRSP animals from IHC data (chapter 7). This data highlights that there are salt specific effects taking place before the onset of hypertension and that the accelerated vasculopathy seen in SHRSP+NaCl may not be due to the combination of salt plus an increase in blood pressure.

SHRSP+NaCl also displayed significant reductions in MBP immunoreactivity, increased astrocytosis and microglial activation on IHC (chapter 7) all indicate secondary vascular damage. Microarray data supported a decrease in MBP expression in the frontal section of SHRSP+NaCl (chapter 8). Additionally our microarray study highlighted a decrease in ACTB (a major structural protein closely associated with tight junction signalling) and Claudin-11 (a tight junction protein) in SHRSP+NaCl versus SHRSP indicating once again how fragile the BBB is in the SHRSP (chapter 8).

Finally our microarray data also showed that SHRSP+NaCl have an up regulation of the same sodium/potassium/calcium channel that was down regulated in WKY+NaCl rats (chapter 8). This difference in the expression of the same gene in response to salt between the WKY and SHRSP could imply a difference in physiological response to salt in the strains - a salt susceptibility effect – or reflect differences in the stage of development of disease between the two strains. Salt-specific effects like this need to be investigated further.

9.5 Aspects of the methodologies used in this thesis

9.5.1 New methodologies and advantages of the approaches used in this thesis

Before conducting any experimental studies, we extensively and systematically searched the literature in order to assess gaps in knowledge in an unbiased and comprehensive fashion. We firstly assessed the human pathology data related to lacunar stroke and tried to harmonise disparate terminology in these studies which can impair the interpretation and understanding of pathology in both humans and experimental models. We applied this knowledge of the disparate terminology when searching for potential animal models of lacunar stroke to devise the most comprehensive search strategy possible. Consequently our finding that the SHRSP was the most appropriate animal model of lacunar stroke was supported by another independent research group looking for animal models of small vessel disease(Hainsworth and Markus 2008). We subsequently systematically assessed available data concerning the cerebral pathology of this strain before designing any experimental work.

We undertook study quality assessments in all our reviews with the help of recognised study reporting guidelines(Stroup et al. 2000;Macleod et al. 2004;von Elm et al. 2007) to highlight reporting issues which could bias publications, hamper interpretation of results and contribute to the low translational success of animal models in stroke. Consequently we made a conscious effort to apply study quality guidelines to all the experimental work conducted in this thesis.

We developed standard sampling protocols for sampling brain tissue from different ages and strains of rat – we can therefore be confident that we sampled the same brain areas from all animals. We applied this protocol across 3 different types of experimental study with success. This approach has not been explicitly used in experimental studies previously but is an obvious extension of methods commonly used in human experimental imaging studies.

We separated out the effects of salt from the spontaneous state of the animals to look at the effects of salt separately in not only the SHRSP but also control animals. We looked at specific brain regions pertinent to regions associated both with SVD pathology in humans and the development of pathology in the SHRSP. We also deliberately geared our approach towards pathological changes in the cerebral vasculature – an aspect which has so far been neglected, especially in young SHRSP.

We used both control animals and experimental animals from the same colony. This ensured exactly the same housekeeping conditions, blood pressure measurements and dietary protocols. Salt loading was administered under exactly the same conditions and for the same period of time for both the WKY and the SHRSP. Additionally, we used separate hemispheres from the same animals for histology and microarray work meaning a direct

comparison between these experimental findings can be made as the spontaneous pathology of the SHRSP and WKY is not hemisphere specific.

We carried out all pathological assessments in a blinded and random fashion. Microarray experiments were randomized to try and prevent any chip effects, batch effects, age and / or strain bias. As mentioned previously these aspects of methodology are important if the 'bench to beside' approach to translational studies is to succeed.

Finally we used two statistical tests to analyse the microarray data to try and limit the number of false positive results and to control for multiple comparisons.

9.5.2 Disadvantages of the approaches used in this thesis

The SHRSP is highly inbred and as well as displaying both tissue and vessel changes strikingly similar to human small vessel disease, it also displays pathology which is not pertinent to the condition e.g. cortical infarcts and haemorrhages although how prevalent these other lesions are is unclear as no official estimates have been undertaken. Incidentally, we saw no cortical lesions or haemorrhages in our animals. Some patients with small vessel disease also get cortical lesions and haemorrhages, but cortical events are common in older humans – it does not necessarily mean they are causally related – perhaps cortical events are simply common in older rats too. This could simply reflect a species difference relating to the make up of the vascular tree and would therefore be an issue in any hypertensive rodent model.

To date the brain and in particular the cerebral vessels of inducible hypertensive rats have not been fully characterised(Patterson et al. 2005), neither have those from models of hypoperfusion which use carotid coils(Shibata et al. 2004), but to compare the data with ours would be extremely valuable. We would argue that it is more advantageous towards our understanding of a human condition for an animal model to possess most of the features of a disease as well as some irrelevant pathology than to have no animal model at all or a very pure model. The SHRSP may reveal one mechanism of many that can contribute to the understanding of SVD – after all, some patients exhibit microbleeds as a result of SVD – therefore like humans, even genetically inbred rats may express different predispositions to end stage pathology.

Our experimental numbers overall were relatively small. However, we were restricted by the availability of animals within a relatively short time frame. To start up our own colony would have a) been expensive and b) taken too long to produce tissue. In this sense all our studies

can be classed as pilot data. Larger studies are easily reproducible from our methodologies and we actively encourage them.

Furthermore, whilst the inclusion of SHR rats would have been desirable, it would have introduced heterogeneity into the experiment. The Glasgow colony do not keep SHR rats therefore variation due to differences in breeding programs, levels of systolic hypertension, animal maintenance, genetic background etc would have been introduced and would have made interpretation of subtle changes (particularly changes in gene expression) very difficult.

Whilst selecting age groups which covered the development of hypertension we did not look at an end stage animal (e.g. >28 weeks). The end stage pathology of the SHRSP is already extensively described in the literature and we were primarily interested in early changes rather than re-characterizing end stage pathology. Despite our lack of an older age group, our 21 week old animals replicated previous reports of end stage pathology with vessel wall thickening and even an old infarct in one SHRSP+NaCl. A wider variety of ages e.g. 9, 12 and 20 week old animals in addition to the age groups we used would be beneficial.

Working with RNA poses challenges, in particular working with small samples, as our attempts at laser capture microdissection highlighted. The smaller the sample, the more rapid the decline of RNA quality. We used an Arcturus laser capture system with an infra red laser which does not allow for tracing around specific structures. It essentially punches holes within the tissue meaning more surface area of the sample will be exposed to the elements. If attempting this in the future we would recommend the use a Leica system with a UV laser which enables entire vessels to be dissected in one piece thereby increasing the chance of preserving RNA quality.

9.6 The potential causes of lacunar stroke and how our data contributes to a non-ischaemic hypothesis.

From data gathered from the literature and our own experimental findings we would propose the following hypothesis for the causative pathological mechanism of lacunar stroke. In the SHRSP (the most pertinent animal model) the vascular pathology originates with both structural and functional alterations inherent in the BBB from the youngest ages coupled with a systemic inflammatory condition and impaired vascular reactivity. The development of hypertension and /or the presence of salt exacerbates this pre-existing state and in addition initiates vascular remodelling leading to small vessel disease pathology within areas of BBB disruption. But how does this apply to human SVD and lacunar stroke?

Recent human studies have revealed increased levels of homocysteine(Hassan et al. 2004;Zylberstein et al. 2008) and other biomarkers of inflammation in small vessel disease and/or lacunar stroke patients(Fornage et al. 2008;Virdis et al. 2010), although unfortunately these studies did not use cortical stroke patients as controls. Therefore interpreting these findings in relation to stroke subtypes is difficult. Furthermore, background BBB leakage on imaging as measured by intravenous gadolinium was higher in the subcortical white matter of lacunar stroke patients versus cortical stroke control patients(Wardlaw et al. 2008).

Endothelial dysfunction is impaired in stroke patients in general but whether the extent or characteristics of this dysfunction differ between stroke subtypes has not yet been fully clarified(Stevenson et al. 2010). This is due to a lack of studies using appropriate controls e.g. cortical stroke patients rather than age matched non neurological patients(Stevenson et al. 2010).

From reviewing the literature and from our own observations, evidence of a thrombotic or embolic cause of infarcts in the SHRSP is rare and thrombi are most often seen as a late secondary event in the SHRSP(Fredriksson et al. 1988). This supports human data which suggests that only 20% of lacunar strokes are due to an embolic source(Chowdhury et al. 2004) along with the rare occurrence of thrombi in autopsy specimens of lacunar stroke patients(Fisher 1982a;Ogata 1999).

Therefore the data gathered from the SHRSP in this thesis adds to increasing amounts of human data supporting the hypothesis that cerebral small vessel disease and lacunar stroke are not primarily caused by an ischaemic mechanism. There are several paths which ultimately lead to either: SVD, lacunar stroke, leukoaraiosis, vascular dementia and / or other related cerebral pathology and we have tried to summarise these in figure 9.1. In simple terms there are a variety of risk factors aside from hypertension and diabetes that can initiate the development of SVD. Polygenetic factors such as the functionality of the nitric oxide system

or levels of oxidative stress plus vulnerability of the BBB could start the process. These risk factors directly influence the function of the BBB, the vasoreactivity of blood vessels and the regulation of cerebral blood flow. In turn, impairment of one or more of these functions will initiate small vessel arteriopathy which will be further exacerbated by the classic cardiovascular risk factors such as hypertension, diabetes and smoking. Then once again depending on partly environmental factors coupled with genetic susceptibility, the end stage disease will range from mild SVD (e.g. increased white matter lesions without cognitive decline) to a series of lacunar strokes with permanent physical and mental deficits.

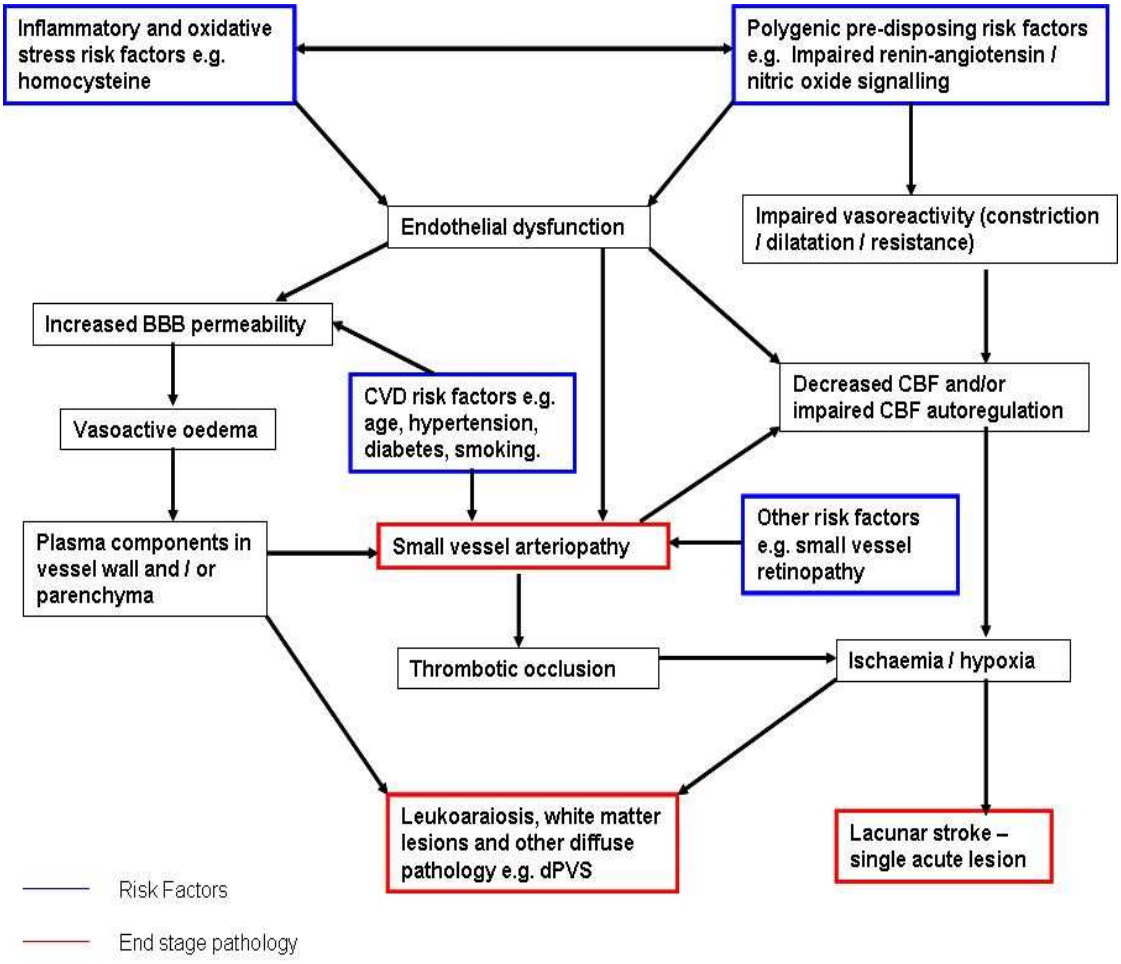

Figure 9.1. A schematic representation of the causative mechanism of small vessel disease, lacunar stroke and associated cerebral pathology.

BBB = blood brain barrier. CBF = Cerebral blood flow. dPVS = Dilated perivascular spaces.

9.7 Recent findings from other experimental models of SVD and/ or related pathology pertinent to our hypothesis.

Aside from the experimental models of lacunar stroke we assessed in chapter 3 of this thesis, there are models of closely related disorders like leukoaraiosis and vascular dementia which can also give insights into the causative mechanisms of SVD. For example, the chronic cerebral hypoperfusion model which ligates both the common carotid arteries is seen as a model of leukoaraiosis (diffuse white matter lesions) and vascular dementia. The white matter lesions created are hypothesized by many to be caused by BBB dysfunction as a direct consequence of the chronic low flow(Fernando et al. 2006).

Huang et al(Huang et al. 2010) found that this model induced the expression of endothelial cell ICAM-1 and VCAM-1 at both the protein and mRNA level in WKY rats. It also induced microglial activation and infiltration of macrophages into the white matter indicating endothelial dysfunction and ultimately causing WMLs(Huang et al. 2010). Ueno et al(Ueno et al. 2002) demonstrated an increase in BBB permeability in the same model using horse radish peroxidase, leakage of which peaked 3 days post surgery. Rats which underwent this procedure also showed an up regulation of MMP2(Ihara et al. 2001). Dysregulation of matrix metalloproteinases seems to be a common feature amongst SVD models with the SHRSP having increased expression of MMP13(Ueno et al. 2009) and our finding that MMP14 mRNA is decreased at 5 weeks of age. Interestingly MMP9 and MMP3 have been shown to be increased in human cases of vascular dementia around WMLs(Rosenberg et al. 2001). Dysregulation of MMPs generally indicates a breakdown in the extracellular matrix(Intengan and Schiffrin 2001). The extracellular matrix directly influences mechanical properties of the vessel wall, cellular adhesion and endothelial proliferation, all processes which if dysregulated can compromise vascular structure(Tunon et al. 2000).

The chronic cerebral hypoperfusion model also produces a marked proliferation of collagen fibrils in the thickened basal lamina of white matter arterioles(Ueno et al. 2002). This appearance is observed in both WKY and SHR rats and the authors postulate that this reflected regressive changes in the endothelial cells. Treatment with an anti-oxidant (lipoic acid) reduced the effects of chronic cerebral hypoperfusion on endothelial cells. They recommended moderating brain inflammation as a therapeutic strategy.

A related model of subcortical ischaemic vascular dementia using bilateral common carotid stenosis rather than ligation is being used to re create the decrease in blood flow due to small vessel arteriopathy and also produces white matter lesions via a similar proposed mechanism(Shibata et al. 2004;Nishio et al. 2010). It is worth noting that the effects of

chronic cerebral hypoperfusion on the BBB in the above models happen independently of any increase in blood pressure. Previous work on the SHRSP has shown there to be a significant decrease (up to 50%) in regional cerebral blood flow (especially in the frontal regions of the brain) from 6 weeks of age(Yamori and Horie 1977;Smeda et al. 1999;Jesmin et al. 2004) well before hypertension is established or any cerebral pathology is evident. Therefore any BBB leak caused by this hypoperfusion will consequently be exacerbated by the onset of hypertension.

Some authors are concerned that the bilateral carotid stenosis mouse model does not develop lacunar infarcts or amyloid deposits in the long term. However, this is not necessarily a disadvantage as it may simply reflect species differences (mouse amyloid does not have a tendency to aggregate like human amyloid) and /or indeed the individual differences in susceptibility to these pathologies seen in humans.

9.8 Future work needed across both human and animal studies.

Standardised quantitative methodologies, like those developed in this thesis, need to be used in order to assess cerebral small vessel pathology across different animal and human models. These approaches (e.g. density counts, vessel measurements and immunohistochemistry with accompanying image analysis) would enable easier comparisons with quantitative human data such as white matter lesion rating scales used in imaging studies(Fazekas et al. 1987). Descriptive qualitative assessments, whilst valuable, can only provide a limited amount of information.

Genetic studies targeted towards tissue type and /or vascular territory plus the use of congenic strains will reveal more about the development of pathology, the susceptibility of different brain areas to that pathology and the true role of hypertension. Our experimental work along with data emerging from experimental models of related conditions (see above) has highlighted nitric oxide signalling, matrix metalloproteinases, collagens and the functional and structural integrity of the BBB as areas which targeted studies could and should focus upon. Again these studies are needed not just in the SHRSP but in other animal models of hypertension, cerebrovascular disorders and SVD as well as models of other relevant risk factors (e.g. diabetes, inflammatory conditions).

Cerebral small vessel disease is often seen as a disease of the arteries, arterioles and very rarely the capillaries. However, it probably affects all components of the small vessels and therefore studies of the veins and venules are also required. Some would say that often it is difficult to distinguish venules from arterioles under a light microscope, but this should no longer be a problem due to major advances in microscope technology. In humans there is now

increasing evidence from retinal photography and imaging that differences in the venular system (e.g. venular diameters) may distinguish small vessel disease from large artery pathologies(Kwa et al. 2002;Delles et al. 2008;Lindley et al. 2009;Doubal et al. 2009;Rodriguez et al. 2010). Retinal studies are extremely valuable to cerebral small vessel disease research as retinal vessels share the same embryological source, size, and physiologic characteristics with cerebral small vessels, and retinopathy itself is associated with and is a risk factor for stroke (Doubal et al. 2009). Eyes are inherently more accessible in both humans and animal models than the brain and they provide a canvas for a larger array of experimental studies particularly in vivo studies in the case of animal models. Retinal work in the SHRSP is scarce, mostly over 20 years old, not published in mainstream journals and is often confounded by the introduction of dietary modulations (e.g. cholesterol)(Affymetrix ;Lin and Essner 1988;Hamada 1991). More assessments of retinal pathology in animal models such as the SHRSP are not only feasible but necessary.

9.9 Conclusion

The data presented in this thesis provides evidence which supports blood brain barrier dysfunction, impaired vascular reactivity and inflammation as primary causative mechanisms for cerebral small vessel disease and lacunar stroke. Any thrombotic vessel lesions encountered in both human tissue and the most relevant animal model, are usually a late stage event. This suggests that patients with an innate susceptibility to increased blood brain barrier permeability and/or inflammatory conditions could be at higher risk of developing small vessel disease pathology and related end stage diseases (e.g. vascular dementia, lacunar stroke). Further research is required to determine if patients with lacunar stroke should be treated differently to those with cortical large artery atherothromboembolic stroke.

Reference List

Adachi T (2010) Modulation of vascular sarco/endoplasmic reticulum calcium ATPase in cardiovascular pathophysiology. In: *Advances in Pharmacology Cardiovascular Pharmacology - Heart and Circulation*, Academic Press, pp 165-195

Alex M, Baron EK, Goldenburg S, BHT (1962) An autopsy study of cerebrovascular accident in diabetes mellitus. *Circulation* 25:663-673

Ambros V (2004) The functions of animal microRNAs. *Nature* 431:350-355

Arboix A, Marti-Vilalta J-L (2004) New concepts in lacunar stroke etiology: The constellation of small vessel arterial disease. *Cerebrovascular Diseases* 17:58-62

Arboix A, Ferrer I, Marti-Vilalta JL (1996) Clinico-anatomopathologic analysis of 25 patients with lacunar infarction. *Rev Clin Esp* 196:370-374

Arboix A, Lopez-Grau M, Casasnovas C, Garcia-Eroles L, Massons J, Balcells M (2006) Clinical study of 39 patients with atypical lacunar syndrome. *Journal of Neurology, Neurosurgery and Psychiatry* 77:381-384

Arribas SM, Gordon JF, Daly CJ, Dominiczak AF, McGrath JC (1996) Confocal microscopic characterization of a lesion in a cerebral vessel of the stroke-prone spontaneously hypertensive rat. *Stroke* 27:1118-1123

Atochin D, Murciano J, Gursoy-Ozdemir Y, Krasik T, Noda F, Ayata C, Dunn A, Moskowitz M, Huang P, Muzykantov V (2004) Mouse model of microembolic stroke and reperfusion. *Stroke* 35:2177-2182

Awad IA, Johnson PC, Spetzler RF, Hodak JA (1986) Incidental subcortical lesions identified on magnetic resonance imaging in the elderly. II. Postmortem pathological correlations. *Stroke* 17:1090-1097

Bailey EL, McCulloch J, Sudlow C, Wardlaw JM (2009) Potential animal models of lacunar stroke. A systematic review. *Stroke* 40:e451-e458

Bailey EL, Smith C, Sudlow C, Wardlaw J (2011a) Is the spontaneously hypertensive stroke prone rat a pertinent model of subcortical ischaemic stroke? A systematic review.

Bailey EL, Wardlaw J, Graham D, Dominiczak A, Sudlow C, Smith C (2011b) Cerebral small vessel endothelial structural changes predate hypertension in stroke prone spontaneously hypertensive rats: a blinded, controlled immunohistochemical study of 5-21 week old rats.

Ballerio R, Gianazza E, Mussoni L, Miller I, Gelosa P, Guerrini U, Eberini I, Gemeiner M, Belcredito S, Tremoli E, Sironi L (2007) Gender differences in endothelial function and inflammatory markers along the occurrence of pathological events in stroke-prone rats. *Experimental and Molecular Pathology* 82:33-41

Baloh RW, Vinters HV (1995) White matter lesions and disequilibrium in older people: II. Clinicopathologic correlation. *Arch Neurol* 52:975-981

Bamford J, Sandercock P, Dennis M, Warlow C, Burn J (1991) Classification and natural history of clinically identifiable subtypes of cerebral infarction. *The Lancet* 337:1521-1526

Bamford J, Sandercock P, Jones L, Warlow C (1987) The natural history of lacunar infarction: The oxfordshire community stroke project. *Stroke* 18:545-551

Bancroft JD, Cook HC (1994) *Manual of histological techniques and thier diagnostic application.*, Churchill Livingstone,

Bancroft JD, Gamble M (2002) *Theory and practice of histological techniques*, Churchill Livingstone,

Bar-Or A, Nuttall RK, Duddy M, Alter A, Kim H, Ifergan I, Pennington CJ, Bourgoin P, Edwards DR, Yong V (2003) Analyses of all matrix metalloproteinase members in leukocytes emphasize monocytes as major inflammatory mediators in multiple sclerosis. *Brain* 126:2738-2749

Barker D (2002) Fetal programming of coronary heart disease. *Trends in Endocrinology and Metabolism* 13:364-368

Bejamini Y, Hochberg Y (1995) Controlling the false discovery rate: a practical and powerful approach to multiple testing. *Journal of the Royal Statistical Society Series B Methodological* 57:289-300

Bejot Y, Catteau A, Caillier M, Rouaud O, Durier J, Marie C, Di CA, Osseby G-V, Moreau T, Giroud M (2008) Trends in incidence, risk factors, and survival in symptomatic lacunar stroke in dijon, france, from 1989 to 2006: A population-based study. *Stroke* 39:1945-1951

Belayev L, Busto R, Zhao W, Fernandez G, Ginsberg MD (1999) Middle cerebral artery occlusion in the mouse by intraluminal suture coated with poly-L-lysine: Neurological and histological validation. *Brain Research* 833(2)*:*181-190

Benhaiem-Sigaux N, Gherardi R, Salama J (1986) Thrombosis of a saccular microaneurysm causing cerebral (pontine) lacunae. *Acta Neuropathologica* 69 (3-4)*:*332-336

Benhaiem-Sigaux N, Gray F, Gherardi R, Roucayrol AM, Poirier J (1987) Expanding cerebellar lacunes due to dilatation of the perivascular space associated with Binswanger's subcortical arteriosclerotic encephalopathy. *Stroke* 18:1087-1092

Bini A, Wu D, Schnuer R, Kudryk B (1999) Characterization of stromelysin 1 (MMP-3), matrilysin (MMP-7), and membrane type 1 matrix metalloproteinase (MT1-MMP) derived fibrin(ogen) fragments d-dimer and d-like monomer: NH_2-terminal sequences of late-stage digest fragments. *Biochemistry* 38:13928-13936

Black PH, Garbutt LD (2002) Stress, inflammation and cardiovascular disease. *Journal of Psychosomatic Research* 52:1-23

Blezer ELA, Schurink M, Nicolay K, Dop Bar PR, Jansen GH, Koomans HA, Joles JA (1998) Proteinuria precedes cerebral edema in stroke-prone rats: A magnetic resonance imaging study. *Stroke* 29:167-174

Bokura H, Kobayashi S, Yamaguchi S (1998) Distinguishing silent lacunar infarction from enlarged Virchow-Robin spaces: a magnetic resonance imaging and pathological study. *Journal of Neurology* 245:1432-1459

Bossuyt PM, Reitsma JB, Bruns DE, Gatsonis CA, Glasziou PP, Irwig LM, Lijmer JG, Moher D, Rennie D, de Vet H, for the STARD Group (2003) Toward complete and accurate reporting of studies of diagnostic accuracy: The STARD initiative. *Academic Radiology* 10:664-669

Boumaza S, Arribas SM, Osborne-Pellegrin M, McGrath JC, Laurent S, Lacolley P, Challande P (2001) Fenestrations of the carotid internal elastic lamina and structural adaptation in stroke-prone spontaneously hypertensive rats. *Hypertension* 37:1101-1107

Bourjeili N, Turner M, Stinner J, Ely D (1995) Sympathetic nervous system influences salt appetite in four strains of rats. *Physiology and Behavior* 58:437-443

Braffman BH, Zimmerman RA, Trojanowski JQ, Gonatas NK, Hickey WF, Schlaepfer WW (1987) Brain MR: Pathologic correlation with gross and histopathology. 1. Lacunar infarction and virchow-robin spaces. *ANJR* 9:628

Breitling R, Armengaud P, Amtmann A, Herzyk P (2004) Rank products: a simple, yet powerful, new method to detect differentially regulated genes in replicated microarray experiments. *FEBS Letters* 573:83-92

Brenowitz G, Yonas H (1990) Selective occlusion of blood supply to the anterior perforated substance of the dog a highly reproducible stroke model. *Surgical Neurology* 33:247-252

Bryan RN, Wells SW, Miller TJ, Elster AD, Jungreis CA, Poirier VC, Lind BK, Manolio TA (1997) Infarctlike lesions in the brain: prevalence and anatomic characteristics at MR imaging of the elderly--data from the Cardiovascular Health Study. *Radiology* 202:47-54

Burton J, Underwood J (2007) Clinical, educational, and epidemiological value of autopsy. *The Lancet* 369:1471-1480

Bush E, Allman J (2003) The scaling of white matter to gray matter in cerebellum and neocortex. *Brain Behav Evol* 61:1-5

Bustin SA (2002) Quantification of mRNA using real-time reverse transcription PCR (RT-PCR): trends and problems. *J Mol Endocrinol* 29:23-39

Challa VR, Bell MA, Moody DM (1990) A combined hematoxylin-eosin, alkaline phosphatase and high-resolution microradiographic study of lacunes. *Clinical Neuropathology* 9:196-204

Chander PN, Rocha R, Ranaudo J, Singh G, Zuckerman A, Stier J (2003) Aldosterone plays a pivotal role in the pathogenesis of thrombotic microangiopathy in SHRSP. *Journal of the American Society of Nephrology* 14:1990-1997

Chen X, Wen W, Anstey KJ, Sachdev PS (2009) Prevalence, incidence, and risk factors of lacunar infarcts in a community sample. *Neurology* 73:266-272

Chen XW, Todd KG, Yang Y, Gordon T, Shuaib A (2001) Patency of cerebral microvessels after focal embolic stroke in the rat. *Journal of Cerebral Blood Flow & Metabolism* 21(4)*:*413-421

Chimowitz MI, Estes ML, Furlan AJ, Awad IA (1992) Further observations on the pathology of subcortical lesions identified on magnetic resonance imaging. *Arch Neurol* 49:747-752

Chowdhury D, Wardlaw JM, Dennis MS (2004) Are multiple acute small subcortical infarctions caused by embolic mechanisms? *J Neurol Neurosurg Psychiatry* 75:1416-1420

Chue C-H, Yukioka N, Yamada E, Hazama F (1993) The possible role of lysosomal enzymes in the pathogenesis of hypertensive cerebral lesions in spontaneously hypertensive rats. *Acta Neuropathologica* 85:383-389

Clemitson J, Dixon RJ, Haines S, Bingham AJ, Patel BR, Hall L, Lo M, Sassard J, Charchar FJ, Samani NJ (2007) Genetic dissection of a blood pressure quantitative trait locus on rat chromosome 1 and gene expression analysis identifies SPON1 as a novel candidate hypertension gene. *Circ Res* 100:992-999

Cole FM, Yates PO (1967) The occurrence and significance of intracerebral micro-aneurysms. *The Journal of Pathology and Bacteriology* 93:393-411

Contard F, Sabri A, Glukhova M, Sartore S, Marotte F, Pomies JP, Schiavi P, Guez D, Samuel J-L, Rappaport L (1993) Arterial smooth muscle cell phenotype in stroke-prone spontaneously hypertensive rats. *Hypertension* 22:665-676

Coyle P (1987) Dorsal cerebral collaterals of stroke-prone spontaneously hypertensive rats shrsp and wistar kyoto rats wky. *Anatomical Record* 218:40-44

Coyle P, Feng X (1993) Risk area and infarct area relations in the hypertensive stroke-prone rat. *Stroke* 24:705-709

Crowell RM, Olsson Y, Klatzo I, Ommaya AK (1970) Temporary focal ischemia in the monkey. *Transactions of the American Neurological Association 95:229-31,*

Cserr HF, Knopf PM (1992) Cervical lymphatics, the blood-brain barrier and the immunoreactivity of the brain: a new view. *Immunology Today* 13:507-512

Davidson AO, Schork N, Jaques BC, Kelman AW, Sutcliffe RG, Reid JL, Dominiczak AF (1995) Blood pressure in genetically hypertensive rats : Influence of the Y chromosome. *Hypertension* 26:452-459

Davis SM, Donnan GA (2004) Why lacunar syndromes are different and important. *Stroke* 35:1780-1781

Dawson SL, Panerai RB, Potter JF (2003) Serial changes in static and dynamic cerebral autoregulation after acute ischaemic stroke. *Cerebrovasc Dis* 16:69-75

de Leeuw F, de Groot JC, Oudkerk M, Witteman JCM, Hofman A, van Gijn J, Breteler MMB (2002) Hypertension and cerebral white matter lesions in a prospective cohort study. *Brain* 125:765-772

Dechambre A (1838) Mémoire sur la curabilité du ramollissement cérébral. *Gaz Méd Paris* 6:305-314

DeGirolami U, Crowell RM, Marcoux FW (1984) Selective necrosis and total necrosis in focal cerebral ischemia. Neuropathologic observations on experimental middle cerebral artery occlusion in the macaque monkey. *Journal of Neuropathology & Experimental Neurology 43(1):57-71,*

del Zoppo GJ, Copeland BR, Harker LA, Waltz TA, Zyroff J, Hanson SR, Battenberg E (1986) Experimental acute thrombotic stroke in baboons. *Stroke* 17:1254-1265

Delles C, McBride MW, Padmanabhan S, Dominiczak AF (2008) The genetics of cardiovascular disease. *Trends in Endocrinology & Metabolism* 19:309-316

Derouesne C, Poirier J (1999) Cerebral lacunae : Still under debate. *Rev Neurol (Paris)* 155:823-831

DiNicolantonio R, Silvapulle MJ (1988) Blood pressure, salt appetite and mortality of genetically hypertensive and normotensive rats maintained on high and low salt diets from weaning. *Clinical and Experimental Pharmacology and Physiology* 15:741-751

Donnan GA, Bladin PF, Berkovic SF, Longley WA, Saling MM (1991) The stroke syndrome of striatocapsular infarction. *Brain* 114A:51-70

Doubal FN, MacGillivray TJ, Hokke PE, Dhillon B, Dennis MS, Wardlaw JM (2009) Differences in retinal vessels support a distinct vasculopathy causing lacunar stroke. *Neurology* 72:1773-1778

Doubal FN, Dennis MS, Wardlaw JM (2010) Characteristics of patients with minor ischaemic strokes and negative MRI: a cross-sectional study. *Journal of Neurology, Neurosurgery & Psychiatry*10.1136/jnnp.2009.190298

Dozono K, Ishii N, Nishihara Y, Horie A (1991b) An autopsy study of the incidence of lacunes in relation to age, hypertension and arteriosclerosis. *Stroke* 22:993-996

Dulli D, D'Alessio D, Palta M, Levine R, Schutta H (1998) Differentiation of acute cortical and subcortical ischemic stroke by risk factors and clinical examination findings. *Neuroepidemiology* 17:80-89

Durand-Fardel M (1843) Traité du ramollissement du cerveau. *Paris JB Bailliere*

Eames PJ, Blake MJ, Dawson SL, Panerai RB, Potter JF (2002) Dynamic cerebral autoregulation and beat to beat blood pressure control are impaired in acute ischaemic stroke. *Journal of Neurology, Neurosurgery & Psychiatry* 72:467-472

Enea I, De Paolis P, Porcellini A, Piras O, Savoia C, Russo R, Giliberti R, Gigante B, Rubattu S, Conte G, Ganten D, Volpe M (2000) Defective suppression of the aldosterone biosynthesis during stroke permissive diet in the stroke-prone phenotype of the spontaneously hypertensive rat. *Basic Research in Cardiology* 95:84-92

Etienne W, Meyer MH, Peppers J, Meyer RA (2004) Comparison of mRNA gene expression by RT-PCR and DNA microarray. *Biotechniques* 36:618-620

Farrall AJ, Wardlaw JM (2009) Blood-brain barrier: Ageing and microvascular disease - systematic review and meta-analysis. *Neurobiology of Aging* 30:337-352

Fazekas F, Kleinert R, Offenbacher H, Schmidt R, Kleinert G, Payer F, Radner H, Lechner.H (1993) Pathologic correlates of incidental MRI white matter signal hyperintensities. *Neurology* 43:1683-1689

Fazekas F, Chawluk JB, Alavi A, Hurtig HI, Zimmerman RA (1987) MR signal abnormalities at 1.5 T in Alzheimer's dementia and normal aging. *Am J Roentgenol* 149:351-356

Feekes JA, Hsu S-W, Chaloupka JC, Cassell MD (2005) Tertiary microvascular territories define lacunar infarcts in the basal ganglia. *Ann Neurol* 58:18-30

Feigin VL, Lawes C, Bennett DA, Anderson CS (2003) Stroke epidemiology: a review of population-based studies of incidence, prevalence, and case-fatality in the late 20th century. *The Lancet Neurology* 2:43-53

Fernando MS, Simpson JE, Matthews F, Brayne C, Lewis CE, Barber R, Kalaria RN, Forster G, Esteves F, Wharton SB, Shaw PJ, O'Brien JT, Ince PG (2006) White matter lesions in an unselected cohort of the elderly: Molecular pathology suggests origin from chronic hypoperfusion injury. *Stroke* 37:1391-1398

Ferrand J (1902) Éssai sur l'hémiplegie des vieillards: Les lacunes de désintegration cérébrale. *Paris Jules Rousset*

Fisher CM (1978) Thalamic pure sensory stroke: A pathologic study. *Neurology* 28:1141

Fisher CM (1965) Lacunes: Small deep cerebral infarcts. *Neurology* 15:774-784

Fisher CM (1968) The arterial lesions underlying lacunes. *Acta Neuropathologica* 12:1-15

Fisher CM (1979) Capsular infarcts: The underlying vascular lesions. *Arch Neurology* 36:65-73

Fisher CM (1982a) Lacunar strokes and infarcts: A review. *Neurology* 32:871-876

Fisher CM (1982b) Pure sensory stroke and allied conditions. *Stroke* 13:434-447

Fornage M, Chiang YA, O'Meara ES, Psaty BM, Reiner AP, Siscovick DS, Tracy RP, Longstreth WT, Jr. (2008) Biomarkers of inflammation and MRI-defined small vessel disease of the brain: The cardiovascular health study. *Stroke* 39:1952-1959

Fredriksson K, Auer RN, Kalimo H, Nordborg C, Olsson Y, Johansson BB (1985) Cerebrovascular lesions in stroke-prone spontaneously hypertensive rats. *Acta Neuropathologica* 68:284-294

Fredriksson K, Kalimo H, Westergren J, Kahrstrom J, Johansson BB (1987) Blood brain barrier leakage and brain edema in stroke-prone spontaneously hypertensive rats. Effect of chronic sympathectomy and low protein/high salt diet. *Acta Neuropathologica* 74:259-268

Fredriksson K, Nordborg C, Kalimo H, Olsson Y, Johansson BB (1988) Cerebral microangiopathy in stroke-prone spontaneously hypertensive rats an immunohistochemical and ultrastructural study. *Acta Neuropathologica* 75:241-252

Frost SB, Barbay S, Mumert ML, Stowe AM, Nudo RJ (2006) An animal model of capsular infarct: Endothelin-1 injections in the rat. *Behavioural Brain Research* 169:206-211

Fujita Y, Lin JX, Takahashi R, Tomimoto H (2008) Cilostazol alleviates cerebral small-vessel pathology and white-matter lesions in stroke-prone spontaneously hypertensive rats. *Brain Research* 1203:170-176

Fujiwara T, Kondo M, Tabei R (1990) Morphological changes in cerebral vascular smooth muscle cells in stroke-prone spontaneously hypertensive rats (SHRSP). A scanning and transmission electron microscopic study. *Virchows Arch B Cell Pathol Incl Mol Pathol* 58:377-382

Futrell N (1991) An improved photochemical model of embolic cerebral infarction in rats. *Stroke* 22:225-232

Futrell N (2004) Lacunar infarction: embolism is the key.[see comment]. *Stroke* 35:1778-1779

Futrell N, Garcia JH, Millikan C (1991) Embolic stroke in aged rats. *Stroke* 22:1582-1591

Fuxe K, Kurosawa M, Cintra A, Hallstrom A, Goiny M, Rosen L, Agnati LF, Ungerstedt U (1992) Involvement of local ischemia in endothelin-1 induced lesions of the neostriatum of the anaesthetized rat. *Experimental Brain Research* 88:131-138

Garosi L, McConnell JF, Platt SR, Barone G, Baron JC, de LA, Schatzberg SJ (2006) Clinical and topographic magnetic resonance characteristics of suspected brain infarction in 40 dogs. *Journal of Veterinary Internal Medicine*311-321

Garrett M, Joe B, Dene H, Rapp J (2002) Identification of blood pressure quantitative trait loci that differentiate two hypertensive strains. *Journal of Hypertension* 20:2399-2406

Garrett MR, Meng H, Rapp JP, Joe B (2005) Locating a blood pressure quantitative trait locus within 117 kb on the rat genome: Substitution mapping and renal expression analysis. *Hypertension* 45:451-459

Ghandehari K, Izadi ZM (2009) Clinical evaulation of 625 lacunar syndrome patients. *Turkish Journal of Medical Science* 39:607-612

Gharbawie OA, Auer RN, Whishaw IQ (2006) Subcortical middle cerebral artery ischemia abolishes the digit flexion and closing used for grasping in rat skilled reaching. *Neuroscience* 137(4)*:*1107-1118

Gotoh K, Kikuchi H, Kataoka H, Nagata I, Nozaki K, Takahashi JC, Hazama F (1996) Altered nitric oxide synthase immunoreactivity in the brain of stroke-prone spontaneously hypertensive rats. *Acta Neuropathologica* 92:123-129

Gould DB, Phalan FC, Van Mil SE, Sundberg JP, Vahedi K, Massin P, Bousser MG, Heutink P, Miner JH, Tournier-Lasserve E, John SWM (2006) Role of COL4A1 in small-vessel disease and hemorrhagic stroke. *New England Journal of Medicine* 354(14):1489-1496

Gouw AA, Seewann A, van der Flier WM, Barkhof F, Rozemuller AM, Scheltens P, Geurts J (2010) Heterogeneity of small vessel disease: a systematic review of MRI and histopathology correlations. *Journal of Neurology, Neurosurgery & Psychiatry*

Graham D, McBride MW, Gaasenbeek M, Gilday K, Beattie E, Miller WH, McClure JD, Polke JM, Montezano A, Touyz RM, Dominiczak AF (2007) Candidate genes that

determine response to salt in the stroke-prone spontaneously hypertensive rat: Congenic analysis. *Hypertension* 50:1134-1141

Grinberg L, Thal DR (2010) Vascular pathology in the aged human brain . *Acta Neuropathologica* 119:277-290

Grunfeld S, Hamilton CA, Mesaros S, McClain SW, Dominiczak AF, Bohr DF, Malinski T (1995) Role of superoxide in the depressed nitric oxide production by the endothelium of genetically hypertensive rats. *Hypertension* 26:854-857

Guerrini U, Sironi L, Tremoli E, Cimino M, Pollo B, Calvio AM, Paoletti R, Asdente M (2002) New insights into brain damage in stroke-prone rats: A nuclear magnetic imaging study. *Stroke* 33:825-830

Gupta SR, Naheedy MH, Young JC, Ghobrial M, Rubino FA, Hindo W (1988) Periventricular white matter changes and dementia. Clinical, neuropsychological, radiological, and pathological correlation. *Arch Neurol* 45:637-641

Hachinski V (2002) Stroke: The next 30 years. *Stroke* 33:1-4

Hainsworth AH, Markus HS (2008) Do in vivo experimental models reflect human cerebral small vessel disease? A systematic review. *J Cereb Blood Flow Metab* 28:1877-1891

Hajdu MA, Baumbach GL (1994) Mechanics of large and small cerebral arteries in chronic hypertension. *American Journal of Physiology* 266:1027-1033

Hamada Y (1991) Ophthalmologic study on the M-strain of stroke-prone spontaneously hypertensive rat (M-SHRSP). Classification of hypertensive fundus changes in M-SHRSP. *Nihon Ganka Gakkai Zasshi* 95:16-30

Hamilton CA, Brosnan MJ, McIntyre M, Graham D, Dominiczak AF (2001) Superoxide excess in hypertension and aging a common cause of endothelial dysfunction. *Hypertension* 37:529-534

Hassan A, Hunt BJ, O'Sullivan M, Bell R, D'Souza R, Jeffery S, Bamford JM, Markus HS (2004) Homocysteine is a risk factor for cerebral small vessel disease, acting via endothelial dysfunction. *Brain* 127:212-219

Hazama F, Ozaki T, Amano S (1979) Scanning electron microscopic study of endothelial cells of cerebral arteries from spontaneously hypertensive rats. *Stroke* 10:245-252

He Z, Yamawaki T, Yang S, Day AL, Simpkins JW, Naritomi H, Rosenblum WI (1999) Experimental model of small deep infarcts involving the hypothalamus in rats: Changes in body temperature and postural reflex. *Stroke* 30(12*):*2743-2751

He Z, Yang SH, Naritomi H, Yamawaki T, Liu Q, King MA, Day AL, Simpkins JW (2000) Definition of the anterior choroidal artery territory in rats using intraluminal occluding technique. *Journal of the Neurological Sciences* 182:16-28

Henning EC, Warach S, Spatz M (2010) Hypertension-induced vascular remodeling contributes to reduced cerebral perfusion and the development of spontaneous stroke in aged SHRSP rats. *J Cereb Blood Flow Metab* 30:827-836

Higashino H, Sirneonova K, Lambev I, Markov M, Suzuki A (1995) Proper measurement of blood pressure and heart rate in SHRSP and WKY by an indirect volume-

oscillometric method. *Clinical and Experimental Pharmacology and Physiology* 22:S292-S293

Higuchi R, Dollinger G, Walsh P, Griffith R (1992) Simultaneous amplification and detection of specific DNA -sequences. *Bio-Technology* 10:413-417

Hilgers KF, Veelken R, Mai M, Ganten U, Ganten D, Luft FC, Mann JFE (1993) Vascular conversion of angiotensin I in stroke-prone spontaneously hypertensive and Wistar-Kyoto rats. *Journal of Hypertension* 11:1053-1059

Hinojos CA, Boerwinkle E, Fornage M, Doris PA (2005) Combined genealogical, mapping, and expression approaches to identify spontaneously hypertensive rat hypertension candidate genes. *Hypertension* 45:698-704

Hirafuji M, Tsunoda M, Machida T, Hamaue N, Endo T, Miyamoto A, Minami M (2002) Reduced expressions of inducible nitric oxide synthase and cyclooxygenase-2 in vascular smooth muscle cells of stroke-prone spontaneously hypertensive rats. *Life Sciences* 70:917-926

Holland PM, Abramson RD, Watson R, Gelfand DH (1991) Detection of specific polymerase chain reaction product by utilizing the 5'----3' exonuclease activity of Thermus aquaticus DNA polymerase. *PNAS* 88:7276-7280

Homeyer P, Cornu P, Lacomblez L (1996) A special form of cerebral lacunae: expanding lacunae. *J Neurol Neurosurg Psychiatry* 61:200-202

Hua R, Walz W (2006) Minocycline treatment prevents cavitation in rats after a cortical devascularizing lesion. *Brain Research* 1090:172-181

Huang Y, Zhang W, Lin L, Feng J, Chen F, Wei W, Zhao X, Guo W, Li J, Yin W, Li L (2010) Is endothelial dysfunction of cerebral small vessels responsible for white matter lesions after chronic cerebral hypoperfusion in rats? *Journal of the Neurological Sciences* 299:72-80

Hughes PM, Anthony DC, Ruddin M, Botham MS, Rankine EL, Sablone M, Baumann D, Mir AK, Perry VH (2003) Focal lesions in the rat central nervous system induced by endothelin-1. *Journal of Neuropathology & Experimental Neurology* 62(12):1276-86,

Hughes W, Dodgson M, Maclennan D (1954) Chronic cerebral hypertensive disease. *The Lancet* 264:770-774

Ihara M, Tomimoto H, Kinoshita M, Oh J, Noda M, Wakita H, Akiguchi I, Shibasaki H (2001) Chronic cerebral hypoperfusion induces MMP-2 but not MMP-9 expression in the microglia and vascular endothelium of white matter. *J Cereb Blood Flow Metab* 21:828-834

Ikeda M, Onda T, Tomita I, Tomita T (1996) The differences in Ca-2+-sensitivity of protein kinase C in platelets from Wistar Kyoto rat and stroke-prone spontaneously hypertensive rat. *Thrombosis Research* 82:417-427

Intengan H, Schiffrin EL (2001) Vascular remodeling in hypertension: Roles of apoptosis, inflammation, and fibrosis. *Hypertension* 38:581-587

Ishizuka T, Niwa A, Tabuchi M, Nagatani Y, Ooshima K, Higashino H (2007) Involvement of thromboxane A2 receptor in the cerebrovascular damage of salt-loaded, stroke-prone rats. *Journal of Hypertension* 25:861-870

Ito H, Takemori K, Suzuki T (2001) Role of angiotensin II type 1 receptor in the leucocytes and endothelial cells of brain microvessels in the pathogenesis of hypertensive cerebral injury. *Journal of Hypertension* 19:591-597

Ito H, Torii M, Suzuki T (1995a) Decreased Superoxide Dismutase Activity and Increased Superoxide Anion Production in Cardiac Hypertrophy of Spontaneously Hypertensive Rats. *Clinical and Experimental Hypertension* 17:803-816

Ito S, Nara Y, Yamori Y (1995b) Distinction of endothelial cell growth and fibrinolytic activity between WKY/Izm and SHRSP/Izm in vitro. *Clinical and Experimental Pharmacology and Physiology*S273-S274

Izzard AS, Graham D, Burnham MP, Heerkens EH, Dominiczak AF, Heagerty AM (2003) Myogenic and structural properties of cerebral arteries from the stroke-prone spontaneously hypertensive rat. *American Journal of Physiology - Heart and Circulatory Physiology* 285:H1489-H1494

Izzard AS, Horton S, Heerkens EH, Shaw L, Heagerty AM (2006) Middle cerebral artery structure and distensibility during developing and established phases of hypertension in the spontaneously hypertensive rat. *Journal of Hypertension* 24:875-880

Jackson C, Sudlow C (2005a) Are lacunar strokes really different?: A systematic review of differences in risk factor profiles between lacunar and nonlacunar infarcts. *Stroke* 36:891-901

Jackson C, Sudlow C (2005b) Comparing risks of death and recurrent vascular events between lacunar and non-lacunar infarction. *Brain* 128:2507-2517

Jackson CA, Hutchison A, Dennis MS, Wardlaw JM, Lindgren A, Norrving B, Anderson CS, Hankey GJ, Jamrozik K, Appelros P, Sudlow C (2010) Differing risk factor profiles of ischemic stroke subtypes: Evidence for a distinct lacunar arteriopathy? *Stroke* 41:624-629

Jeffs B, Clark J, Anderson NH, Gratton.J, Brosnan MJ, Gauguier D, Reid J, Macrae I, Dominiczak AF (1997a) Sensitivity to cerebral ischaemic insult in a rat model of stroke is determined by a single genetic locus. *Nature Genetics* 16:364-367

Jeffs B, Clark JS, Anderson NH, Gratton J, Brosnan M, Gauguier D, Reid JL, Macrae I, Dominiczak AF (1997b) Sensitivity to cerebral ischaemic insult in a rat model of stroke is determined by a single genetic locus. *Nat Genet* 16:364-367

Jellinger K (2007) The enigma of vascular cognitive disorder and vascular dementia. *Acta Neuropathol* 113:349-388

Jesmin S, Togashi H, Mowa CN, Ueno K, Yamaguchi T, Shibayama A, Miyauchi T, Sakuma I, Yoshioka M (2004) Characterization of regional cerebral blood flow and expression of angiogenic growth factors in the frontal cortex of juvenile male SHRSP and SHR. *Brain Research* 1030:172-182

Kanbe T, Nara Y, Tagami M, Yamori Y (1983) Studies of hypertension-induced vascular hypertrophy in cultured smooth muscle cells from spontaneously hypertensive rats. *Hypertension* 5:887-892

Kato N, Nabika T, Liang Y, Mashimo T, Inomata H, Watanabe T, Yanai K, Yamori Y, Yazaki Y, Sasazuki T (2003) Isolation of a chromosome 1 region affecting blood pressure and vascular disease traits in the stroke-prone rat model. *Hypertension* 42:1191-1197

Kawamoto Y, Akiguchi I, Tomimoto H, Shirakashi Y, Honjo Y, Budka H (2006) Upregulated expression of 14-3-3 proteins in astrocytes from human cerebrovascular ischemic lesions. *Stroke* 37:830-835

Kim-Mitsuyama S, Yamamoto E, Tanaka T, Zhan Y, Izumi Y, Izumiya Y, Ioroi T, Wanibuchi H, Iwao H (2005) Critical role of angiotensin II in excess salt-induced brain oxidative stress of stroke-prone spontaneously hypertensive rats. *Stroke* 36:1083-1088

Kimura S, Saito H, Minami M, Togashi H, Nakamura N, Nemoto M, Parvez HS (2000) Pathogenesis of vascular dementia in stroke-prone spontaneously hypertensive rats. *Toxicology* 153:167-178

Kishi T, Hirooka Y, Kimura Y, Ito K, Shimokawa H, Takeshita A (2004) Increased reactive oxygen species in rostral ventrolateral medulla contribute to neural mechanisms of hypertension in stroke-prone spontaneously hypertensive rats. *Circulation* 109:2357-2362

Kitazono T, Heistad DD, Faraci FM (1995) Enhanced responses of the basilar artery to activation of endothelin-B receptors in stroke-prone spontaneously hypertensive rats. *Hypertension* 25:490-494

Klee A, Vater S, Schmid-Schonbein GW, Seiffge D, Heistad DD (1993) Evidence from comparative investigations that impaired platelet activation is not specific for stroke-prone spontaneously hypertensive rats. *Stroke* 24:1528-1533

Kloss S, Furneaux H, Mulsch A (2003) Post-transcriptional regulation of soluble guanylyl cyclase expression in rat aorta. *Journal of Biological Chemistry* 278:2377-2383

Knottnerus ILH, Ten Cate H, Lodder J, Kessels F, van Oostenbrugge RJ (2009) Endothelial dysfunction in lacunar stroke: A systematic review. *Cerebrovasc Dis* 27:519-526

Knox CA, Yates RD, Chen I, Klara PM (1980) Effects of aging on the structural and permeability characteristics of cerebrovasculature in normotensive and hypertensive strains of rats. *Acta Neuropathologica* 51:1-13

Kobayashi A, Nara Y, Nishio T, Mori C, Yamori Y (1990) Increased Na+/ H+ exchange activity in cultured vascular smooth muscle cells from stroke-prone spontaneously hypertensive rats. *Journal of Hypertension* 8:153-157

Kobayashi M, Hirawa N, Yatsu K, Kobayashi Y, Yamamoto Y, Saka S, Andoh D, Toya Y, Yasuda G, Umemura S (2009) Relationship between silent brain infarction and chronic kidney disease. *Nephrology Dialysis Transplantation* 24 (1):201-207

Kubista M, Andrade J, Bengtsson M, Forootan A, Jonβk J, Lind K, Sindelka R, Sjoback R, Sjogreen B, Strombom L, Stσhlberg A, Zoric N (2004) The real-time polymerase chain reaction. *Molecular Aspects of Medicine* 27:95-125

Kurtz TW, Montano M, Chan L, Kabra P (1989) Molecular evidence of genetic heterogeneity in Wistar-Kyoto rats: implications for research with the spontaneously hypertensive rat. *Hypertension* 13:188-192

Kurtz TW, Morris RC, Jr. (1987) Biological variability in Wistar-Kyoto rats. Implications for research with the spontaneously hypertensive rat. *Hypertension* 10:127-131

Kuwabara S, Uno J, Ishikawa S (1988) A new model of brainstem ischemia in dogs. *Stroke* 19:365-371

Kwa VIH, Van der Sande JJ, Stam J, Tijmes N, Vrooland JL (2002) Retinal arterial changes correlate with cerebral small-vessel disease. *Neurology* 59:1536-1540

Lafleur M, Handsley M, Edwards D (2003) Metalloproteinases and their inhibitors in angiogenesis. *Expert Reviews in Molecular Medicine* 5:1-39

Laloux P, Brucher JM (1991) Lacunar infarctions due to cholesterol emboli. *Stroke* 22:1440-1444

Lammie GA (2000) Pathology of small vessel stroke. *British Medical Bulletin* 56:296-306

Lammie GA (2002a) Pathology of lacunar infarction. In: *Subcortical Stroke* (Donnan GA, Norrving B, Bamford J, Bogousslavsky J, eds), Oxford University Press, pp 37-47

Lammie GA, Brannan F, Slattery J, Warlow C (1997) Nonhypertensive cerebral small-vessel disease : An autopsy study. *Stroke* 28:2222-2229

Lammie GA, Brannan F, Wardlaw JM (1998) Incomplete lacunar infarction (type 1b lacunes). *Acta Neuropathologica* 96:163-171

Lammie GA (2002b) Hypertensive cerebral small vessel disease and stroke. *Brain Pathology* 12:358-370

Laurent S (1995) Arterial wall hypertrophy and stiffness in essential hypertensive patients. *Hypertension* 26:355-362

Lawlor DA, Smith G, Leon DA, Sterne J, Ebrahim S (2002) Secular trends in mortality by stroke subtype in the 20th century: a retrospective analysis. *The Lancet* 360:1818-1823

Leary M, Saver JL (2003) Annual incidence of first silent stroke in the united states: A preliminary estimate. *Cerebrovasc Dis* 16:280-285

Lee J, Zhai G, Liu Q, Gonzales ER, Yin K, Yan P, Hsu CY, Vo KD, Lin W (2007) Vascular permeability precedes spontaneous intracerebral hemorrhage in stroke-prone spontaneously hypertensive rats. *Stroke* 38:3289-3291

Lee PH, Oh SH, Bang OY, Joo IS, Huh K (2004) Isolated middle cerebral artery disease: clinical and neuroradiological features depending on the pathogenesis. *Journal of Neurology, Neurosurgery & Psychiatry* 75:727-732

Lin J-X, Tomimoto H, Akiguchi I, Wakita H, Shibasaki H, Horie R (2001) White matter lesions and alteration of vascular cell composition in the brain of spontaneously hypertensive rats. *Neuroreport* 12:1835-1839

Lin W, Essner E (1988) Ultrastructural and permeability characteristics of retinal vessels in stroke-prone spontaneously hypertensive rats. *Graefe's Archive for Clinical and Experimental Ophthalmology* 226:559-566

Lindley RI, Wang J, Wong M, Mitchell P, Liew G, Hand P, Wardlaw J, De Silva DA, Baker M, Rochtchina E, Chen C, Hankey GJ, Chang HM, Fung V, Gomes L, Wong TY (2009) Retinal microvasculature in acute lacunar stroke: a cross-sectional study. *The Lancet Neurology* 8:628-634

Lindner MD, Gribkoff VK, Donlan NA, Jones TA (2003) Long-lasting functional disabilities in middle-aged rats with small cerebral infarcts. *J Neurosci* 23:10913-10922

Lippoldt A, Kniesel U, Liebner S, Kalbacher H, Kirsch T, Wolburg H, Haller H (2000) Structural alterations of tight junctions are associated with loss of polarity in stroke-prone spontaneously hypertensive rat blood-brain barrier endothelial cells. *Brain Research* 885:251-261

Loeb C, Gandolfo C, Caponnetto C, Del SM (1990) Pseudobulbar palsy: A clinical computed tomography study. *European Neurology* 30:42-46

Longstreth WT, Jr., Bernick C, Manolio TA, Bryan N, Jungreis CA, Price TR, for the Cardiovascular Health Study Collaborative Research Group (1998) Lacunar infarcts defined by magnetic resonance imaging of 3660 elderly people: The cardiovascular health study. *Arch Neurol* 55:1217-1225

Lozano JD, Abulafia DP, Danton GH, Watson BD, Dietrich W (2007) Characterization of a thromboembolic photochemical model of repeated stroke in mice. *Journal of Neuroscience Methods* 162:244-254

Luft FC, Demmert G, Rohmeiss P, Unger T (1986) Baroreceptor reflex effect on sympathetic nerve activity in stroke-prone spontaneously hypertensive rats. *J Auton Nerv Syst* 17:199-209

Ma K-C, Olsson Y (1997) The role of chronic brain edema in the formation of lacunes in binswanger's encephalopathy. *Cerebrovascular Diseases* 7:324-331

Ma XL, Gao F, Nelson AH, Lopez BL, Christopher TA, Yue TL, Barone FC (2001) Oxidative inactivation of nitric oxide and endothelial dysfunction in stroke-prone spontaneous hypertensive rats. *Journal of Pharmacology & Experimental Therapeutics* 298:879-885

Macdonald RL, Kowalczuk A, Johns L (1995) Emboli enter penetrating arteries of monkey brain in relation to their size. *Stroke 26(7):1247-50; discussion 1250-1,*

Macleod MR, O'Collins T, Howells DW, Donnan GA (2004) Pooling of animal experimental data reveals influence of study design and publication bias. *Stroke* 35:1203-1208

Mancardi GL, Romagnoli P, Tassinari T, Gandolfo C, Primavera JM, Loeb C (1988) Lacunae and cribriform cavities of the brain. *Eur Neurol* 28:11-17

Mangiarua EI, Lee RMKW (1992) Morphometric study of cerebral arteries from spontaneously hypertensive and stroke-prone spontaneously hypertensive rats. *Journal of Hypertension* 10:1183-1190

Marie P (1901) Des foyers lacunaires de désintégration et des differents autres états cavitaires du cerveau. *Rev Méd* 21:281-298

Marshall VG, Bradley J, Marshall CE, Bhoopat T, Rhodes RH (1988) Deep white matter infarction: Correlation of MR imaging and histopathologic findings. *Radiology* 167:517-522

Masineni SN, Chander PN, Singh GD, Powers C, Stier CT, Jr. (2005) Male gender and not the severity of hypertension is associated with end-organ damage in aged stroke-prone spontaneously hypertensive rats. *American Journal of Hypertension* 18:878-884

Masuda J, Tanaka K, Omae T, Ueda K, Sadoshima S (1983) Cerebrovascular diseases and their underlying vascular lesions in Hisayama, Japan--a pathological study of autopsy cases. *Stroke* 14:934-940

Matsumoto M, Hatakeyama T, Morimoto K, Yanagihara T (1990) Cerebral blood flow and neuronal damage during progressive cerebral ischemia in gerbils. *Stroke* 21(10):1470-7,

Matsuo O, Okada K, Fukao H, Suzuki A, Ueshima S (1992) Cerebral plasminogen activator activity in spontaneously hypertensive stroke-prone rats. *Stroke* 23:995-999

Matsuo T, Nagaoka A (1981) Postnatal undernutrition accelerates incidence of stroke in stroke-prone spontaneously hypertensive rats. *Stroke* 12:509-512

Mayer SA, Tatemichi TK, Hair LS, Goldman JE, Camac A, Mohr JP (1993) Hemineglect and seizures in Binswanger's disease: Clinical-pathological report. *Journal of Neurology Neurosurgery and Psychiatry* 56:816-819

McBride MW, Brosnan M, Mathers J, McLellan LI, Miller WH, Graham D, Hanlon N, Hamilton CA, Polke JM, Lee WK, Dominiczak AF (2005) Reduction of Gstm1 expression in the stroke-prone spontaneously hypertension rat contributes to increased oxidative stress. *Hypertension* 45:786-792

McBride MW, Carr FJ, Graham D, Anderson NH, Clark JS, Lee WK, Charchar FJ, Brosnan MJ, Dominiczak AF (2003) Microarray analysis of rat chromosome 2 congenic strains. *Hypertension* 41:847-853

Memezawa H, Smith M-L, Siesjo BK (1992) Penumbral tissues salvaged by reperfusion following middle cerebral artery occlusion in rats. *Stroke* 23:552-559

Menzies SA, Betz A, Hoff J (1993) Contributions of ions and albumin to the formation and resolution of ischemic brain edema. *J Neurosurg* 78:257-266

Michihara A, Sawamura M, Yamori Y, Akasaki K, Tsuji H (2001) Mevalonate pyrophosphate decarboxylase in stroke-prone spontaneously hypertensive rat is reduced from the age of two weeks. *Biological and Pharmaceutical Bulletin* 24:1417-1419

Michihara A, Shimatani M, Anraku M, Tomida H, Akasaki K (2010) High levels of oxidative stress exist in the brain than serum or kidneys in stroke-prone spontaneously hypertensive rats at ten weeks of age. *Biol Pharm Bull* 33:518-521

Mies G, Hermann D, Ganten U, Hossmann K (1999) Hemodynamics and metabolism in stroke-prone spontaneously hypertensive rats before manifestation of brain infarcts. *J Cereb Blood Flow Metab* 19:1238-1246

Mihara T (1980) Study on pathogenesis of lacunar softening in the basal ganglia and thalamus. *Kitakanto Med J* 36:387-402

Milan C, Beuriat P, Gras P, Essayagh E, Arveux P, Dumas R (1991) Incidence and survival rates during a two-year period of intracerebral and subarachnoid haemorrhages, cortical infarcts, lacunes and transient ischaemic attacks. The stroke registry of Dijon:1985-1989 (1991). *Int J Epidemiol* 20:892-899

Miller M (2006) Hyponatremia and arginine vasopressin dysregulation: Mechanisms, clinical consequences, and management. *Journal of the American Geriatrics Society* 54:345-353

Minami M, Togashi H, Koike Y (1985) Changes in ambulation and drinking behavior related to stroke in stroke-prone spontaneously hypertensive rats. *Stroke* 16:44-48

Miyake K, Takeo S, Kaijihara H (1993) Sustained decrease in brain regional blood flow after microsphere embolism in rats. *Stroke* 24:415-420

Mizuno H, Ikeda M, Harada M, Onda T, Tomita T (1999) Sustained contraction to angiotensin II and impaired Ca2+-sequestration in the smooth muscle of stroke-prone spontaneously hypertensive rats. *American Journal of Hypertension* 12:590-595

Mohr JP (1982) Lacunes. *Stroke* 13:3-11

Molinari GF (1970a) Experimental cerebral infarction. II. Clinicopathological model of deep cerebral infarction. *Stroke 1(4):232-44,*-Aug

Molinari GF (1970b) Experimental Cerebral Infarction. I. Selective segmental occlusion of intracranial arteries in the dog. *Stroke* 1:224-237

Moody DM, Thore CR, Anstrom JA, Challa VR, Langefeld CD, Brown WR (2004) Quantification of afferent vessels shows reduced brain vascular density in subjects with leukoaraiosis. *Radiology* 233:883-890

Morris Z, Whiteley WN, Longstreth WT, Weber F, Lee Y, Tsushima Y, Alphs H, Ladd S, Warlow C, Wardlaw JM, Al-Shahi Salman R (2009) Incidental findings on brain magnetic resonance imaging: systematic review and meta-analysis. *BMJ* 339:b3016

Nabika T, Cui Z, Masuda J (2004) The stroke-prone spontaneously hypertensive rat: How good is it as a model for cerebrovascular diseases? *Cellular and Molecular Neurobiology* 24:639-646

Negishi H, Ikeda K, Sagara M, Sawamura M, Yamori Y (1999) Increased oxidative DNA damage in stroke-prone spontaneously hypertensive rats. *Clinical and Experimental Pharmacology and Physiology* 26:482-484

Nelson RF, Pullicino P, Kendall BE, Marshall J (1980) Computed tomography in patients presenting with lacunar syndromes. *Stroke* 11:256-261

Ng Y, Stein J, Ning M, Black-Schaffer RM (2007) Comparison of clinical characteristics and functional outcomes of ischemic stroke in different vascular territories. *Stroke* 38:2309-2314

Nishida N, Ogata J, Yutani C, Minematsu K, Yamaguchi T (2000) Cerebral artery thrombosis as a cause of striatocapsular infarction. a histopathological case study. *Cerebrovascular Diseases* 10:151-154

Nishio K, Ihara M, Yamasaki N, Kalaria RN, Maki T, Fujita Y, Ito H, Oishi N, Fukuyama H, Miyakawa T, Takahashi R, Tomimoto H (2010) A mouse model characterising features of vascular dementia with hippocampal atrophy. *Stroke* 41:1278-1284

Nitta T, Hata M, Gotoh S, Seo Y, Sasaki H, Hashimoto N, Furuse M, Tsukita S (2003) Size-selective loosening of the blood-brain barrier in claudin-5-deficient mice. *J Cell Biol* 161:653-660

Nordborg C, Fredriksson K, Johansson BB (1985) The morphometry of consecutive segments in cerebral arteries of normotensive and spontaneously hypertensive rats. *Stroke* 16:313-320

Norrving B (2004) Lacunar infarction: embolism is the key: against.[see comment][comment]. *Stroke* 35:1779-1780

Ogata J, Fujishima M, Tamaki K, Nakatomi Y, Ishitsuka T, Omae T (1980) Stroke-prone spontaneously hypertensive rats as an experimental model of malignant hypertension. *Acta Neuropathologica* 51:179-184

Ogata J (1999) The arterial lesions underlying cerebral infarction. *Neuropathology* 19:112-118

Ogata J, Fujishima M, Tamaki K, Nakatomi Y, Ishitsuka T, Omae T (1981) Vascular changes underlying cerebral lesions in stroke-prone spontaneously hypertensive rats. A serial section study. *Acta Neuropathologica* 54:183-188

Ogata J, Fujishima M, Tamaki K, Nakatomi Y, Ishitsuka T, Omae T (1982) Stroke-prone spontaneously hypertensive rats as an experimental model of malignant hypertension. A pathological study. *Virchows Archiv A, Pathological Anatomy & Histology* 394:185-194

Ogata J, Yutani C, Otsubo R, Yamanishi H, Naritomi H, Yamaguchi T, Minematsu K (2008) Heart and vessel pathology underlying brain infarction in 142 stroke patients. *Annals of Neurology* 63:770-781

Okamoto K, Aoki K (1963) Development of a strain of spontaneously hypertensive rat. *Japanese Circulation Journal* 27:282-293

Okamoto K, Yamori Y, Nagaoka A (1974) Establishment of the stroke prone spontaneously hypertensive rat. *Circulation Research* 34:143-153

Pantoni L, Sarti C, Alafuzoff I, Jellinger K, Munoz DG, Ogata J, Palumbo V (2006) Postmortem examination of vascular lesions in cognitive impairment: A survey among neuropathological services. *Stroke* 37:1005-1009

Papamitsakis N (2007) Lacunar Syndromes: eMedicine Neurology.

Patterson ME, Mouton CR, Mullins JJ, Mitchell KD (2005) Interactive effects of superoxide anion and nitric oxide on blood pressure and renal hemodynamics in transgenic rats with inducible malignant hypertension. *American Journal of Physiology - Renal Physiology* 289:F754-F759

Paxinos G, Watson C (2007) *The rat brain in stereotaxic coordinates.*, New York: Elsevier/Academic Press,

Pevsner PH, Eichenbaum JW, Miller DC, Pivawer G, Eichenbaum KD, Stern A, Zakian KL, Koutcher JA (2001) A photothrombotic model of small early ischemic infarcts in the rat brain with histologic and MRI correlation. *Journal of Pharmacological & Toxicological Methods* 45(3):227-233

Pico F, Labreuche J, Seilhean D, Duyckaerts C, Hauw J, Amarenco P (2007) Association of small-vessel disease with dilatative arteriopathy of the brain: Neuropathologic evidence. *Stroke* 38:1197-1202

Piechowski-Józwiak B, Bogousslavsky J (2008) Posterior circulation strokes. In: *Handbook of clinical neurology* (Fisher M, ed), Elsevier, pp 537-558

Poirier J, Gray F, Gherardi R, Derouesne C (1985) Cerebral lacunae.A new neuropathological classiication. *Rev Neurol (Paris)* 141:3-17

Polke JM (2008) Functional genomics in the stroke-prone spontaneously hypertensive rat: Genome wide and candidate gene analysis. University of Glasgow,

Pope F, Narcisi P, Nicholls AC, Germaine D, Pals G, Richards A (1996) Col3a1 mutations cause variable clinical phenotypes including acrogeria and vascular rupture. *British Journal of Dermatology* 135:163-181

Potter G, Doubal F, Jackson C, Sudlow C, Dennis MS, Wardlaw J (2010a) Associations of clinical stroke misclassification ('clinical-imaging dissociation') in acute ischemic stroke. *Cerebrovasc Dis* 29:395-402

Potter GM, Doubal FN, Jackson CA, Chappell FM, Sudlow CL, Dennis MS, Wardlaw JM (2010b) Counting cavitating lacunes underestimates the burden of lacunar infarction. *Stroke* 41:267-272

Potter GM, Marlborough FJ, Wardlaw JM (2011) Wide variation in definition, detection, and description of lacunar lesions on imaging. *Stroke* 42:359-366

Pullicino P, Nelson RF, Kendall BE, Marshall J (1980) Small deep infarcts diagnosed on computed tomography. *Neurology* 30:1090

Purves D, Augustine G, Fitzpatrick D, Hall W, LaMantia A, McNamara JWL (2007) *Neuroscience*, Sinauer Associates,

Racasan S, Braam B, Koomans HA, Joles JA (2005) Programming blood pressure in adult SHR by shifting perinatal balance of NO and reactive oxygen species toward NO: the inverted Barker phenomenon. *American Journal of Physiology - Renal Physiology* 288:F626-F636

Reed D, Jacobs J, Hayashi T, Konishi M, Nelson J, Iso H, Strong J (1994) A comparison of lesions in small intracerebral arteries among Japanese men in Hawaii and Japan. *Stroke* 25:60-65

Revesz T, Hawkins CP, du Boulay EP, Barnard RO, McDonald WI (1989) Pathological findings correlated with magnetic resonance imaging in subcortical arteriosclerotic encephalopathy (Binswanger's disease). *Journal of Neurology, Neurosurgery & Psychiatry* 52:1337-1344

Rieke GK, Bowers DE, Jr., Penn P (1981) Vascular supply pattern to rat caudatoputamen and globus pallidus: scanning electronmicroscopic study of vascular endocasts of stroke-prone vessels. *Stroke* 12:840-847

Rodda RA, Brain T, Jones S (1983) Parenchymal brain lesions in spontaneously hypertensive stroke-prone rats. *Clinical & Experimental Neurology* 19:147-158

Rodriguez I, Lema I, Blanco M, Rodriguez-Yanez M, Leira R, Castillo J (2010) Vascular retinal, neuroimaging and ultrasonographic markers of lacunar infarcts. *International Journal of Stroke* 5 (5):360-366

Roman GC, Erkinjuntti T, Wallin A, Pantoni L, Chui HC (2002) Subcortical ischaemic vascular dementia. *The Lancet Neurology* 1:426-436

Roos MW, Sperber GO (1998) Effects of microemboli on local blood flow in the rabbit brain. *Experimental Neurology* 149(2):384-389

Roos MW, Sperber GO, Johansson A, Bill A (1996) An experimental model of cerebral microischemia in rabbits. *Experimental Neurology* 137:73-80

Roozen P, van Kempen, L (2010) LCM Staining Effects on Real-Time RT-PCR.

Rosenberg GA, Sullivan N, Esiri MM, Sobel RA (2001) White matter damage is associated with matrix metalloproteinases in vascular dementia (editorial comment) : Matrix metalloproteinases and diffuse white matter injury. *Stroke* 32:1162-1168

Ross M, Pawlina W (2005) *Histology: A text and atlas*, Lippincott Williams & Wilkins,

Rossi R, Joachim C, Geroldi C, Combrinck M, Esiri MM, Smith AD, Frisoni GB (2004) Association between subcortical vascular disease on CT and neuropathological findings. *International Journal of Geriatric Psychiatry* 19:690-695

Rossmeisl JH, Jr., Rohleder JJ, Pickett JP, Duncan R, Herring IP (2007) Presumed and confirmed striatocapsular brain infarctions in six dogs. *Veterinary Ophthalmology 10(1):23-36,*-Feb

Rothermund L, Luckert S, Mehl P, Paul M, Kreutz R (2001) Renal endothelin ETA/ETB receptor imbalance differentiates salt-sensitive from salt-resistant spontaneous hypertension. *Hypertension* 37:275-280

Rothwell PM, Coull AJ, Giles MF, Howard SC, Silver LE, Bull LM, Gutnikov SA, Edwards P, Mant D, Sackley CM, Farmer A, Sandercock PAG, Dennis MS, Warlow CP, Bamford JM, Anslow P (2004) Change in stroke incidence, mortality, case-fatality, severity, and risk factors in Oxfordshire, UK from 1981 to 2004 (Oxford Vascular Study). *The Lancet* 363:1925-1933

Rubattu S, Lee-Kirsch M, DePaolis P, Giliberti R, Gigante B, Lombardi A, Volpe M, Lindpaintner K (1999) Altered structure, regulation, and function of the gene encoding the atrial natriuretic peptide in the stroke-prone spontaneously hypertensive rat. *Circ Res* 85:900-905

Rubattu S, Volpe M, Kreutz R, Ganten U, Ganten D, Lindpaintner K (1996) Chromosomal mapping of quantitative trait loci contributing to stroke in a rat model of complex human disease. *Nat Genet* 13:429-434

Ruchoux MM, Domenga V, Brulin P, Maciazek J, Limol S, Tournier-Lasserve E, Joutel A (2003b) Transgenic mice expressing mutant Notch3 develop vascular alterations characteristic of cerebral autosomal dominant arteriopathy with subcortical infarcts and leukoencephalopathy. *American Journal of Pathology 162(1):329-42,*

Sadoshima S, Heistad D (1982) Sympathetic nerves protect the blood-brain barrier in stroke-prone spontaneously hypertensive rats. *Hypertension* 4:904-907

Sadoshima S, Heistad DD (1983) Regional cerebral blood flow during hypotension in normotensive and stroke-prone spontaneously hypertensive rats: Effect of sympathetic denervation. *Stroke* 14:575-579

Saito H, Togashi H, Yoshioka M, Nakamura N, Minami M, Parvez H (1995) Animal models of vascular dementia with emphasis on stroke-prone spontaneously hypertensive rats. *Clinical and Experimental Pharmacology and Physiology* 22:S257-S259

Samuelsson M, Lindell D, Norrving B (1994) Gadolinium-enhanced magnetic resonance imaging in patients with presumed lacunar infarcts. *Cerebrovascular Diseases* 4:12-19

Schlaich MP, Parnell MM, Ahlers BA, Finch S, Marshall T, Zhang W, Kaye DM (2004) Impaired l-arginine transport and endothelial function in hypertensive and genetically predisposed normotensive subjects. *Circulation* 110:3680-3686

Schmidlin O, Tanaka M, Bollen AW, Yi S-L, Morris J (2005) Chloride-dominant salt sensitivity in the stroke-prone spontaneously hypertensive rat. *Hypertension* 45:867-873

Schneider JA, Bienias JL, Wilson RS, Berry-Kravis E, Evans DA, Bennett DA (2005) The apolipoprotein E epsilon4 allele increases the odds of chronic cerebral infection detected at autopsy in older persons. *Stroke* 36:954-959

Schuff N, Capizzano AA, Du AT, Amend DL, O'Neill J, Norman D, Jagust WJ, Chui HC, Kramer JH, Reed BR, Miller BL, Yaffe K, Weiner MW (2003) Different patterns of N-acetylaspartate loss in subcortical ischemic vascular dementia and AD. *Neurology* 61:358-364

Sekiguchi F, Miyake Y, Hirakawa A, akahira T, amaoka M, himamura K, amamoto K, unano S (2001) Hypertension and impairment of endothelium-dependent relaxation of arteries from spontaneously hypertensive and L-NAME-treated Wistar rats. *Journal of Smooth Muscle Research* 37:67-79

Sena E, van der Worp H, Howells D, Macleod M (2007) How can we improve the pre-clinical development of drugs for stroke? *Trends in Neurosciences* 30:433-439

Seubert JM, Xu F, Graves JP, Collins JB, Sieber SO, Paules RS, Kroetz DL, Zeldin DC (2005) Differential renal gene expression in prehypertensive and hypertensive spontaneously hypertensive rats. *Am J Physiol Renal Physiol* 289:F552-F561

Sharkey J, Ritchie IM, Kelly PA (1993) Perivascular microapplication of endothelin-1: A new model of focal cerebral ischaemia in the rat. pp 865-871

Shibata M, Ohtani R, Ihara M, Tomimoto H (2004) White matter lesions and glial activation in a novel mouse model of chronic cerebral hypoperfusion. *Stroke* 35:2598-2603

Shimamura T, Nakajima M, Iwasaki T, Hayasaki Y, Yonetani Y, Iwaki K (1999) Analysis of circadian blood pressure rhythm and target-organ damage in stroke-prone spontaneously hypertensive rats. *Journal of Hypertension* 17:211-220

Shimizu S, Nara Y, Yamada K, Keiser HR, Yamori Y (1988) Cellular mechanisms of hypertension and atherosclerosis: hypoxia-induced lipid accumulation in cultured vascular smooth muscle cells from the stroke-prone spontaneously hypertensive rat. *Journal of Hypertension* 6:S163-S165

Sironi L, Calvio A, Bellosta S, Lodetti B, Guerrini U, Monetti M, Tremoli E, Mussoni L (2003) Endogenous proteolytic activity in a rat model of spontaneous cerebral stroke. *Brain Research* 974:184-192

Sironi L, Guerrini U, Tremoli E, Miller I, Gelosa P, Lascialfari A, Zucca I, Eberini I, Gemeiner M, Paoletti R, Gianazza E (2004) Analysis of pathological events at the onset of brain damage in stroke-prone rats: A proteomics and magnetic resonance imaging approach. *Journal of Neuroscience Research* 78(1):115-122

Sironi L, Tremoli E, Miller I, Guerrini U, Calvio AM, Eberini I, Gemeiner M, Asdente M, Paoletti R, Gianazza E (2001) Acute-phase proteins before cerebral ischemia in stroke-prone rats: Identification by proteomics. *Stroke* 32:753-760

Smeda JS, King S (1999) Cerebrovascular alterations in protein kinase C-mediated constriction in stroke-prone rats. *Stroke* 30:656-661

Smeda JS, King S (2000) Electromechanical alterations in the cerebrovasculature of stroke-prone rats. *Stroke* 31:751-759

Smeda JS, VanVliet BN, King SR (1999) Stroke-prone spontaneously hypertensive rats lose their ability to auto-regulate cerebral blood flow prior to stroke. *Journal of Hypertension* 17:1697-1705

Sounni NE, Dehne K, van Kempen L, Egeblad M, Affara NI, Cuevas I, Wiesen J, Junankar S, Korets L, Lee J, Shen J, Morrison CJ, Overall CM, Krane SM, Werb Z, Boudreau N, Coussens LM (2010) Stromal regulation of vessel stability by MMP14 and TGFb. *Disease Models & Mechanisms* 3:317-332

Stevenson SF, Doubal FN, Shuler K, Wardlaw JM (2010) A systematic review of dynamic cerebral and peripheral endothelial function in lacunar stroke versus controls. *Stroke* 41:e434-e442

Stier C, Benter IF, Levine S (1988) Thromboxane A2 in severe hypertension and stroke in stroke-prone spontaneously hypertensive rats. *Stroke* 19:1145-1150

Stroup DF, Berlin JA, Morton SC, Olkin I, Williamson GD, Rennie D, Moher D, Becker BJ, Sipe T, Thacker SB, for the Meta-analysis Of Observational Studies in Epidemiology Group (2000) Meta-analysis of observational studies in epidemiology: A proposal for reporting. *JAMA* 283:2008-2012

Su MY, Head E, Brooks W, Nalcioglu O (1998) Magnetic Resonance Imaging of Anatomic and Vascular Characteristics in a Canine Model ofHuman Aging [abstract]. *Neurobiology of Aging* 19 (5):479-485

Sudlow CLM, Warlow CP (1997) Comparable studies of the incidence of stroke and its pathological types: Results from an international collaboration. *Stroke* 28:491-499

Sunano S, Watanabe H, Tanaka S, Sekiguchi F, Shimamura K (1999) Endothelium-derived relaxing, contracting and hyperpolarizing factors of mesenteric arteries of hypertensive and normotensive rats. *British Journal of Pharmacology* 126:709-716

Syme PD, Byrne AW, Chen R, Devenny R, Forbes JF (2005) Community-based stroke incidence in a scottish population: The scottish borders stroke study. *Stroke* 36:1837-1843

Tabuchi M, Umegaki K, Ito T, Suzuki M, Tomita I, Ikeda M, Tomita T (2002) Fluctuation of serum NOx concentration at stroke onset in a rat spontaneous stroke model (M-SHRSP): Peroxynitrite formation in brain lesions. *Brain Research* 949:147-156

Tagami M, Kubota A, Sunaga T (1981) Permeability of intracranial extracerebral vessels in stroke-prone SHR. *Stroke* 12:852-857

Tagami M, Nara Y, Kubota A, Sunaga T, Maezawa H, Fujino H, Yamori Y (1987) Ultrastructural characteristics of occluded perforating arteries in stroke-prone spontaneously hypertensive rats. *Stroke* 18:733-740

Taka T, Ohta Y, Seki J, Giddings JC, Yamamoto J (2002) Impaired flow-mediated vasodilation in vivo and reduced shear-induced platelet reactivity in vitro in response to nitric oxide in prothrombotic, stroke-prone spontaneously hypertensive rats. *Pathophysiology of Haemostasis and Thrombosis* 32:184-189

Takeshita A, Imaizumi T, Ashihara T, Nakamura M (1982) Adrenergic mechanisms do not contribute to salt-induced vasoconstriction in stroke-prone spontaneously hypertensive rat. *Hypertension* 4:288-293

Takiguchi K (1983) Experimental hypertension pathological study of the cerebrovascular lesions of stroke-prone spontaneously hypertensive rat. *Acta Medica Nagasakiensia* 28:46-63

Tamaki K, Sadoshima S, Baumbach GL, Iadecola C, Reis DJ, Heistad DD (1984a) Evidence that disruption of the blood-brain barrier precedes reduction in cerebral blood flow in hypertensive encephalopathy. *Hypertension* 6:75-81

Tamaki K, Sadoshima S, Heistad DD (1984b) Increased susceptibility to osmotic disruption of the blood-brain barrier in chronic hypertension. *Hypertension* 6:633-638

Tanaka Y, Imai H, Konno K, Miyagishima T, Kubota C, Puentes S, Aoki T, Hata H, Takata K, Yoshimoto Y, Saito N (2008) Experimental model of lacunar infarction in the gyrencephalic brain of the miniature pig: Neurological assessment and histological,

immunohistochemical, and physiological evaluation of dynamic corticospinal tract deformation. *Stroke* 39:205-212

Thompson CS, Hakim AM (2009) Living beyond our physiological means: Small vessel disease of the brain is an expression of a systemic failure in arteriolar function: A unifying hypothesis. *Stroke* 40:e322-e330

Thompson LE, Rinaldi GJ, Bohr DF (1988) Sodium-calcium exchange in vascular smooth muscle of Wistar-Kyoto and stroke-prone spontaneously hypertensive rats. *Journal of Hypertension* 6:S160-S162

Thorvaldsen P, Kuulasmaa K, Rajakangas A, Rastenyte D, Sarti C, Wilhelmsen L (1997) Stroke Trends in the WHO MONICA Project. *Stroke* 28:500-506

Tomimoto H, Shibata M, Ihara M, Akiguchi I, Ohtani R, Budka H (2002) A comparative study on the expression of cyclooxygenase and 5-lipoxygenase during cerebral ischemia in humans. *Acta Neuropathologica* 104:601-607

Tomita T, Umegaki K, Hayashi E (1984) Hypoaggregability of washed platelets from stroke-prone spontaneously hypertensive rats (SHRSP). *Stroke* 15:70-75

Topakian R, Barrick TR, Howe FA, Markus HS (2010) Blood brain barrier permeability is increased in normal-appearing white matter in patients with lacunar stroke and leucoaraiosis. *Journal of Neurology, Neurosurgery & Psychiatry* 81:192-197

Toshima Y, Satoh S, Ikegaki I, Asano T (2000) A new model of cerebral microthrombosis in rats and the neuroprotective effect of a Rho-kinase inhibitor. *Stroke 31(9):2245-50,*

Tunon J, Ruiz-Ortega M, Egido J (2000) Regulation of matrix proteins and impact on vascular structure. *Current Hypertension Reports* 2:106-113

Tuszynski MH, Petito CK, Levy DE (1989) Risk factors and clinical manifestations of pathologically verified lacunar infarctions. *Stroke* 20:990-999

Udaka F, Sawada H, Kameyama M (2002) White matter lesions and dementia. *Ann N Y Acad Sci* 977:411-415

Uehara Y (2003) The world of endothelin in the brain of the stroke-prone spontaneously hypertensive rat. *Journal of Hypertension* 21:23-25

Ueno M, Sakamoto H, Liao Y, Onodera M, Huang C, Miyanaka H, Nakagawa T (2004a) Blood-brain barrier disruption in the hypothalamus of young adult spontaneously hypertensive rats. *Histochemistry and Cell Biology* 122:131-137

Ueno M, Tomimoto H, Akiguchi I, Wakita H, Sakamoto H (2002) Blood brain barrier disruption in white matter lesions in a rat model of chronic cerebral hypoperfusion. *J Cereb Blood Flow Metab* 22:97-104

Ueno M, Sakamoto H, Tomimoto H, Akiguchi I, Onodera M, Huang C-L, Kanenishi K (2004b) Blood-brain barrier is impaired in the hippocampus of young adult spontaneously hypertensive rats. *Acta Neuropathologica* 107:532-538

Ueno M, Wu B, Nishiyama A, Huang C-L, Hosomi N, Kusaka T, Nakagawa T, Onodera M, Kido M, Sakamoto H (2009) The expression of matrix metalloproteinase-13 is

increased in vessels with blood-brain barrier impairment in a stroke-prone hypertensive model. *Hypertension Research* 32:332-338

Umegaki K, Nakamura K, Tomita T (1986) Primary dysfunction in aggregation and secretion of stroke-prone spontaneously hypertensive rat platelets not secondary to the circulation of exhausted platelets. *Blut* 52:17-28

Unger T (2002) The role of the renin-angiotensin system in the development of cardiovascular disease. *The American Journal of Cardiology* 89:3-9

Ursino M, Gianessi M (2010) A model of cerebrovascular reactivity including the circle of willis and cortical anastomoses. *Ann Biomed Eng* 38:955-974

Vajda J, Branston NM, Ladds A, Symon L (1985) A model of selective experimental ischaemia in the primate thalamus. *Stroke* 16:493-501

van Swieten JC, van den Hout J, van Ketel BA, Hijdra A, Wokke J, van Gijn J (1991) Periventricular lesions in the white matter on magnetic resonance imaging in the elderly. *Brain* 114:761-774

Vinters HV, Ellis W, Jagust W, Ellis C, Zaias B, Chui H, Mack W (2000) Neuropathologic substrates of ischemic vascular dementia. *Journal of Neuropathology and Experimental Neurology* 59:931-945

Virdis A, Ghiadoni L, Giannarelli C, Taddei S (2010) Endothelial dysfunction and vascular disease in later life. *Maturitas* 67:20-24

Volpe M, Iaccarino G, Vecchione C, Rizzoni D, Russo R, Rubattu S, Condorelli G, Ganten U, Ganten D, Trimarco B, Lindpaintner K (1996) Association and cosegregation of stroke with impaired endothelium- dependent vasorelaxation in stroke prone, spontaneously hypertensive rats. *Journal of Clinical Investigation* 98:256-261

von Elm E, Altman DG, Egger M, Pocock SJ, Gotzsche PC, Vandenbroucke JP (2007) The Strengthening the Reporting of Observational Studies in Epidemiology (STROBE) Statement: Guidelines for reporting observational studies. *Preventive Medicine* 45:247-251

Wagerle L, Orr JA, Shirer HW, Kiorpes AL, Fraser DB, DeSoignie RC (1983) Cerebrovascular response to acute decreases in arterial PO2. *J Cereb Blood Flow Metab* 3:507-515

Walters FJM (1998) Intracranial pressure and cerebral blood flow. *Update in Anaesthesia* 8:1-4

Wang K, Walz W (2003) Unusual topographical pattern of proximal astrogliosis around a cortical devascularizing lesion. *Journal of Neuroscience Research 73(4):497-506,*

Wang L, Larson E, Sonnen J, Shofer J, McCormick W, Bowen J, Montine T, Li G (2009) Blood pressure and brain injury in older adults: Findings from a community-based autopsy study. *J Am Geriatr Soc* 57:1975-1981

Wardlaw J, Doubal F, Armitage P, Chappell F, Carpenter T, Munoz Maniega S, Farrall A, Sudlow C, Dennis MS, Dhillon B (2009) Lacunar stroke is associated with diffuse blood brain barrier dysfunction. *Ann Neurol* 65:194-202

Wardlaw JM, Farrall A, Armitage PA, Carpenter T, Chappell F, Doubal F, Chowdhury D, Cvoro V, Dennis MS (2008) Changes in background blood-brain barrier integrity between lacunar and cortical ischemic stroke subtypes. *Stroke* 39:1327-1332

Wardlaw JM, Dennis MS, Warlow CP, Sandercock PA (2001) Imaging appearance of the symptomatic perforating artery in patients with lacunar infarction: Occlusion or other vascular pathology? *Ann Neurology* 50:208-215

Wardlaw JM (2005) What causes lacunar stroke? *Journal of Neurology, Neurosurgery and Psychiatry* 76:617-619

Wardlaw JM (2008) What is a lacune? *Stroke* 39:2921-2922

Wardlaw JM, Doubal FN, Eadie E, Chappell F, Shuler K, Cvoro V (2011) Little association between intracranial arterial stenosis and lacunar stroke. *Cerebrovascular Diseases* 31(1):12-18

Wardlaw JM, Sandercock PAG, Dennis MS, Starr J, Kalimo H (2003) Is breakdown of the blood-brain barrier responsible for lacunar stroke, leukoaraiosis, and dementia? *Stroke* 34:806-812

Warlow C, van Gijn J, Dennis MS, Wardlaw J, Bamford J, Hankey GJ, Sandercock P, Rinkel GJ, Langhorne P, Sudlow C, Rothwell PM (2008a) Specific treatment of primary intracerebral haemorrhage. In: *Stroke: Practical Management* Blackwell Science, pp 509-518

Warlow C, van Gijn J, Dennis MS, Wardlaw J, Bamford J, Hankey GJ, Sandercock P, Rinkel GJ, Langhorne P, Sudlow C, Rothwell PM (2008b) What caused this transient or persisting ischaemic event? In: *Stroke: Practical management* Blackwell Science, pp 223-300

Warlow C, van Gijn J, Dennis MS, Wardlaw J, Bamford J, Hankey GJ, Sandercock P, Rinkel GJ, Langhorne P, Sudlow C, Rothwell PM (2008c) What pathological type of stroke is it? In: *Stroke: Practical Management* Blackwell Science, pp 151-222

Warlow C, van Gijn J, Dennis MS, Wardlaw J, Bamford J, Hankey GJ, Sandercock P, Rinkel GJ, Langhorne P, Sudlow C, Rothwell PM (2008d) Which arterial territory is involved? Developing a clnically-based method of subclassification. In: *Stroke: Practical Management* Blackwell Science, pp 106-151

Warlow C, van Gijn J, Dennis MS, Wardlaw J, Bamford JM, Hankey GJ, Sandercock P, Rinkel GJ, Langhorne P, Sudlow C, Rothwell PM (2008e) Is it a vascular event and where is the lesion? Identifying and interpreting the symptoms and signs of cerebrovascular disease. In: *Stroke: Practical management* Blackwell Science, pp 28-105

Werber AH, Heistad DD (1984) Effects of chronic hypertension and sympathetic nerves on the cerebral microvasculature of stroke-prone spontaneously hypertensive rats. *Circulation Research* 55:286-294

Whitehead SN, Hachinski VC, Cechetto DF (2005) Interaction between a rat model of cerebral ischemia and {beta}-amyloid toxicity: Inflammatory responses. *Stroke* 36:107-112

Wit E, McClure J (2004) *Statistics for microarray: Design, analysis, and inference.*, Wiley-Blackhall,

Wuerfel J, Haertle M, Waiczies H, Tysiak E, Bechmann I, Wernecke KD, Zipp F, Paul F (2008) Perivascular spaces--MRI marker of inflammatory activity in the brain? *Brain*171-180

Yamada T, Miyazaki K, Koshikawa N, Takahashi M, Akatsu H, Yamamoto T (1995) Selective localization of gelatinase A, an enzyme degrading ß-amyloid protein, in white matter microglia and in Schwann cells. *Acta Neuropathologica* 89:199-203

Yamamoto E, Tamamaki N, Nakamura T, Kataoka K, Tokutomi Y, Dong Y-F, Fukuda M, Matsuba S, Ogawa H, Kim-Mitsuyama S (2008) Excess salt causes cerebral neuronal apoptosis and inflammation in stroke-prone hypertensive rats through angiotensin II-induced NADPH oxidase activation. *Stroke* 39:3049-3056

Yamori Y, Horie R, Sato M, Sasagawa S, Okamoto K (1975) Experimental studies on the pathogenesis and prophylaxis of stroke in stroke-prone spontaneously hypertensive rats. 1. Quantitative estimation of cerebrovascular permeability. *Japanese Circulation Journal* 39:611-615

Yamori Y, Horie R (1977) Developmental course of hypertension and regional cerebral blood flow in stroke-prone spontaneously hypertensive rats. *Stroke* 8:456-461

Yamori Y, Horie R, Handa H, Sato M, Fukase M (1976a) Pathogenetic similarity of strokes in stroke-prone spontaneously hypertensive rats and humans. *Stroke* 7:46-53

Yamori Y, Horie R, Sato M, Fukase M (1976b) Hypertension as an important factor for cerebrovascular atherogenesis in rats. *Stroke* 7:120-125

Yang TLC, Chai CY, Yen C-T (1995) Enhanced sympathetic reactivity to glutamate stimulation in medulla oblongata of spontaneously hypertensive rats. *American Journal of Physiology - Heart and Circulatory Physiology* 268:H1499-H1509

Yang Y, Shuaib A, Li Q (1998) Quantification of infarct size on focal cerebral ischemia model of rats using a simple and economical method. *Journal of Neuroscience Methods* 84:9-16

Yonas H, Wolfson SK, Jr., Dujovny M, Boehnke M, Cook E (1981) Selective lenticulo striate occlusion in the primate a highly focal cerebral ischemia model. *Stroke* 12:567-572

Yoshimoto T, Sakamoto T, Suzuki J (1978) Experimental cerebral infarction. Part 1: Production of thalamic infarction in dogs. *Stroke 9(3):211-4*,-Jun

Youman P, Wilson K, Harraf F, Kalra L (2003) The economic burden of stroke in the United Kingdom. *Pharmacoeconomics* 21:43-50

Zanchi A, Brunner HR, Hayoz D (1997) Age-related changes of the mechanical properties of the carotid artery in spontaneously hypertensive rats. *Journal of Hypertension* 15:1415-1422

Zhang A-J, Yu X-J, Wang M (2010) The clinical manifestations and pathophysiology of cerebral small vessel disease. *Neuroscience Bulletin* 26 (3):257-264

Zhang K, Sejnowski TJ (2000) A universal scaling law between gray matter and white matter of cerebral cortex. *Proceedings of the National Academy of Sciences* 97:5621-5626

Zhu Y, Tzourio C, Soumare A, Mazoyer B, Dufouil C, Chabriat H (2010) Severity of dilated virchow-robin spaces is associated with age, blood pressure, and MRI markers of small vessel disease: A population-based study. *Stroke* 41:2483-2490

Zylberstein D, Skoog I, Björkelund C, Guo X, Hultén B, Andreasson L, Palmertz B, Thelle D, Lissner L (2008) Homocysteine levels and lacunar brain infarcts in elderly women: The prospective population study of women in gothenburg. *Journal of the American Geriatrics Society* 56:1087-1091

APPENDIX A) THE SEARCH STRATEGY DEVISED FOR RETRIEVING HUMAN LACUNAR STROKE PATHOLOGY LITERATURE.

This search strategy was applied across both Medline and Embase databases. Mesh terms were altered automatically to match each database by the programme as both are owned by Ovid.

1. brain edema/ or cerebrovascular disorders/ or basal ganglia cerebrovascular disease/ or brain ischemia/ or cadasil/ or cerebral arterial diseases/ or intracranial arteriosclerosis/ or "intracranial embolism and thrombosis"/ or stroke/ or brain infarction/ or vasospasm, intracranial/ or hypoxia, brain/ or hypertensive encephalopathy/

2. (Stroke$ or cerebrovasc$).mp. or cerebral vasc$.tw. [mp=title, original title, abstract, name of substance word, subject heading word]

3. 1 or 2

4. lacun$.tw.

5. ((lacunar or small or subcortical or silent or micro) adj5 (infarct$ or lesion$ or stroke$)).tw.

6. (small vessel adj5 (stroke$ or occlusion or disease)).tw.

7. 4 or 5 or 6

8. (leukoaraiosis or leucoaraiosis or leukoariosis or leucoariosis or MARCD or microangiopathy related cerebral damage or microangiopathy-related cerebral damage).tw.

9. (white matter lesion$ or WML or white matter hyperintensit$ or WMH or white matter change$ or small vessel disease or small-vessel disease or microangiopath$ or white matter hypointensit$ or white matter hyperdens$ or white matter hypodens$).tw.

10. 8 or 9

11. (caus$ or histolog$ or immunohisto$ or patholog$ or autopsy).tw.

12. (Lipohyalinosis or fibrinoid necrosis or hyaline thickening).tw.

13. ((enlarged or dilated) adj3 perivascular spaces).tw.

14. 7 or 13 or 10 or 12

15. 3 and 14

16. 11 and 15

17. limit 16 to humans

18. (CADASIL or Notch3 or NOTCH3).tw.

19. 18 and 17

20. (vascular dementia or VaD or Alzheimer$).tw.

21. 17 and 20

22. 21 not 18

23. from 22 keep 1-259

24. 16 not (19 or 22).

APPENDIX B) The data extraction form used to compile the systematic review of human lacunar stroke pathology.

HT = Hypertension. DM = Diabetes Mellitus, AF = Atrial Fibrillation. DWI = Diffusion Weighted Imaging.

STUDY CHARACTERISTICS	Options	
Author		
Date of Publication		
Prospective / Retrospective Study		
Population Type & Source	e.g. General, Stroke Specific, Outpatient, Brain Bank etc	
Number of Subjects		
PATIENT CHARACTERISTICS		
Clinical History Available?		
Vascular Risk Factors analysed.	HT, DM, Smoking, AF, Hypercholestrolaemia etc	
Cognitive Status	Dementia scale?	
Medication (e.g. Anti-Hypertensives)		
Mean Age at Death		
Cause(s) of Death		
CLINICAL METHODOLOGY		
Time from Stroke to Admission		
Presence of a Lacunar Syndrome?		
Imaging Method	MRI, CT, Both, DWI etc	
Other clinical methods	Angiography, blood samples etc.	

Data extraction form continued……

PATHOLOGICAL METHODOLOGY	
Time from death to post mortem / post mortem to histopathology	
Post Mortem Imaging?	Whole brain, specific blocks etc
Histopathology methods	Fixative, stains
Who performed the histological assessment?	Pathologist, Technician, Neuropathologist?
Number of observers	
RESULTS	
Mean number of Infarcts per patient	
Infarct /Lesion – symptomatic / asymptomatic	Lesion directly related to syndrome / symptoms / imaging feature?
Brain region studied / affected	
Mean size of lesion / lesion classed as lacunar.	Diameter / volume?
Vessels studied	Territory / specific vessel
Description of vascular pathology	
Proposed causative mechanism	

APPENDIX C) The search strategy used to find potential animal models of lacunar stroke within the published literature.

Like the human lacunar pathology search strategy above, Mesh terms were converted by Ovid to match those in Medline and Embase respectively. Mesh terms were also matched as closely as possible with terms in Biosis Previews.

1. exp Models, Biological/ or exp Disease Models, Animal/ or exp Models, Animal/

2. (experimental adj5 stroke).tw.

3. Animals/

4. exp mammals/ or exp primates/ or exp mice/ or exp rats/ or exp rats, inbred strains/ or exp rats, mutant strains/

5. 1 or 2 or 3 or 4

6. exp cerebrovascular disorders/ or exp basal ganglia cerebrovascular disease/ or exp brain ischemia/ or exp cerebrovascular accident/ or exp brain infarction/ or exp hypoxia-ischemia, brain/

7. brain edema/ or cerebrovascular accident/ or exp dementia, vascular/ or exp intracranial arterial diseases/ or exp "intracranial embolism and thrombosis"/ or exp vasospasm, intracranial/

8. (Stroke$ or cerebrovasc$ or cerebral vasc$ or cerebral$).tw.

9. 6 or 7 or 8

10. 5 and 9

11. limit 10 to animals

12. (((micro or small or perforat$) adj3 vessel) or arteriole).tw.

13. (lacunar stroke or lacunar infarct).tw.

14. (focal or multifocal or subcortical).tw.

15. (emboli or microemboli).tw.

16. (Blood brain barrier or BBB or plasma proteins).tw.

17. ((small or micro) adj5 (stroke$ or occlusion$ or disease$)).tw.

18. ((lacun$ or small or subcortical or deep or silent) adj5 (infarct$ or lesion$ or stroke$)).tw.

19. (microgli$ or astrocyte).tw.

20. 12 or 13 or 14 or 15 or 16 or 17 or 18 or 19

21. 11 and 20

22. limit 21 to humans

23. 21 not 22

24. (heart or bone or eye or lung or kidney or liver or renal or intestin$ or spinal or pulmonary or hepatic or global).mp. [mp=title, abstract, subject headings, heading word, drug trade name, original title, device manufacturer, drug manufacturer name]

25. 23 not 24

26. (AD or PD or Alzheimer$ or Parkinson$ or epilepsy or MS or Multiple Sclerosis).tw.

27. 25 not 26.

APPENDIX D) THE DATA EXTRACTION FORM USED TO COMPILE THE SYSTEMATIC REVIEW OF POTENTIAL ANIMAL MODELS OF LACUNAR STROKE.

1.1	Author	
1.2	Country of origin	
1.3	Reference and date of publication	
1.4a 1.4b 1.4c	Stated purpose of research Explicitly lacunar related? Yes/No Which aspect of pathology is the paper trying to model?	
1.5	Species and strain of animals used (Rat,Wistar etc.)	
1.6	Total number of animals used	
1.7a 1.7b 1.7c	Weight Age Sex of animals used	
1.8	Comorbidities of animals used: Diabetes Hypertension Hypercholestrolaemia Cardiac problems Other – please state None	

Data extraction form continued……..

1.9a 1.9b	Method of stroke induction: Intraluminal thread ET-1 Injection Photothrombosis Spontaneous Embolism Other (please state) Blinded Induction (Yes/No)	
1.10	Anaesthetic used: Halothane Isoflurane Ketamine Sodium Pentobarbital Enflurane Urethane Other (please state)	
1.11	Control of physiological variables: Body Temperature (Y/N) Blood pressure (Y/N) Respiration rate (Y/N)	
1.12a 12b	Method of sacrifice: Cardiac Perfusion Other (please state) Time of sacrifice in relation to administration of ischemia (hours/days/weeks)	

Data extraction form continued……..

1.13a 1.13b	Size of infarct produced and units of measurement (area, volume, diameter etc.) Method of measurement (e.g. microscopic calibrator, imaging, area on histology sections etc.)	
1.14	Territory of infarct produced	
1.15	Definition of infarct	
1.16	Outcome measure(s): Histology Imaging Neurobehavioural assessment Microscopy Other (please state)	
 1.17a 1.17b 1.17c 1.17d	If Histology……. Type of staining used Number of sections taken Size of sections taken (µm / mm) Blood vessel separated (Y/N)	

Data extraction form continued……

1.18a 1.18b	Results: Neurological symptoms? How many had infarcts on MRI? Etc Mortality rate (% total of animals used)	
1.19	Blinded assessment of outcome (Y/N)	
1.20	Observer reliability (e.g. more than one observer?)	
Notes	Any additional useful information	

APPENDIX E) SUMMARY OF THE STUDIES INCLUDED FOR ANALYSIS IN THE SYSTEMATIC REVIEW OF THE CEREBRAL PATHOLOGY OF THE SHRSP, IN CHRONOLOGICAL ORDER;

Abbreviations: n/a = information unobtainable, unclear or irrelevant. BG = basal ganglia, BA = basilar artery, MCA = middle cerebral artery, ACA = anterior cerebral artery, PCA = posterior cerebral artery, CC = corpus callosum, AC = anterior commisure, IC = internal capsule, CP = caudate and putamen, GP = globus pallidus, WM = white matter, CB = cerebellum, MB = midbrain, HT = hypothalamus, MO = medulla oblongata, HP = hippocampus, ST = striatum. N= total number of experimental animals used – in general this equated to 50% WKY and 50% SHRSP unless otherwise stated. $ = All SHRSP, # = SHR included as well as WKY.

Author	Date	N	Age at sacrifice	Salt loaded?	Aspect of pathology studied	Specific brain territory?
Yamori (Yamori et al. 1975)	1975	24	32wks	No	Brain parenchyma	No
Okuma(Okuma and Yamori 1976) #	1976	29	14-16wks	No	Serum, urine or CSF biomarkers	No
Yamori(Yamori et al. 1976)	1976	1278	n/a	No	All cerebral arteries	No
Yamori(Yamori and Horie 1977)	1977	150	20-40wks	No	All cerebral arteries	Frontal cortex
Hazama(Hazama et al. 1979) #	1979	17	8-52wks	No	Basal arteries	No
Knox(Knox et al. 1980)	1980	43	12-108wks	No	Intraparenchymal arteries	Frontal cortex
Tagami(Tagami et al. 1981) $	1981	62	8-40wks	No	Intracranial extracerebral	No
Rieke(Rieke et al. 1981)	1981	13	13-20wks	No	Supply to BG etc including perforators & parent.	CP & GP
Ogata(Fisher 1965)	1981	5	40-80wks	No	Cerebral arterioles	No
Matsuo(Matsuo and Nagaoka 1981) $	1981	75	0-22wks	Yes	Brain parenchyma	No
Sadoshima(Sadoshima and Heistad 1982)	1982	24	4-26wks	Yes	Brain parenchyma	Cerebrum / frontoparietal cortex.
Takeshita(Takeshita et al. 1982) $	1982	59	8-16wks	Yes	Serum, urine or CSF biomarkers	No
Sadoshima(Sadoshima and Heistad 1983)	1983	n/a	n/a	No	All cerebral vessels	No

Author	Date	N	Age	Salt loaded?	Aspect of pathology studied	Specific brain territory?
Kanbe(Kanbe et al. 1983) #	1983	n/a	12-24wks	No	Aorta	No
Takiguchi (Takiguchi 1983) $	1983	n/a	n/a	No	Brain parenchyma	No
Rodda(Rodda et al. 1983)	1983	57	n/a	No	Brain parenchyma	No
Tamaki(Tamaki et al. 1984b) #	1984	96	20-30wks	No	Carotid & pial vessels	No
Werber(Werber and Heistad 1984)	1984	37	3-64wks	No	Aorta & cortical pial vessels	No
Yamada(Yamada et al. 1985) #	1984	n/a	5-24wks	No	Serum, urine or CSF biomarkers	HT
Tomita(Tomita et al. 1984) #	1984	n/a	4-25wwks	No	Serum, urine or CSF biomarkers	No
Yamada(Yamada et al. 1984) #	1985	n/a	5-24wks	No	Serum, urine or CSF biomarkers	HT
Norborg(Nordborg et al. 1985) #	1985	48	28-52wks	No	Intracranial, pial, basal & extracranial cervical.	No
Minami(Minami et al. 1985)	1985	27	15-60wks	No	Brain parenchyma	No
Fredriksson(Fredriksson et al. 1985) $	1985	23	24-36wks	No	Brain parenchyma	No
Umegaki(Umegaki et al. 1986)	1985	100	4-41wks	No	Serum, urine or CSF biomarkers	No
Luft(Luft et al. 1986)	1986	n/a	n/a	No	All cerebral vessels	No
Coyle(Coyle 1987)	1987	11	5-69wks	No	Dorsal cerebral collaterals	No
Fredriksson (Fredriksson et al. 1987)	1987	n/a	20-36wks	No	MCA territory	No
Tagami(Tagami et al. 1987) $	1987	84	4-52wks	No	Perforating arteries	Anteriomedial & occipital cortex

Author	Date	N	Age	Salt loaded?	Aspect of pathology studied	Specific brain territory?
Fredriksson(Fredriksson et al. 1988) #	1988	32	24-36wks	No	Cerebral microvessels extraparenchymal.	Cerebral cortex & BG
Lee(Lee et al. 1988)	1988	278	24-37wks	No	BA, Circle of Willis, MCA & ACA	No
Stier(Stier et al. 1988)	1988	43	6-18wks	Yes	Serum, urine or CSF biomarkers	No
Shimizu(Shimizu et al. 1988) $	1988	n/a	12wks	No	Serum, urine or CSF biomarkers	No
Thompson(Thompson et al. 1988)	1988	24	24wks	No	Serum, urine or CSF biomarkers	No
Schober(Schober et al. 1989)	1989	41	16-52wks	No	Serum, urine or CSF biomarkers	Adrenal medulla
Furspan(Furspan and Bohr 1990)	1990	36	16-24wks	No	Serum, urine or CSF biomarkers	No
Kobayashi(Kobayashi et al. 1990)	1990	n/a	12wks	No	Serum, urine or CSF biomarkers	No
Mangiarua(Mangiarua and Lee 1992) #	1992	45	28wks	No	Basilar, superior cerebellar, PCA & MCA	No
Matsuo(Matsuo et al. 1992)	1992	12	24wks	No	Serum, urine or CSF biomarkers	No
Contard(Contard et al. 1993)	1993	24	6-13wks	Yes	Aorta & coronary vessels	No
Coyle(Coyle and Feng 1993)	1993	36	8-13wks	No	MCA and connecting vessels	No
Furspan(Furspan and Webb 1993)	1993	36	16-20wks	No	Serum, urine or CSF biomarkers	No
Chue(Chue et al. 1993)	1993	76	8-24wks	No	Serum, urine or CSF biomarkers	Cortex & subcortical WM
Liu(Liu et al. 1994)	1994	46	16-24wks	No	Serum, urine or CSF biomarkers	No
Wilde(Wilde et al. 1994)	1994	62	>17wks	No	Serum, urine or CSF biomarkers & "cerebral arteries"	No

Author	Date	N	Age	Salt loaded?	Aspect of pathology studied	Specific brain territory?
Kanagy(Kanagy et al. 1994)	1994	20	20-24wks	No	Serum, urine or CSF biomarkers	No
Hajdu(Hajdu and Baumbach 1994)	1994	14	24-32wks	No	PCA (large 2nd order and small 3rd order branches.	No
Kitazono(Kitazono et al. 1995)	1995	77	24-36wks	No	Basilar	No
Ito(Ito et al. 1995a)	1995	n/a	n/a	No	Serum, urine or CSF biomarkers	No
Grunfeld(Grunfeld et al. 1995)	1995	13	5-16wks	No	Serum, urine or CSF biomarkers	No
Yang(Yang et al. 1995) #	1995	89	12-16wks	No	Serum, urine or CSF biomarkers	MO
Volpe(Volpe et al. 1996) #	1996	80	6-18wks	Yes	Aorta & basilar artery	No
Arribas(Arribas et al. 1996)	1996	84	16-44wks	No	Basilar artery	No
Ikeda(Ikeda et al. 1996)	1996	n/a	14-18wks	No	Serum, urine or CSF biomarkers	No
Ono(Ono et al. 1996) #	1996	45	12-13wks	No	Serum, urine or CSF biomarkers	No
Gotoh(Gotoh et al. 1996)	1996	n/a	n/a	No	Serum, urine or CSF biomarkers	No
Togashi(Togashi et al. 1996)	1996	n/a	15-40wks	No	Serum, urine or CSF biomarkers	CB, MB, HP, HT, MO & ST.
Cabrera(Cabrera et al. 1996)	1996	12	12wks	No	Serum, urine or CSF biomarkers	No

Author	Date	N	Age	Salt loaded?	Aspect of pathology studied	Specific brain territory?
Zanchi(Zanchi et al. 1997) #	1997	133	4-32wks	No	Carotid artery	No
Lin(Lin et al. 1997)	1997	n/a	12-38wks	No	Serum, urine or CSF biomarkers	No
Takeda(Takeda et al. 1997)	1997	156	2-9wks	No	Serum, urine or CSF biomarkers	No
Blezer(Blezer et al. 1998) $	1998	23	7-16wks	Yes	Serum, urine or CSF biomarkers	No
Smeda(Smeda et al. 1999)	1999	25	10-27wks	Yes	MCA	No
Smeda(Smeda and King 1999)	1999	24	10-22wks	Yes	MCA & PCA	No
Sunano(Sunano et al. 1999)	1999	60	16wks	No	2^{nd} branch arterioles	No
Mies(Mies et al. 1999) $	1999	20	6-12wks	Yes	All cerebral arteries	No
Negishi(Negishi et al. 1999)	1999	35	6-17wks	No	Serum, urine or CSF biomarkers	No
Shimamura(Shimamura et al. 1999) #	1999	63	7-17wks	No	Serum, urine or CSF biomarkers	No
Kerr(Kerr et al. 1999)	1999	88	12-16wks	No	Serum, urine or CSF biomarkers	No
Kimoto - Kinoshita(Kimoto-Kinoshita et al. 1999)	1999	80	15-31wks	No	Serum, urine or CSF biomarkers	HP & Cortex
Mizuno(Mizuno et al. 1999)	1999	100	10-12wks	No	Serum, urine or CSF biomarkers	No

Author	Date	N	Age	Salt loaded?	Aspect of pathology studied	Specific brain territory
Lippoldt(Lippoldt et al. 2000) #	2000	39	13wks	No	Capillaries	No
Enea(Enea et al. 2000) #	2000	133	6-10wks	Yes	Serum, urine or CSF biomarkers	No
Boumaza(Boumaza et al. 2001)	2001	44	13wks	No	Internal carotid & aorta	No
Lin(Lin et al. 2001)	2001	38	4-20wks	No	Cerebral arteries	CC, AC, IC & CP.
Sironi(Sironi et al. 2001) #	2001	18	6-13wks	Yes	Serum, urine or CSF biomarkers	No
Hamilton(Hamilton et al. 2001)	2001	150	12-52wks	No	Serum, urine or CSF biomarkers	No
Ito(Ito et al. 2001)	2001	n/a	19-23wks	No	Serum, urine or CSF biomarkers & "cerebral microvessels"	No
Ma(Ma et al. 2001)	2001	44	12-25wks	Yes	Serum, urine or CSF biomarkers	No
Michihara(Michihara et al. 2001)	2001	n/a	1-9wks	No	Serum, urine or CSF biomarkers	No
Sekiguchi(Sekiguchi et al. 2001)	2001	62	5-15wks	No	Serum, urine or CSF biomarkers & carotid, aorta & iliac arteries	No
Hirafuji(Hirafuji et al. 2002)	2002	n/a	6-7wks	No	Aorta	No
Guerrini(Guerrini et al. 2002)	2002	68	6-52wks	Yes	Brain parenchyma	No
Yamashita(Yamashita et al. 2002)	2002	12	10-23wks	No	Serum, urine or CSF biomarkers & arterioles 20-25μm in diameter	No
Taka(Taka et al. 2002)	2002	n/a	28-31wks	No	Serum, urine or CSF biomarkers	No

Author	Date	N	Age	Salt loaded?	Aspect of pathology studied	Specific brain territory?
Tabuchi(Tabuchi et al. 2002) $	2002	127	4-10wks	No	Serum, urine or CSF biomarkers	No
Izzard(Izzard et al. 2003) #	2003	27	4-12wks	Yes	MCA	No
Sironi(Sironi et al. 2003) $	2003	50	8-14 wks	Yes	Brain parenchyma	No
Chander(Chander et al. 2003)	2003	58	8-12wks	Yes	Serum, urine or CSF biomarkers	No
Ueno(Ueno et al. 2004b) #	2004	18	12wks	No	All cerebral arteries, arterioles & capillaries	HP & cortex
Sironi(Sironi et al. 2004) $	2004	28	6-11wks	Yes	Brain parenchyma	CP
Jesmin(Jesmin et al. 2004)	2004	71	6wks	No	Serum, urine or CSF biomarkers & all cerebral vessels	No
Kishi(Kishi et al. 2004)	2004	10	14-18wks	No	Serum, urine or CSF biomarkers	No
Schmidlin(Schmidlin et al. 2005) $	2005	83	6-15wks	Yes	Serum, urine or CSF biomarkers	No
Kim-Mitsuyama(Kim-Mitsuyama et al. 2005) $	2005	235	8-14wks	Yes	Serum, urine or CSF biomarkers	HP & Cortex
Masineni(Masineni et al. 2005)$	2005	18	53wks	No	Serum, urine or CSF biomarkers	No
Izzard(Izzard et al. 2006)	2006	20	5-24wks	Yes	MCA	No
Ballerio(Ballerio et al. 2007) $	2007	100	6-18wks	Yes	Serum, urine or CSF biomarkers	No
Lee(Lee et al. 2007) $	2007	10	8-18wks	Yes	All cerebral vessels	No
Ishizuka(Ishizuka et al. 2007) $	2007	n/a	9-14wks	Yes	Serum, urine or CSF biomarkers	No
Ueno(Ueno et al. 2009)	2009	36	4-12wks	No	‘Randomly sampled’ microvessels	Frontal cortex & HP
Henning(Henning et al. 2010)	2010	12	24 wks +	No	Vessels within lesions – 100-250µm diameter.	Whole brain – wherever there was a lesion.

APPENDIX F) H&E staining protocol – used for both qualitative and quantitative assessments.

Sections to water

1. 2 x 5 mins deparaffin Xylene (in hood).
2. 2 x 5 mins 74ºP.
3. 2 x 5mins 70% Alcohol.
4. 30 mins Picric Acid.
5. Wash in water until all excess picric acid removed.

Staining

6. Stain in Harris Hematoxylin for 8-10 mins.
7. Wash with water until all excess stain removed.
8. Differentiate staining in acid alcohol (~3 dips).
9. 'Blue' slides in Lithium Carbonate (~3 dips).
10. Place slide rack straight into Putt's Eosin solution for ~10mins.
11. Wash with water until all excess stain is removed.
12. If necessary dip slides in pot aluminium solution and replace in Eosin for 1-2 mins to fix staining.
13. Dehydrate slides through alcohols (70%, 74ºP & 2x absolute alcohol) ~ 5 dips in each.
14. Clear in xylene for 2 x 5 mins.
15. Mount slides with pertex.

APPENDIX G) Immunohistochemistry ABC protocol

Sections to water – same as H&E

2 x 5 mins deparaffin Xylene (in hood).

2 x 5 mins 74ºP.

2 x 5mins 70% Alcohol.

30 mins Picric Acid.

ABC Method –

1. Wash off picric acid in water until clear.
2. Block in hydrogen peroxide (H_2O_2) for 10 mins in a glass container on top of a rocker. (Dilution = 1:10 in distilled water).
3. Pretreatment step if required (e.g. Citric acid).
4. Wash in water.
5. Transfer slides to Sequenza (separate the negative). Mount with Tris (TBS) Buffer in squeezy bottle (1:10 in saline – make 500mls). Check flow.
6. Wash in TBS buffer for 5 mins.
7. Treat with 100µl/slide of Serum (NRS – 1:5 dilution with TBS for 10 mins.
8. Treat with 100µl/slide of primary antibody (e.g. GFAP – made to recommended dilution e.g.1:250) for 30 mins. Omit from negative control – treat this with serum.
9. Wash in buffer 2 x 5 mins.
10. Incubate in RAMBO (or other secondary antibody made to dilution e.g. 1:200) for 30 mins.
11. Prepare ABC – 30 mins prior to use. (5ml TBS, 1 drop A, 1 drop B).
12. Wash in buffer 2 x 5 mins.
13. Incubate in ABC for 30 mins.
14. Wash in buffer 2 x 5 mins.
15. Remove slides from coverplates and place in water.
16. Treat with DAB on relevant bench for 1 minute. (DAB – 5 ml distilled water, 2 drops H_2O_2, 2 drops buffer, 4 drops DAB from kit in fridge.) Use immediately – drop enough to cover tissue.
17. Wash off excess DAB in water. Check staining.
18. Counterstain in Haematoxylin (15-20 seconds). Blue in Lithium carbonate.
19. Dehydrate through alcohols, clear in xylene & mount.

APPENDIX H) IPA – the statistical methods used to analyse uploaded data. Ingenuity® Systems www.ingenuity.com.

1. Network Generation

A data set containing gene (or chemical) identifiers and corresponding expression values was uploaded into in the application. Each identifier was mapped to its corresponding object in the Ingenuity® Knowledge Base. A <*insert expression value type here*> cutoff of <*insert expression value cutoff here*> was set to identify molecules whose expression was significantly differentially regulated. These molecules, called Network Eligible molecules, were overlaid onto a global molecular network developed from information contained in the Ingenuity Knowledge Base.Networks of Network Eligible Molecules were then algorithmically generated based on their connectivity.

2. Functional Analysis of an Entire Data Set

The Functional Analysis identified the biological functions and/or diseases that were most significant to the data set. Molecules from the dataset that met the <*insert expression value type here*> cutoff of <*insert expression value cutoff here*> and were associated with biological functions and/or diseases in the Ingenuity Knowledge Base were considered for the analysis.Right-tailed Fisher's exact test was used to calculate a p-value determining the probability that each biological function and/or disease assigned to that data set is due to chance alone.

3. Functional Analysis of a Network

The Functional Analysis of a network identified the biological functions and/or diseases that were most significant to the molecules in the network. The network molecules associated with biological functions and/or diseases in the Ingenuity Knowledge Base were considered for the analysis. Right-tailed Fisher's exact test was used to calculate a p-value determining the probability that each biological function and/or disease assigned to that network is due to chance alone.

4. Canonical Pathway Analysis: Entire Data Set

When publishing part of or an entire Ingenuity canonical pathway(s), cite IPA (see options above) in the reference section of your publication. You may also want to cite some of the references contained within that canonical pathway(s).Canonical pathways analysis identified the pathways from the IPA library of canonical pathways that were most significant to the data set. Molecules from the data set that met the <*insert expression value type here*> cutoff of <*insert expression value cutoff here*> and were associated with a canonical pathway in the Ingenuity Knowledge Base were considered for the analysis. The significance of the association between the data set and the canonical pathway was measured in 2 ways:

1) A ratio of the number of molecules from the data set that map to the pathway divided by the total number of molecules that map to the canonical pathway is displayed.

2) Fisher's exact test was used to calculate a p-value determining the probability that the association between the genes in the dataset and the canonical pathway is explained by chance alone.

5. Network/My Pathways/ Path Designer Graphical Representation

A network/My Pathways is a graphical representation of the molecular relationships between molecules. Molecules are represented as nodes, and the biological relationship between two nodes is represented as an edge (line). All edges are supported by at least one reference from the literature, from a textbook, or from canonical information stored in the Ingenuity Knowledge Base. Human, mouse, and rat orthologs of a gene are stored as separate objects in the Ingenuity Knowledge Base, but are represented as a single node in the network. The intensity of the node color indicates the degree of up- (red) or down- (green) regulation. Nodes are displayed using various shapes that represent the functional class of the gene product. Edges are displayed with various labels that describe the nature of the relationship between the nodes (e.g. P for phosphorylation, T for transcription).

APPENDIX I) Standard PCR protocol performed on DNA taken from the liver of WKY and SHRSP rats for sequencing.

Kod Hot Start DNA polymerase (Novagen®) kits contained the following reaction mix for each well;

Reaction Mix	**Volume (µl)**
10x PCR buffer	5
dNTPs (1mM ea.)	5
MgSO4 (25mM)	3
Fwd primer (5pmol/µl)	1.5
Rvs primer (5pmol/µl)	1.5
DNA	1.0-5.0
Kod	1
H_2O	up to 50

Heat cycling

Polymerase activation	94°C	2 min
Denature	94°C	15 secs
Annealing	52°C	30 secs
Extension	68°C	2.5 min
	68°C	10 min

APPENDIX J) DNA sequencing reaction mix and temperature cycling.

Applied Biosystems BigDye Terminator n3.1 Cycle Sequencing kits included the following reaction mix ;

Reaction Mix	**Volume (µl)**
5x Sequencing buffer	3.5
Ready Reaction	0.5
Template (purified PCR product)	8
Primer (1pmol/µl)	3.2
H_2O	4.8

Heat Cycling

1) 96°C	45 secs
2) 50°C	25 secs
3) 60°C	4 min

Repeat steps 1)-2) x25

APPENDIX K) Figures of immunohistochemical staining – all antibodies across all ages and both strains

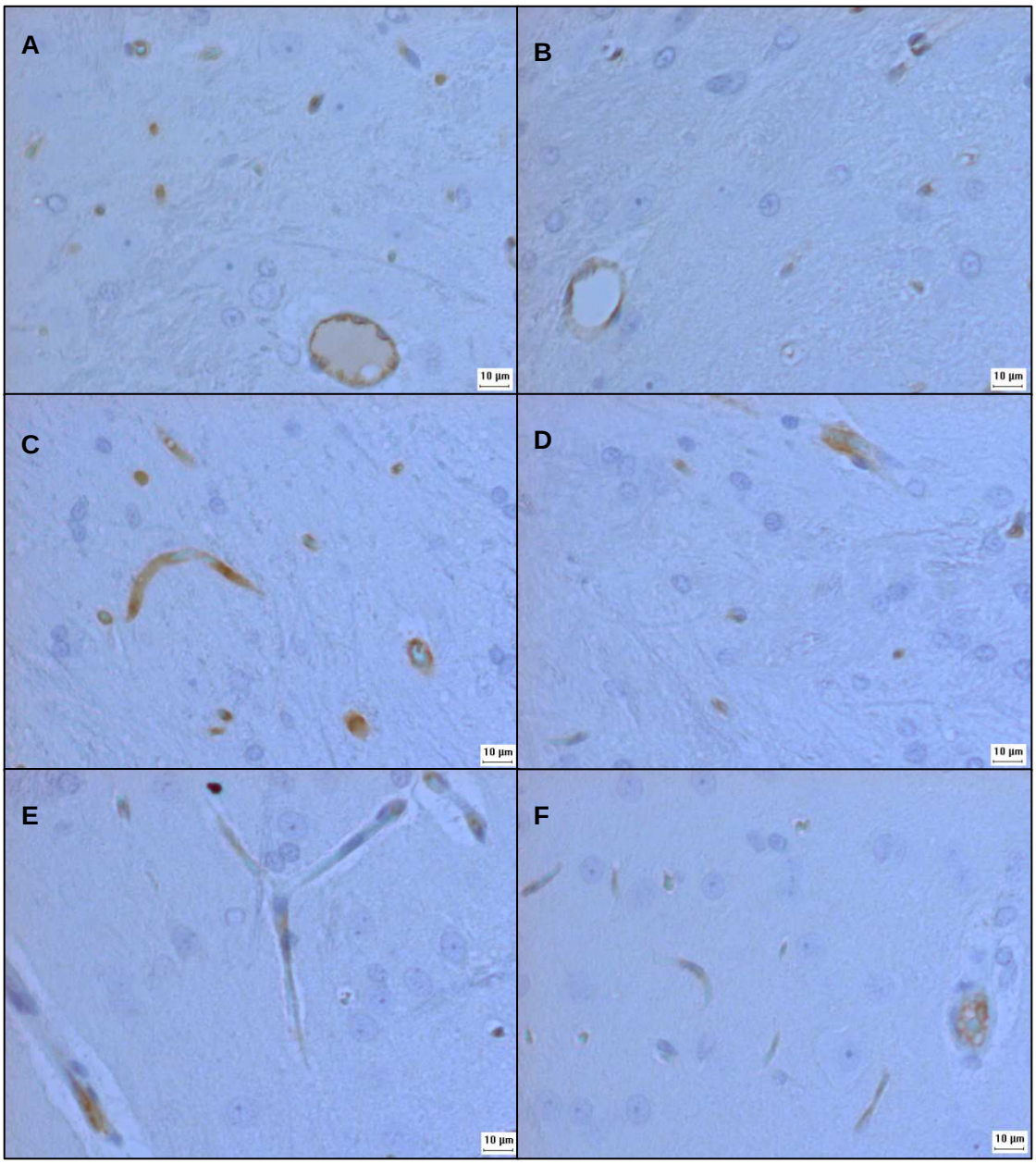

Figure K.1 – Claudin-5 staining from WKY and SHRSP rats aged 5-21 weeks raised on standard rat chow.

A&B represent 5 weeks of age. C&D represent 16 weeks of age. E&F represent 21 weeks of age. In all images WKY is on the left and SHRSP is on the right. Images taken at x20 objective from the deep grey matter of mid coronal sections. Scale bar = 10µm. We found a significant decrease in Claudin-5 staining in SHRSP at all ages including at 5 weeks (panel B vs A).

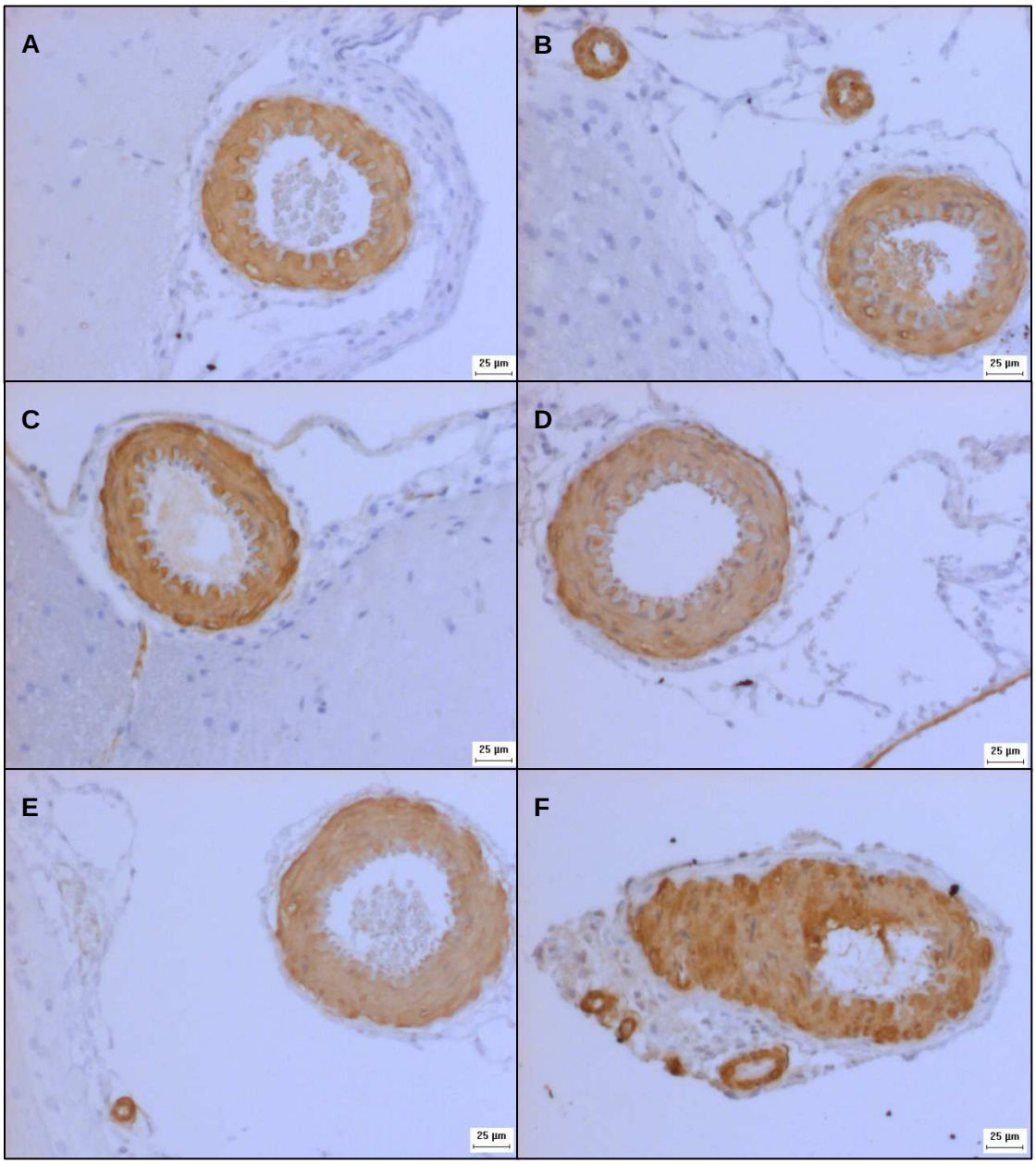

Figure K.2 – SMA staining from WKY and SHRSP rats aged 5-21 weeks raised on standard rat chow.

A&B represent 5 weeks of age. C&D represent 16 weeks of age. E&F represent 21 weeks of age. In all images WKY is on the left and SHRSP is on the right. Images taken at x10 objective from frontal brain sections and show meningeal arteries. Scale bar = 25µm. Note the increasing wall thickness with age in the SHRSP (panels B,D & F).

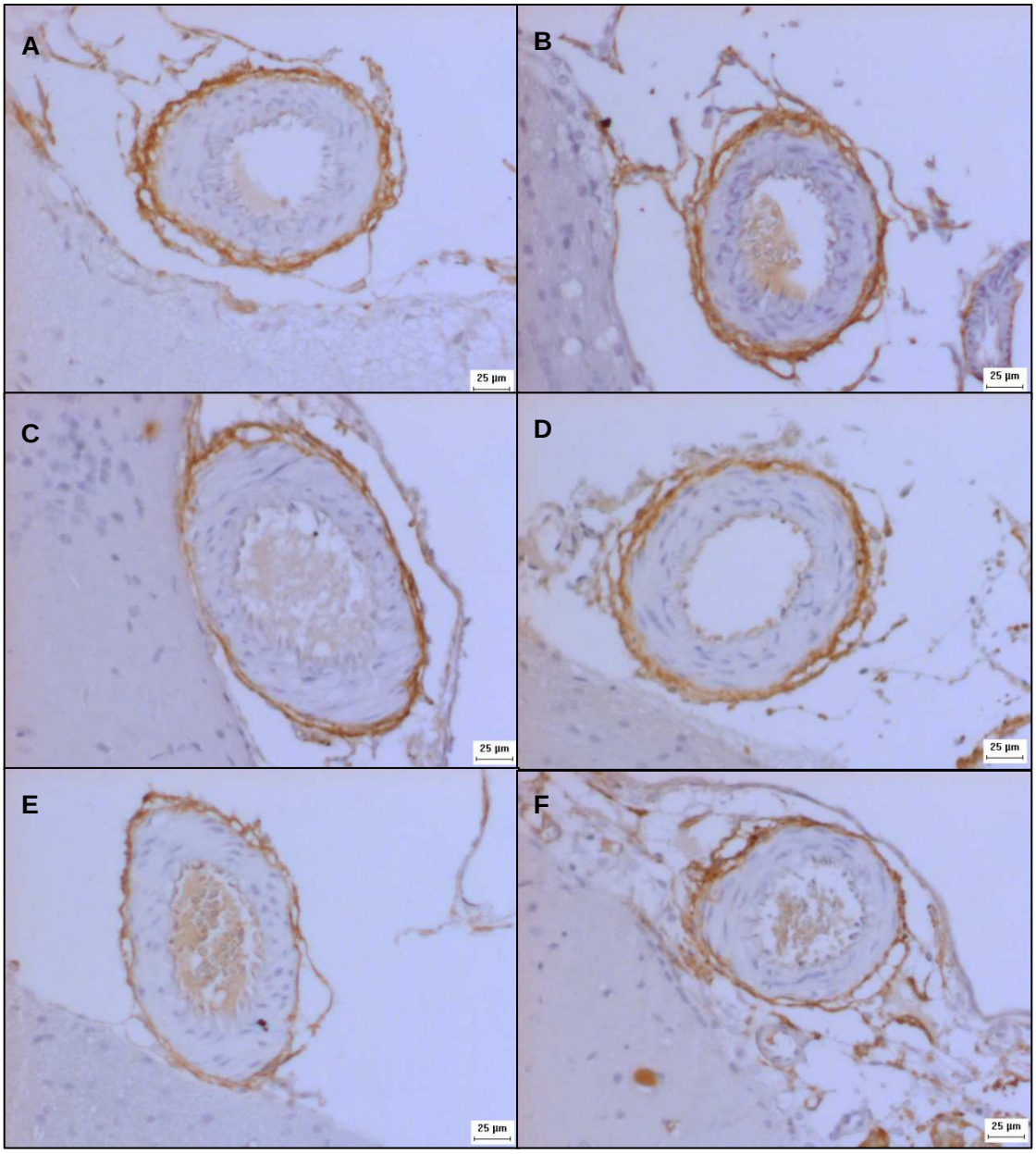

Figure K.3 – Collagen I staining from WKY and SHRSP rats aged 5-21 weeks raised on standard rat chow.

A&B represent 5 weeks of age. C&D represent 16 weeks of age. E&F represent 21 weeks of age. In all images WKY is on the left and SHRSP is on the right. Images taken at x10 objective from frontal brain sections and show meningeal arteries. Scale bar = 25µm. We found no significant difference in Collagen I staining in this section.

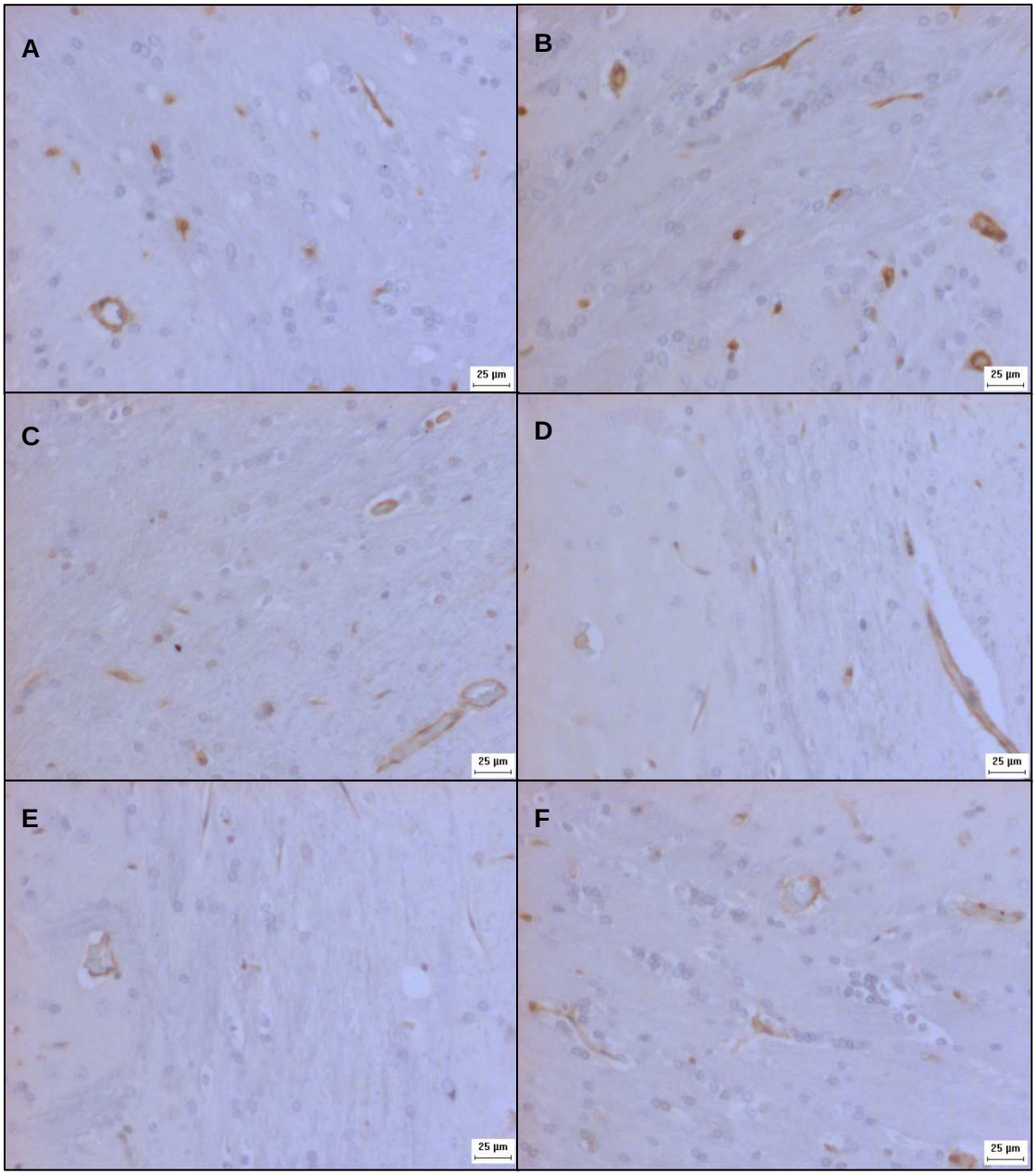

Figure K.4 – Collagen IV staining from WKY and SHRSP rats aged 5-21 weeks raised on standard rat chow.

A&B represent 5 weeks of age. C&D represent 16 weeks of age. E&F represent 21 weeks of age. In all images WKY is on the left and SHRSP is on the right. Images taken at x10 objective in the deep grey matter of mid coronal sections. Scale bar = 25µm. We found no significant difference in Collagen IV staining in this region.

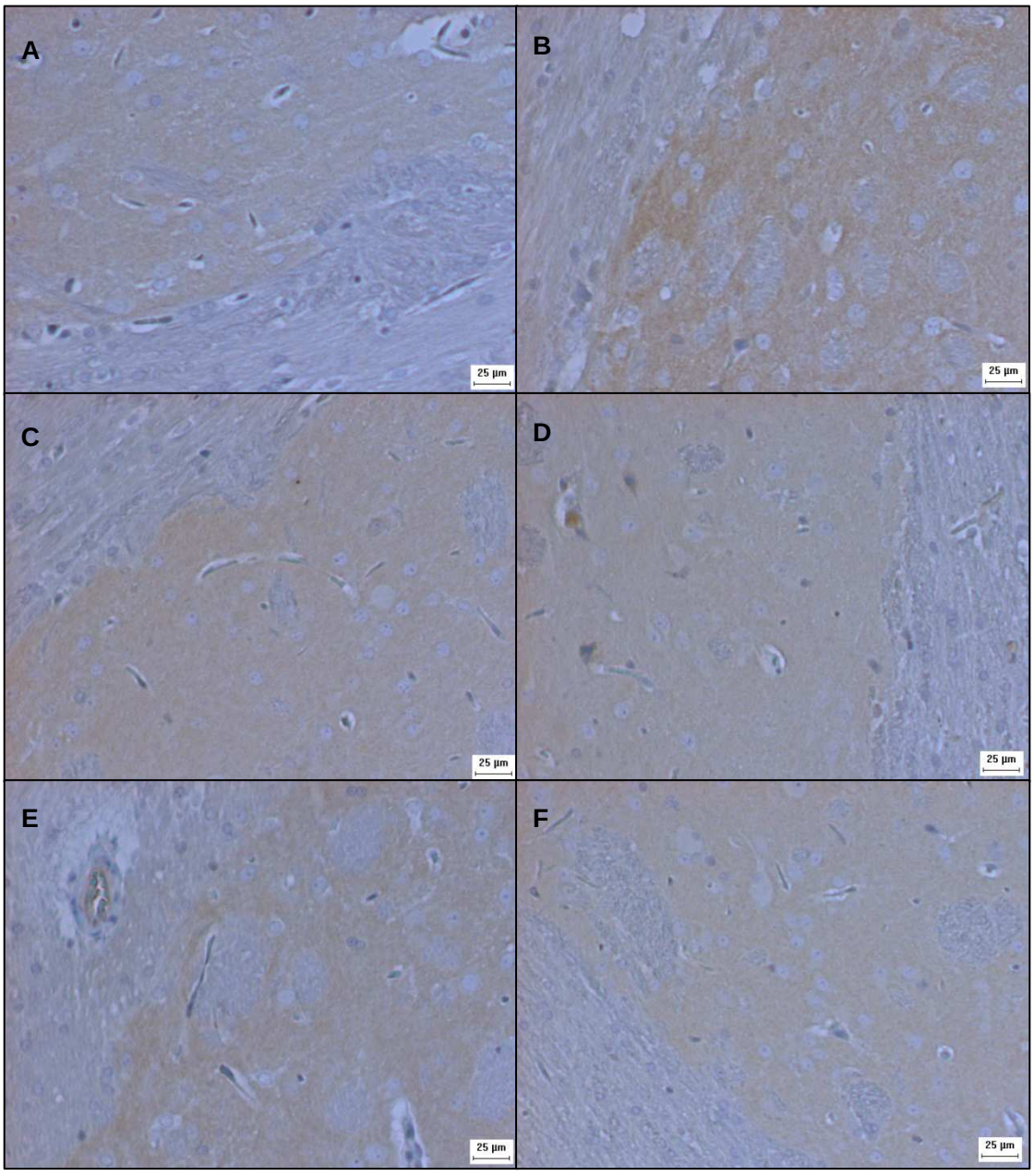

Figure K.5 – MMP9 staining from WKY and SHRSP rats aged 5-21 weeks raised on standard rat chow.

A&B represent 5 weeks of age. C&D represent 16 weeks of age. E&F represent 21 weeks of age. In all images WKY is on the left and SHRSP is on the right. Images taken at x10 objective from the border of the white matter and deep grey matter from mid coronal brain sections. Scale bar = 25µm. MMP9 staining did not significantly differ between SHRSP and WKY, however not the increased staining intensity in 5 week old SHRSP (panel B versus A).

Figure K.6 – GFAP staining from WKY and SHRSP rats aged 5-21 weeks raised on standard rat chow.

A&B represent 5 weeks of age. C&D represent 16 weeks of age. E&F represent 21 weeks of age. In all images WKY is on the left and SHRSP is on the right. Images taken at x10 objective in the deep grey matter from frontal brain sections. Scale bar = 25µm. Quantitatively SHRSP showed increased GFAP staining at 5 weeks of age versus WKY.

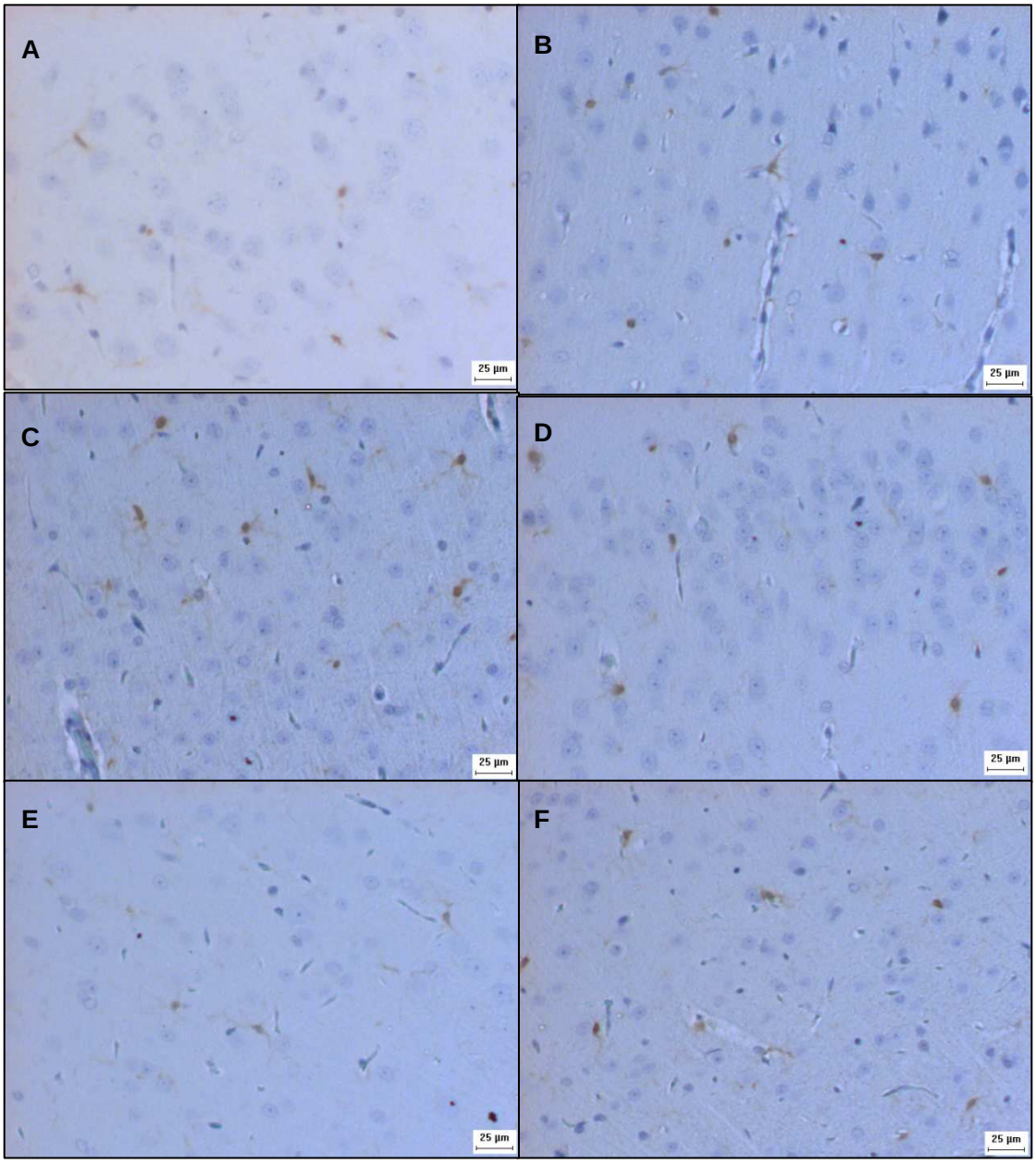

Figure K7 – Iba-1 staining from WKY and SHRSP rats aged 5-21 weeks raised on standard rat chow.

A&B represent 5 weeks of age. C&D represent 16 weeks of age. E&F represent 21 weeks of age. In all images WKY is on the left and SHRSP is on the right. Images taken at x10 objective in the cortical grey matter of frontal brain sections. Scale bar = 25µm. Quantitatively SHRSP showed higher levels of Iba-1 staining in this section.

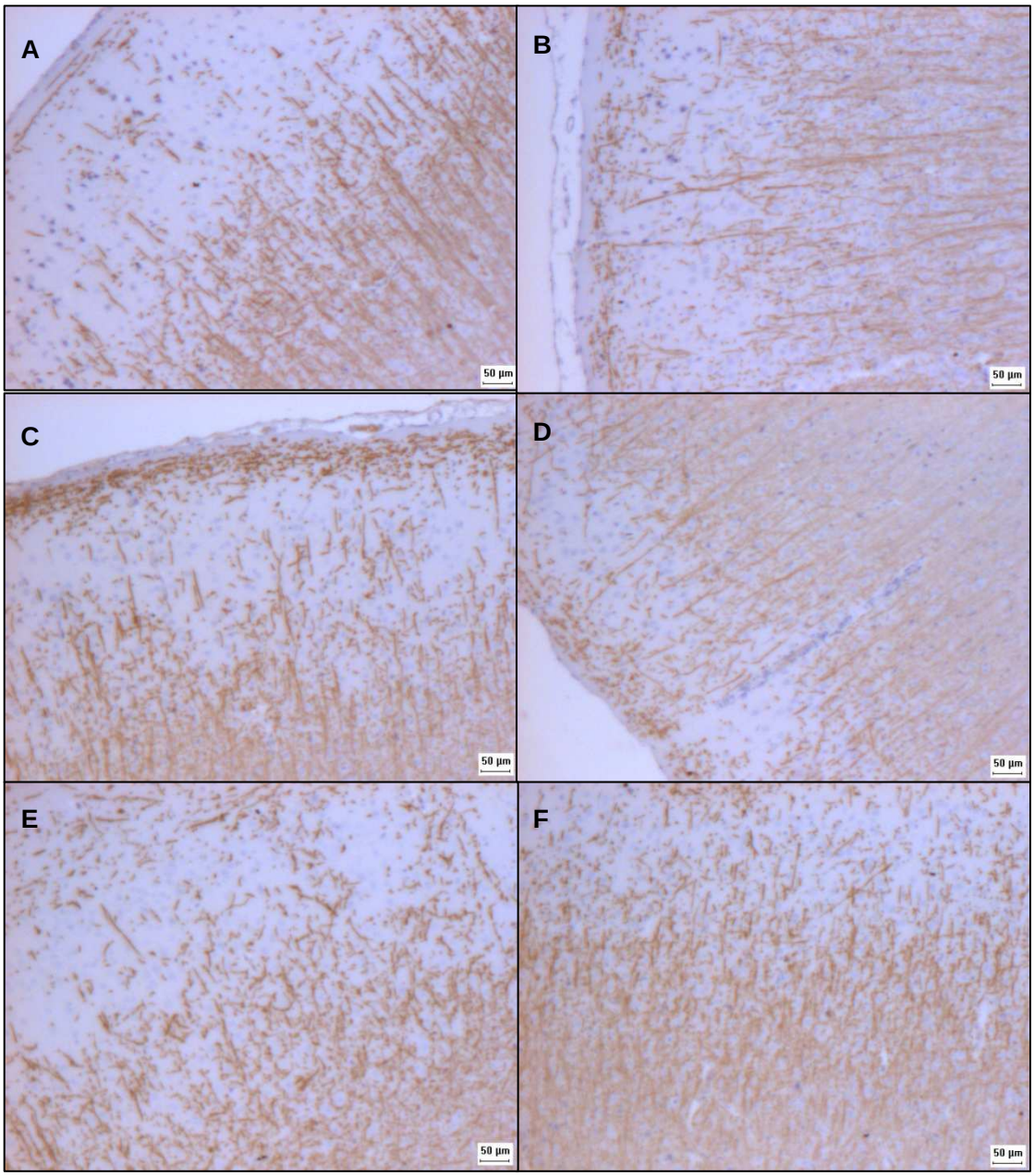

Figure K8 – MBP staining from WKY and SHRSP rats aged 5-21 weeks raised on standard rat chow.

A&B represent 5 weeks of age. C&D represent 16 weeks of age. E&F represent 21 weeks of age. In all images WKY is on the left and SHRSP is on the right. Images taken at x4 objective in the cortical grey matter of frontal brain sections. Scale bar = 50µm. We found a significant decrease in MBP staining in SHRSP (displayed most prominently in panel D).

APPENDIX L) Immunohistochemical staining from salt-loaded versus non salt-loaded 21 week old WKY and SHRSP. All antibodies.

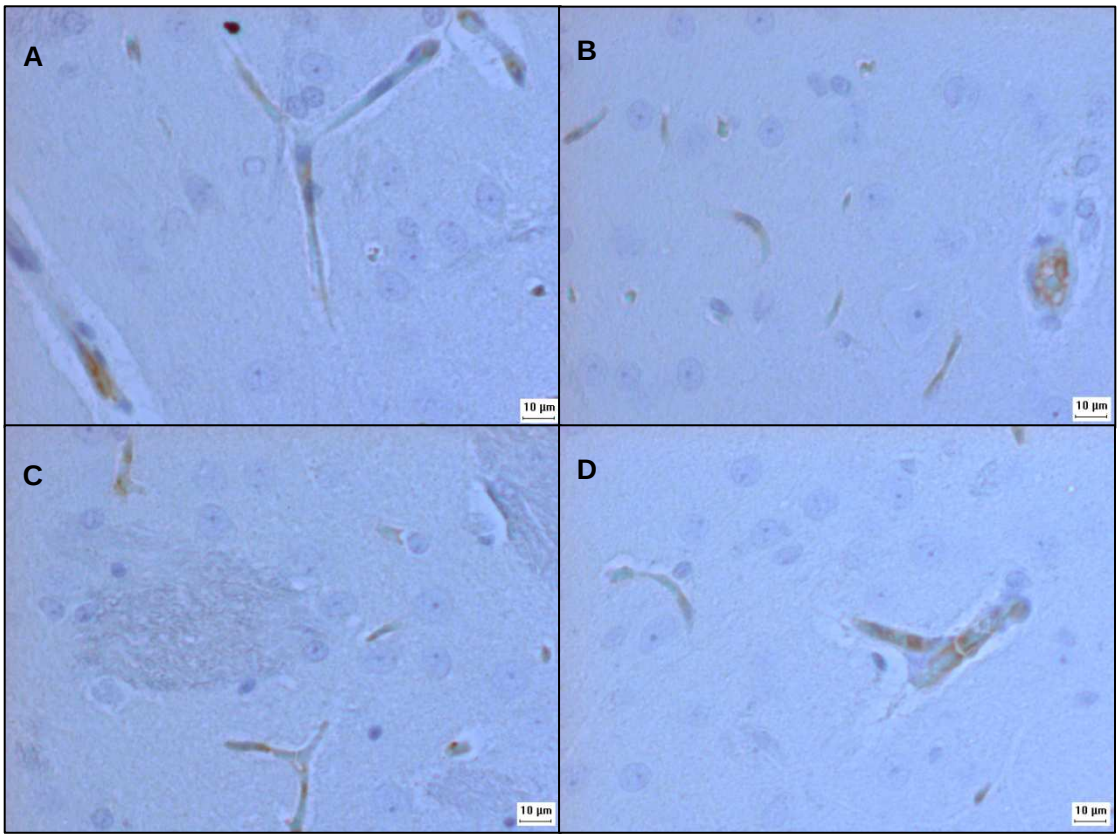

Figure L.1 -.Immunoreactivity of Claudin-5 in 21 week old animals A) WKY B) WKY+NaCl C) SHRSP D) SHRSP+NaCl.

All images taken at x20 objective in the deep grey matter of mid coronal brain sections. Scale bar = 10µm. We found no significant differences in Claudin-5 staining due to salt loading.

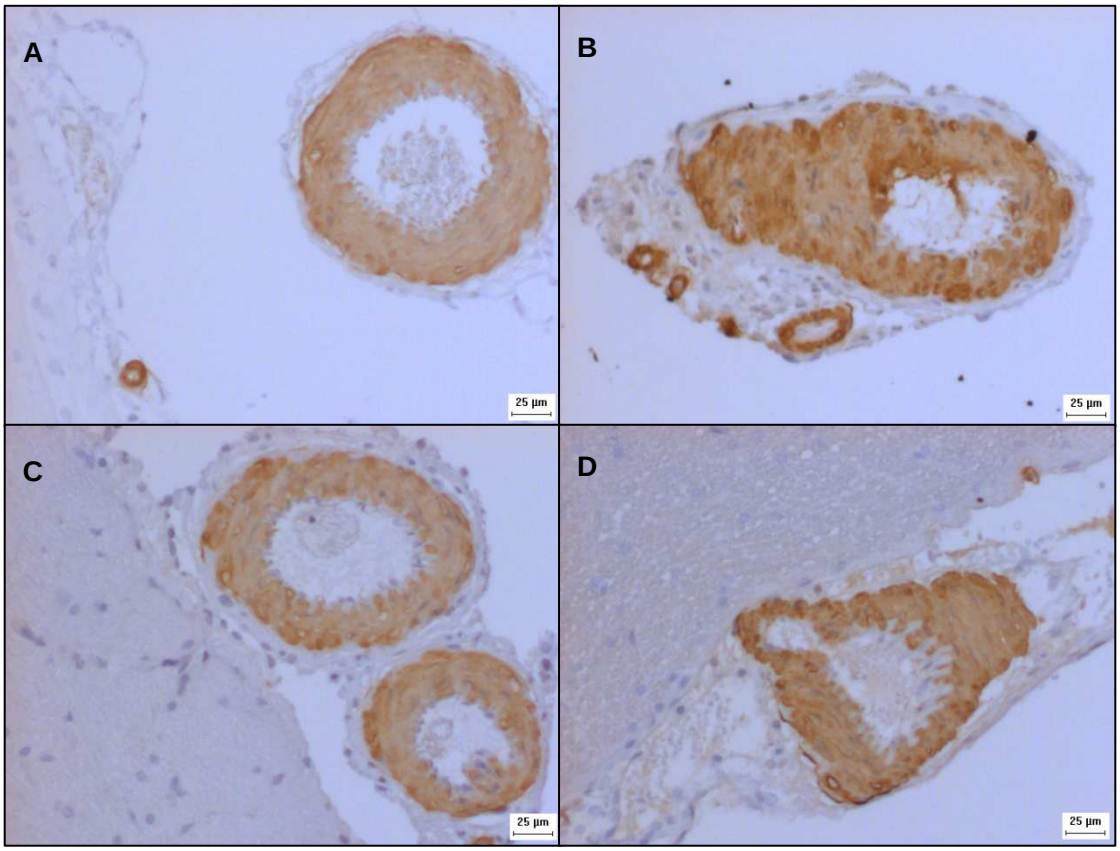

Figure L.2 -.Immunoreactivity of SMA in 21 week old animals A) WKY B) WKY+NaCl C) SHRSP D) SHRSP+NaCl.

All images taken at x10 objective and show meningeal arteries from frontal brain sections. Scale bar = 25µm. We found no significant difference due to salt loading in this brain section. SHRSP had significantly more SMA staining than WKY in both salt loaded and non salt loaded WKY.

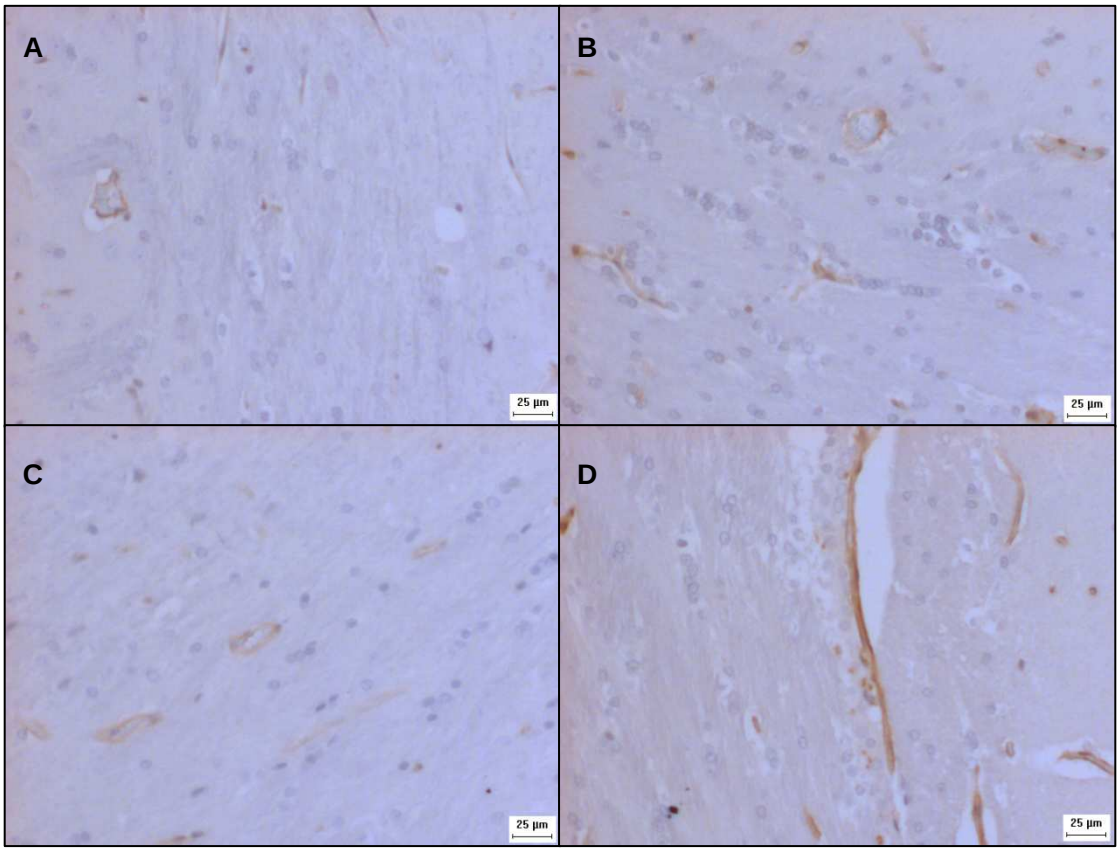

Figure L.3 -.Immunoreactivity of Collagen I in 21 week old animals A) WKY B) WKY+NaCl C) SHRSP D) SHRSP+NaCl.

All images taken at x10 objective and show meningeal arteries from frontal brain sections. Scale bar = 25µm. We found no significant differences in Collagen I staining due to salt loading in this brain section.

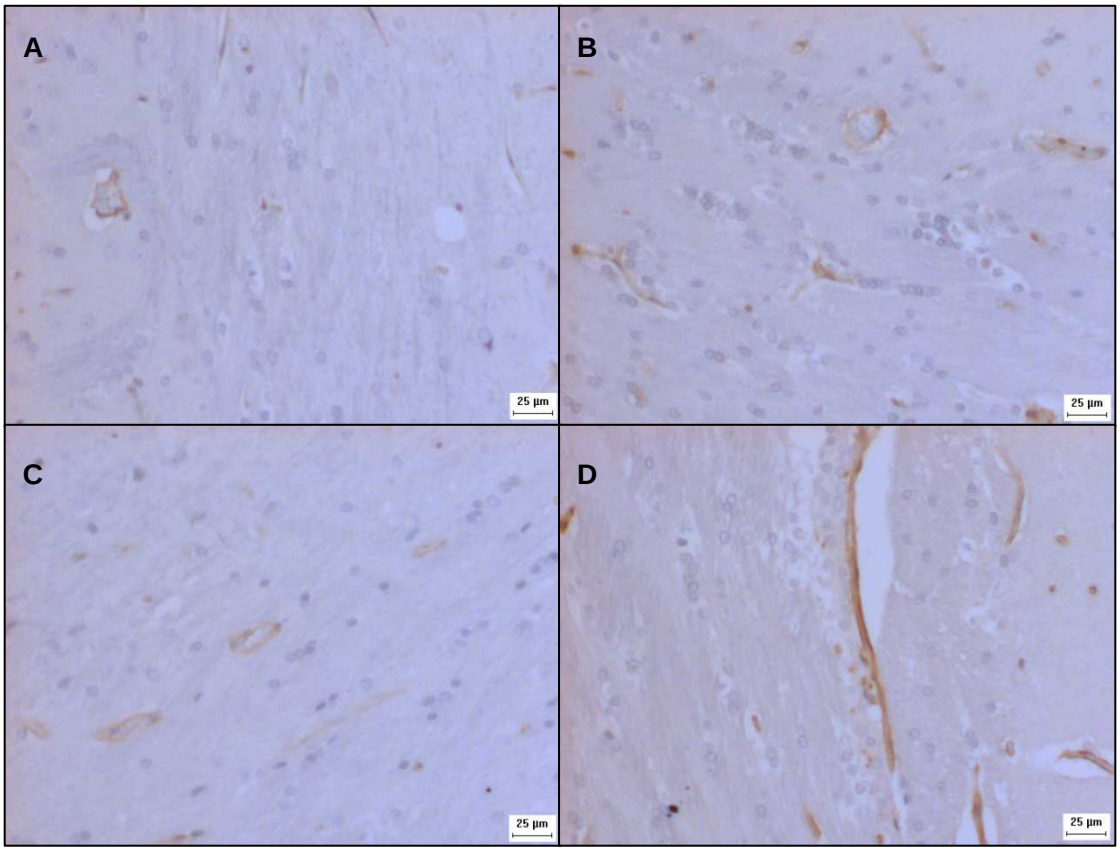

Figure L.4 -.Immunoreactivity of Collagen IV in 21 week old animals A) WKY B) WKY+NaCl C) SHRSP D) SHRSP+NaCl.

All images taken at x10 objective in the deep grey matter / white matter border fron mid coronal brain sections. Scale bar = 25µm. We found no significant differences in Collagen IV staining due to salt loading in this section.

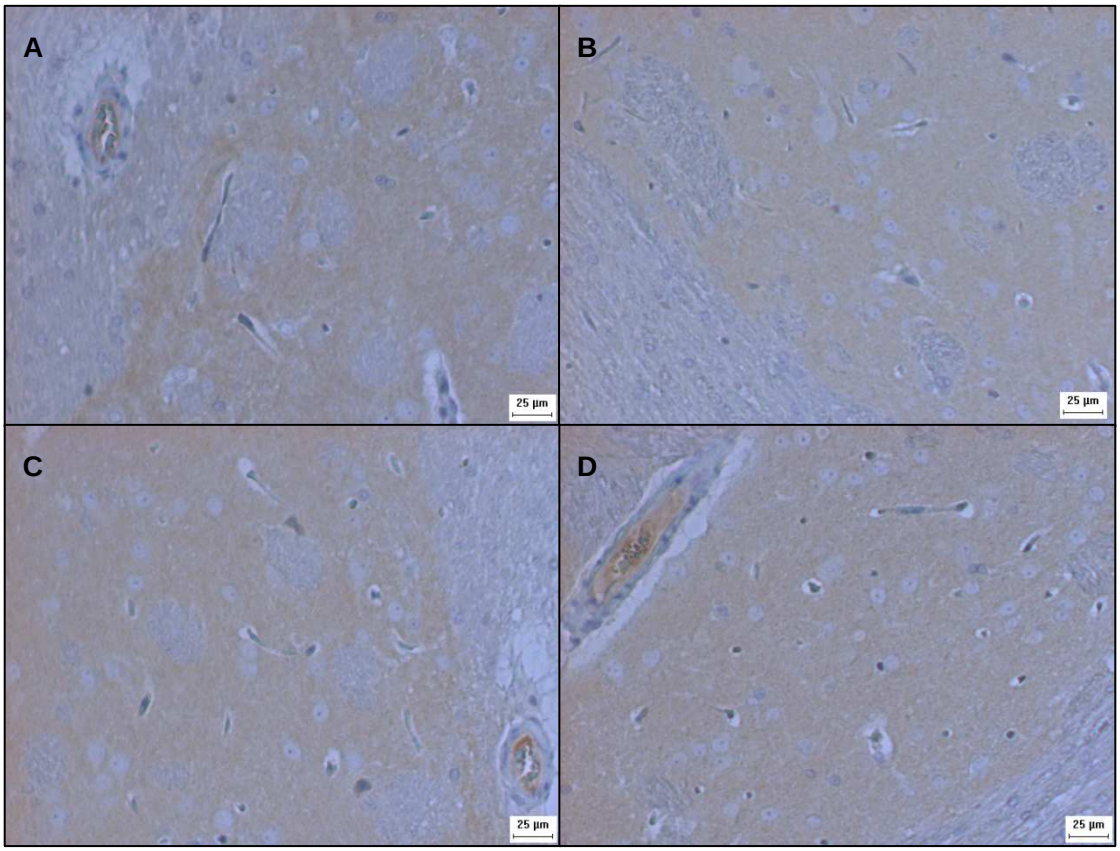

Figure L.5 -.Immunoreactivity of MMP9 in 21 week old animals A) WKY B) WKY+NaCl C) SHRSP D) SHRSP+NaCl.

All images taken at x10 objective in the deep grey matter of mid coronal brain sections. Scale bar = 25µm. We found no significant differences in MMP9 staining due to salt in this region.

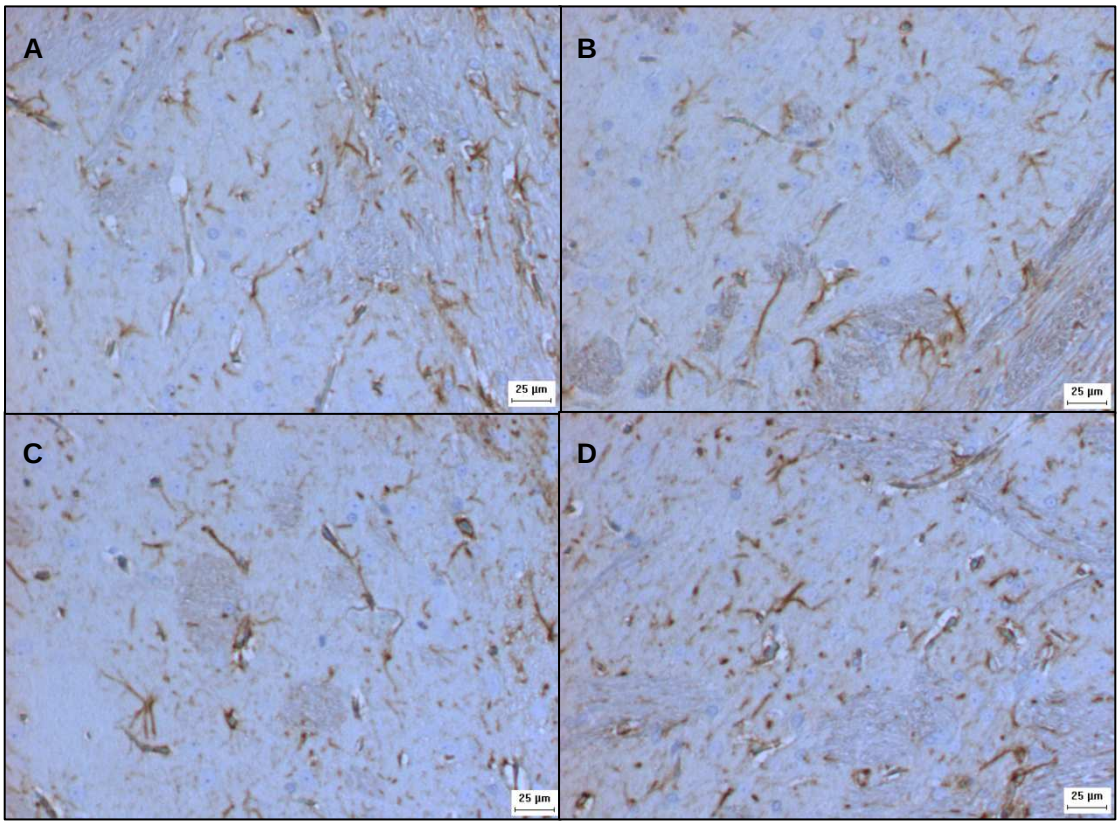

Figure L.6 -.Immunoreactivity of GFAP in 21 week old animals A) WKY B) WKY+NaCl C) SHRSP D) SHRSP+NaCl.

All images taken at x10 objective in the deep grey matter from frontal brain sections. Scale bar = 25µm. We found no significant differences due to salt loading in this brain region due to salt.

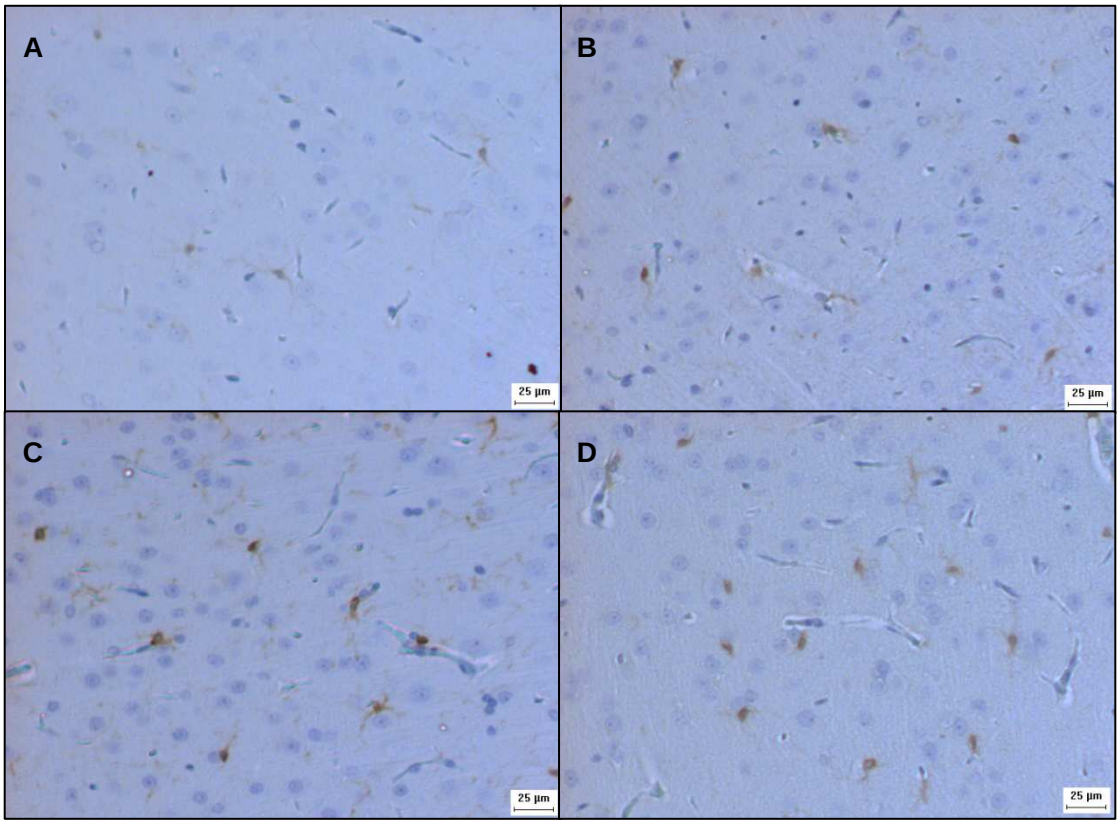

Figure L.7 -.Immunoreactivity of Iba-1 in 21 week old animals A) WKY B) WKY+NaCl C) SHRSP D) SHRSP+NaCl.

All images taken at x10 objective in the cortical grey matter of frontal brain sections. Scale bar = 25µm. Note the increase in intensity of microglia staining in WKY+NaCl versus WKY (C vs A).

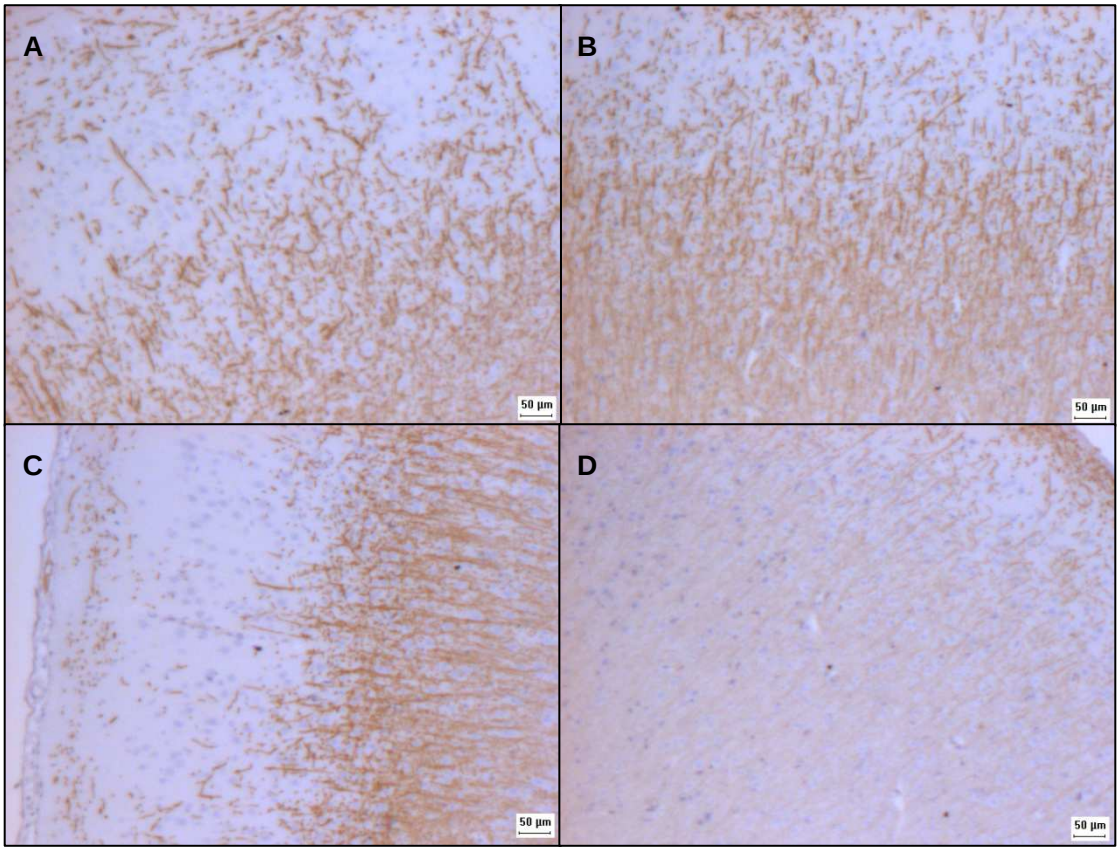

Figure L.8 -.Immunoreactivity of MBP in 21 week old animals A) WKY B) WKY+NaCl C) SHRSP D) SHRSP+NaCl.

All images taken at x4 objective in the cortical grey matter of frontal brain sections. Scale bar = 50µm. Note the signifiifant decrease in SHRSP+NaCl (D) versus both SHRSP and WKY+NaCl.

APPENDIX M) Data from Rank Products Analysis of mRNA expression in the frontal section of SHRSP versus WKY of all ages. Data shown are genes commonly differentially expressed over all three age groups. N=62 (see figure 8.1 for corresponding Venn diagram).

ABC	FRONTAL SECTIONS				
			A	B	C
PROBE_ID	ILMN_GENE	CHROMOSOME	FDR.WKY.5wk.F-SP.5wk.F	FDR.WKY.16wk.F-SP.16wk.F	FDR.WKY.21wk.F-SP.21wk.F
ILMN_1365113	RGD1564649_PREDICTED		0	0	0
ILMN_2038795	RPS9	1	0	0	0
ILMN_1371357	LOC497757		0	0	0
ILMN_2038796	RPS9	1	0	0	0
ILMN_1359040	RGD1561110_PREDICTED	2	0	0	0
ILMN_1368735	RGD1311103_PREDICTED		0	0	0
ILMN_1361865	ZFP597	10	0	0	0
ILMN_1372230	RNF149	9	4.13E-05	0.000710227	0
ILMN_1351340	LOC500950		7.27E-05	0	0.004449036
ILMN_1371004	RPS16		0.000117302	0	0
ILMN_1367530	LOC497727		0.000160428	0.001326781	0.013008264
ILMN_1372711	LOC502316		0.000160428	0.000118577	0.003023715
ILMN_1366713	ZNF575_PREDICTED		0.000227273	0.008311688	0.00799609
ILMN_1353766	RGD1566136_PREDICTED	X	0.000317125	0	0
ILMN_1360786	FKBP8	16	0.000317125	0.000242424	0
ILMN_1363342	SLC1A3	2	0.000618182	0.001748252	0.000633609
ILMN_1364120	POLL	1	0.000714286	0.000962567	0.000501567
ILMN_1349793	LOC684139		0.000651801	0.007204117	0.000828877

ILMN_1376530	RT1-A3		20	0.000861244	0.00026393	0.00012987
ILMN_1369562	LOC499096			0.00119697	0.01525974	0.005090909
ILMN_1368305	LOC499613			0.001124807	0.001194805	0.001181818
ILMN_1373217	ADPGK			0.001633729	0	0.00020979
ILMN_1650689	CPE		16	0.006217839	0.039892473	0.001048951
ILMN_1357461	ZFP61		1	0.003237998	0.002136364	0.003570248
ILMN_1368780	CLIC2		20	0.004415584	0.000798898	0.000933661
ILMN_1372466	ZCCHC9		2	0.008783107	0.004161616	0.007932068
ILMN_1353304	RGD1561287_PREDICTED			0.009307057	0.001262626	0.003827751
ILMN_1364975	LOC298980			0.00540054	0.008730408	0.002156448
ILMN_1362409	BAI2_PREDICTED		5	0.008701299	0.008730408	0.006522727
ILMN_1362692	MAP1B		2	0.015577014	0.016491677	0.004967062
ILMN_1370371	TM4SF2_MAPPED	X		0.01756993	0.033048128	0.000857143
ILMN_1357368	LOC497841			0.03056229	0.036713287	0.003493761
ILMN_1356949	COL6A1_PREDICTED		20	0.01375383	0.000242424	0.00012987
ILMN_1359375	LOC499418		20	0.012542188	0.042884972	0.007390374
ILMN_1364683	NECAB2			0.017802335	0.007946128	0.007463002
ILMN_1349772	FTCD		20	0.039682259	0.007058824	0.004060606
ILMN_1360243	LOC362350			0.021338056	0.043158861	0.017813674
ILMN_1371662	PPP2R1A		1	0.048310249	0.009379509	0.001028708
ILMN_1369541	TCF4		18	0.011252914	0.000174825	0.003827751
ILMN_1357413	LOC360443			0.007355372	0.001411483	0.00023569
ILMN_1361722	RBM8_PREDICTED			0.011111111	0.009225037	0.017185771
ILMN_1372988	FHL2		9	0.002472284	0.022260766	0.024813249

ILMN_1357163	SYMPK		0.001251863	0.004624506	0.032288401
ILMN_1349624	KIF5C_PREDICTED		0.002223587	0.009013867	0.005176768
ILMN_1358541	IGFBP6	7	0.000117302	0.002505543	0.032739475
ILMN_1363262	CSNK2A1		0.000395257	0.007058824	0.003487941
ILMN_1358234	RGD1562351_PREDICTED		0.000142045	0.000227273	0.001884701
ILMN_1364214	LOC497864		0.000117302	0.007204117	0.047861517
ILMN_1351068	RGD1309829_PREDICTED		7.27E-05	0.000151515	0.003570248
ILMN_1368752	LOC499378		7.27E-05	0.000174825	0.005172855
ILMN_1351487	RT1-A1	20	0	0.00582205	0.000292208
ILMN_1353260	PXMP4	3	0	0	0.000145455
ILMN_1353156	COLQ		0	0.002835498	0.040998943
ILMN_1651096	RGD1560364_PREDICTED		0	8.26E-05	0.000545455
ILMN_2038792	ALB	14	0	4.33E-05	4.78E-05
ILMN_1650062	RGD1563903_PREDICTED		0	4.33E-05	0.000145455
ILMN_1370031	LOC362068		0	4.33E-05	0.000145455
ILMN_1371684	LOC499103		0	0	4.78E-05
ILMN_1358480	LOC365566		0	0	0
ILMN_1376663	LOC287167	10	0	4.33E-05	0
ILMN_1349205	RGD1562905_PREDICTED	1	0	0	0
ILMN_1359180	MRPL18_PREDICTED	1	0	0	0

APPENDIX M CONTINUED

ii) Data from Rank Products Analysis of mRNA expression in the mid coronal section of SHRSP versus WKY of all ages. Data shown are genes commonly differentially expressed over all three age groups. N=55 (see figure 8.1 for the corresponding Venn diagram).

ABC	MID CORONAL SECTIONS				
			A	B	C
PROBE_ID	ILMN_GENE	CHROMOSOME	FDR.WKY.5wk.M-SP.5wk.M	FDR.WKY.16wk.M-SP.16wk.M	FDR.WKY.21wk.M-SP.21wk.M
ILMN_1365113	RGD1564649_PREDICTED		0	0	0
ILMN_2038796	RPS9	1	0	0	0
ILMN_2038795	RPS9	1	0	0	0
ILMN_1371357	LOC497757		0	0	0
ILMN_1359040	RGD1561110_PREDICTED	2	0	0	0
ILMN_1368735	RGD1311103_PREDICTED		0	0	0
ILMN_1361865	ZFP597	10	0	0	0
ILMN_1372230	RNF149	9	0	0.000227273	4.13E-05
ILMN_1371004	RPS16		0	0	0
ILMN_1376530	RT1-A3	20	0	0.00037037	0
ILMN_1353766	RGD1566136_PREDICTED	X	8.26E-05	0.000165289	7.27E-05
ILMN_1367530	LOC497727		0.000146628	0.00037037	0.018295455
ILMN_1368305	LOC499613		0.000277778	0.000666667	0.001267943
ILMN_1351340	LOC500950		0.000187166	0.00037037	0.000668449
ILMN_1360786	FKBP8	16	0.000125392	0.000823864	0.004242424
ILMN_1372711	LOC502316		0.000146628	0.000438871	0.00025974
ILMN_1373217	ADPGK		0.000847107	0.00038961	0

ILMN_1368780	CLIC2	20	0.000847107	0.00248337	0.002509881
ILMN_1357461	ZFP61	1	0.002540107	0.003555556	0.003075435
ILMN_1349793	LOC684139		0.002306649	0.001767677	0.001450216
ILMN_1363342	SLC1A3	2	0.001018182	0.011109399	0.00031348
ILMN_1353304	RGD1561287_PREDICTED		0.004159402	0.005581818	0.010681818
ILMN_1369562	LOC499096		0.007554545	0.010606061	0.00465035
ILMN_1356949	COL6A1_PREDICTED	20	0.006753247	0.001480519	0.000469208
ILMN_1359375	LOC499418	20	0.013913949	0.047282717	0.020363636
ILMN_1371662	PPP2R1A	1	0.024218835	0.012227273	0.019676214
ILMN_1357368	LOC497841		0.030909091	0.02981588	0.001606765
ILMN_1650271	LOC498813		0.046209617	0.025381818	0.028419913
ILMN_1649874	RGD1559605_PREDICTED		0.04476785	0.002400932	0.026121979
ILMN_1372988	FHL2	9	0.007204301	0.022369146	0.031024033
ILMN_1359627	LOC360919	14	0.01020475	0.027655502	0.031678322
ILMN_1349336	ADD3	1	0.005140693	0.008330579	0.011160839
ILMN_1357413	LOC360443		0.004427391	0.002344498	4.13E-05
ILMN_1649821	HAGHL		0.001603306	0.003810445	0.017844156
ILMN_1349624	KIF5C_PREDICTED		0.002306649	0.003095238	0.033049242
ILMN_1357163	SYMPK		0.000868687	0.031829545	0.002121212
ILMN_1350743	PRMT5_PREDICTED	15	0.002164502	0.001294766	0.016933514
ILMN_1369541	TCF4	18	0.000871212	0.000823864	0.004821429
ILMN_1364214	LOC497864		0.000170455	0.018636364	0.040458874
ILMN_1358234	RGD1562351_PREDICTED		0.000233766	4.33E-05	0.000884521

ILMN_2038792	ALB	14	0.000871212	0	0
ILMN_1353156	COLQ		9.74E-05	0.003553719	0.008166915
ILMN_1368752	LOC499378		9.74E-05	4.33E-05	0.000393939
ILMN_1351068	RGD1309829_PREDICTED		9.74E-05	0.000197628	7.27E-05
ILMN_1651096	RGD1560364_PREDICTED		9.74E-05	4.33E-05	0.00020202
ILMN_1363262	CSNK2A1		0.000187166	0	0.001328671
ILMN_1351487	RT1-A1	20	9.74E-05	0.00248337	0.000805195
ILMN_1353260	PXMP4	3	4.33E-05	4.33E-05	0.000174825
ILMN_1370031	LOC362068		0	0	0
ILMN_1650062	RGD1563903_PREDICTED		0	0	7.27E-05
ILMN_1371684	LOC499103		0	0	0
ILMN_1358480	LOC365566		0	0	0
ILMN_1376663	LOC287167	10	0	4.33E-05	0
ILMN_1349205	RGD1562905_PREDICTED	1	0	0	0
ILMN_1359180	MRPL18_PREDICTED	1	0	0	0

APPENDIX N) Data from Rank Products Analysis of significant differences in mRNA expression between WKY and SHRSP in both brain sections at 5 weeks of age. N=162. For the corresponding Venn diagram see figure 8.2.

AB

			A	B
PROBE_ID	ILMN_GENE	CHROMOSOME	FDR.WKY.5wk.F-SP.5wk.F	FDR.WKY.5wk.M-SP.5wk.M
ILMN_1365113	RGD1564649_PREDICTED		0	0
ILMN_2038795	RPS9	1	0	0
ILMN_1371357	LOC497757		0	0
ILMN_2038796	RPS9	1	0	0
ILMN_1359040	RGD1561110_PREDICTED	2	0	0
ILMN_1368735	RGD1311103_PREDICTED		0	0
ILMN_2039673	ARC	7	0	0
ILMN_1361865	ZFP597	10	0	0
ILMN_1372230	RNF149	9	4.13E-05	0
ILMN_1350784	JUNB	19	0.00010101	0.00030303
ILMN_1351340	LOC500950		7.27E-05	0.000187166
ILMN_1368356	FOS	6	0.000117302	0.00030303
ILMN_1367486	DUSP1	10	0.00010101	0
ILMN_1371004	RPS16		0.000117302	0
ILMN_1367530	LOC497727		0.000160428	0.000146628
ILMN_1372711	LOC502316		0.000160428	0.000146628
ILMN_1367467	PER2	9	0.000383838	0.000465632

ILMN_1367162	GPM6A		16	0.000317125	0.000386364
ILMN_1352667	NAB1			0.000317125	0.000890538
ILMN_1366713	ZNF575_PREDICTED			0.000227273	0.001603306
ILMN_1353766	RGD1566136_PREDICTED	X		0.000317125	8.26E-05
ILMN_1353839	PER1			0.000317125	0.00030303
ILMN_1360786	FKBP8		16	0.000317125	0.000125392
ILMN_1363342	SLC1A3		2	0.000618182	0.001018182
ILMN_1359704	LOC307332			0.000371901	0.00161442
ILMN_1364120	POLL		1	0.000714286	0.000847107
ILMN_1362834	DUSP6		7	0.001124807	0.01020475
ILMN_1369573	LOC688712		19	0.001792208	0.006753247
ILMN_1375922	NR4A3		5	0.000482375	0.007217069
ILMN_1349793	LOC684139			0.000651801	0.002306649
ILMN_1358205	RGD1560975_PREDICTED			0.008009404	0.028941878
ILMN_1360210	LOC499068			0.001805378	0.01180303
ILMN_1376530	RT1-A3		20	0.000861244	0
ILMN_1369562	LOC499096			0.00119697	0.007554545
ILMN_1368305	LOC499613			0.001124807	0.000277778
ILMN_1373217	ADPGK			0.001633729	0.000847107
ILMN_1355124	GALNT2_PREDICTED			0.000714286	0.008354978
ILMN_1368809	BTG2		13	0.01057352	0.013769231
ILMN_1364113	CTGF		1	0.002249417	0.004427391

ILMN_1367428	ZFP189_PREDICTED			0.004554637	0.013664773
ILMN_1370045	TRAPPC2	X		0.002683983	0.008354978
ILMN_1364821	LOC500720			0.009307057	0.028941878
ILMN_1350533	RGD1563551_PREDICTED		4	0.017192118	0.00161442
ILMN_1367827	LOC298998			0.003996212	0.005117845
ILMN_1352722	LOC316550			0.003839458	0.025268474
ILMN_1349422	PTGS2		13	0.004818182	0.016441558
ILMN_1359441	PLA2G2A		5	0.009950187	0.024345238
ILMN_1357461	ZFP61		1	0.003237998	0.002540107
ILMN_1368780	CLIC2		20	0.004415584	0.000847107
ILMN_1359630	LOC679663	16|NW_047479.1		0.008343109	0.045305577
ILMN_1372466	ZCCHC9		2	0.008783107	0.001607143
ILMN_1353304	RGD1561287_PREDICTED			0.009307057	0.004159402
ILMN_1374612	TM9SF4_PREDICTED			0.01004329	0.023941242
ILMN_1368506	LOC497770			0.012253444	0.021175449
ILMN_1362561	LOC498378			0.023521336	0.029085968
ILMN_1359795	LOC499555			0.009918495	0.024214876
ILMN_1356628	NFKBIA		6	0.01039312	0.046209617
ILMN_1374199	GIOT1		7	0.006464646	0.013769231
ILMN_1353935	FARP1_PREDICTED			0.009307057	0.027335423
ILMN_1362409	BAI2_PREDICTED		5	0.008701299	0.002714097
ILMN_1370369	EGR2		20	0.009307057	0.003713188
ILMN_1372919	CYR61		2	0.003996212	0.006986166

ILMN_1355401	RGD1563543_PREDICTED			0.021554002	0.0188
ILMN_1362451	RGS2		13	0.007420147	0.0072147
ILMN_1365095	DHX40		10	0.011252914	0.030909091
ILMN_1376434	PGRMC1	X		0.008343109	0.033276328
ILMN_1349269	SGK		1	0.011998871	0.002164502
ILMN_1361423	RKHD2_PREDICTED			0.011998871	0.036649595
ILMN_1649981	STRN3		6	0.01487781	0.042800325
ILMN_1361139	TMPRSS8		10	0.015932282	0.033140909
ILMN_1357368	LOC497841			0.03056229	0.030909091
ILMN_1356949	COL6A1_PREDICTED		20	0.01375383	0.006753247
ILMN_1368116	LOC367398			0.017802335	0.015773059
ILMN_1359375	LOC499418		20	0.012542188	0.013913949
ILMN_1352529	IER2		19	0.01724612	0.043680416
ILMN_1354120	LOC691762	Un|NW_047990.1		0.012963959	0.027361039
ILMN_1373383	TIPARP_PREDICTED			0.009131615	0.004731935
ILMN_1364683	NECAB2			0.017802335	0.002306649
ILMN_1360868	RNF40		1	0.021361686	0.015614973
ILMN_1373434	RAB28		14	0.01620753	0.043683386
ILMN_1354535	ZNF386		6	0.014258893	0.029966683
ILMN_1374435	C1GALT1C1	X		0.024523282	0.030423928
ILMN_1362029	LOC502490			0.04383255	0.022875929
ILMN_1351127	PLCL1		9	0.019282511	0.020445748

ILMN_1361932	MLL5		4	0.037223421	0.029966683
ILMN_1369005	EGR1		18	0.035286665	0.010340909
ILMN_1360758	RGD1308626		15	0.044931617	0.043680416
ILMN_1359043	EGR4		4	0.030741362	0.027467899
ILMN_1368493	RGD1562629_PREDICTED			0.038248485	0.034655248
ILMN_1349772	FTCD		20	0.039682259	0.009592184
ILMN_1361370	RYBP_PREDICTED		4	0.017995019	0.023480201
ILMN_1373798	PLCB1		3	0.024981672	0.020053129
ILMN_1372236	ZFP36L1		6	0.038386514	0.040504587
ILMN_1349546	MDGA2		6	0.047363636	0.017687075
ILMN_1353576	GPR149		2	0.04383255	0.024593868
ILMN_1354065	LOC686053	Un|NW_047874.1		0.042841958	0.014360902
ILMN_1357903	RGD1564171_PREDICTED		2	0.028060375	0.033276328
ILMN_1361346	RGD1564940_PREDICTED		5	0.031886608	0.033533363
ILMN_1370101	LOC499058			0.046880878	0.022875929
ILMN_1352135	CEACAM10		1	0.045470541	0.003838384
ILMN_1371662	PPP2R1A		1	0.048310249	0.024218835
ILMN_1363414	LOC365025			0.043867069	0.005140693
ILMN_1370033	LOC498604			0.037413057	0.04984
ILMN_1359027	RGD1563482_PREDICTED		12	0.047780599	0.019192584
ILMN_1350094	SDPR		9	0.019282511	0.011280632
ILMN_2039346	HLA-DMA		20	0.017802335	0.00802139
ILMN_1349530	CRSP6			0.02584	0.007749775
ILMN_1369447	RGD1565673_PREDICTED		3	0.015577014	0.043683386

ILMN_1355984	TPX2_PREDICTED		0.036723549	0.016383399
ILMN_1350525	XPNPEP1	1	0.011273885	0.036497199
ILMN_1360785	LOC361929	2	0.01569697	0.004775604
ILMN_1651182	ANKRD15	1	0.013436679	0.029966683
ILMN_1360040	NUDT14_PREDICTED		0.007355372	0.01180303
ILMN_1354941	COL3A1	9	0.008265852	0.007226814
ILMN_1374043	ERAF_PREDICTED		0.011252914	0.012742299
ILMN_1351156	GNAI1	4	0.038758971	0.006236786
ILMN_1352524	USMG5	1	0.012053872	0.004427391
ILMN_1374825	LOC294789		0.00608658	0.029223587
ILMN_1369541	TCF4	18	0.011252914	0.000871212
ILMN_1357413	LOC360443		0.007355372	0.004427391
ILMN_1650955	IFI27L		0.028212577	0.01020475
ILMN_1375028	HTATIP2_PREDICTED		0.023521336	0.036142857
ILMN_1348843	SLC17A6	1	0.009307057	0.016441558
ILMN_1361722	RBM8_PREDICTED		0.011111111	0.001194296
ILMN_1359627	LOC360919	14	0.002249417	0.01020475
ILMN_1358978	RGD1306126	10	0.002584885	0.007217069
ILMN_1350985	INPP5D	9	0.002191781	0.004427391
ILMN_1367329	PPP1R16A_PREDICTED	7	0.002684492	0.00848199
ILMN_1361915	PDE10A	1	0.001931818	0.008296558
ILMN_1365885	MMP14	15	0.002472284	0.043683386
ILMN_1371064	RPS18	20	0.002236842	0.01076555

ILMN_1372988	FHL2	9	0.002472284	0.007204301
ILMN_1651148	POLR2I_PREDICTED	1	0.0015427	0.001276224
ILMN_1350743	PRMT5_PREDICTED	15	0.001505682	0.002164502
ILMN_1350481	LOC499790		0.000482375	0.014687924
ILMN_1352269	RT1-149		0.0015427	0.016747759
ILMN_1362726	HMGN3	8	0.001564171	0.011285266
ILMN_1357163	SYMPK		0.001251863	0.000868687
ILMN_1357432	CYP11B1	7	0.000641711	0.003168831
ILMN_1359619	LYZL4_PREDICTED	8	0.001564171	0.049642205
ILMN_1360418	RGD1302996	20	0.000714286	0.001320755
ILMN_1649821	HAGHL		0.00040619	0.001603306
ILMN_1349624	KIF5C_PREDICTED		0.002223587	0.002306649
ILMN_1358541	IGFBP6	7	0.000117302	0.002201705
ILMN_1363262	CSNK2A1		0.000395257	0.000187166
ILMN_1359301	IGF2		0.000181818	0.011375291
ILMN_1358234	RGD1562351_PREDICTED		0.000142045	0.000233766
ILMN_1364214	LOC497864		0.000117302	0.000170455
ILMN_1351068	RGD1309829_PREDICTED		7.27E-05	9.74E-05
ILMN_1368752	LOC499378		7.27E-05	9.74E-05
ILMN_1351487	RT1-A1	20	0	9.74E-05
ILMN_1353260	PXMP4	3	0	4.33E-05
ILMN_1353156	COLQ		0	9.74E-05
ILMN_1651096	RGD1560364_PREDICTED		0	9.74E-05

ILMN_2038792	ALB	14	0	0.000871212
ILMN_1650062	RGD1563903_PREDICTED		0	0
ILMN_1370031	LOC362068		0	0
ILMN_1371684	LOC499103		0	0
ILMN_1358480	LOC365566		0	0
ILMN_1376663	LOC287167	10	0	0
ILMN_1349205	RGD1562905_PREDICTED	1	0	0
ILMN_1359180	MRPL18_PREDICTED	1	0	0

APPENDIX O) Data from Rank Products Analysis of mRNA expression between WKY+NaCl and WKY in the frontal brain section alone. N=31. For the corresponding Venn diagram see figure 8.7.

B.only

PROBE_ID	ILMN_GENE	CHROMOSOME	B	FDR.WKY.21wkS.F-WKY.21wk.F
ILMN_1351310	NCKAP1		3	0.018383838
ILMN_1365134	DBC1		5	0.018383838
ILMN_1363732	VARS2			0.022932551
ILMN_1367140	ACVR1C		3	0.045470219
ILMN_1367508	EEF1A2		3	0.039690522
ILMN_1349150	RGD1565099_PREDICTED		1	0.048243451
ILMN_1365487	LOC501282			0.041616162
ILMN_1348958	RAB14		3	0.044074675
ILMN_1350522	NFIX			0.032464115
ILMN_1352293	BMPR2		9	0.022932551
ILMN_1363601	RGD1560020_PREDICTED			0.039690522
ILMN_1374435	C1GALT1C1	X		0.039943182

ILMN_1363881	LOC498449			0.016098485
ILMN_1352524	USMG5		1	0.040055659
ILMN_1356910	RGD1560729_PREDICTED			0.039556025
ILMN_1350873	NTS_PREDICTED		7	0.041423671
ILMN_1359630	LOC679663	16|NW_047479.1		0.019278997
ILMN_1358592	CYP2E1		1	0.044194577
ILMN_1352722	LOC316550			0.009760766
ILMN_2038793	ALB		14	0.01
ILMN_1350338	GC		14	0.022954545
ILMN_1352471	AHSG		11	0.028353808
ILMN_1353635	ALDOB		5	0.018072727
ILMN_1351672	APOH		10	0.019155844
ILMN_1369573	LOC688712		19	0.003116883
ILMN_1374571	LOC297568		4	0.00973262
ILMN_1370481	AMBP		5	0.011185771
ILMN_1371501	SERPINA3K		6	0.001636364
ILMN_1361155	LOC682605			0
ILMN_1355639	MUP5		5	0
ILMN_1370140	MUP4		5	0

APPENDIX O) CONTINUED II) DATA FROM RANK PRODUCTS ANALYSIS OF MRNA EXPRESSION BETWEEN SHRSP+NACL AND SHRSP IN THE FRONTAL BRAIN SECTION ALONE. N=83. FOR THE CORRESPONDING VENN DIAGRAM SEE FIGURE 8.7.

A.only

PROBE_ID	ILMN_GENE	CHROMOSOME	A FDR.SP.21wkS.F-SP.21wk.F
ILMN_1650700	LOC360941		0.00012987
ILMN_1366732	RGD1306494_PREDICTED	4	0.000227273
ILMN_1355142	LOC500959		0.011558442
ILMN_1360197	RGD1565117_PREDICTED		0.009683794
ILMN_1353667	LOC681549		0.020646853
ILMN_1359238	ROCK2	6	0.021338843
ILMN_1368898	RGD1561587_PREDICTED		0.023318903
ILMN_1358078	HBXIP_PREDICTED	2	0.02952862
ILMN_1352300	LOC363306		0.036497326
ILMN_1351707	RGD1560706_PREDICTED		0.032959381
ILMN_1358943	MYEF2		0.035502392
ILMN_2040245	MAP1B	2	0.041172472

ILMN_1360715	LOC360303		0.015159705
ILMN_1363538	NAV3_PREDICTED		0.042966942
ILMN_1371109	RGD1561135_PREDICTED		0.011558442
ILMN_1369996	SDK2_PREDICTED		0.049123377
ILMN_1365861	LOC687298		0.032959381
ILMN_1358768	LOC503192		0.041793161
ILMN_1348850	HNRPA2B1_PREDICTED	4	0.040969125
ILMN_1359382	AMPH	17	0.040969125
ILMN_1358980	ATP6V0E2	4	0.041557239
ILMN_1350087	NS5ATP4	3	0.035754452
ILMN_1354352	LOC314472		0.036497326
ILMN_1354875	LOC497991		0.039276258
ILMN_1351551	MLC1_PREDICTED	7	0.032959381
ILMN_1650386	GNB5	8	0.025376623
ILMN_1358379	LOC315496		0.023337856
ILMN_1366333	CACNG3	1	0.048034398
ILMN_1373428	LONRF2_PREDICTED		0.032959381

ILMN_1348848	TMEFF1			0.029102564
ILMN_1356275	RGD1561850_PREDICTED	Un|NW_047851.1		0.036054545
ILMN_1370876	ANK2			0.02952862
ILMN_1358657	RIMS1		9	0.023337856
ILMN_1356423	SYTL2_PREDICTED			0.032959381
ILMN_1649757	PPP2R5B		1	0.029355581
ILMN_1373124	MFRP_PREDICTED			0.022399404
ILMN_1373296	SCGB1C1_PREDICTED		1	0.023049853
ILMN_1368395	DDX23_PREDICTED		7	0.025376623
ILMN_1363928	PTBP2		2	0.026737235
ILMN_1353696	HBB		1	0.028696172
ILMN_1368109	DDX21A_PREDICTED			0.03286631
ILMN_1349428	RGD1565052_PREDICTED		2	0.023337856
ILMN_1374082	SLC25A11		10	0.029879518
ILMN_1368188	LOC690262		7	0.016807611
ILMN_1358663	ENPP5		9	0.022399404
ILMN_1371000	DNAJB4			0.025200535

ILMN_1357622	CAPNS1		1	0.017414141
ILMN_1650851	GOLPH3		2	0.040017483
ILMN_1352570	VAMP7		12	0.018330241
ILMN_1358347	PLS3			0.02084048
ILMN_1350658	SACS_PREDICTED			0.036054545
ILMN_1370967	SNAP91		8	0.015159705
ILMN_1367994	GLRB		2	0.022399404
ILMN_1365940	SPTBN1		14	0.016807611
ILMN_1369132	PRAF2_PREDICTED	X		0.02057041
ILMN_1351568	KBTBD2_PREDICTED		4	0.026737235
ILMN_1371457	KCNIP4			0.029879518
ILMN_1373796	RGD1561932_PREDICTED		10	0.013210227
ILMN_1350714	OXR1		7	0.022399404
ILMN_1350875	LOC365214			0.015159705
ILMN_1351182	APLP2			0.018330241
ILMN_1366848	GPSN2		19	0.016807611
ILMN_1650120	CLDN11		2	0.012507837

ILMN_1362283	YY1	6	0.015159705
ILMN_1358924	LOC501116		0.029102564
ILMN_1363443	RGD1564087_PREDICTED		0.01576555
ILMN_1355098	RGD1562658_PREDICTED		0.016807611
ILMN_1370118	RPL7		0.015159705
ILMN_1357805	RGD1563441_PREDICTED	10	0.0104
ILMN_1651181	CAP1	5	0.007561983
ILMN_1354897	JAK1		0.012844575
ILMN_1365855	ATP6V1A1_PREDICTED		0.018330241
ILMN_1362105	DSTN_PREDICTED	20	0.012545455
ILMN_1352103	RGD1312005_PREDICTED		0.003787879
ILMN_1373102	LOC316573	9	0.005545455
ILMN_1352752	CTNNB1	8	0.004545455
ILMN_1355138	CLN6_PREDICTED		0.001871658
ILMN_1349652	OPCML	8	0.001871658
ILMN_1363490	NPM1	10	0.017414141
ILMN_1360728	OXT	3	0.018563636
ILMN_1650420	VSNL1	6	0.000974026
ILMN_1371753	F5_MAPPED	13	0.000363636
ILMN_1365900	OTX2	15	0.00012987

APPENDIX P) HEATMAP - 5 WEEKS OF AGE

Heatmap showing 37 genes of interest (a subset of 149 genes) which were differentially expressed between 5 week old SHRSP versus 5 week old WKY in the frontal brain section. (See 5 week IPA network figure for representation of the interactions between these genes).

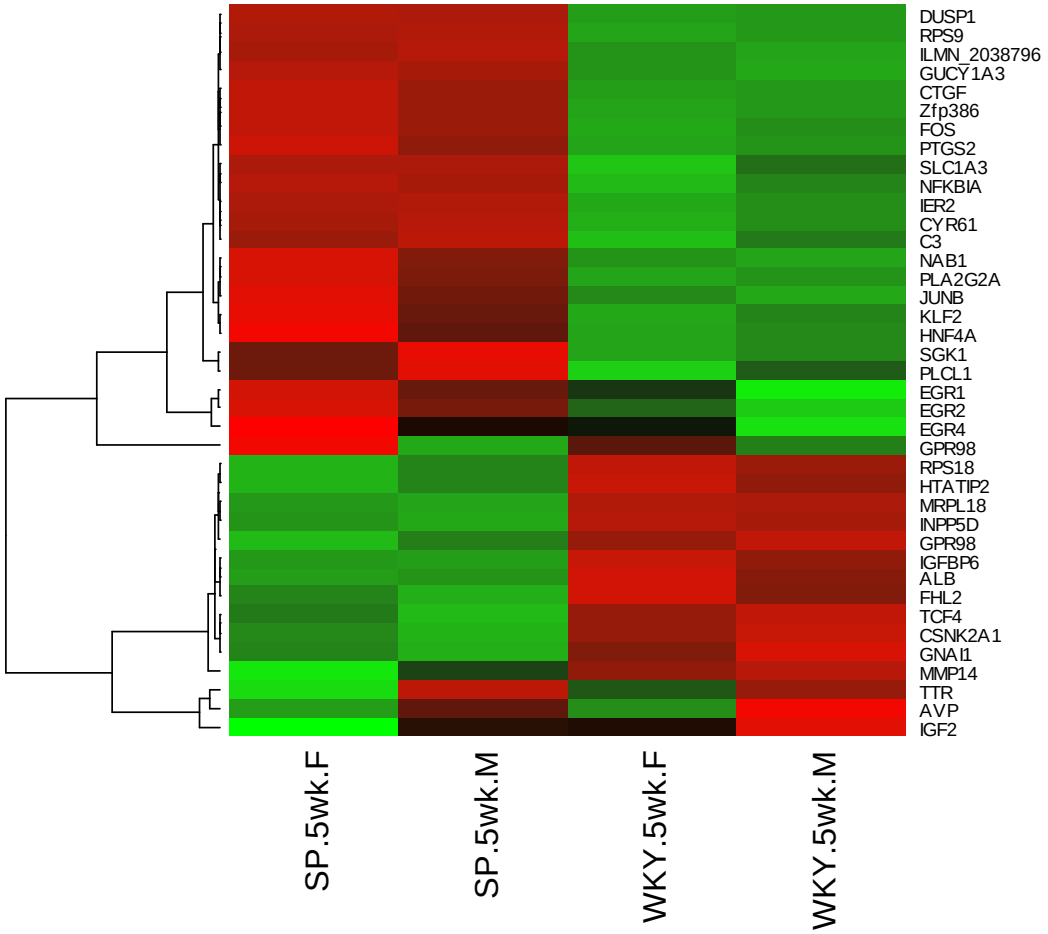

Data represents the median intensities for each group (horizontal axis) (n=4 per group), scaled per gene (vertical axis) by the mean and standard deviation. Green is low intensity and red is high intensity; Black is intermediate. The black lines on the left side are a dendrogram illustrating how the genes shown cluster.

APPENDIX Q) SALT COMPARISON HEAT MAPS

P1. Heatmap showing 31 genes differentially expressed between WKY+NaCl versus WKY aged 21 weeks in the frontal brain section.

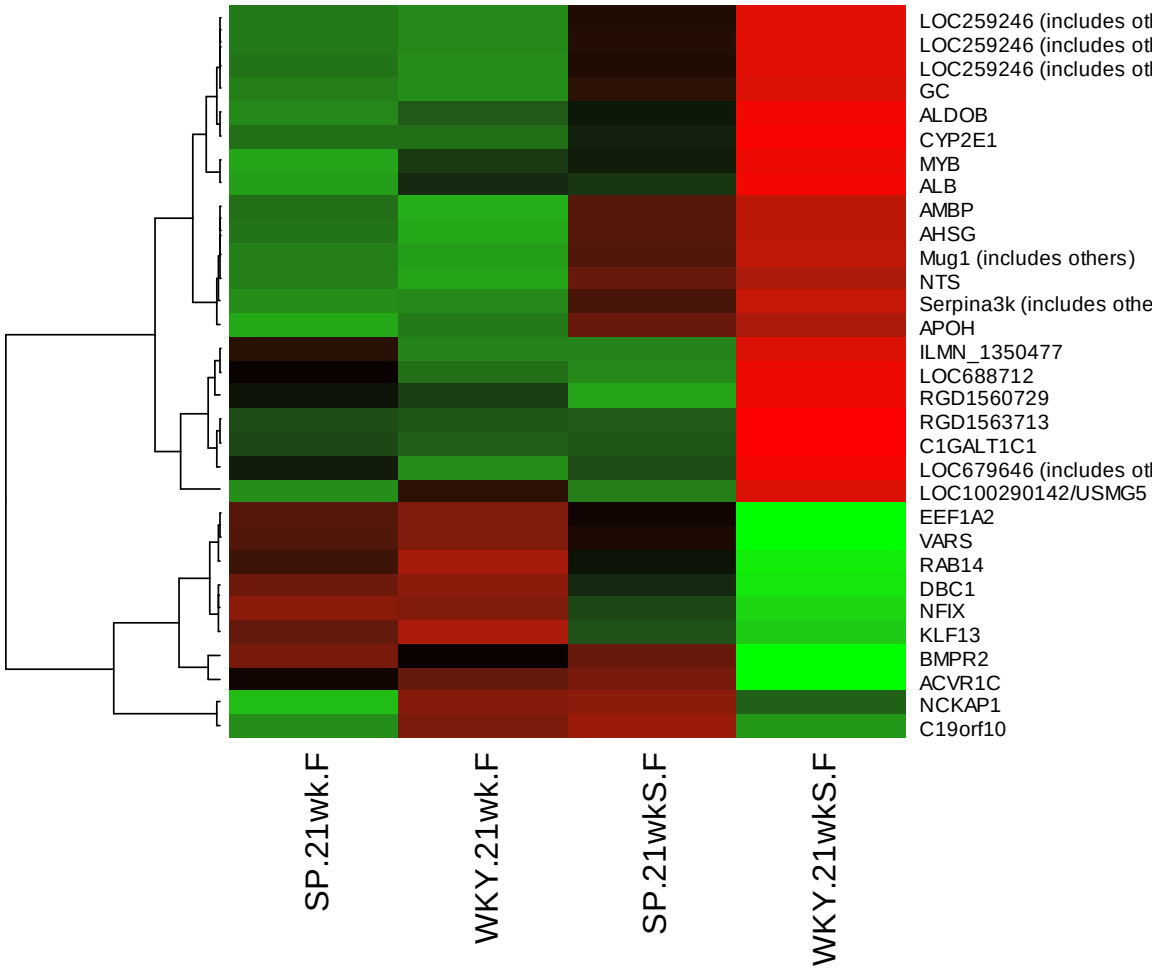

Data represents the median intensities for each group (horizontal axis) (n=4 per group), scaled per gene (vertical axis) by the mean and standard deviation. Green is low intensity and red is high intensity; Black is intermediate. The black lines on the left side are a dendrogram illustrating how the genes shown cluster.

P2. Heatmap showing 29 genes of interest (a subset of 83 genes) differentially expressed between SHRSP+NaCl versus SHRSP aged 21 weeks in the frontal brain section.

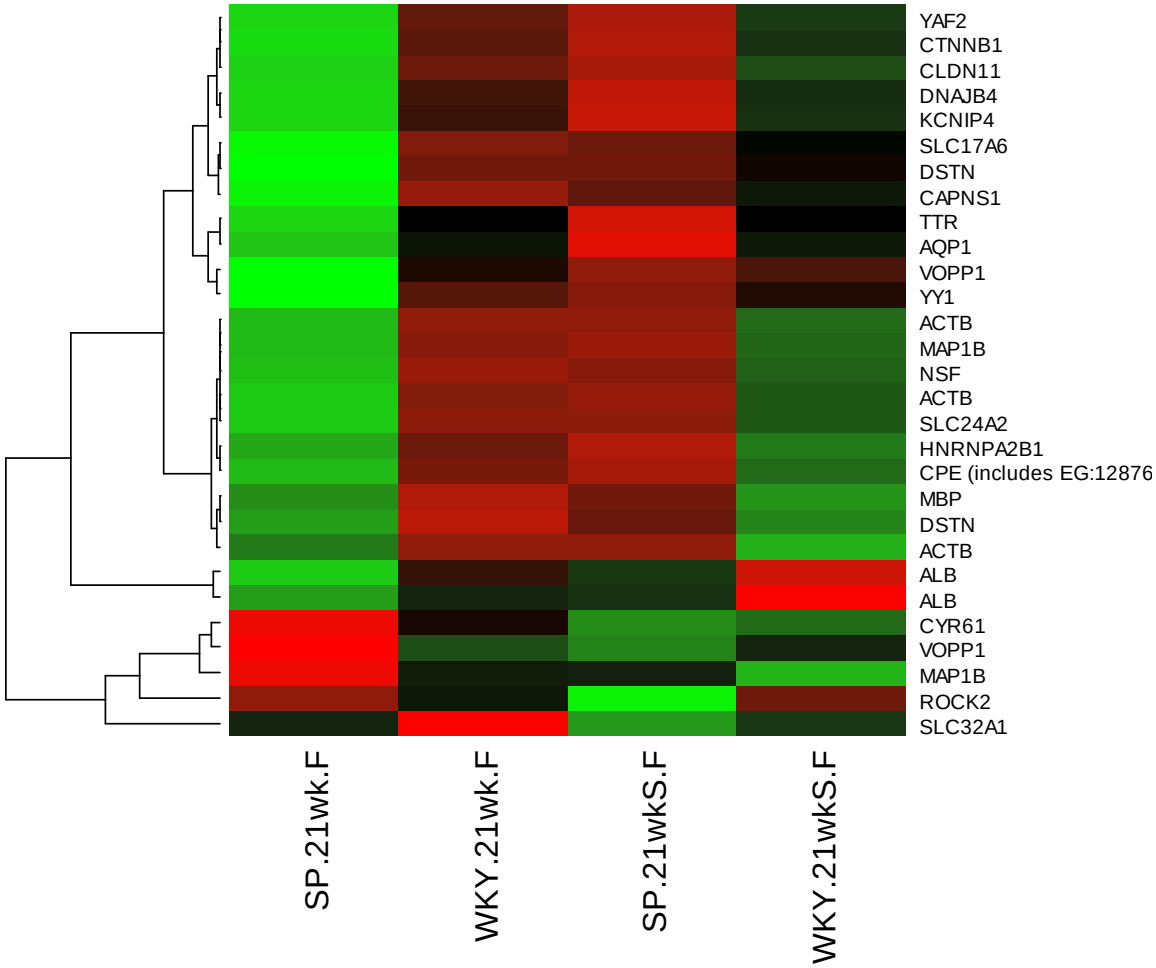

Data represents the median intensities for each group (horizontal axis) (n=4 per group), scaled per gene (vertical axis) by the mean and standard deviation. Green is low intensity and red is high intensity; Black is intermediate. The black lines on the left side are a dendrogram illustrating how the genes shown cluster.

P3. Heatmap showing 7 genes differentially expressed between SHRSP+NaCl versus SHRSP *and* WKY+NaCl versus WKY aged 21 weeks in the frontal brain section.

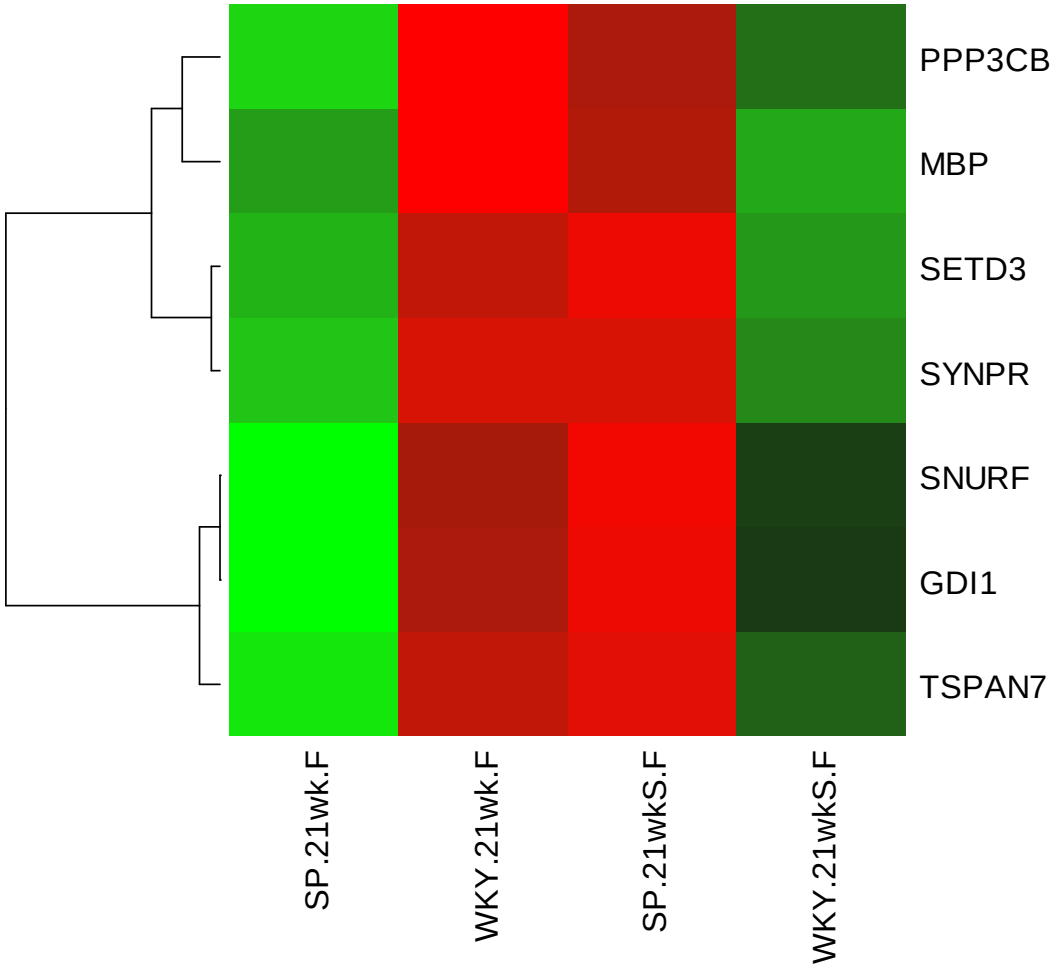

Data represents the median intensities for each group (horizontal axis) (n=4 per group), scaled per gene (vertical axis) by the mean and standard deviation. Green is low intensity and red is high intensity; Black is intermediate. The black lines on the left side are a dendrogram illustrating how the genes shown cluster.

Note: although significant for both comparisons, the direction of the differenetial expression changes (i.e.all genes are down-regulated in WKY+NaCl and up-regulated in SHRSP+NaCl).

APPENDIX R) Image of PCR gels showing no difference in signal intensity between WKY and SHRSP corresponding to expression of portions of the GUCY1a3 gene within the region of the Illumina GUCY1a3 probe binding site.

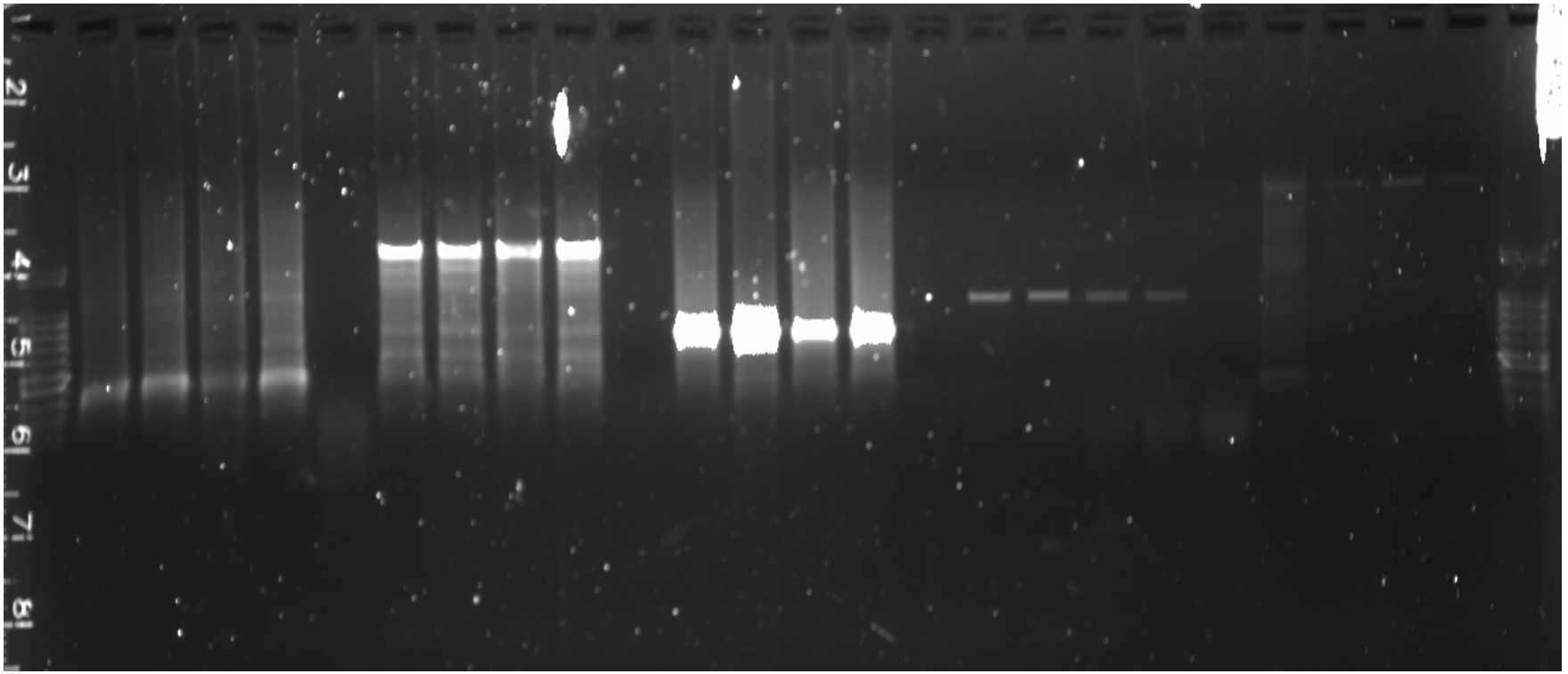

Samples left to right in each block of 4 are WKY, WKY, SHRSP and SHRSP. Each block of four corresponds to a different pairing of forward and reverse primers. The gel shows no difference in the size of the gene products formed, indicating the sequence is the same length in both WKY and SHRSP and no insertions or deletions exist in the SHRSP.